Epigenetic modulation of intestinal homeostasis and tumorigenesis by Brm SWI/SNF chromatin remodelling factor

Thesis submitted for the award of PhD

By

Joanna Krzystyniak

Cardiff School of Biosciences

Cardiff University

September 2014

Acknowledgments

I dedicate this thesis to my parents, Jolanta and Dariusz.

I would like to thank my parents for never-ending support throughout the eight years I have been living and studying in the United Kingdom. I would also like to thank my brother for providing me with fresh waves of critique which motivated me to aim even higher.

I would like to thank everyone in the ARC group, past and present, for their help, guidance and acceptance as a member of a research team. First and foremost, I must thank my supervisor Professor Alan Clarke for his academic wisdom and guidance, at the same time allowing me to make my own decisions and learn. Secondly, I would like to thank Aliaksei Holik for setting up the initial project and being my mentor during the first year of my PhD. I would like to thank Mark Bishop and Matt Zverev for genotyping of animals as well as Derek Scarborough for undertaking tissue processing and sectioning. I would like to thank Meera Raja for her support and advice, and teaching me a patient approach to Western blotting. I would like to thank Valerie Meniel for all the help and support, and our conversations in French. I would like to thank Giusy Tornillo for keeping me company during the weekends spent in the lab and for telling me when I talk too much. Boris and my three favourite clinicians for hours of discussion about cuisine, travelling and how it is to be “a real doctor”. Finally I would like to thank everyone on the 4th floor in the Biosi3 building as well as on the ECSCRI floor in the Hadyn Elis building for their advice and friendliness.

Contents

Declarations i

Acknowledgements ii

Contents iii

List of figures vii

List of tables xi

Abbreviations and definitions xiii

Abstract xv

1. Introduction 1
    1.1 The Mammalian small intestine 1
        1.1.1 Anatomy and functions of gastrointestinal tract 1
        1.1.2 Micro-architecture of small intestinal epithelium 4
            1.1.2.1 Stem cell niche and identity 8
        1.1.3 The homeostasis in the intestinal epithelium 11
            1.1.3.1 Hedgehog and PDGF pathway 12
            1.1.3.2 TGF-β and BMP pathway 14
            1.1.3.3 Wnt pathway 17
            1.1.3.4 Notch pathway 20
    1.2 Colorectal cancer 25
        1.2.1 Incidence of colorectal cancer and environmental risk factors 25
        1.2.2 Genetic predisposition to colorectal cancer 25
            1.2.2.1 Familial adenomatous polyposis 26
            1.2.2.2 Hamartomatous polyposis syndromes 26
            1.2.2.3 Hereditary nonpolyposis colorectal cancer syndrome 27
        1.2.3 Major signalling pathways involved in the development, progression and metastasis of CRC 29
            1.2.3.1 Wnt signalling 29
                1.2.3.1.1 Human mutations in the Wnt pathway 29
                1.2.3.1.2 Mouse models of alterations in the Wnt pathway 31
            1.2.3.2 TGF-β and BMP pathway 31
                1.2.3.2.1 Human mutations in the TGF-β and BMP pathway 31
                1.2.3.2.2 Mouse models of alterations in the TGF-β and BMP pathway 32
            1.2.3.3 Ras-Raf-MAPK pathway 33
                1.2.3.3.1 Human mutations in the Ras-Raf-MAPK pathway 33
                1.2.3.3.2 Mouse models of alterations in the Ras-Raf-MAPK pathway 34
            1.2.3.4 PI3K pathway 34
                1.2.3.4.1 Human mutations in the PI3K pathway 34
                1.2.3.4.2 Mouse models of alterations in the PI3K pathway 35
        1.2.4 Genetic model of CRC progression 36
        1.2.5 Colorectal cancer stem cell 39
        1.2.6 Mouse models as a tool for recapitulating human colorectal tumorigenesis and translational research 40
            1.2.6.1 Constitutive transgenesis 41
            1.2.6.2 Conditional transgenesis 42

1.3 Brm as a potential therapeutic target for Wnt-driven tumorigenesis 43
1.3.1 Chromatin structure and chromatin remodelling 43
1.3.2 Mammalian SWI/SNF and its subunits 44
1.3.3 Comparison between paralogues: Brm and Brg1 46
1.3.4 Physiological functions of Brm 49
1.3.4.1 Brm interaction with Notch signalling 50
1.3.5 The role of Brm in mammalian development 50
1.3.6 The role of Brm as tumour suppressor 51
1.4 Aims and objectives 53
2 Materials and Methods 54
2.1 Experimental animals 54
2.1.1 Transgenic constructs and animals used in the project 54
2.1.2 Animal husbandry 57
2.1.3 Experimental procedures 57
2.1.4 PCR genotyping 58
2.2 Tissue harvesting and processing 63
2.2.1 Tissue harvesting 63
2.2.2 Tissue fixation 64
2.2.3 Tissue processing for light microscopy 64
2.2.4 Tissue preservation for DNA, RNA and protein extraction 64
2.3 Histological analysis 65
2.3.1 Haematoxylin and Eosin staining of tissue sections 65
2.3.2 Quantitative histological analysis of H&E sections 65
2.3.3 Quantification of histological traits by the use of cell specific Stains 66
2.4 Immunohistochemistry 69
2.5 Gene expression analysis 74
2.5.1 RNA extraction from tissue 74
2.5.2 Preparation of cDNA 76
2.5.3 Quantitative real-time PCR analysis 76
2.5.4 *In situ* hybridization 80
2.6 Protein analysis 83
2.6.1 Protein extraction from collected tissues 83
2.6.2 Quantification of protein concentrations 83
2.6.3 Analysis of protein levels by Western blotting 84
2.7 Statistical and quantitative analysis 88
2.7.1 Quantitative analysis of histological traits 88
2.7.2 Comparisons of means 88
2.7.3 Kolmogorov-Smirnov Z test 89
2.7.4 Kaplan-Meier survival analysis 90
3 Investigating the effects of Brm loss in the epithelium of small and large intestine 91
3.1 Introduction 91
3.2 Results 92
3.2.1 Brm null mice are viable and not prone to tumorigenesis 92
3.2.2 The complete loss of Brm in Brm null mice 93
3.2.3 Brm loss has mild effects on the small intestinal homeostasis 102
3.2.4 Brm loss changes the shape of proliferative compartment in the epithelium of small intestine 105
3.2.5 Brm loss does not affect the cell migration in the small intestinal epithelium 106
3.2.6 Brm loss affects the differentiation of the certain intestinal epithelial cell types 107

3.2.7 Brm loss does not affect CD44 expression 113
3.2.8 Brm loss does not directly interact with Wnt signalling 116
3.2.9 Brm loss leads to changes in Notch signalling..... 118
3.2.10 Brm loss does not affect stem cell compartment..... 123
3.2.11 The pattern of Brm expression in the large intestinal epithelium 125
3.2.12 Brm loss has mild effects on the homeostasis of large intestinal epithelium..... 127
3.2.13 Brm deficiency results in a shift in the differentiation pattern towards the secretory lineages 129

3.3. Discussion..... 133

4 Investigating the effects of Brm loss in the Wnt-activated epithelium of small and large intestine .....
4.1 Introduction 139
4.2 Results 140
4.2.1 Placing Brm in the context of aberrant Wnt signalling 140
4.2.2 Brm loss does not improve the survival of Apc-deficient animals 141
4.2.3 Brm loss is compatible with nuclear β-catenin 144
4.2.4 Brm deficiency in permissive of Apc loss and accentuates some of the manifestations associated with Wnt signalling activation..... 145
4.2.5 Brm loss leads to a change in distribution pattern of proliferating cells in the Wnt-activated epithelium of small intestine..... 149
4.2.6 Brm loss affects the differentiation of certain intestinal epithelial cell types 151
4.2.7 Brm loss does not modulate the β-catenin levels and localisation following Apc loss 159
4.2.8 Brm deficiency modulates the expression of genes crucial to development and progression of CRC 161
4.2.9 Brm deficiency leads to the reduction of the Wnt-mediated expansion of stem cell population 164
4.2.10 Brm loss has mild effects on the homeostasis of large intestinal epithelium..... 166
4.2.11 Brm loss results in a change in the distribution of proliferating cells in the Apc-deficient colonic epithelium 169
4.2.12 Brm deficiency does not alter differentiation status in Wnt-activated colonic epithelium..... 170
4.2.13 Brm deficiency leads to the attenuation of the β-catenin-activated transcription of Wnt target genes 173
4.3 Discussion 176

5 Investigating the effects of Brg1 loss in the context of Brm null in the small intestinal epithelium.....
5.1 Introduction 188
5.2 Results 189
5.2.1 Concomitant loss of Brm and Brg1 results in animals that are viable and not prone to tumorigenesis 189
5.2.2 AhCreERrecombinase drives mosaic loss of Brg1 and subsequent repopulation in the small intestinal epithelium of AhCre^{+}Brg1$^{fl/fl}$Brm null mice..... 190
5.2.3 Brg1 loss in the context of a Brm null allele has mild effects on small intestinal homeostasis..... 193

5.2.4 Mosaic loss of Brg1 changes the pattern of distribution of proliferating cells in the Brm null epithelium of small epithelium 196
5.2.5 Brg1 deficiency affects the differentiation of goblet cells in the small intestinal epithelium of AhCreER^{+}Brg1$^{fl/fl}$Brm null Animals 197
5.2.6 Mosaic loss of Brg1 in Brm-deficient colonic epithelium of AhCreER^{+}Brg1$^{fl/fl}$Brm null animals is characterized by a long-term retention of Brg1–negative clusters of epithelial cells 202
5.2.7 Brg1 loss in the context of Brm null allele leads to severe decrease in apoptosis levels and an expansion of proliferative zone in colonic epithelium 204
5.2.8 Brg1 deficiency in the context of concomitant Brm loss results in a decrease in the differentiation of epithelial cells along the secretory lineage 208
5.2.9 Concomitant deficiency in Brm and Brg1 under the expression of AhCreER in the context of Apc loss results in the abrogation of intestinal architecture 210
5.2.10 Brg1 deficiency potentiates the effects of Brm loss on the transcriptional program of Wnt target genes in the context of Wnt activation 215
5.2.11 The upregulation of Brm in the Brg1-deficient neoplastic lesions of AhCreER^{+}Apc$^{fl/fl}$Brg1$^{fl/fl}$ colonic epithelium 217
5.2.12 The expression levels of Brm and Brg1 in the small intestinal and colonic epithelium are context- and tissue-dependent 219
5.3 Discussion 222

6 General discussion 227
7 Reference List 242
8 Appendix I 262

List of Figures

Figure 1.1 The basic anatomy of gastrointestinal tract consisting of small and large intestine supported in their function by multiple glands 2

Figure 1.2 Histology of small and large intestinal epithelium including the underlying layers of tissue 3

Figure 1.3 The epithelial cell lining of small intestine forms invaginations into the mucosa and finger-like projections into the gut lumen and consists of numerous cell populations.....5

Figure 1.4 Hedgehog is one of the major pathway playing role in the maintenance of intestinal homeostasis and represents epithelium-to-mesenchyme signalling with Ptch playing a dual role in the signal transduction 14

Figure 1.5 TGF-β and BMP pathways together with Hedgehog pathway regulate activation of Wnt signalling and intestinal homeostasis acting through their common co-effector SMAD4.....16

Figure 1.6 Wnt signalling pathway is responsible for the maintenance of intestinal homeostasis by regulating stem cell renewal and progenitor cell differentiation.....20

Figure 1.7 Notch signalling pathway represents cell-to-cell signalling within small intestinal epithelium and regulates cell fate decision of progenitor cells as they exit the crypt compartment 21

Figure 1.8 In order to maintain the intestinal homeostasis the interplay between different signalling pathways: Wnt, Notch, BMP/TGF-β and Hedgehog is necessary to control all processes regulating cell renewal, proliferation, differentiation, migration and cell death.....24

Figure 1.9 Genetic model of CRC progressionfrom adenoma to carcinoma.....38

Figure 1.10 Structural domains of Brg1 and Brm ATPase subunits include six common domains that are evolutionarily conserved 47

Figure 2.1 Schematic representation of the targeted disruption of*Brm* gene and loxP targeted *Brg1* and *Apc*alleles and their primer positions 56

Figure 2.2 The differences between SYBR Green-based and TaqMan-Based qRT-PCR reactions 79

Figure 3.1 The complete loss of Brm in Brm null knock-out mice. Brm null animals along with Brm $^{+/+}$ controls were dissected at 70 days of age .....

Figure 3.2 The expression pattern of Brm in the small intestinal epithelium. 95-99

Figure 3.3 The mosaic expression of Brm and Brg1 in liver. 99-100

Figure 3.4 Brm loss affects the expression levels of Brg1 101

Figure 3.5 Histological analysis of the effects of constitutive Brm loss in the small intestinal epithelium 104

Figure 3.6 Immunohistochemical analysis of Ki67 staining of control and experimental animals at day 70 of age detected no gross differences in distribution of Ki67-positive cells within the epithelium. 105

Figure 3.7 Brm deficiency does not affect the population of BrdU positive cells and the migration pattern of those cells remains unchanged. Cumulative frequency analysis of BrdUimmunostaining.....107

Figure 3.8 Alkaline phosphatase staining detected the normal brush border pattern corresponding to the membrane of differentiated enterocytes. 109

Figure 3.9 Alcian Blue staining was used in order to mark goblet cells within small intestinal epithelium 110

Figure 3.10 Immunohistochemistry against lysozyme was carried out in order to mark Paneth cells within small intestinal epithelium.....111

Figure 3.11 Grimelius staining of small intestinal sections was carried out to visualize the number of enteroendocrine cells on small intestinal sections of control and Brm null mice dissected at day 70 of age. 112

Figure 3.12 Analysis of the expression of CD44. 114

Figure 3.13 Immunofluorescent staining for CD44 for (A) small intestinal epithelium (B) stomach (C) lung (D) liver.....115

Figure 3.14 The analysis of expression of β-catenin in small intestinal epithelium in Brm null and Brm wild-type animals harvested at 70 days of age. 117

Figure 3.15 Western blots for numerous elements of Notch signalling such as Hes1, Math1, Notch1 ICD. 120

Figure 3.16 Analysis of Hes5 expression in the small intestinal epithelium. 121

Figure 3.17 The transcriptional levels of Hes5, Hes1 and Math1 were quantified by quantitative real-time-PCR (qRT-PCR) as shown in bar graph form. 122

Figure 3.18 Analysis of intestinal stem cell niche in Brm null animals. 124

Figure 3.19 The expression pattern of Brm in the colonic epithelium. 126

Figure 3.20 Histological analysis of the effects of constitutive Brm loss in the colonic epithelium. 129

Figure 3.21 Alcian Blue staining was used in order to mark goblet cells within colonic epithelium 131

Figure 3.22 Grimelius staining of colonic sections was carried out to visualize the number of enteroendocrine cells on colonic epithelium sections of control and Brm null mice dissected at day 70 of age. 132

Figure 4.1 Brm deficiency does not alter the survival of animals with a homozygous inactivation of Apc.....142

Figure 4.2 Brm deficiency is compatible with Wnt pathway activation in the stem cells and progenitors cells of small intestinal epithelium. 144

Figure 4.3 Histological analysis of the effects of Brm loss in the Wnt-activated small intestinal epithelium.....148

Figure 4.4 Analysis of proliferative compartment by Ki67 staining of control and experimental Apc-deficient animals at day 10-12 post induction. 150

Figure 4.5 Alkaline phosphatase staining detected a decreased brush border enterocytes in the epithelium of Apc deficient animals. 154

Figure 4.6 Alcian Blue staining was used to identify goblet cells within small intestinal epithelium. 155

Figure 4.7 Immunohistochemistry against lysozyme was carried out to visualize Paneth cells

within small intestinal epithelium.....156

Figure 4.8 Grimelius staining of small intestinal sections was carried out to label enteroendocrine cells. 157

Figure 4.9 The transcriptional levels of Hes1, Math1 and Muc2 were assessed by quantitative real-time-PCR (qRT-PCR) as shown in bar graph form.....158

Figure 4.10 Brm loss does not affect the levels of stabilized β-catenin in the small intestinal epithelium of Apc-deficient animals.....160

Figure 4.11 Brm loss suppresses the expression of the Wnt target genes and genes involved in development and progression of CRC 162

Figure 4.12 Brm deficiency results in the diminished expression of CD44 in context of aberrant Wnt signalling.....163

Figure 4.13 Analysis of intestinal stem cell niche in Brm null animals. 165

Figure 4.14 Histological analysis of the effects of Brm loss in the Wnt-activated colonic epithelium. 168

Figure 4.15 Analysis of proliferative compartment by Ki67 staining of AhCreER^{+}Apc$^{fl/fl}$Brm$^{+/+}$ and AhCreER^{+}Apc$^{fl/fl}$Brm null epithelium animals at day 10-12 post induction. 169

Figure 4.16 Alcian Blue staining was used in order to mark goblet cells within colonic epithelium. 171

Figure 4.17 Grimelius staining of colonic sections was carried out to visualize the number of enteroendocrine cells on colonic epithelium sections of AhCreER^{+}Apc$^{fl/fl}$Brm$^{+/+}$ and AhCreER^{+}Apc$^{fl/fl}$Brm null animals.....172

Figure 4.18 Brm loss suppresses the expression of the Wnt target genes. 174

Figure 4.19 Brm deficiency leads to decrease in the expression of CD44 in context of activated Wnt pathway in the colonic epithelium. 175

Figure 5.1 Brg1 loss under the expression of AhCreERrecombinase is characterized by mosaic pattern of Brg1-deficient and Brg1-proficient crypts 192

Figure 5.2 Histological analysis of the effects of mosaic Brg1loss in the small intestinal epithelium of Brm null animals 195

Figure 5.3 A change in shape of proliferative zone in the small intestinal epithelium of AhCreER^{+}Brg1$^{fl/fl}$Brm null animals. 196

Figure 5.4 Alkaline phosphatase staining detected the normal brush border pattern corresponding to the membrane of differentiated enterocytes.....199

Figure 5.5 Cell-specific stains were performed for identification of cells of secretory

lineage. 200

Figure 5.6 Immunohistochemistry against lysozyme was performed to mark Paneth cells within small intestinal epithelium. 201

Figure 5.7 Mosaic loss of Brg1 under the expression of AhCreERrecombinase is maintained within the colonic epithelium.....203

Figure 5.8 Histological analysis of the effects of induced mosaic Brg1 loss in the Brm null colonic epithelium.....206

Figure 5.9 Brg1 loss in the context of Brm null epithelium leads to significant reduction in the goblet and enteroendocrine cells of large intestine. 209

Figure 5.10 Deficiency in both Brm and Brg1 does not alter the survival of animals with a homozygous inactivation of Apc. 212

Figure 5.11 Microscopical analysis of H&E sections of small intestinal and colonic epithelium of AhCreER^{+}Apc$^{fl/fl}$Brg1$^{fl/fl}$Brm null animals reveals severe intestinal dysplasia across the tissue.....213

Figure 5.12 Deficiency in Brm and Brg1 ATPases is tolerated at much lower levels in the colonic epithelium of animals carrying a homozygous inactivation of Apc. 214

Figure 5.12 Brg1 deficiency suppresses the expression of the Wnt target genes in the small intestine with concurring upregulation of the same genes in the colonic epithelium of AhCreER^{+}Apc$^{fl/fl}$Brg1$^{fl/fl}$Brm null animals. 216

Figure 5.13 The upregulation of the expression of Brm in the colonic epithelium of AhCreER^{+}Apc$^{fl/fl}$Brg1$^{fl/fl}$ animals. 218

Figure 5.14 The fluctuations in the gene expression of Brm and Brg1 in the small intestinal and colonic epithelium in the context of normal homeostasis and Wnt-driven tumorigenesis.221

List of tables

Page

Table 2.1 Genotyping PCR reaction components and cycling conditions.....61
Table 2.2 Primer sequences and size of products of genotyping PCR reaction 62
Table 2.3 Antibody-specific conditions for immunohistochemical staining.....73
Table 2.4 Primer and probe sequences for qRT-PCR analysis.....77
Table 2.5 Components of probe-labelling reaction.....81
Table 2.6 Gels and solutions used for quantitative protein analysis by Western blotting.....85
Table 2.7 Outline of antibody-specific conditions for Western blotting 87
Table 3.1 Quantitative analysis of the effects of Brm loss on the small intestinal histology .103
Table 3.2 Quantitative analysis of the effects of Brm loss on the histology of colonic epithelium 128
Table 4.3 Quantitative analysis of the effects of Brm loss on the histology of Wnt-activated small intestinal epithelium 147
Table 4.2 Quantitative analysis of the effects of Brm loss on the histology of Wnt-activated colonic epithelium.....167
Table 5.1 Quantitative analysis of the effects of Brg1 deficiency on the small intestinal histology in the context of constitutive Brm loss.....194
Table 5.2 Quantitative analysis of the effects of Brg1 deficiency on the histology of Brm null colonic epithelium.....205
Table 6.1 The summary of histological analyses of all phenotypes involving Brm null allele in both small intestinal and colonic epithelium 230

Abbreviations and definitions

Symbols

°C	Degrees Celsius
µg	Micrograms
µl	Microlitres
µm	Micrometre
µM	Micromolar

A

ABC	Avidin Biotin Complex
AhCreER	ArylHydrocarbonCrerecom-binase Estrogen Receptor transgene
Ascl2	AchaeteScutelike 2
APC	AdenomatousPolyposisColi

B

BCA	BicinchoninicAcid
Bmi1	polycomb ring fingeroncogene
BMP	BoneMorphogenicProtein
BMPRII	BoneMorphogenic Receptor type II
bp	Base Pair
BrdU	5-Bromo-2-deoxyuridine
Brg1	Brahma related gene 1
Brm	Brahma
BSA	BovineSerumAlbumin

C

CRC	ColorectalCancer
CBC cells	Crypt-Base-Columnar cells
cm	Centimetre
CSL	CBF1/RBP-J_/Suppressor of Hairless/LAG-1
CreER	Cre recombinase-Estrogen receptor fusiontransgene
C_T	Cycle Time

D

DAB	3,3-diaminobenzidine
dATP	DeoxyadenosineTriphosphate
DCAMKL1	Doublecortin and Calcium/ Calmodulin-dependentprotein Kinase-Like-1
DCC	Deleted in Colorectal Cancer
ddH2O	double distilled water
dGTP	Deoxyguanosine Triphosphate
Dhh	Desert Hedgehog
dH2O	deionised water
DNA	Deoxyribonucleic Acid
DNase	Deoxyribonuclease
dNTP	Deoxynucleotide Triphosphate
DSH	Dishevelled
DTT	Dithiothreitol
dTTP	Deoxythymidine Triphosphate

E

E-cadherin	Epithelial Cadherin
ECL	Electrochemiluminescence
EDTA	Ethylenediamine Tetra-acetic Acid
EGFP	Enhanced Green Fluorescent Protein
EpCAM	Epithelial Cell Adhesion Molecule
ER	Estrogen Receptor
Erk	Extracellular regulated MAP kinase
ES cells	Embryonic Stem cells

F

FAP	Familial Adenomatous Polyposis
FLP	flippase
FRT	FLP Recognition Target

G

GSK-3	Glycogen Synthase Kinase-3
GTP	Guanosine Triphosphate
GTPase	GuanosineTriphosphatase

H

H&E	Haematoxylin and Eosin
HNPCC	Hereditary Nonpolyposis ColorectalCancer
h	Hour
HRP	Horse Radish Peroxidase

I

IGF-1	Insulin-Like Growth Factor-1
IHC	Immunohistochemistry
Ihh	Indian Hedgehog
IP	Intraperitoneal

J

JPS	JuvenilePolyposis Syndrome

K

KDa	Kilodaltons
kg	Kilograms
KRAS	Kirsten Rat Sarcoma viral oncogeneshomolog

L

l	Litre
Lgr5	Leucine-rich repeat-containing Gprotein coupled receptor 5
LN2	Liquid Nitrogen
LOH	loss of heterozygosity
loxP	Locus of crossover of BacteriophageP1

M

MAPK	Mitogen Activated Protein Kinase
MEK	Mitogen Activated Erk Kinase1/2
mg	Milligrams

MIN	Multiple Intestinal Neoplasia
min	minutes
MLH1	MutL homolog 1
mm	Millimetre
MMR	Mismatch Repair
MSH2	MutSE.Coli homolog of 2
mTERT	mouse telomerase reverse transcriptase
mTOR	mammalian target of rapamycin
M/W	Microwave

N

NCID	Notch Receptor Intracellular Domain
NGS	Normal Goat Serum
NRS	Normal Rabbit Serum

O

Olfm4	Olfactomedin 4
o/n	Overnight

P

PBS	Phosphate Bu_ered Saline
P/C	Pressure Cooker
PCR	Polymerase Chain Reaction
PKA	Protein Kinase A
PLL	Poly-L-Lysine
PTEN	Phosphatase and tensin homologdeleted on chromosome ten
PI	Post induction
PI3K	Phosphatidylinositol-3-Kinase

Q

qRT-PCR	Quantitative ReversetranscriptionPCR

R

RNA	Ribonucleic Acid
RNase	Ribonuclease
RPM	Revolutions Per Minute
rt	Room Temperature
RTK	Receptor Tyrosine Kinase

S

SDS	Sodium Dodecyl Sulphate
SDS-PAGE	Sodium Dodecyl Sulphate-Polyacrylamide Gel Electrophoresis
sec	Seconds
Shh	Sonic Hedgehog

T

TA	Transit-Amplifying
TACE	Tumour Necrosis Factor ConvertingEnzyme
Taq	DNA polymerase from Thermusaquaticus
TBE	Tris Borate EDTA
TBS/T	Tris Buffered Saline with Tween20
Tcf/Lef	T-cell factor and Lymphoid enhancerfactor
TEMED	N,N,N,N-teramethylethylenediamine
TGF-β	Transforming Growth Factor-β

V

V	Volts
VillinCreER	VillinCrerecombinase ER transgene
v/v	Volume per Volume

W

W/B	Waterbath
w/v	Weight per Volume
WT	Wild Type
Wnt	Wingless-type murine mammarytumour virus Integration site family

X

x g	times gravity

Other

3HTdR	Tritiated Thymidine

Abstract

SWI/SNF chromatin remodelling complexes are one of the well-characterized cellular machineries capable of regulation of gene expression. Numerous lines of evidence indicate that SWI/SNF complexes are involved in a wide range of cellular processes and the maintenance of homeostasis whereas aberrant expression of those proteins contributes towards cancer development. Colorectal cancer remains one of the most clinically significant cancers due to its high incidence in developed countries and previous studies have demonstrated that SWI/SNF complexes are aberrantly regulated in a significant proportion of patients with this disease. However, whilst the sequence of molecular events leading to CRC has been well-established, the role of SWI/SNF chromatin remodelling complex ATPase subunits Brm and its paralogue Brg1 in the colorectal tumorigenesis remains elusive.

The chromatin remodelling catalytic subunit Brm has been found to interact with the Notch pathway effectors ICD-22 and CBF-1 and also to be necessary for expression of the Wnt target gene CD44 and for Rb-mediated cell cycle arrest. In this PhD thesis, the potential of Brm to modulate Wnt-driven intestinal tumorigenesis was addressed. Initially, a murine model carrying constitutively deleted Brm was used to assess the consequences of this loss on homeostasis of the small intestinal and colonic epithelia. The effects of Brm deficiency were also examined in the context of Wnt-activated epithelium via conditional loss of Apc. Additionally, the effect of concomitant loss of Brm and Brg1 was addressed in the contexts of both normal homeostasis and aberrant Wnt signalling.

The results presented here demonstrate that Brm plays an important role in the small intestine by regulating the distribution of proliferating cells and cell fate decisions mediated through Notch pathway effectors. Furthermore, Brm deficiency was found to modulate intestinal phenotype of Wnt activation through the attenuation of the Wnt transcriptional programme and the suppressed expression of the intestinal stem cell marker Olfm4. Thus while Brg1 has been widely characterized as a *bone fide* tumour suppressor, the function of Brm continues to remain elusive especially in the light of contrasting effects co-mediated by Brm on proliferation, differentiation and gene expression.

Taken together, these results elucidate the tissue-specific role of Brm, the catalytic subunit of SWI/SNF chromatin remodelling complex, on both normal intestinal homeostasis and acute activation of Wnt pathway while the extent of these Brm-dependent effects depend upon the gradient of Wnt signalling throughout the epithelium of small and large intestine.

Chapter 1
General introduction

1.1 The Mammalian intestines

1.1.1 Anatomy and functions of gastrointestinal tract

The human digestive tract is a central part of the digestive system where different elements of this tract have some distinct functions assigned. The main function of the digestive tract is to convert the consumed food into the basic nutrients as it passes through its different parts, gets digested and absorbed in the form of elementary molecules. Gastrointestinal tract is the largest part of the digestive tract and consists of the stomach and the intestines (Figure 1.1).

Stomach primarily functions as storage and mixing chamber as the body of the stomach consists of series of ridges called rugae which are produced by numerous folds that can stretch in and therefore allow the expansion of the stomach volume upon the entry of the food. Once the food enters this compartment of the digestive tract, it is mixed with stomach secretions to form chyme which also undergoes some initial and very limited digestion and absorption. The gastric glands of stomach epithelium secrete hydrochloric acid, digestive enzymes such as pepsinogen and mucus that provides the lubrication and protects the stomach mucosa from damage by acidic chyme and digestive enzymes. Three muscular layers within the stomach enable the mixing of its contents and help with the movement of those partially digested gastric contents into the intestine where the majority of digestion and absorption occurs (Seeley *et al.*, 2002). The intestine is divided into two major parts: the small intestine and the large intestine, each organised into smaller compartments. The small intestine consists of the duodenum, the jejum, and the ileum. All three parts of small intestine can be characterized by similar organization (Figure 1.2) with some exceptions to duodenum where Brunner glands are present in the submucosa and two papillae through which the duodenal lumen receives the secretions from bile duct and pancreatic duct.

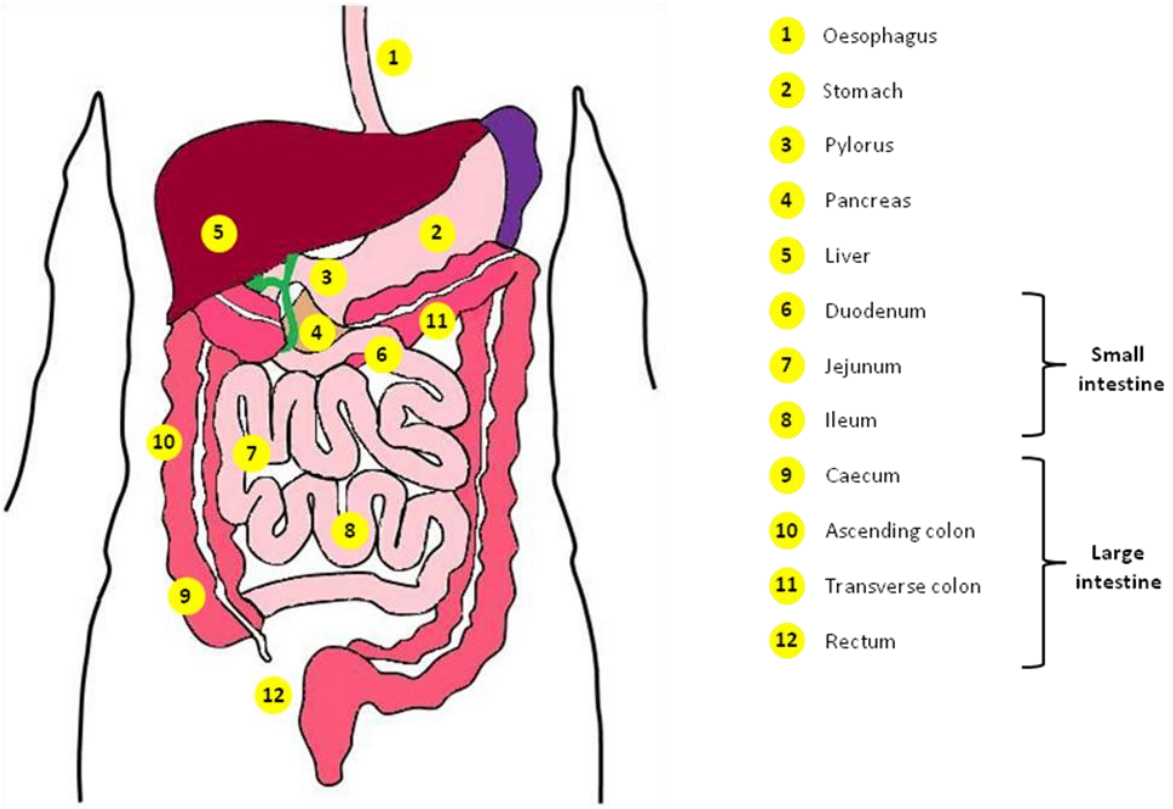

Figure 1.1 The basic anatomy of gastrointestinal tract consisting of small and large intestine supported in their function by multiple glands. Both small and large intestine can be further subdivided into three sections that bear some structural differences as well as minor changes in pH.

Those four histologically different layers are serosa, muscularis, submucosa and mucosa and they are present within the length of gastrointestinal tract from the esophagus to the anus. The outermost layer, serosa consists of a connective tissue and simple squamous epithelium that is lining the abdominal cavity. The next underlying layer is muscularis which is represented by longitudinal smooth muscle and circular smooth muscle. The myenteric plexus, a network of nerve cells lays between those two muscle layers and it is responsible for controlling the motility of the gastrointestinal tract. A layer of connective tissue containing blood and lymphatic vessels and nerves, the submucosa, provides the support for the innermost layer of mucosa as well as connection between mucosa and muscularis due to the presence of the submucosal plexus. The submucosal plexus and myenteric plexus together form the enteric nervous system which plays a crucial role in the secretion and movement control within gastrointestinal tract. The mucosa surrounding the lumen of the gut is composed of three distinct layers: a thin layer of smooth muscle - muscularis mucosae, loose connective tissue called lamina propria and mucous epithelium. This epithelium differs from that of the esophagus which is stratified, squamous epithelium as in the intestine it is represented by simple columnar epithelium specialized for absorption. The lymphatic nodules in the mucosa

and submucosa of ileum called Payer's patches protect the intestine as they trigger the immune responses against microorganisms.

The surface of the small intestine can be greatly enhanced about 600-fold by the presence of specific histological structures that allow for the most efficient digestion and absorption of the passing chyme. First of those are plicae ciculares, a series of folds formed within the mucosa and submucosa that run perpendicularly to the intestinal axis. Furthermore, the mucosa forms long finger-like projections covered by simple columnar epithelium that are protruding into the lumen called villi. As the small intestine is traced towards the ileum, the number of those circular folds, the density and the length of the villi decrease gradually. At the base of the villi, the epithelium produces the pocket-like tubular invaginations into the lamina propria termed crypts of Lieberkuhn. Lastly, the majority of the cells that cover the surface of the villus possess numerous cytoplasmic extensions termed microvilli that enhance the surface for digestion and absorption even further.

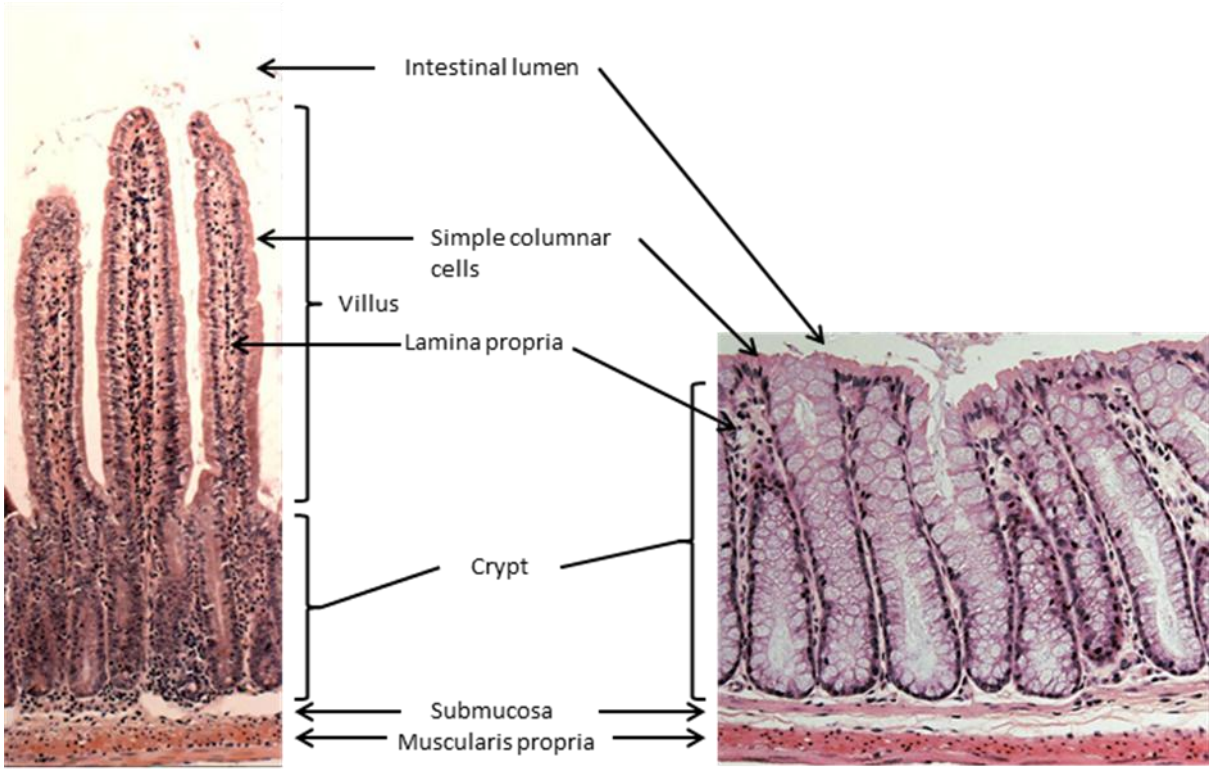

Figure 1.2 Histology of small and large intestinal epithelium including the underlying layers of tissue. The small intestine consists of finger-like projections into the lumen called villi and invaginations called crypts. The large intestine is made up of single layer of epithelial cells similarly to small intestine, however those cells form a flat surface of epithelium with no villi.

The small intestine possesses a variety of functions the most important of which include the digestion and absorption. As the acidic chyme is entering the duodenum from the stomach, it is neutralized by bicarbonate ions from pancreas and bile from the liver. This produces the pH conditions suitable for further digestion of passing chyme by pancreatic and intestinal enzymes. Those final stages of the breakdown of the food molecules are achieved mostly by the enzymes entering the small intestine from pancreas with the aid of intestinal enzymes bound to the membranes of the microvilli. Although the latter are exclusively associated with epithelium surface, it is indeed due to the extremely large surface area of the intestinal epithelium that they are able to perform their digestive function so efficiently. Once the digestion of food is completed, the absorption of the majority of the nutrients, water and electrolytes occurs through the microvilli in the duodenum and jejum of the small intestine, whereas the remainder is absorbed in the large intestine.

The large intestine can be subdivided into caecum, colon, rectum and anal canal where the colon constitutes the major part of the large intestine. The absorption of the remaining water and salts from the chyme occurs in the proximal part of the colon as the chyme is converted further into faeces.

The mucosa in the colon bears some crucial differences from that of small intestine as it lacks plicae ciculares and villi in the epithelium (Figure 1.2). The crypts similar to those found in the small intestinal mucosa are also present in the colon however the most apparent is the change in major populations of cell types present in the epithelium. The predominant cell population in the colon are mucus secreting cells whereas in the small intestine the majority of the cells are absorptive cells. This shift in the cell type abundance correlates closely with the main functions conducted by small and large intestine.

1.1.2 Micro-architecture of small intestinal epithelium

As mentioned in the previous section, gastrointestinal tract is comprised of different parts and each of those possesses specific functions including digestion, absorption or protection which are supported and accomplished by cells of multiple lineages localised within the epithelium. In the intestinal epithelium those cells are arranged in crypt-villus structures that run along the vertical axis of the gut lumen. The intestinal crypts are compartments at the base of which intestinal stem cells are localised, whereas above we can find originating from those stem cells highly proliferative cell progenitors. Progenitor cells create a transit-amplifying zone within the crypt where cells undergo few rounds of cell division as well as initial stages of the

differentiation that determine their cell fate. As those incompletely differentiated progenitor cells migrate towards the crypt-villus junction they steadily begin to lose their proliferative capacities and differentiate towards one of two differentiated cell lineages that populate the villi. Fully differentiated cells are continuing to migrate upwards towards the tip of the villi, once there they undergo the apoptosis and are shed into the gut lumen (Gregorieff *et al.*, 2005). This migration pattern is followed by all mature cells of intestinal epithelium with exception of Paneth cells that in contrast upon differentiation migrate towards the base of the intestinal crypt. The progenitor cells are actively dividing producing on the daily basis around 200 cells per crypt and upon the differentiation they continue to migrate towards the tip of the villus, fundamentally all fully differentiated cells of intestinal epithelium are renewed every 5 days in humans (Figure 1.3) (Marshman *et al.*, 2002).

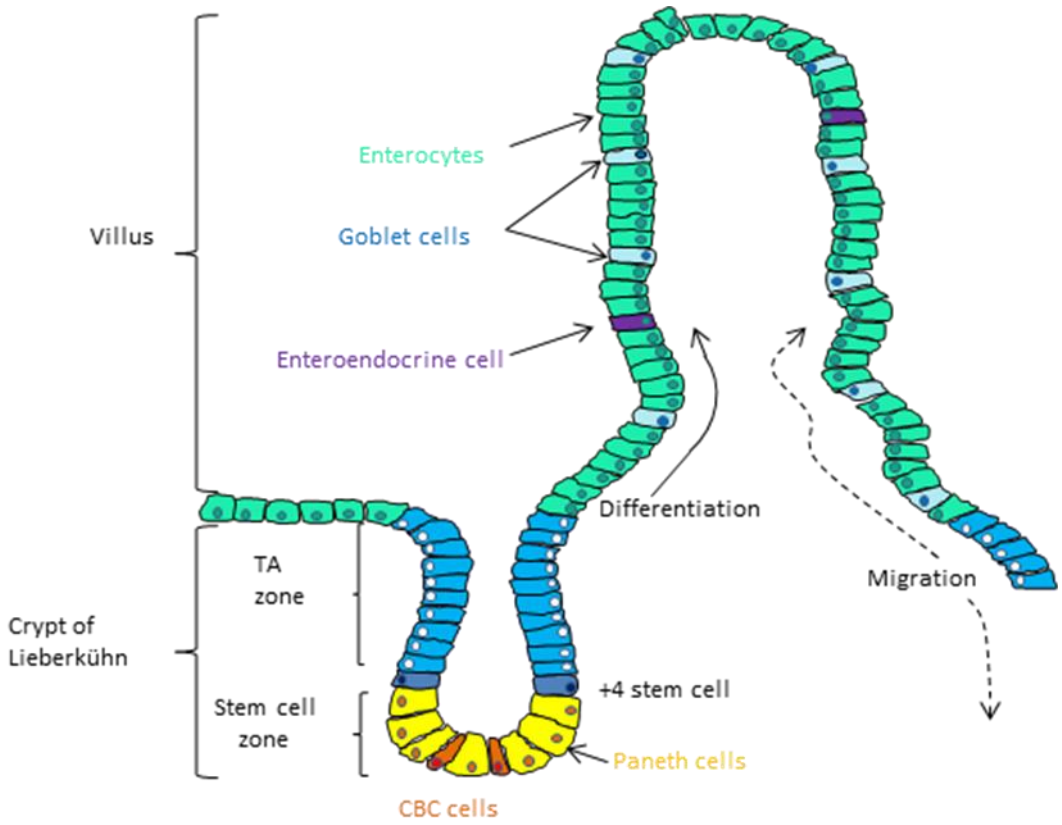

Figure 1.3 The epithelial cell lining of small intestine forms invaginations into the mucosa and finger-like projections into the gut lumen and consists of numerous cell populations. Intestinal stem cell and Paneth cells are located at the bottom of the crypt escaping the general trend of upward migration. Other differentiated cell types reside along the length of villus migrating upward and eventually being shed off the villus tip.

We can distinguish between four major epithelial cells types that can be divided into two distinct lineages: absorptive or secretory lineage. Absorptive lineage consists of enterocytes

while Paneth, goblet and enteroendocrine cells belong to secretory lineage. Whereas the epithelium of small intestine comprises of all four main differentiated cells (notably, enterocytes, goblet, Paneth and enteroendocrine cells), the colonic epithelium consists of mostly the absorptive enterocytes and goblet cells.

The vast majority of the differentiated cells within intestinal epithelium are enterocytes. Enterocytes represents more than 80% of all intestinal epithelial cells and they are present in the top part of the crypt compartment and all along the length of the villus. The main characteristic of enterocytes is the presence of the microvilli on their surface whereas the combined microvilli of all epithelial surfaces form a brush border. In contrast to secretory lineage cells, absorptive enterocytes do not contain secretory granules. Instead the brush border membrane vesicles contain multiple hydrolases that function to aid the final breakdown of complex molecules such as peptides and disaccharides into simple compounds that can be absorbed. The transporter proteins within apical and basolateral membranes actively transport various ions and nutrients from the lumen to the blood capillaries (Smith 1985). Furthermore enterocytes can be distinguished from other three mature cell types of intestinal epithelium by the expression of intestinal alkaline phosphatase which functions as a marker for fully differentiated enterocytes. Alkaline phosphatase (AP) activity is not present in the stomach with the highest levels detected within brush border membrane of the duodenum and substantially decreasing towards the large intestine (Hinnebusch *et al.*, 2003).

Amongst the mature cell types of secretory lineage, goblet cells are the most abundant cells of epithelium with the numbers of cells varying between different parts of the gastrointestinal tract. Goblet cells are localized in between enterocytes from top half of the crypt all the way upwards to the tip of the villus and similarly to enterocytes they are renewed every 3 days. Those cells contain of large granules that are filled with mucin and large endoplasmic reticulum. Goblet cells produce a protective mucous lining that lubricates the intestinal wall in order to facilitate the passing of food, prevents the injury from the acidic chyme as well as autodigestion by digestive enzymes.

Another secretory lineage cell type is represented by enteroendocrine cells. Although these cells are very rare within the small intestinal epithelium accounting for less than 1% of all differentiated cells amongst themselves they can be subdivided into 15 distinct cell types according to the morphology of their granules, the type of secretory product, the expression of the specific marker molecule and their capacity for expressing particular transgenes. This

highly heterogeneous population of cells shares one common function which is the expression and secretion of hormones including serotonin, secretin, substance P, cholecystokinin, gastric inhibitory polypeptide, neuropeptide Y and many others (Hocker and Wiedenmann 1998).

As mentioned before, the last cell type belonging to the secretory lineage as well as the only where instead of migrating up towards the tip of villus cells are migrating towards the crypt base is Paneth cells. Within the secretory lineage, they are the second most abundant cell type after goblet cells in the intestinal epithelium and in comparison to other 3 cell types they have much longer lifespan. The Paneth cell turnover has been extensively investigated in the past by injection of [^{3}H]-thymidine labelling agent that is allowed to be incorporated into the nuclei of cells actively synthesizing DNA showing that Paneth cells whose nuclei contain the label are present at 18-22 days post-injection (Cheng 1969) and at 29 days post injection (Troughton and Trier 1969). Nevertheless both groups have confirmed that Paneth cells do not possess proliferative capacities. Most recently, a new method exploiting a distinct ability of progenitor cells but not Paneth cells to express inducible AhCre transgene and furthermore to express Cre-activated the enhanced yellow fluorescent protein (EYFP) was applied to determine the life span of Paneth cells. Ireland *et al.* (2005) found that contrary to previous data published, Paneth cells are capable of surviving up to 57 days meaning their turnover is 19 times longer than that of any other differentiated cell type of the intestinal epithelium. As other cells of secretory lineage, one of the crucial features of Paneth cells is the presence in abundance of well-pronounced secretory granules in the apical cytoplasm (Troughton and Trier 1969). The protective function of Paneth cells against the bacteria is indeed achieved through the presence of various antimicrobial substances in their granules. Fully differentiated Paneth cells secrete antimicrobial peptides (AMP) α-defensins (cryptdins in mice) and enzymes such as lysozyme and phospholipase A2 type IIA that are specifically targeting the bacterial cell walls (Keshav *et al.*, 2006, Ouellette *et al.*, 2005). Other components of granules, notably immunoglobulin IgA, secretory leukocyte inhibitor and pancreatitis-associated protein may be involved in supporting AMPs in fighting the intestinal inflammation (Porter *et al.*, 2002). Consequently, Paneth cells play a central role in the intestinal immunity and may as well contribute towards the immunopathology. The recent data also suggests that Paneth cells are necessary in maintaining the intestinal stem cell niche (Sato *et al.*, 2010) with this particular aspect discussed in more detail in later sections of this PhD thesis.

With the exception of the above mentioned four main differentiated cell types, two small populations of cells can be found in the small intestinal epithelium. M (microfold) cells are very distinct epithelial cells present in the follicle-associated epithelium, adjacent to Peyer's patches. In contrast to enterocytes, M cells do not possess microvilli but instead they can be characterized by the presence of the microfolds on their apical surface. They are capable of the uptake and transporting of microorganisms and foreign antigens from the lumen of the gut, across the epithelium by transcytosis (endo- or phagocytosis). Upon the delivery to the basolateral memebrane, those antigens are presented to dendritic cells and B and T lymphocytes within the lymphoid tissues. The mechanism of functioning of M cells is believed to act as an antigen sampling system and therefore very important in inducing an immune response within the intestinal epithelium (Kraehenbuhl *et al.,* 2000, Kucharzik *et al.,* 2000). Tuft cells (also known as brush, caveolated or fibrillovesicular cells) are present throughout the organs of digestive and respiratory tract and comprise up to 0.4% of the epithelial cells in ileum (Gerbe *et al.,* 2012). They can be characterized by goblet-like shape, shorter than enterocytes and blunt brush border associated with much weaker alkaline phosphatase activity and multiple vesicles in the apical cytoplasm (Sato 2007). Since their discovery in 1956 in both trachea and glandular stomach (Järvi and Keyrilainen 1956) the origin, differentiation and functions of tuft cells have not been unveiled yet. Some of existing data suggests they may be playing role in secretion or absorption or function as chemoreceptors and until the determination of their differentiation and specification their principal function and the relationship with other cells of intestinal epithelium remain undefined (Gerbe *et al.,* 2012, Sato *et al.,* 2007).

1.1.2.1 Stem cell niche and identity

Considering that the rate of renewal of cells within the intestinal epithelium where nearly all differentiated cell types (with exception to Paneth cells) are replaced every few days, the maintenance of renewal rate requires tightly regulated stem cell activity. In the context of adult organism, stem cells are defined as undifferentiated cells that maintained their capacity for long-term self-renewal as well as multipotency to generate several particular cell types (Siminovitch and Axelrad, 1963).

In the absence of discreet set of intestinal stem cell markers, the identification of stem cells within the intestinal crypts has been a subject of large debate in the field.

Nearly four decades ago Potten *et al.* (1974) performed tritated thymidine- ^{3}HTdR-labelling of intestinal epithelium incorporates into DNA during S phase of cell cycle and identified a population of slowly cycling cells located at the +4 cell position in regards to the crypt base. Interestingly, these cells were found directly above Paneth cells and further experiments utilizing irradiation as means to stem cell expansion revealed that ^{3}HTdR label was incorporated into the DNA of +4 stem cells that underwent regeneration and the label was retained for more than one week (Potten 1974, 1978). The most recent data from the same group further confirms previous results showing that labelling of intestinal epithelium post-irradiation using both ^{3}HTdR and BrdU detected a population of cells that were double-labelled with one template DNA stand carrying ^{3}HTdR label whereas the daughter stand incorporated BrdU (Potten *et al.* 2002). The localisation of intestinal stem cells at the +4 position in the epithelium resulted in the identification of numerous potential stem cell markers expressed specifically in that area of crypt including Musashi-1 however further studies indicated that Musashi-1 is not limited to +4 cells but also to CBC and early progenitor cells negating its use as stem cell marker (Potten *et al.* 2003). Bmi-1 (polycomb ring finger oncogene) was amongst other potential stem cell markers found to be expressed in the +4 cells. Linage tracing with inducible Bmi1-CreER in the small intestinal epithelium found that Bmi1^{+} cells were located predominantly at +4 position. This notion together with a finding that a single Bmi1^{+} cell can generate 3D organoid structures *in vitro* highlight the "+4 position" cells as intestinal stem cell niche (Sangiorgi and Capecchi, 2008). DCAMKL-1 (doublecortin and calcium/calmodulin-dependent protein kinase-like-1) was another stem cell marker that showed expression around +4 position however it was also found expressed in some differentiated cells of villus as well as being co-expressed with tuft cells markers (May *et al.* 2008, Gerbe *et al.* 2009). A well-known hematopoietic stem cell marker CD133 (Prominin 1 in mice) was also proposed as intestinal stem cell marker as Prom1 was found to be expressed exclusively within CBC cells (Zhu et al., 2009) in contrast to data from Snippert *et al.* (2009) suggesting that Prom1 expression is not restricted to CBC cells only and furthermore showing that reporter-labelled cells were removed from the intestinal epithelium in a short period of time suggesting Prom1 as a marker for progenitor cells as well as stem cells (Snippert *et al.* 2009). Throughout the decades of experiments investigating stem cells of intestinal epithelium, numerous novel markers specifically expressed at +4 position were identified such as Hopx homeobox protein (Takeda *et al*., 2011), mTert (mouse telomerase reverse transcriptase) (Montgomery *et al.*, 2011) and Lrig1 (pan-ErbB inhibitor) (Powell *et al.*, 2012) marking long-lived, slow-cycling and label-retaining cells at +4 position.

In the context of the downward migration of Paneth cells towards the crypt base which generates two differential migration gradients that originate directly above Paneth cells, it is plausible that intestinal stem cells niche can be found at the crypt base neighbouring with Paneth cells (Cairnie *et al.,* 1965). As alternative to +4 stem cell theory, crypt-base columnar cells (CBC) cells found between Paneth cells at the crypt base were proposed as intestinal stem cells. They have been characterized as being undifferentiated cell type that is multipotent and capable of generating all differentiated cell types of epithelium and sensitive to irradiation as ^{3}HTdR labelling prior to irradiation showed that some CBC cells became phagocytosed by neighbouring CBC cells and those ^{3}HTdR-labelled phagosomes were detected later in mature epithelial cell types suggesting they are the progeny of phagocytosed CBC cells (Cheng and Leblond 1974). This notion indicating CBC cells as potential intestinal stem cells have been overlooked for decades at the cost of "+4 stem cell" model however most recent studies have provided the field with new evidence in support of this notion. Lineage tracing in murine intestinal epithelium found that CBC cell expressing leucine-rich repeat-containing G-protein coupled receptor 5 (Lgr5) were actively cycling and displayed a multipotency potential in a long-term study (Barker *et al.,* 2007). Moreover the isolation of Lgr5-positive cells and their culture *in vitro* in 3D matrix revealed they were capable of generating organoid structures (Sato *et al.,* 2009). Further characterization of Lgr5^{+} cells have implicated Ascl2 (Achaete scute-like 2) and Olfm4 (Olfactomedin-4) as additional stem cell markers that are exclusively co-expressed with Lgr5 in CBC cells (van der Flier *et al.,* 2009).

Taken together, extensive data from +4 position and CBC cell stem cell studies implicate the existence of two different pools of intestinal stem cells: quiescent stem cells located at the +4 position characterised by the presence of Bmi1 expression and actively cycling Lgr5^{+} CBC cells. Accordingly, each of those two populations of intestinal stem cells possess very particular but at the same time collaborative functions contributing towards a reciprocal back-up system that is capable of the maintenance of intestinal epithelium and its regeneration in case of the damage (Li and Clevers, 2010). Bmi1+ cells were previously shown to proliferate at a slower rate than Lgr5-expressing CBC cells which divide approximately once a day providing further evidence for the presence of two separate populations of intestinal stem cells (Baker *et al.* 2007, Sangiorgi and Capecci, 2008).

Despite this indications, the identification and nature of quiescent intestinal stem cells remains elusive as many studies failed to recapitulate the above findings using "+4 position"-specific stem cell markers. Recent study by Muñoz *et al.* (2012) showed that in Lgr5^{+} cells

Bmi1, Hopx, Tert and Lrig1 are found to be expressed at high levels in contrast to Lgr5^{-} cells in which no such enrichment was detected using transcriptome and proteomic analysis. These results are contrary to previous data obtained by Bmi1 lineage tracing experiments (Muñoz *et al.,* 2012).

In summary, the existence of population of quiescent stem cell pool cannot be excluded however the use of mentioned "+4 position" stem cell markers does not guarantee the correct identification of those cells. Furthermore, an alternative hypothesis exists suggesting that the transit-amplifying cells in close proximity to the stem cell niche might display plasticity and subsequently be capable of reverting to intestinal stem cell phenotype in order to support the regeneration process in case of damage (Cheng and Leblond 1974, Potten *et al.* 1974).

1.1.3 The homeostasis in the intestinal epithelium

As a majority of functions performed by the intestinal epithelium of gastrointestinal tract relies on the continuous renewal of the intestinal epithelium it requires very strict and coordinated regulation to maintain the balance between proliferation and differentiation of epithelial stem cells and immature progenitor cells in order to preserve this unique multicellular tissue architecture. The maintenance of the homeostasis is based on three principal mechanisms, first of which involves the active proliferation dictated by the small population of the stem cells at the crypt base which safeguards the renewal of all epithelial surface. Secondly, the differentiation of newly produced cells along secretory or absorptive lineage ensures the right balance between cell numbers and enables them to perform their functions. Thirdly, the continuous migration of cells up the crypt-villus axis provides the means for the complete replenishment of epithelial cell layer as the cells are shed of the tip of the villus to accommodate newly produced cells within the crypt.

Therefore the maintenance of small intestinal homeostasis which involves numerous processes that control the structure as well as functions within intestinal epithelium is tightly coordinated by a network of signalling pathways including Wnt, Notch, Hedgehog, BMP, PDGF and TGFβ (Andrae *et al.,* 2008, Büller *et al.,* 2012, Clevers 2006, He *et al.,* 2004, Katoh and Katoh 2006, Karlsson *et al.,* 2000, Shi and Massague 2003). This section will briefly describe each of those pathways and its role in maintaining homeostasis in the small intestine.

1.1.3.1 Hedgehog and Platelet-derived growth factor pathways

The mesenchyme-to-epithelium signalling is governed by the Hedgehog and PDGF pathways whereas the other side of this interaction from mesenchyme to epithelium is dictated by TGF-β/BMP pathway (Sancho 2004). Within Hh pathway we can distinguish between three different transmembrane receptors: Smootherned (Smo), Patched (Ptch) and Hedgehog-interacting protein (HIP) present on the surface of hedgehog-responsive cells as well as three ligands that are paralogues: Sonic hedgehog (Shh), Indian hedgehog (Ihh) and Desert hedgehog (Dhh). Sonic Hh and Indian Hh are both expressed in the epithelium and play crucial role in formation of intestinal structures of crypts and villi.

In the absence of secreted Hh ligands, Ptch is believed to inhibit the Smo activity. The inactive form of Smo functions as an assembly core of a complex comprising of Costal-2 (Cos-2) and Fused (Fu) whereas Cos-2 binds several other molecules such as glycogen synthase kinase-3β (GSK3β), casein kinase 1α (CK1α) and protein kinase (PKA). This complex impounds Glioblastoma (Gli) transcription factors and targets them for proteasomal degradation. GLI family of zinc-finger transcription factors consists of Gli1, Gli2 and Gli3. Resulted from the proteasomal degradation truncated Gli2 and Gli3 proteins are not capable of transducing the Hh signal and therefore act as Hh suppressors. Upon the Hh ligand binding to the PTCH, its inhibitory action upon Smo is lifted and downstream signalling cascade blocks the formation of GLI destruction complex (Figure 1.4). The stabilisation and translocation of GLI transcription factors from cytoplasm into the nucleus triggers the transcription and expression of Hh target genes (reviewed in Sancho 2004, Katoh and Katoh 2006).

In the intestinal epithelium Gli2 and Gli3 are the major transducers of Hh signalling. In early development of mouse, the Hh ligands Shh and Ihh are both produced in the endodermal epithelium and play crucial role in controlling the cell fate specification processes. With time as the villi develop their expression becomes confined to proliferative crypt compartment whereas the expression of Hh receptors and effector molecules is strictly restricted to stromal cells. Inactivation of Ihh or Shh leads to the death of animals soon after birth restricting the possibilities to investigate the role of Hh signalling in stem cell renewal and normal intestinal homeostasis in adult mice. Moreover Ihh deficient mice display greatly reduced numbers of proliferating progenitor cells, decline in enteroendocrine cell differentiation and short villi. In contrast, $Shh^{-/-}$ animals can be characterized by the enlarged villi structures advocating for the

opposite phenotype and in turn, increased proliferation levels (Ramalho-Santos 2000). These results suggest that Ihh and Shh each possess a specific role within the intestinal epithelium although they are expressed in the same compartments. Inhibition of Hh signalling using Hhip hedgehog interacting protein is capable of blocking both Hh ligands and was conducted in tissue-specific manner being restricted to the intestine. The high expression of Hhip leads to significantly increased rates of proliferation and complete abrogation of villi structures. However the lower expression levels of Hhip are capable of inducing a milder phenotype that includes the formation of abnormal villi containing crypt-like structures near their tips as well as presence of ectopic sites of Wnt activation through Tcf4/β-catenin target gene enhancement and increased proliferation. These results have led Madison and his lab to hypothesis that Shh and Ihh are both released in the crypt compartment of intestinal epithelium and Hh signalling is paracrine from the epithelium surface to myofibroblasts and smooth muscle cells successively controls the patterning along crypt-villus axis safeguarding the correct size and localization of newly arising crypt compartments (Madison *et al.,* 2005).

Platelet-derived growth factor (PDGF) pathway is another signalling pathway that governs the epithelium-to-mesenchyme interactions. This signalling network consists of four ligands: PDGF-A, PDGF-B, PDGF-C and PDGF-D that are capable of binding receptor tyrosine kinases, PDGFR-α and PDGFR-β. Upon the activation of PDGF signalling, these receptors form dimers and undergo phosphorylation which enables the signal transduction through numerous pathways such as phosphatidylinositol 3-kinase (PI3K/Akt), signal transducer and activator of transcription (STAT) and Mitogen-activated protein kinase (MAPK) (reviewed in Andrae *et al*,. 2008).

Mice deficient of PDGF-A or PDGFR-α develop villi that are aberrant in their shape and present at much lower density within the epithelium as well as loss of pericryptal mesenchyme (Karlsson *et al.,* 2000). The theory explaining the abnormal villus patterning suggested that PDGF-A expression from epithelial cells maintains the self-renewal and proliferation of PDGFR-α positive mesenchymal cells thus preventing their premature differentiation and depletion (Karlsson *et al.,* 2000). Those PDGFR-α positive cells are clustering into “villus clusters” supporting the morphogenesis of villi therefore the inability to form those clusters results in decrease in villi numbers.

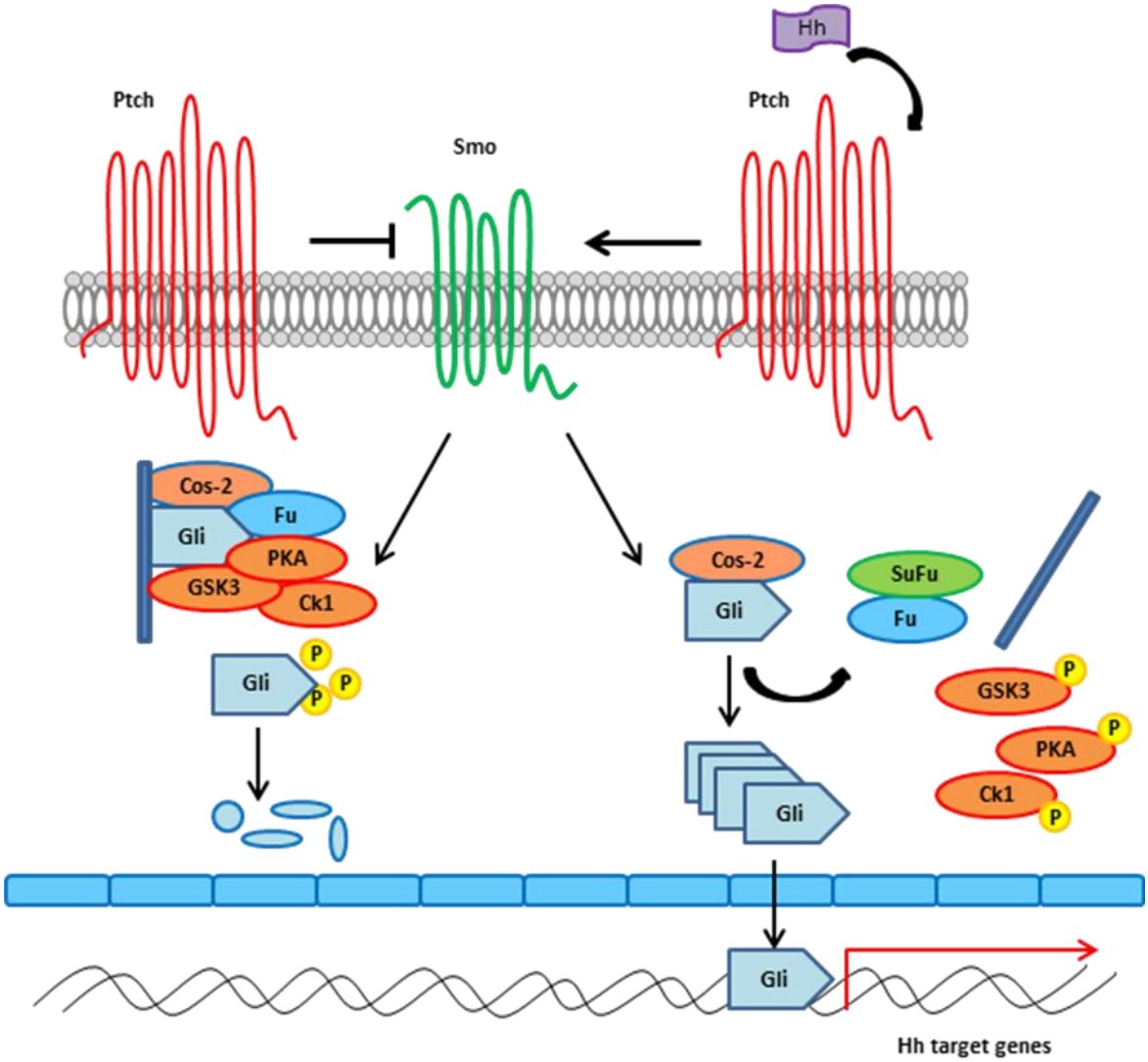

Figure 1.4 Hedgehog is one of the major pathway playing role in the maintenance of intestinal homeostasis and represents epithelium-to-mesenchyme signalling with Ptch playing a dual role in the signal transduction.

1.1.3.2 TGF-β and BMP pathways

TGF-β signalling pathway regulates the abundance of the processes such as embryonic development, angiogenesis, proliferation and differentiation (Shi and Massague 2003) and mediates the mesenchyme-to-epithelium signalling. TGF-β family of cytokines comprises of TGF-β, bone morphogenetic protein (BMP) and activins molecules which are all ligands for type I and type II serine-threonine kinase receptors. TGF-β signalling also possesses a wide range of SMAD intracellular messengers that can be subdivided into three different classes of molecules: receptor-regulated SMADs (R-Smads: Smad1, 2, 3, 5 and 8), co-mediator SMAD (Smad 4) and inhibitory SMADs (I-Smads: Smad6 and 7).

The binding of ligands to type I and type II kinase receptors leads to colocalisation of those two types of receptors allowing type II receptor of phosphorylating the type I receptor and therefore activating the signalling cascade. Further phosphorylation of R-Smads through the action of activated type I receptor results in the formation of heterodimeric complex consisting of R-Smads and Co-Smad, Smad4 which together translocate to the nucleus. Once within the nucleus, Smad complex regulates the expression of TGF-β target genes. Although this mechanism of pathway activation is common for all cytokines members of TGF-β family, some preferential binding exists between the ligands and particular Smads where TGF-β ligands signal through Smad2 and 3 however BMP ligands through Smad3, 5 and 8. The inhibition of TGF-β pathway occurs via the association of I-Smads with kinase receptors as they are competing for receptor binding with R-Smads (Figure 1.5).

The majority of the TGF-β family members are expressed non-epithelial parts of the gut notably lamina propria and muscularis with some restricted expression of some of the Smads in villi of small intestine. No expression of TGF-β molecules is detected in the crypt compartments of either small or large intestine (Winesett *et al.,* 1996). In particular, BMP2 and BMP4 ligands are found to be expressed in the intravillus mesenchyme being positively regulated by the Hh pathway (Madison *et al.,* 2005). Other BMPs such as BMP receptor Bmpr1a and Smads: Smad1, 5 and 8 are expressed in the epithelial cells of villi (Karlsson *et al.,* 2000). Loss of Bmpr1a in the intestinal epithelium disturbs the intestinal homeostasis causing an expansion of the stem and progenitor cell populations leading to the intestinal phenotype including development of multiple polyps resembling that of human juvenile polyposis syndrome (He *et al.,* 2004). Noggin is an inhibitor of BMP pathway expressed in the submucosa surrounding the crypt compartment (Figure 1.8) abrogating the signalling from mesenchyme (He *et al.,* 2004). Overexpression of Noggin results in development of ectopic crypts on the sides of villi (Haramis *et al.,* 2004) suggesting that both loss of Bmpr1a and overexpression of Noggin lead to similar phenotype consisting of excessive formation of abnormal structures closely resembling intestinal crypts and development of polyps with enlarged proliferative compartment.

These results indicate the importance of BMP signalling in controlling the proliferation of continuously self-renewing intestinal epithelium. The proliferation of stem and progenitor cells is restricted to the crypt compartment by the presence of Noggin in the inter-villus zone. Moreover the BMP signals from stroma underlying the epithelial cell layer of villi are inhibiting proliferation in that region halting the ectopic formation of crypt-like structures.

The mismanagement of crypt fission and excessive formation of intestinal crypts is repressed by active BMP signalling.

In all the expression patterns of different elements of BMP and Hh signalling contribute towards explaining crypt-villus organisation of intestinal epithelium. From the epithelial layer Hh signals are released influence underlying mesenchyme layer which consecutively releases BMP ligands.

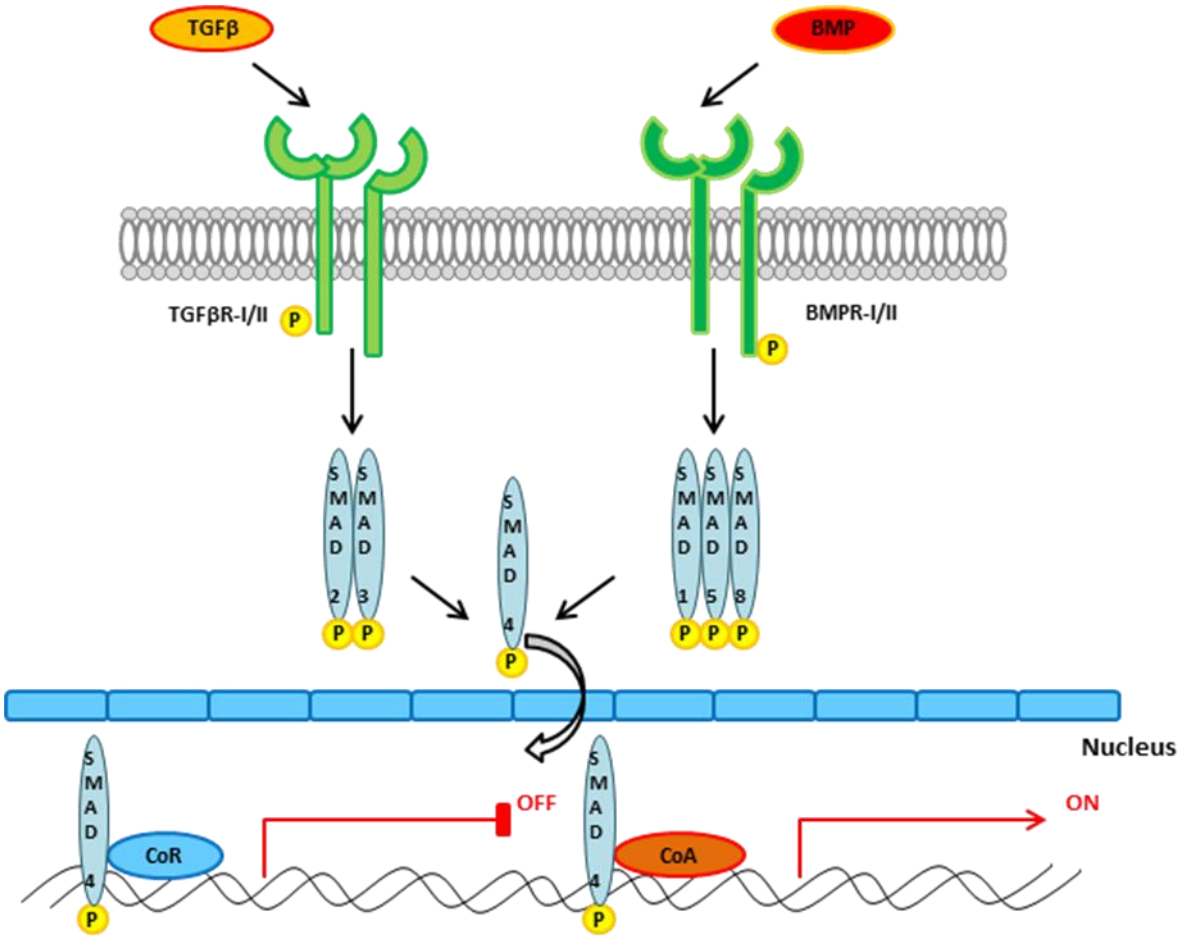

Figure 1.5 TGF-β and BMP pathways together with Hedgehog pathway regulate activation of Wnt signalling and intestinal homeostasis acting through their common co-effector SMAD4.

1.1.3.3 Wnt pathway

One of the most important pathways that conveys the maintenance of the intestines is Wnt signalling (Figure 1.6). This pathway has been implicated in a wide spectrum of cellular processes being one of the fundamental signalling pathways in development and disease and has been extensively investigated over the last 30 years (Nusse and Varmus 2012, Reya and

Clevers 2005). Wnt ligands and its downstream effectors were first discovered in *Drosophila* and Wnt ligands and downstream effectors of the Wnt pathway are conserved within the animal kingdom (Rijsewijk *et al.,* 1987). Wnt signaling is playing a central role in embryonic development especially in body patterning and formation of anterior-posterior axis. It is also involved in the maintenance of homeostasis and self-renewal processes in various adult tissues and therefore in many pathological events that result from disturbance of this state (reviewed in Clevers 2006). In normal circumstances within intestinal epithelium Wnt signalling regulates proliferation within the intestinal crypt (Muncan *et al.,* 2006, Pinto 2003), differentiation of progenitor cells towards secretory lineage (Andreu *et al.,* 2005, Pinto 2003) as well as controls spatial segregation of cell populations via Eph/ephrin receptor-ligand system (Batlle 2002). Equally Wnt signalling is also a major pathway involved in intestinal tumorigenesis and colorectal cancer.

The family of Wnt genes consists of 19 cysteine-rich glycoprotein members in humans and mice. In order to render those Wnts biologically active the palmitoylation of a conserved cysteine residue is required during their production and secretion (Willert *et al.,* 2003).
Upon their release into the intracellular space, Wnts activate responding cells by interacting with Frizzled (Fz) receptor transmembrane proteins and single-span LRP5/6 receptor protein. The binding of Wnts to Frizzled and LRP5/6 proteins is an initial step in canonical Wnt pathway and involves a cascade of events that changes the amount of β-catenin present in nucleus.

The phosphorylation of the cytoplasmic domain of LPR5/6 upon the binding between Wnt, Fz and LPR5/6, aided by Fz-bound Dishevelled (Dsh) leads to the recruitment of Axin to the plasma membrane. Subsequently Axin becomes degraded and dissociated from β-catenin "destruction complex" which disturbs the integrity of the complex and non-phosphorylated β-catenin accumulates in the cytoplasm. This stabilized form of β-catenin then further translocated into the nucleus. Once in the nucleus, β-catenin binds to TCF/ LEF transcription factors which converts TCF/LEF factors from repressors into activators, thus activating the transcription of downstream Wnt target genes.
In the absence of Wnt ligand, cytoplasmic pool of β-catenin is sequestered by the "destruction complex". This "destruction complex" comprises of two scaffolding proteins APC and Axin that bind synthesized β-catenin. CK1 phosphorylates the N-terminus of β-catenin at the Ser45 residue and further action of GSK3β kinase drives the phosphorylation of

serine and threonine residues at N terminus of β-catenin. This pattern of phosphorylation of β-catenin recruits β-TrCP ligase and β-catenin is ubiquitinated. Once ubiquitinated, β-catenin is targeted for degradation by proteasome machinery (Figure 1.6) (Reya and Clevers 2005, Ricci-Vitiani *et al.,* 2009).

In case of cells that are not responding to Wnt signals, Tcf proteins associate with general transcription repressors like Groucho and this binding result in the repression of Tcf-responsive genes. This form of silencing is achieved by recruitment of histone deacetylases (HDACs) that transform the chromatin structure into form that is inaccessible for transcription machinery. Upon the activation of Wnt signalling and binding of β-catenin to Tcf proteins, it displaces the Groucho and recruits numerous nuclear factors that are capable of transactivating Tcf target genes such as chromatin remodelling factors.

Wnt signalling is crucial for the maintenance of proliferation within crypt compartment

The extensive studies of Wnt signalling over the last decade have gathered strong line of evidence suggesting that Wnt signalling and β-catenin are necessary for the survival of the crypt proliferative population therefore aberrant Wnt signalling by its ablation inhibits the proliferation and by its activation expands the proliferative compartment of intestinal epithelium. The importance of particular elements of the Wnt pathway in the crypt homeostasis is emphasized by the severity of phenotype resulting from their abnormal expression.

Tissue-specific ablation of β-catenin in the small intestine leads to quickly progressing loss of cells of epithelium layer, including loss of crypt compartment and inhibition of proliferation. Moreover the loss of β-catenin disrupts the maintenance of homeostasis within the stem cell niche inducing stem cells to terminally differentiate and rendering them incapable of self-renewal and therefore disturbing normal functioning of small intestinal epithelium (Fevr *et al.,* 2007). Corresponding phenotype of loss of crypt compartment and increase in apoptosis was observed upon the conditional deletion of β-catenin under the expression of inducible *AhCre* promoter (Ireland 2005).

Disruption of both alleles of TCF-4 gene in the germline resulted in death of those animals shortly after birth due to their inability to maintain a proliferative stem cell compartment in the small intestinal epithelium (Korinek *et al.,* 1998). Similarly the inhibition of canonical Wnt pathway through the expression of Wnt inhibitor Dickkopf-1 (Dkk1) results in the levels of proliferation being significantly repressed together with disruption of normal intestinal architecture involving loss of crypt and villus structures (Kuhnert *et al.,* 2004).

Deletion of one of main Wnt target genes, c-myc in the small intestinal epithelium under the expression of the same transgene as Ireland et al (2005) resulted in reduction of the crypt length, significant decline in the proliferation rates and cell cycle progression in the progenitor cells. This triggers the response in the crypts that escaped the c-myc ablation that consequently repopulate the c-myc deficient crypts leading to their complete elimination from the epithelium of small intestine (Muncan *et al.,* 2006).

Wnt signalling directs progenitor cells towards the secretory lineage

Wnt signalling has been showed to be involved not only in the maintenance of proliferation in the crypt compartment of intestinal epithelium but also in regulation of cell fate decision of early progenitor cells. Specifically the Paneth cell differentiation is affected due to the fact that unlike other differentiated cell types of intestinal epithelium that migrate towards the tip of the villus, Paneth cells migrate down towards the crypt base where they remain throughout their lifespan. Moreover similarly to crypt proliferating cells they are characterized by the presence of active Wnt signalling and express high levels of nuclear β-catenin. Wnt signalling has been shown to drive the expression of Paneth-specific genes (van Es *et al.,* 2005) and ablation of β-catenin significantly reduced the numbers of Paneth cells as well as caused their mislocalisation. Dkk1 overexpression driving the inhibition of Wnt signalling results in the loss of cells belonging to all three secretory lineages however not affecting the enterocytes (Pinto 2003). Different studies found that the loss of β-catenin increases the differentiation of enterocytes (Fevr 2007).

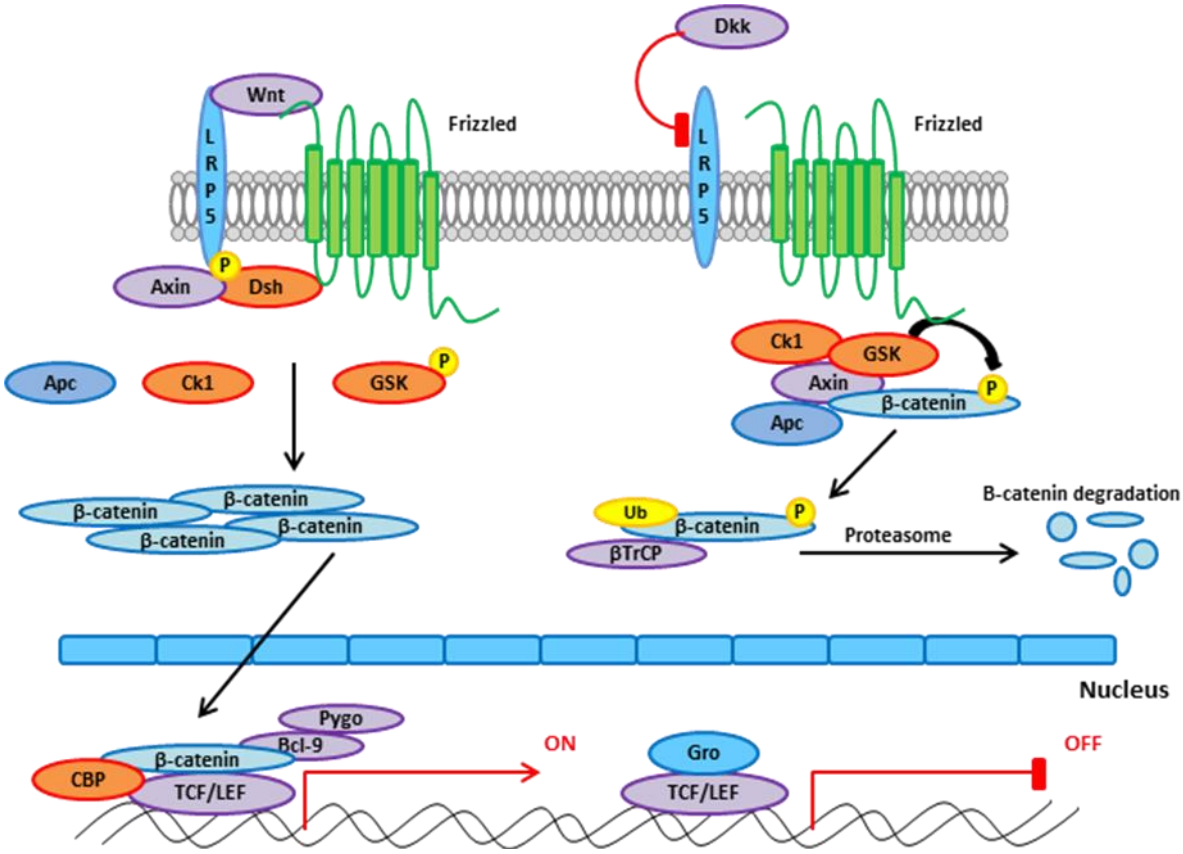

Figure 1.6 Wnt signalling pathway is responsible for the maintenance of intestinal homeostasis by regulating stem cell renewal and progenitor cell differentiation. In a normal cell, β-catenin degradation complex prevents the accumulation of β-catenin in the cytoplasm and active transcription of Wnt target genes.

1.1.3.4 Notch pathway

Notch pathway mediates cell-to-cell signal transduction due to the interactions between Notch receptors and ligands between the adjacent cells. Multiple biological functions are regulated by Notch including cell proliferation, apoptosis, spatial patterning and cell fate determination.

Mammalian Notch includes 4 receptors: Notch1, Notch2, Notch3 and Notch4 and 5 ligands: Delta-like 1, Delta-like 2, Delta-like 3, Jagged 1 and Jagged 2 and the association between each ligand and each receptor command different Notch response. Notch signalling receptors are evolutionary conserved large transmembrane glycoproteins that consist of two domains: extracellular domain (ECD) and intracellular domain (ICD). Initially, Notch receptor is synthesised as an inactive form that upon the cleavage by Furin protease at first cleavage site (S1) in the trans-Golgi produces Notch ICD and Notch ECD heterodimer at the cell surface.

Prior to the full integration into the cell membrane, both domains undergo O-glycosylation by Fringe and O-fucosylation by O-fucosyl transferase.

The binding between Notch ligands and Notch receptor triggers the activation of the Notch signalling as the two cleavage events of the receptor occur. The second cleavage site (S2) becomes exposed as a result of endocytosis action of E3 ligases and then cleaved by tumour necrosis factor-α-converting-enzyme (TACE) to release NECD. Consecutively, the final third cleavage (S3) is triggered and achieved by γ-secretase leading to release of NICD and its translocation into the nucleus. Within the nucleus, NICD forms a transcriptional complex with Notch mediator CSL (CBF-1/RBP-jκ) and Mastermind-like co-activator proteins that triggers the transcription of Notch target genes. In the absence of the Notch signalling, CSL acts as the repressor of the transcription (Figure 1.7).

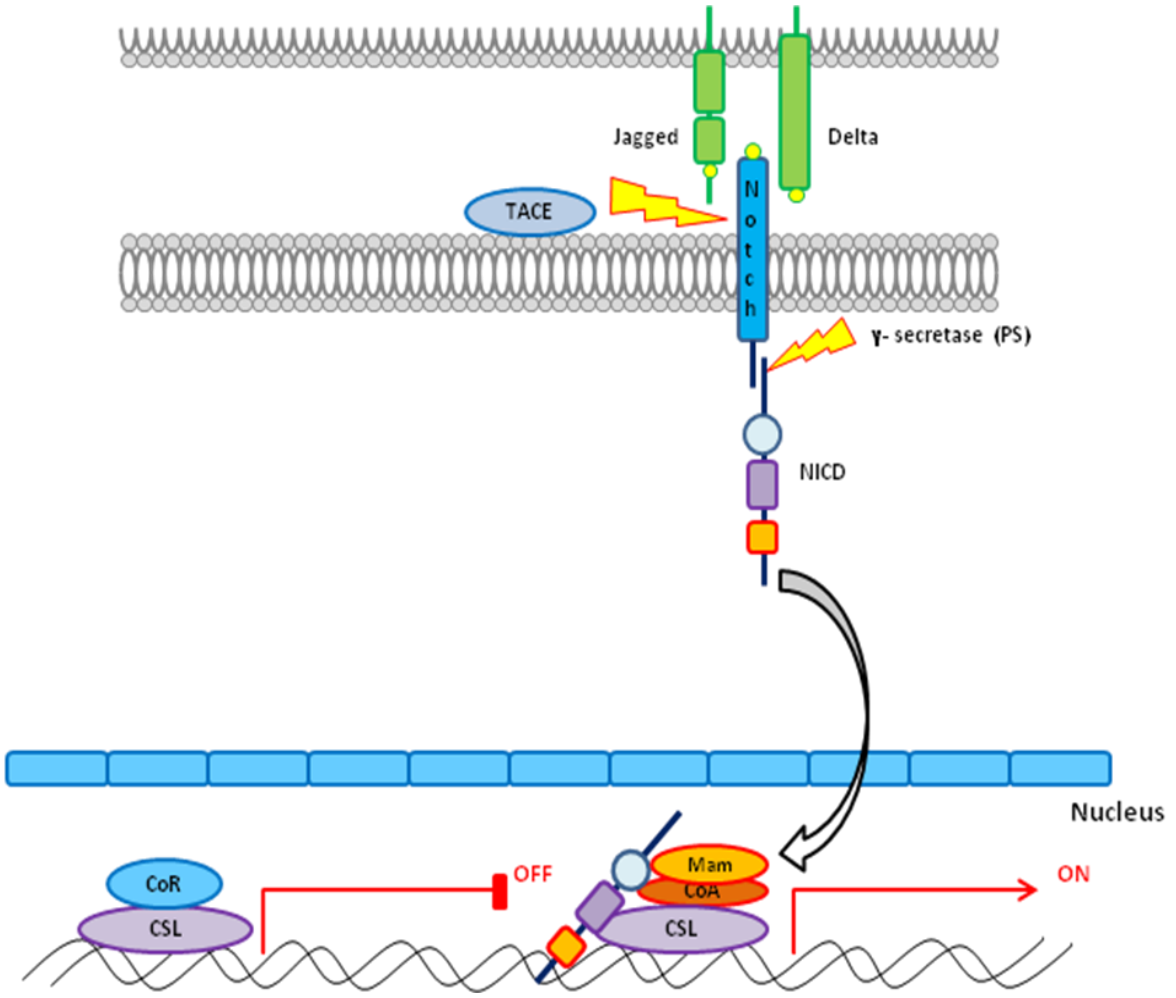

Figure 1.7 Notch signalling pathway represents cell-to-cell signalling within small intestinal epithelium and regulates cell fate decision of progenitor cells as they exit the crypt compartment.

In the intestinal epithelium Notch receptors and ligands are expressed in the crypt compartment of small intestine and colon (Sander *et al.,* 2004). Canonical Notch signalling to CSL-NICD-Mastermind complex inhibits the differentiation of stem cells and progenitor cells however in case of unnatural Notch ligands to the Notch receptor triggers non-canonical Notch signalling acting via CSL-NICD-Deltex complex. This non-canonical signalling unlike canonical Notch promotes the differentiation of progenitor cells by activation of the transcription of genes such as MAG that induce terminal differentiation of cells.

The best characterized Notch target is a large family of hairy enhancer of split (Hes) transcriptional repressors which in turn regulate the expression of many downstream Notch genes. Upon the activation of Notch signalling, Hes together with Hey family becomes upregulated and consequently inhibits the transcription of other downstream tissue-specific transcription factors such as Math1 leading to repression of differentiation and maintenance of stem and progenitor cells. Hes1 is normally promoting the differentiation towards the absorptive enterocyte lineage whereas loss of Hes1 shifts the cell fate determination leading to increase in goblet and enteroendocrine cell numbers (van Es *et al.,* 2005). Removal of CSL or similarly inhibition of Notch signalling via introduction of γ-secretase in the small intestinal epithelium results in the loss of proliferating crypts and concurrently immense changes in cell fate decisions as all proliferating cells turn into post-mitotic goblet cells (van Es *et al.,* 2005). Therefore it seems like the differentiation of cells towards secretory lineages in particular goblet cells is a default choice in the absence or Notch signalling deficiencies.

Mimicking the effects of the activation of Notch signalling is possible by gain-of-function studies involving Notch receptors. The activation of Notch receptor (Notch1 IC) under the expression of *Villin* promoter revealed the inhibition of cell differentiation into either absorptive or secretory lineage and most importantly in the expansion of immature intestinal progenitor cells (Fre *et al.,* 2005). As the upregulation of Notch signalling results in high Hes1 and thus Math1 inhibition the phenotype of Math1 deficient mice was investigated. $Math^{-/-}$ animals displayed normal intestinal architecture with a depletion of all differentiated cell types of secretory lineage but not affecting the differentiation of enterocytes. This is due to the fact that absorptive lineage enterocytes arise from a Math1-independent progenitor as opposed to secretory lineage cells (Yang *et al.,* 2001).

Accordingly Notch together with Wnt signalling is suggested as one of the main gatekeepers of intestinal progenitor compartment as both pathways are required for the maintenance of proliferating and non-differentiating cell in the intestinal crypts.

To summarize, the maintenance of intestinal homeostasis requires a firmly controlled interplay between numerous signalling pathways transducing signals between different layers of epithelium. Presence of high Wnt and Notch signals in the crypts safeguards the undifferentiated state of stem cells and progenitors within that niche whereas as those signal levels decline as cells migrate up towards the crypt-villus junction progenitor cells lose their proliferating capacities and differentiate into mature epithelial cell types. The expression of Hh ligands by the epithelial cells of crypt compartment consequently induces Hh signalling in the surrounding stroma leading to BMP ligand activation. BMP signalling suppresses Wnt pathway activation in the villus area restricting the proliferation whereas BMP antagonist Noggin protects the crypts from BMP signalling ensuring controlled self-renewal of stem cell strictly within that intestinal niche (Figure 1.8).

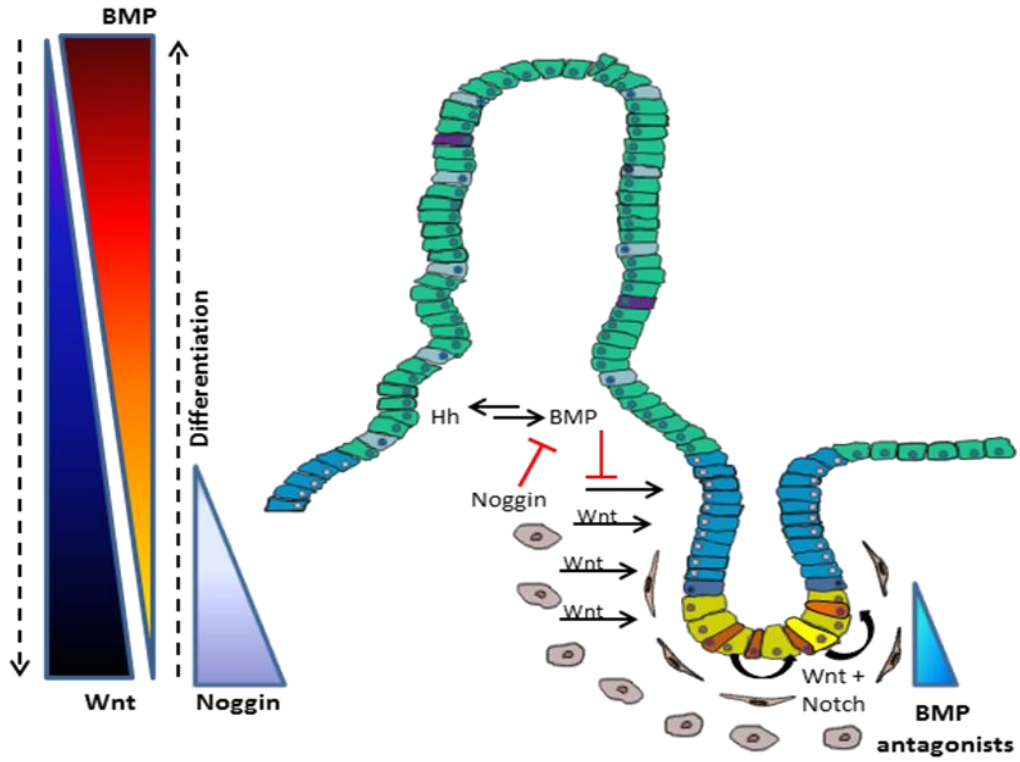

Figure 1.8 In order to maintain the intestinal homeostasis the interplay between different signalling pathways: Wnt, Notch, BMP/TGF-β and Hedgehog is necessary to control all processes regulating cell renewal, proliferation, differentiation, migration and cell death. While BMP/TGF-β and Hedgehog pathways are crucial for regulating Wnt signalling, the Wnt pathway is crucial for proliferation and self-renewal within a stem cell niche. Notch signalling directs the differentiation of intestinal progenitor cells safeguards the immature state in the crypt in particular within stem cell niche through high levels of Notch in those compartments.

1.2 Colorectal cancer

1.2.1 Incidence of colorectal cancer and environmental risk factors

Colorectal cancer (CRC) is the third most common cancer in UK accounting for 12.5% of all new cancer cases. In 2010 over 40,000 new cases of CRC have been diagnosed with male to female ratio of 13:10 and this incidence has persisted at the similar levels since last decade.

There is a geographical variation in incidence of CRC across the world which can be associated with environmental and dietary factors previously implied in increased risk of developing CRC. High consumption of red and processed meat (Norat *et al.,* 2000), diet deficient in natural fibres (Park *et al.,* 2005) as well as other lifestyle factors including lack of physical activity (Wolin *et al.,* 2011), obesity (Moghaddam *et al.,* 2007), smoking (Liang *et al.,* 2009) and alcohol consumption (Fedirko *et al.,* 2011) have been reported to predispose and therefore rapidly increase the risk for CRC.

As with vast majority of cancers, relative survival for CRC has been improving with 1-, 5- and 10-year survival rates increasing two-fold since 1970's. Nevertheless CRC remains the second most common cause of cancer death in UK accounting for over 600,000 deaths worldwide in 2008 (Cancer Research UK).

1.2.2 Genetic predisposition to colorectal cancer

Colorectal cancer can be subdivided into sporadic and familial cases and it is estimated that around 20-25% of all CRC cases is considered to have a hereditary origin whereas another 5-10% of all cases are inherited according to the Mendelian laws implying that the causing mutation is inherited in the autosomal dominant manner (Lynch and de la Chapelle, 2003, de la Chapelle 2004).

Therefore, except the environmental and dietary, genetics factors play a major role in predisposing towards CRC. For that reason hereditary syndromes conferring susceptibility to CRC development have been of a great value in identification and understanding of roles of genes important for colorectal carcinogenesis to occur as well as in the design of novel diagnostic and therapeutic strategies.

Hereditary CRC syndromes can be organised into two main categories on the ground of presence or absence of intestinal polyps. Furthermore polyposis syndromes can be classified

into two separate groups of adenomatous and hamartomatous polyposis depending on the type of tissue present predominantly within those polyps.

1.2.2.1 Familial adenomatous polyposis

Familial adenomatous polyposis can be characterized by the emergence of hundreds to thousands of adenomas in the colon in the late childhood or adolescence primarily composed of epithelial cells. From an average age of 40 years old the malignant degeneration occurs where due to the extremely high numbers of proliferating adenomas present, one or few of those develop into adenocarcinoma. One of the common features of tumours from FAP patients is the presence of chromosomal instability and aneuploidy as well as more aggressive phenotype. Mutations in several key oncogenes and tumour suppressor genes such as APC, P53, KRAS have been identified in those tumours (reviewed in Lynch and de la Chapelle 2003).

Years of cohort studies have led to the discovery that APC gene mutations are responsible for the development of FAP by Groden *et al.* in 1991 and that the vast majority of germ-line APC mutations involve truncating or nonsense mutations often leading to the alteration of the reading frame. The location of those germ-line mutations seems to be correlated with the number of polyps present in the colorectum of FAP patients: truncating mutations in the 5' region of APC gene upstream of codon 157 result in the "attenuated" FAP phenotype which involves delayed adenoma formation (reviewed in Sancho *et al.,* 2004) and in general fewer adenomas predominantly located at the proximal end of colon (Nagase and Nakamura, 1993) whereas mutations in the other parts of the gene lead to "classical" FAP. Furthermore, the mutations in APC gene have been identified in around 80% of early adenomas in sporadic cases of colorectal cancer (Nagase and Nakamura, 1993).

1.2.2.2 Hamartomatous polyposis syndromes

Hamartomatous polyposis syndromes are a heterogenous group of inherited non neoplastic conditions that encompasses Peutz-Jeghers syndrome, Cowden syndrome, Bannayan-Riley-Ruvalcaba syndrome and familial juvenile polyposis (Eng and Ji 1998). All of those disorders can be characterized by the overgrowth of normal tissue within the colon with a marked expansion of cells derived predominantly from stroma. Although all of those syndromes are rare and comprise a very small proportion of familial CRC, in particular two of them, notably

Peutz-Jeghers Syndrome and juvenile polyposis are associated with a significantly increased risk of gastrointestinal and other malignancies (de la Chapelle 2004).

Mutations in PTEN gene have been identified in both Cowden syndrome and Bannayan-Riley-Ruvalcaba syndrome and with only some subtle distinctions between the two and considerable overlap in symptoms the argument exists that they both represent same syndrome (Lachlan and Lucassen 2007, Eng and Li 1998). Furthermore as both lead to development of benign non-neoplastic lesions which only in rare cases result in malignant adenocarcinoma, the thorough involvement of Cowden syndrome and Bannayan-Riley-Ruvalcaba syndrome in development of colorectal malignancies remains to be explored.

The main clinical criteria of Peutz-Jeghers syndrome in patients are multiple hamartomatous polyps throughout the gastrointestinal tract as well as the presence of mucocutaneous melanin deposition. Those polyps are frequently present in the jejunum and ileum, they are large and pedunculated with entrapped glands containing mucus-producing goblet cells (Tomlinson and Houlston, 1997). Germline mutations in tumour suppressor gene, *LKB1* are responsible for 50% of Peutz-Jeghers cases (Lim *et al*., 2003).

Juvenile polyposis syndrome involves the development from few to few hundred polyps in the colorectum. These juvenile polyps possess a distinct histology from that of adenomatous polyps present in FAP patients where mucous cysts are surrounded by cells derived from lamina propria. Several genes are known to be associated with JPS with approximately 20% of affected individuals carrying mutations in *SMAD4* (Howe *et al.*, 1998), another 20% - in *BMPR1A* (Howe *et al.*, 2001). Both of those belong to the superfamily of transforming growth factor-beta (TGF-β) indicating the involvement of this signalling pathway in the development of colorectal cancer.

1.2.2.3 Hereditary nonpolyposis colorectal cancer syndrome

Hereditary nonpolyposis colorectal cancer syndrome is also commonly known as Lynch syndrome due to the fact that it predisposes not only to CRC, but also several other cancers such as endometrial cancer, ovarian and brain cancer. Depending upon the clinical definition of this syndrome, it is responsible for 2.5-5% of all CRC cases (de la Chapelle 2004). Patients with Lynch syndrome occasionally develop colon polyps that at the accelerated rate progress toward CRC characterized by poorly differentiated tumours (Lynch and de la Chapelle, 2003) and relatively late onset in comparison to other hereditary CRC syndromes (Hampel *et al.*, 2005). Lynch syndrome is caused by mutations in the mismatch repair (MMR) genes MLH1,

MSH2, MSH6 and PMS2 where mutations in MLH1 and MSH2 account for approximately 90% of all patient cases (Lynch and de la Chapelle 2003) with different levels of penetrance of those disease alleles for various cancers ranging from 80% for CRC, 60% for endometrial cancer and less than 20% for all other cancer types. Whereas the mutations in MLH1 and MSH2 display no apparent differences in expressivity, MSH6 mutations result in an "attenuated" form of Lynch syndrome distinguished by lower penetrance and higher age of onset however the mechanism behind this phenotype needs to be further explored due to very low numbers of MSH6 mutations identified so far (de la Chapelle 2004). The deficiency in the MMR mechanism leads to microsatellite instability which is known as the hallmark of Lynch syndrome (Thibodeau *et al.* 1996, 1998) and therefore an excellent diagnostic marker.

Each of syndromes governing the inherited susceptibility to CRC described above involves a separate class of genes that when mutated, contributes towards tumorigenesis. According to Kinzler and Vogelstein (1998), there are 3 main groups of "gatekeeper", "landscaper" and "caretaker" genes. Inactivation of gatekeeper genes such as APC which normally act as tumour suppressors leads to formation of benign neoplastic polyps. The penetrance is approximately 100% due to the abundance of those polyps throughout the colon as eventually few of those growths will progress towards malignant degeneration. In case of defects in the caretaker genes i.e. MMR pathway genes, the rate of polyp development is similar to that of observed in the general population as in comparison to gatekeeper genes, those genes suppress neoplasia indirectly. However those mutations lead to the mutator phenotype where increases rate of mutagenesis eventually results in development of CRC. The last class of genes is represented by landscaper genes that lead to hamartomatous polyps in which the abnormal microenvironment of bulk of stromal cells increases the risk of associated epithelial cells to undergo neoplastic transformation and therefore becoming malignant.

1.2.3 Major signalling pathways involved in the development, progression and metastasis of CRC

As mentioned previously, hereditary cancer syndromes account for approximately 20% of all CRC cases with the remainder of cases having a sporadic origin. However the genes and the pathways found to be causative of those conditions are often found mutated in the sporadic cases too.

Hereditary CRC syndromes and analysis of mutations occurs in sporadic CRC provide us with a valuable insight into the signalling pathways involved in the complex nature of colorectal tumours, their development and progression (reviewed in Sancho 2004).

1.2.3.1 Wnt signalling

1.2.3.1.1 Human mutations in the Wnt pathway

The discovery that APC mutations are implicated in the development of FAP by Groden et al (1991) provided one of the first hints towards the association between Wnt pathway and CRC.

As previously described in (Chapter 1.1.3 The homeostasis in the intestinal epithelium), APC is a one of the crucial components of the β-catenin destruction complex where together with GSK3β and Axin it is responsible for β-catenin phosphorylation, subsequent ubiquitination and degradation (Figure from pathways). Therefore any mutations leading to the loss of APC and its function within the destruction β-catenin complex result in the failure to regulate β-catenin levels in the cytoplasm as well as the failure to inhibit transcriptional activation of downstream Wnt target genes (reviewed in Giles *et al.* 2003, Fodde *et al*, 2001).

Although APC mutations detected in FAP patients account for a very limited proportion of all CRC cases, approximately 80% of CRC patients possess mutations in *APC* gene (Nagase and Nakamura, 1993). Mutations in *CTNNB1* gene encoding β-catenin are found in 10% of CRC cases. In those patients, alteration of several important phosphorylation sites leads to inability to target β-catenin for proteasomal degradation and eventually β-catenin stabilization (Morin et al., 1997). Therefore activating mutations of the Wnt pathway are found in over 90% of all CRC cases, interestingly mutations in *APC* and *CTNNB1* genes are suggested to be mutually exclusive insinuating that both of them have similar effect on the β-catenin stabilization and activation of downstream elements of Wnt signalling pathway. Nonetheless, some differences

in tumour phenotype have been observed as the vast majority of β-catenin mutations have been identified in small adenomas in comparison with a small proportion in invasive colorectal tumours. This observation suggested that small adenomas containing β-catenin mutations are less likely to progress to large adenomas and invasive cancer raising the notion that despite *APC* and *CTNNB1* genes performing similar function in regards to β-catenin destruction, *APC* can possibly possess some other tumour suppressor functions yet to be explored (Samowitz *et al*., 1999).

Remarkably, mutations of the Wnt pathway components have been found in other cancers types such as gastric, melanoma and ovarian. Mutations in Axin and aberrant expression of several Wnt ligands have been identified amongst many others genetic alterations, however their role in colorectal tumorigenesis appears to be minimal (reviewed in Giles *et al.,* 2003).

Activating mutations of the Wnt pathway have been identified as the only known genetic modifications present in the early premalignant lesions in the intestine, such as aberrant crypt foci and small polyps. In particular, the maintenance of the frequency of mutations in APC gene throughout the sequential progression from benign to malignant cancer further provides evidence suggesting that aberrant activation of Wnt signalling is one of the initial stages in the development of colorectal tumours.

Years of studies of FAP syndrome revealed that the nature and position of germ-line APC mutation account for a great clinical variability amongst the individuals with FAP. The most common human *APC* mutations are located between codon 450 and 1578 resulting in stable truncated proteins. This genotype-phenotype correlation gives even further insight into APC-related tumorigenesis where majority of CRC cases with APC mutations do not result in the complete ablation of APC protein. As indicated by a "just right" hypothesis the function of APC must be impaired in a very particular manner - at the level sufficient for the accumulation of β-catenin but at the same time below the threshold triggering the apoptosis. In those CRC cases, one allele of APC is lost due to truncating mutations whereas the other one acquires another truncating mutation or undergoes a loss of heterozygosity. This hypothesis suggests the interdependence of different mutations which allow for the successive accumulation of β-catenin sufficient for tumour progression however limited to a certain level in order to avoid programmed cell death (Lamlum *et al.,* 1999, Albuquerque *et al.,* 2002, Crabtree *et al.,* 2003).

1.2.3.1.2 Mouse models of alterations in the Wnt pathway

As the molecular processes involved in development of hereditary cancer syndromes and thus CRC have been of a great interest for many years numerous animal models comprising mutations in Wnt pathway components have been generated. The first model of intestinal tumorigenesis, named Multiple Intestinal Neoplasia was stably expressing a truncated APC protein as a result of a nonsense mutation at codon 850. Mice heterozygous for Apc^{Min} show changes which are characteristic for early preneoplastic tissue such as increased β-catenin and expansion of proliferative compartment, developing a large number of adenomas in the gastrointestinal tract which eventually leads to shortened lifespan (Su *et al.,* 1992). Mice carrying one allele with a truncating mutation in the codon 716 of *Apc* gene ($Apc^{\Delta 716}$) are one of the most extensively used mouse models to study FAP and CRC. Similarly to Apc^{Min} animals, they develop up to 100 adenomas with a vast majority of tumours arising in the small intestine (Oshima *et al.,* 1995). In contrast to the two models of *Apc* mutations described above, mice heterozygous for *Apc* mutation at the codon 1638 (Apc^{1638N}) develop only few intestinal tumours however they display a large spectrum of extra-intestinal phenotypes characteristic for FAP patients (Fodde *et al.,* 1994). Another CRC model characterised by a conditional deletion of exon 14 of *Apc* gene using a colon-specific Cre recombinase (Apc^{580S}) results in the adenoma formation within 4 weeks post-induction (Shibata *et al.,* 1997). Intestinal adenomas also develop in animals expressing oncogenic forms of *β-catenin* as the activation of Wnt signalling is a dominant driver of intestinal neoplasia. Conditional deletion of exon 3 of *β-catenin* resulted in a phenotype similar to that one observed in $Apc^{\Delta 716}$ animals (Harada *et al.,* 1999). Studies of Apc^{Min} have allowed identifying two modifier loci of tumour development called Mom 1 (Modifier of Min 1) and Mom2 (Modifier of Min 2) that can modify the number as well as the size of colon tumours (Gould *et al.,* 1996, Silverman *et al.,* 2002).

1.2.3.2 TGF-β and BMP pathways

1.2.3.2.1 Human mutations in the TGF-β and BMP pathway

As previously described, TGF-β cytokines family comprises of TGF-β, bone morphogenetic protein (BMP) and activins molecules which are all ligands for type I and type II serine-threonine kinase receptors and share SMAD4 as the common signal mediator. Therefore, both TGF-β and BMP pathway have similar effect on the target tissue favouring apoptosis and differentiation and opposing proliferation. Two specific mutations - in a co-mediator SMAD4 and a BMP receptor BMPR1 have been identified in families with Juvenile polyposis syndrome (Chow *et al.* 2005). A 4 base deletion in exon 9 of *Smad4* gene is a

mutational hotspot and resulting loss of growth inhibition and neoplasia. Mutation in the BMPR1 results in a receptor missing its intracellular serine-threonine kinase domain halting the signal transduction through SMAD4 eventually. These two mutations account for approximately 50% of JPS cases with the remaining cases of JPS possibly carrying mutations in different components of BMP pathway (reviewed in Sancho 2004). Mutations in SMAD-2 and SMAD-4 generating truncated proteins are frequent in colorectal cancer (Eppert *et al.,* 1996). The most common mutation in TGF-β pathway is inactivation of receptor type II (TGFβR2) present in the vast majority of microsatellite instable (MSI) tumours as well as in more than 50% of microsatellite stable (MSS) tumours. MSI tumours can be characterized by the accumulation of mutations in a 10 bp coding polyadenine tract (Grady *et al.,* 1999).

According to the current hypotheses about the general tumour suppressor roles of TGF-β and BMP pathways in tumorigenesis, those two pathways are critical for the maintenance of homeostasis by regulating the growth of non-neoplastic cells as well as cells that are already progressing through early stages of tumorigenesis (Roberts and Orkin 2004).

1.2.3.2.2 Mouse models of alterations in the TGF-β and BMP pathway

Over the years numerous mouse models targeting TGF-β superfamily were generated. Animals with heterozygous mutations inactivating the components of this family of cytokines such as TGF-β ligands, TGF-β1, -2 and -3 or SMAD2 have failed to recapitulate the increase in tumorigenesis in the colon with the homozygous mutations being embryonic lethal. The exception to this rule seemed to be SMAD3-deficient animals which survive until adulthood and later develop metastatic colorectal carcinomas (Zhu *et al.,* 1998) however this finding was not confirmed by other studies on SMAD3 loss. Heterozygous mutation in SMAD4 results in the development of polyps in the stomach and duodenum of SMAD4-deficient animals with intestinal polyps being similar to those observed in JPS patients (Takaku *et al.,* 1999). Moreover heterozygous loss of SMAD4 leads to acceleration of progression of benign adenomas carrying $Apc^{\Delta 716}$ mutation to more aggressive carcinomas (Takaku *et al.,* 1998). In similar manner, homozygous loss of TGF-β1 in immunocompromised animals results in the more rapid progression of lesions towards CRC (Engle 1999). Overexpression of the BMP inhibitor, Noggin results in development of crypt-resembling structures on the sides of villi and development of adenomatous polyps with enlarged proliferative compartment which is identical to the phenotype observed in JPS patients (Haramis *et al.,* 2004). While results from *in vivo* animal studies may not be able to fully recapitulate the effects of TGF-β signalling

deficiency on intestinal tissue it has been reported that the loss of TGF-β and BMP signalling is a frequent occurrence in the advance stages of CRC cancer (Markowitz *et al.*, 1995) suggesting that the loss of signalling is a necessary step in the process of progression of pre-neoplastic lesions towards CRC.

1.2.3.3 Ras-Raf-MAPK pathway

1.2.3.3.1 Human mutations in the Ras-Raf-MAPK pathway

In many cases of CRC, except genetic alterations in Wnt and TGF-β pathway, mutations in Ras-Raf-MAPK pathway are very common. Human Rat Sarcoma viral oncogene homology (Ras) family consists of three genes: Kirsten (K-Ras), Harvey (H-Ras) and neuroblastoma (N-Ras) with all of them encoding GTP-binding proteins that are involved in the signal transduction from various receptor tyrosine kinases (RTK). Depending whether those Ras proteins are bound by GDP or GTP, they can become activated or inactive. Upon the binding of an EGF ligand to the extracellular portion of receptor tyrosine kinase, the dimerization of RTK subunits occurs which in turn catalyses the phosphorylation of both RTK subunits. The growth factor receptor-bound protein 2 (GRB2) binds to the phosphorylated RTK while SOS proteins can be activated by GRB2 and bind membrane-bound Ras. Inactive Ras is GDT-bound however SOS catalyses the dissociation of GDP and binding of GTP to Ras leading to the activation of Ras. Once activated, Ras can bind and phosphorylate many downstream effectors of this transduction pathway such as Raf serine/threonine kinases which consequently phosphorylate and activate mitogen activated protein (MAP) kinase cascade including Mek1 and 2, and ERK1 and 2. This kinase cascade translocates to the nucleus and activates transcriptional factors such as c-jun and fos resulting in the expression of many genes that control cell cycle. In the normal cell the active Ras is inactivated immediately after its activation by the GTPase activating protein (GAP) which binds to the Ras-GTP complex and assists in the hydrolysis of GTP to GDP. With Ras-GDT complex being inactive, the MAP signalling pathway is switched off.

The Ras oncogenes are often activated by point mutations that prevent the activation of GAP with those mutations being very frequent in CRC with around 50% of colorectal carcinomas and adenomas containing some kind of Ras mutation. More than 30% of CRCs display activating mutations in the *K-Ras* gene (Bos *et al*. 1987) whereas another 20% of cases with functional K-Ras have activating mutations in *B-Raf* gene (Rajagopalan *et al*. 2002). The vast

majority of all mutations in Ras is found in the more advanced stages of CRC tumorigenesis being very rare in the pre-neoplastic lesions (Vogelstein *et al*. 1988).

1.2.3.3.2 Mouse models of alterations in the Ras-Raf-MAPK pathway

The role of Ras genes in the progression of CRC have been explored using several mouse models. Transgenic animals that carry activating mutations of K-Ras display no or very few gastrointestinal tumours suggesting that Ras does not play role in the initiation of CRC (Coopersmith *et al*., 1997; Kim *et al*., 1993). However Janssen *et al.* (2002) observed that over 80% of experimental animals that express K-Ras (V12G) mutation under the control of *Villin* Cre recombinase have developed few intestinal lesions. Detected lesions included a wide spectrum of neoplastic structures ranging from aberrant crypt foci (ACF) to invasive adenocarcinomas all characterized by the deregulated proliferation (Janssen *et al*., 2002). What is specific for this particular murine model is that expression of K-Ras from the *Villin* promoter leads to constitutive activation as well as over-expression of Ras oncogenes. Another study investigating the effects of K-Ras activation from the endogenous promoter failed to detect any alterations such as misregulation of proliferation in the intestinal epithelium (Guerra *et al*. 2003). Whereas the expression of K-Ras (V12) on its own have not been associated with abrogation of intestinal homeostasis or intestinal tumorigenesis, when combined with heterozygous loss of Apc in a long-term study it leads to acceleration of tumorigenesis as well as more invasive properties in comparison to animals with a functional K-ras oncogene (Sansom *et al.*, 2006).

Although many mouse models with activating mutations in Ras genes have been generated over the years, these results suggest that K-ras plays a minor role in the maintenance of intestinal homeostasis and tumour initiation however together with other elements of Ras-Raf-MAP pathway it plays a crucial role in the progression of pre-existing lesions.

1.2.3.4 PI3K pathway

1.2.3.4.1 Human mutations in the PI3K pathway

Phosphoinositide-3-kinase (PI3K) pathway is one of the most frequently mutated pathways in CRC however due to the number of different signalling transducers involved as well as various feedback loops it is still far from being understood. Similarly to MAP pathway activation, PI3K signalling may be activated by binding of EGF to RTKs or it may also become activated indirectly by K-Ras. In first instance, the binding results in the dimerization

and subsequent phosphorylation of both monomers. The type of proteins that may bind depends upon the different receptors such as insulin receptor substrate 1 (IRS1) may bind to the activated IGF1 receptor with receptor-bound IRS1 functioning as a binding and activation site for PI3K. Additionally in some cases, PI3K may bind directly to the phosphorylated RTK. A different mechanism of PI3K activation is accomplished by Ras where PI3K binds to the activated Ras-GTP complex. Migration of the active PI3K and its binding to the phosphatidylinositol 4,5-bisphosphate (PI[4,5]P_2 (PIP2) leads to the phosphorylation of PIP2 to phosphatidylinositol 3,4,5-triphosphate (PI[3,4,5]P_3 (PIP3). Once PIP3 is formed, it can activate serine/threonine kinase AKT which upon further phosphorylation and full activation is subsequently capable of activating mammalian target of Rapamycin (mTOR). Downstream effects of activated AKT involve many different substrates and processes such as inhibition of apoptosis by binding and preventing the activity of BAX, activation of protein synthesis via mTOR and translation factor S6K or regulating proliferation by maintenance of low concentrations of FOXO protein.

In normal PI3K signalling, the antagonist of the PI3K, the phosphatase and tensin homologue (PTEN) dephosphorylates PIP3 terminating PI3K signalling. However in many cases of cancer, *PTEN* is mutated or lost leading to the accumulation of PIP3. Mutations in *PTEN* gene have been previously identified in both Cowden syndrome and Bannayan-Riley-Ruvalcaba syndrome belonging to the hamartomatous polyposis syndromes (Blumenthal and Dennis, 2008). Sporadic mutations in *PTEN* gene are associated with many different types of cancer such as skin, prostate, breast cancer as well as CRC (Salmena *et al.,* 2008). With exception to PTEN, mutations in *AKT* gene were found in 6% of CRCs (Carpten *et al.,* 2007).

1.2.3.4.2 Mouse models of alterations in the PI3K pathway

The germ-line mutations in PTEN tumour suppressor gene of PI3K signalling have been previously reported in Cowden syndrome which predisposes affected individuals towards colorectal tumorigenesis. Early studies on PTEN function showed that *Pten* is required during murine embryogenesis whereas a small proportion of Pten heterozygous animals revealed the presence of colonic carcinomas (Di Cristofano *et al*., 1998, Suzuki *et al*., 1998). The etiology of juvenile polyps developed by CS patients remained elusive for many years implicating the loss of PTEN in the stromal compartment as a contributing factor. Transgenic mouse model of PTEN loss recapitulating the juvenile polyposis in the colonic epithelium reported that the absence of requirement for stromal PTEN deletion for the formation of juvenile polyps

further implicating that polyps found in the colorectum of CS patients are early precursor lesions of neoplastic transformation (Marsh *et al.,* 2014). Furthermore the same group previously showed that in the context of intestinal homeostasis loss of PTEN does not lead to abrogation of normal crypt-villus architecture however in the context of Apc loss and aberrant Wnt signalling it accelerates the formation of adenocarcinoma through increased activation of Akt levels (Marsh *et al.,* 2008).

1.2.4 Genetic model of CRC progression

Considering the numerous molecules and signalling pathways involved in the maintenance of intestinal homeostasis, indication by Foulds (1958) that cancer is a multistep process where several irreversible changes "in one or more characters of its cells" occur appears to be perfectly thought. The identification of molecular events determinant of the initiation as well as progression of tumorigenesis required years of extensive research nowadays it not only provides us with an insight into basics governing tumorigenesis but also is critical for the development of novel therapies to treat cancer. Over 30 years after Foulds, Fearon and Vogelstein proposed their genetic model of colorectal cancer progression based on the extensive study of genetic and histopathological data which remains the most comprehensive model until today (Fearon and Vogelstein 1990). At the core of this model lies the notion that in regards to tumorigenesis seen as continuum, the accumulation of mutations in multiple tumour suppressor genes and proto-oncogenes results in the transformation and progression of tumorigenesis from early neoplastic lesions into advanced and invasive forms of tumour. Importantly, although genetic alterations in particular genes frequently occur along the preferred sequence, in regards to tumour progression it is the gradual accumulation rather than chronological order of genetic changes that is responsible for biological features of CRC tumours (Figure 1.9) (Fearon and Vogelstein 1990). Consistent with the proposed order of genetic alterations, mutations in the Wnt pathway such as stabilizing mutations in β-catenin or most frequently loss of Apc tumour suppressor gene leading to the aberrant activation of signalling lay are critical event for CRC initiation. As adenomas progress towards more advanced stages of adenoma, they acquire activating mutations in KRAS oncogene and allelic loss of chromosome 18q. Detailed mapping of this region identified *Deleted in colorectal cancer* (DCC) as potential candidate with tumour suppressor capacities however transgenic studies later revealed that DCC does not predispose or accelerates the progression of tumours in Apc^{Min} mice (Fazeli *et al.* 1997). In the absence of phenotype of DCC loss, other genes such as SMAD2 and SMAD4 effectors of TGF-β/BMP pathway mapped to the

same region on the chromosome 18q have been suggested as tumour suppressors (Eppert *et al.* 1996). Lastly, the loss of chromosome 17 short arm containing *TP53* locus encoding p53 tumour suppressor was one of the final steps of CRC tumorigenesis involving the progression to malignant disease (Fearon and Vogelstein 1989). The mutations in p53 were reported in over 50% of carcinomas and often coincided with the allelic loss of 17p leading to its association with the progression of tumours from adenoma to carcinoma (Nigro *et al.* 1989, reviewed in Iacopetta 2003).

Presented genetic model of CRC progression suggests that formation of carcinoma would require more than five genetics events with adenoma arising as a result of fewer alterations (Fearon and Volgelstein 1990) however taking into the account the mutation rate in normal human tissue such a number of independent genetic changes is implausible to be achieved (Kinzel and Vogelstein 1996). In regards to this, two other pathways of CRC tumorigenesis exist allowing for cancer progression (reviewed in Dunican *et al.*, 2002). Microsatellite instability (MIN) pathway involves alterations in the mismatch repair system such as those reported in HNPCC leading to a marked increase in mutation rate and eventually microsatellite instability. In contrast, chromosomal instability (CIN) pathway is characterized by chromosomal lesions due to the escalation in the chromosomal rearrangements where CIN is frequently associated with loss of Apc function (Fodde *et al.*, 2001). The predominant form of genetic instability in CRC is CIN accounting for 85% and MIN respectively for 15% of sporadic CRC cases. Moreover, mutations found in CIN colorectal cancer frequently involve Wnt, Ras-Raf-MAPK, TGF-β/BMP and p53 pathways further accentuating the role of those signalling cascades in the CRC (reviewed in Dunican *et al.*, 2002).

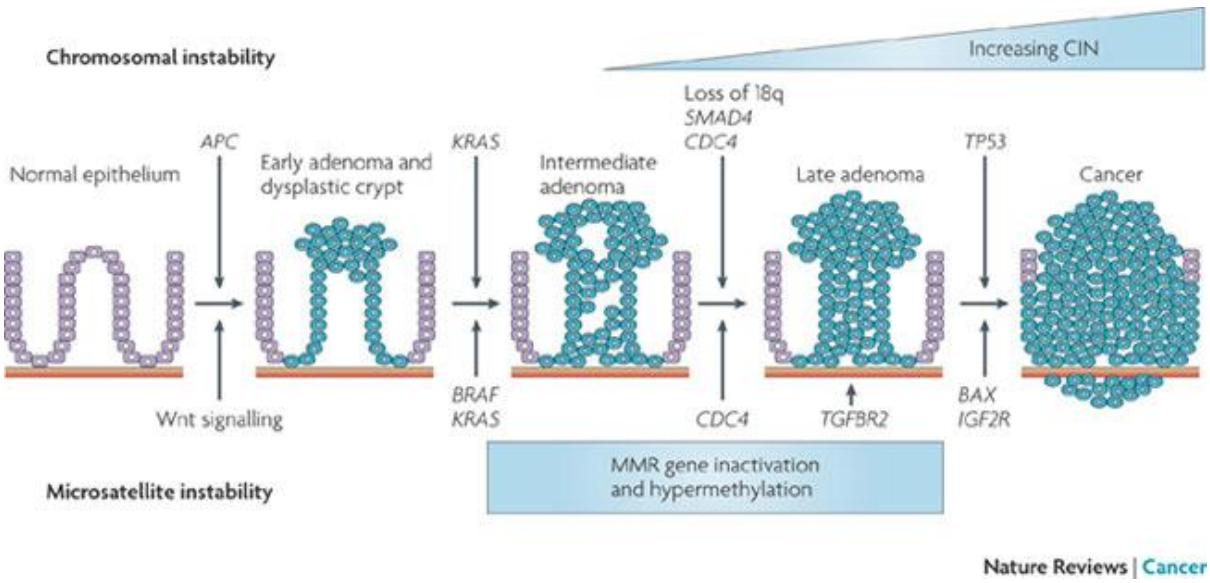

Figure 1.9. Genetic model of CRC progression from adenoma to carcinoma. The initial step in the CRC tumorigenesis involving the transformation of normal intestinal epithelium into adenoma is associated with loss of *APC*. As the tumour progresses towards more advanced stages it accumulates additional mutations - large adenomas and early carcinomas acquire mutations in the *KRAS*, followed by loss of chromosome 18q with *SMAD4* and mutations in *TP53*. The original source of diagram: Walther *et al.* 2009

1.2.5 Colorectal cancer stem cell

The concept of colorectal cancer stem cells as the means by which tumours are propagated has become of a great interest in the last few decades. Unveiling of such a mechanism would in turn have major implications on the detection of cancer, therapeutic compound discovery as well as metastasis amongst all (Wicha *et al.* 2006). Early observations of tumours revealed the heterogeneity amongst them leading to the formulation of the stochastic model. According to this model, all cell types ranging from stem cells to early differentiated cells had equal capacity to become cancer cell of origin whereas the genomic instability of those cells and microenvironment accounted for the differential phenotypical characteristics (Lobo *et al.* 2007). An alternative model, notably cancer stem cell model suggested that the existence of a specific subpopulation of cancer cells characterized by the self-renewal capacity and pluripotency that drive tumour progression and heterogeneity (Vries *et al.* 2010). Consistent with this notion, targeting of the cancer stem cells clinically would result in the eradication of tumour in contrast to targeting other cancer cells (He *et al.* 2009).

The requirement for accurate markers of those cancer stem cells exist in order to pursue the idea of developing the therapy specifically targeting this subpopulation of cancer cells. One of the first colorectal cancer stem cells markers identified was CD133 (Prominin-1). A study using renal capsule transplantation into non-obese diabetic/severe combined immune deficiency (NOD/SCID) mice found that only a $CD133^{+}$ cells were capable of initiation of tumour growth showing over 200 fold enrichment for cancer initiating cells in comparison to CD133- cells (O'Brien *et al.*, 2007). The identification of other colorectal cancer stem cell markers including CD24, CD29, CD166 and Lgr5 was based on their expression in the $CD133^{+}$-derived cultures (Vermeulen *et al.*, 2008). In contrast to reports by O'Brien *et al.* (2007), Shmekov and his colleagues showed that CD133 is widely expressed in the human and mouse metastatic colon cancers undermining its potential as colorectal cancer stem cell marker (Shmelkov *et al.* 2008) Another study by Dalerba *et al.* (2007) found that highly proliferative cells capable of forming tumour morphologically resembling the original lesion were characterised by the high expression levels of epithelial cell adhesion molecule (EpCAM) and the presence of the cell surface marker CD44 suggesting they act as potential cancer stem cell markers (Dalerba et al., 2007). Whereas the identification of numerous cancer stem cells markers would facilitate the targeting of this subset of cancer cells, the question of which of those cell surface markers are required for cancer cell survival remained unresolved. Recent study by Barker *et al.* (2009) has provided strong evidence in support of

the notion that the intestinal cancer stem cell is a cell of origin of CRC. The activation of aberrant Wnt signalling through conditional loss of Apc in the Lgr5^{+} intestinal stem cells but not in progenitor or early differentiated cells resulted in the rapid adenoma formation (Barker *et al.* 2009). Lineage tracing using multicolor Cre-reporter R26R-Confetti by Schepers *et al.* (2012) identified Lgr5 intestinal stem cell marker as a marker of adenoma cells that are fuel the growth of established intestinal adenomas (Schepers *et al.*, 2012). This notion indicating that intestinal stem cell markers can equally be expressed in a subset of colorectal cancer stem cells was confirmed by an analysis of gene expression signatures by Merlos-Suarez et al. (2011). EphB2-enriched intestinal stem cells were shown to be capable of tumour initiation in immunodeficient animals together with the enrichment of cells characterised by this gene expression signature in recurrent and metastatic CRC cases (Merlos-Suarez *et al.*, 2011).

In summary, whereas these observations support the cancer stem cell hypothesis, several important questions including the nature of tumour relapse and the role of tumour microenvironment will have to be addressed prior to the development of cancer stem cell targeted therapies.

1.2.6 Mouse models as a tool for recapitulating human colorectal tumorigenesis and translational research

Due to the nature of CRC tumorigenesis comprising of an array of molecular changes in different signalling pathways involved it requires appropriate models to recapitulate all aspects of the disease which would enable discovery and validation of novel compounds and therapies in future. Use of human cancer cell lines for validation of potential candidates and drug testing was one of the first platforms allowing for examination of some crucial cellular features of cancer cells such as proliferation and apoptosis levels, clonal survival, invasiveness capacities and in particular their ability to generate tumours in immunocompromised mice. Whereas human cancer cell lines provide relatively cheap means of assessment of drug validation there are several shortcoming worth considering. Importantly, many of human cancer cell lines have been isolated many decades ago and since then they have been continuously propagated implicating that due to the native mutation rate as well as some genomic instability they might no longer recapitulate the phenotype of their tumours of origin. Another issue is the setting of the *in vitro* experiments as those cancer cells are taken out of the context of their natural microenvironment and factors *in vivo*. The

mentioned limitations are overcome partially by the use of method of transplantation of cancer cells into immunodeficient animals however injections of cells into the skin flank do not mimic their normal setting. In the light of the importance and dependence of those cancer cells upon the factors and interactions with microenvironment such as with surrounding stroma or immune system, the absence of full recapitulation of tumour microenvironment by xenotransplant procedure provides an avenue for cancer cells to become more susceptible to anti-cancer therapies. Consequently this leads to significantly reduced pool of potential anti-cancer compounds after validation in appropriate murine models that are successfully applied in human studies (Olive *et al.* 2009). Therefore the recapitulation of molecular events and cancer phenotype of such a complex disease like colorectal cancer requires the development of murine models of human cancers capable of mimicking both natural tumour environment as well as being easily reproducible. Despite of some genetic differences between humans and mice, these animals are a great animal cancer model characterised by short reproductive period, the presence of well-established transgenic techniques and similar gene expression regulation. The use genetically modified mouse models (GEMMs) in CRC studies carries some limitations revealed by early transgenic experiments showing that often the control of transgene expression levels is somehow limited with expression levels of many proteins surpassing those found in human counterparts. The localisation of intestinal neoplasia in the murine models of CRC differs significantly from that found in humans with a vast majority of lesions found in the small intestinal epithelium. Moreover the progression of CRC towards more malignant phenotype according to the model proposed by Fearon and Vogelstein (1990) has not been successfully recapitulated in mice.

In summary, whereas the process of the CRC initiation have been well-described appropriate advanced murine models are required in order to overcome all limitations imposed by *in vitro* studies or xenotransplantation approach. Considering the intercalating roles of different signalling pathways in CRC tumorigenesis, more “humanised” models of cancers in mice would provide the better learning platform for understanding of cancer progression as well as a validation platform for novel compounds.

1.2.6.1 Constitutive transgenesis

The generation of GEMMs recapitulating the phenotype of human cancers requires the use of transgenic techniques in order to mimic the mutations that comprise of that particular phenotype. The generation of first targeted deletion of hypoxanthine-guanosine

phosphoribosyl transferase (HPRT) by Kuehn *et al.* (1987) set the stepping stone for the decades of studies in generating mouse models of gene deletion *in vivo*. Numerous murine models of constitutive gene deletion have been generated since then providing a great deal of insight into the redundancy and function of many genes in the embryogenesis. However this technique carries some restrictions due to the nature of the gene deletions.

Most importantly, physiological functions of many genes have not been uncovered as they have been found to be necessary for normal embryonic development whereas constitutive loss of those genes resulted in the pre-implantational or embryonic lethality. This have subsequently led to situations where the role of particular gene could not been investigated in the context of adult tissue homeostasis and tumorigenesis due to its role in the early development of the embryo such as in case of *Pten* tumour suppressor loss (Di Cristofano *et al*., 1998). Another limitation is the use of constitutive knock-down is that the expression of targeted gene is lost in the whole organism. Tissue-specific effects of gene deletion cannot be investigated and accounted for as complications in other systems may lead to severe phenotype besides tissue of interest. Moreover constitutive deletion of a particular gene in all cells of the organism might mask the extend of tissue-specific consequences through the changes in other systems and tissue microenvironment.

1.2.6.2 Conditional transgenesis

Considering the limitations imposed by the constitutive transgenesis together with the fact that in many cases heterozygous deletion of a gene is insufficient for tumour development, an alternative approaches were required for the investigation of tissue-specific effects of gene targeting. Conditional transgenesis systems such as site–specific recombination using LoxP sites or Tet-on and Tet-off system ensures more stringent control over gene manipulation.

Cre-loxP (Causes recombination (Cre) - Locus of crossover of bacteriophage P1 (loxP)) involves the Cre, a DNA recombinase driven under the expression of a particular promoter and LoxP sites that are 34 base pair sequences from bacteriophage P1(Sauer and Henderson, 1988). Upon the induction of Cre activity, the recombination between LoxP sites occurs leading to the excision or inversion of flanked sequence. Recombination may lead to loss of tumour suppressor gene when LoxP sites flank the sequence necessary for its activity. The excision of transcription stop cassette results in the constitutive activation of an oncogene. Cre-LoxP system is most frequently used to exploit inducible promoter that are normally transcriptionally silenced however upon the induction with xenobiotic they become

expressed. One of the most commonly used inducible Cre recombinases is AhCre recombinase consisting of a rat cytochrome P4501A1 gene (*Cyp1A1*) which is transcriptionally silent in normal conditions whereas the administration of xenobiotic such as β-naphthoflavone results in the interaction with aryl hydrocarbon receptor, translocation to the nucleus where it binds to the Cyp1A1 promoter and initiates transcription (Ireland *et al.* 2004). The control of transgenesis at the translational level is achieved by tissue-specific promoters. An example of such a promoter is CreER transgene encoding Cre recombinase-estrogen receptor fusion protein which is activated in the presence of the estrogen antagonist Tamoxifen. The binding of Tamoxifen to the ER domain of the protein allows for translocation of Cre into the nucleus subsequently leading to the catalysis of recombination between loxP sites. Dual control at both transcriptional and post-translational level ensures stringent control over expression of transgene which is illustrated by AhCreER transgene.

FLP/FRT is similar to Cre-LoxP system of control of expression of genes. FLP recombinase is extracted from Saccharomyces cerevisiae (Dymecki, 1996) and together with FLP recognition target (FRT) sites are inserted into the genome. One of the crucial limitations of this mechanism is a substantial thermolability and limited activity.

Overcoming of the main disavantages of both Cre-LoxP and FLP/FRP systems which is the irreversibility of the genetic alterations driven by the excision or inversion of targeted sequence was generation of Tet-on and Tet-off gene expression system controlled by the tetracycline. Tet repressor protein utilized in this system originates from *Escherichia coli* (Gossen and Bujard, 1992) and it can induce or suppress expression of target gene in response to administration of the tetracycline derivative doxycycline (Gossen and Bujard, 1992, Gossen et al., 1995).

1.3 Brm as a potential therapeutic target for Wnt-driven tumorigenesis

1.3.1 Chromatin structure and chromatin remodelling

DNA is tightly packaged into chromatin which importantly serves as a very important mechanism of controlling the expression of genes within that sequence. The core unit of chromatin structure is nucleosome consisting of 147 base pairs of DNA that are wrapped

around an octameric core of histone proteins: H2A, H2B, H3 and H4. These repeating nucleosome structures are bundled together in order to form a higher-order organized, condensed chromatin. Such a condense assembly of DNA prevents the interactions of some DNA sequences with elements of transcription machinery, consequently regulating the gene expression. However as the chromatin is a very dynamic structure capable of responding to the external signals the process termed chromatin remodelling may later the level of DNA packaging. The chromatin remodelling may be achieved by three different mechanisms: DNA methylation, histone modifications or ATP-dependent chromatin remodelling. DNA methylation is one of the major means for epigenetic signalling and it involves the addition of methyl groups to cytosine residues by DNA methyltransfereses converting them from cytosines into 5-methylcytosines. Usually those methylated cytosine residues are adjacent to guanine residues forming methylated CpG sequences dispersed across the whole length of the genome with exception of CpG islands comprising of large clusters of CpG sites that remain unmethylated. The methylation of those CpG islands results in inappropriate gene silencing such as silencing of the tumour suppressor gene sequences and it is therefore widely recognized as an important component of cancer development. Histone-modifying enzymes catalyze the changes at N-terminal tails of histone proteins such as methylation, acetylation, phosphorylation, ubiquitination, sumoylation and ADP-ribosylation. Those modifications affect interactions between the negatively charged backbone of DNA and the positively charged residues within histones and hence tighten or loosen the chromatin structure. Finally, ATP-dependent chromatin remodelling complexes are regulating the gene expression by being capable of moving, ejecting and stabilizing nucleosomes. Each complex comprises of an ATPase subunit which together with the energy from ATP hydrolysis enables them to perform their function.

1.3.2 Mammalian SWI/SNF and its subunits

SWI/SNF chromatin remodelling complex was initially identified in *Saccharomyces cerevisiae* and subsequent purification of complexes containing homologous ATP-dependent nucleosome remodelling activity identified related complexes in *Drosophila melanogaster* and mammalians (Wang *et al.*, 1996). SWI/SNF chromatin remodelling complex is one of four families of SWI-like, ATP-dependent chromatin remodelling complexes which share an evolutionarily conserved SWI-like ATPase catalytic domain with other functional domains being unique to particular family. The main function of SWI/SNF complexes is coordinated

regulation of gene expression playing a crucial role in development and stem cell pluripotency.

The main components of mammalian SWI/SNF complexes are catalytic ATPase subunits: brahma (BRM; SMARCA2) or brahma-related gene 1 (BRG1; SMARCA4) which are mutually exclusive. These complexes also consist of a minimum 8 highly conserved subunits referred as Brm or Brg1-associated factors (BAFs) such as BAF47, BAF155, BAF170, BAF53, BAF57, BAF60A, BAF250 or BAF180 and other variant subunits that are contributing towards targeting, assembly and regulation of those complexes (Muchardt 1999). Whereas 13 BAFs have been identifies so far, no SWI/SNF complex containing all of those subunits exists. The number of mammalian SWI/SNF components greatly exceeds those found in *Drosophila* and *Saccharomyces* suggesting exceeding structural and possibly functional diversity (Wang *et al.,* 1996).

Recently SWI/SNF complexes have become a novel link between chromatin remodelling and cancer development as alterations in chromatin structure can lead to changes in gene expression leading to tumorigenesis in some cases. Mutations in subunits of these complexes have been found to be present in different types of cancers and suggest having an effect on the tumour suppression (Cohet *et al.,* 2010, Glaros *et al.,* 2008, Sevenet *et al.,* 1999, Sun *et al.,* 2007, Wilson *et al.,* 2011). One of the core members of SWI/SNF, SNF5 (BAF47, INI1) has been identified as *bona fide* tumour suppressor gene that is lost (one allele of BAF47 being deleted whereas the other allele is mutated or silenced by methylation) in nearly all cases of paediatric malignant rhabdoid tumours (Biegel *et al.,* 1999, Versteege *et al.,* 1998) and currently is used as a marker gene for those tumours in the field of diagnostics. Mice heterozygous for SNF5 gene develop rhabdoid tumours histologically resembling those found in humans characterized by high aggressiveness and invasiveness and frequent metastasis to lungs and lymph nodes (DelBove *et al.,* 2011, Guidi *et al.,* 2001, Klochendler *et al.,* 2000, Roberts 2000). Heterozygous deletion of BAF47 subunit has been detected in many cases of chronic myeloid leukemia (CML) (Grand *et al.,* 1999) and conditional inactivation of one allele in mice results in lymphomas or rhabdoid tumours with 100% penetrance (Roberts 2002). BAF60A has been found to bind p53 and has been linked to lung cancer risk (Hsiao *et al.,* 2003, Gorlov *et al.,* 2005). Furthermore BRG1 heterozygosity confers mice being more prone (10%) to develop mammary tumours indicating that its haplosufficiency of that gene can drive tumorigenesis (Bultman *et al.,* 2007). Furthermore, approximately 10% of human

primary lung tumours are deficient in both Brg1 and Brm indicating a poorer prognosis than patients whose tumours express either of ATPases (Reisman *et al.*, 2003, Fukuoka *et al.*, 2004).

Strong evidence exists supporting the role of SWI/SNF complexes in a number of processes that are critical for self-renewal and proliferation, cell cycle control, and cell differentiation whose abrogation is essential for tumour development and growth suggesting SWI/SNF complexes to function as potential tumour suppressors.

1.3.3 Comparison between paralogues Brm and Brg1

Human Brm catalytic subunit is highly homologous with Brg1 (75% in humans) in its amino acid sequence and possesses highly conserved structures. At the BRG1-N terminus between residues 1-282 we find a region with high sequence divergence from corresponding region of Brm. Within that particular region between the residues 216-254 Brm contains a polyQ domain encoding about 33 glutamines which is absent from Brg1 (Reisman *et al.*, 2009). The role of this polyQ repeat has not yet been explored however the data from C33 and SW13 cell lines revealed the presence of the variable length polyQ repeats among those cell lines. Brg1 contains 99 base pair exon located between 1235-1334 bp that is unique to this protein and not present in Brm (Kadam and Emerson 2003, Reyes 1998).

The other six conserved domains in Brm and Brg1 include: QLQ domain, a proline-rich domain, a *h*elicase/*SA*NT-associated domain, an ATPase domain, an Rb-binding domain and a Bromo domain. At the N-terminus QLQ domain (Brm 168-208, Brg1 170-200aa) contains conserved glutamine-leucine-glutamine motif and is believed to mediate the protein-protein interactions. A proline-rich domain is distal to the polyQ domain of Brm and proximal to HSA domain of both Brm and Brg1 (Brm 255-375, Brg1 210-345aa). The ATPase domain of Brm and Brg1 consists of helicase and DEAD box domains which are the main elements of ATP-dependent DNA unwinding mechanism. The free energy released from the ATP hydrolysis stimulates the translocation of those helicases along the length of DNA which in turn unwind the duplex DNA. *h*elicase/*SA*NT-associated domain (Brm 450-500, Brg1 475-525aa) is often associated with helicase activity and DNA binding. Rb domain comprises of LxCxE motif (Brm 1356, Brg1 1292aa) which is essential for binding to members of the Rb tumour suppressor family. At the C-terminal, a bromo domain is present (Brm 1380-1500, Brg1 1455-1575aa) functioning as a binding element for acetylated histones and it is an

important element securing the association between SWI/SNF remodelling complexes and chromatin (Figure 1.10).

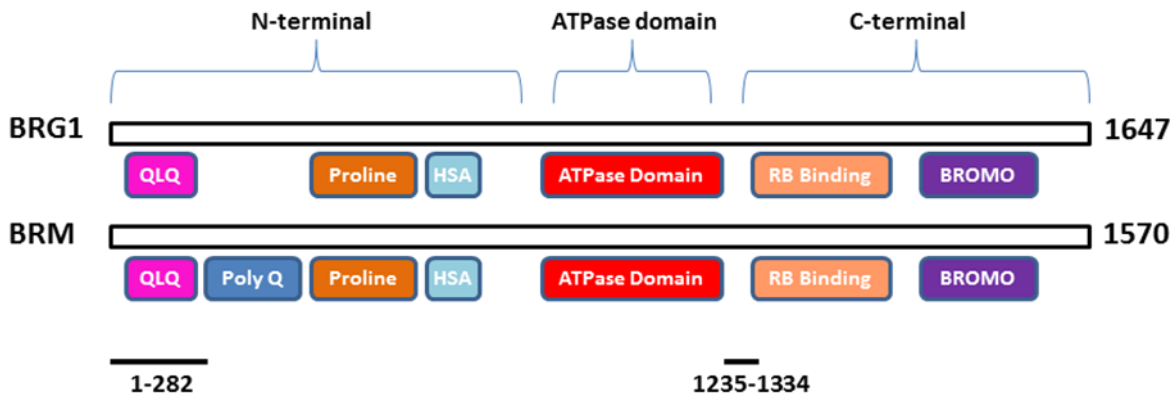

Figure 1.10 Structural domains of Brg1 and Brm ATPase subunits include six common domains that are evolutionarily conserved: QLQ, proline-rich, HSA, ATPase, RB and bromodomain. Proximal to QLQ domain, polyQ domain is present exclusively in Brm whereas a 99bp exon located before the LxCxE Rb binding sequence is unique for Brg1.

Taken together, Brm and Brg1 subunits are sharing multiple domains within their structure most of which are evolutionarily conserved however non-homologous region near N-terminus and 99bp unique exon which may account for some differences in functions of those two ATPases.

Biochemical activity of Brm and Brg1 differs significantly as deletion of Brg1 but not Brm results in aberrant chromatin organisation involving redistribution of histone modifications and dissolution of pericentromeric heterochromatin domains (Bourgo *et al.*, 2009). These differences in biochemical properties may account for difference in severance of the phenotype of murine knockout of Brm and Brg1 as those ATPases are likely to possess distinctive roles in chromatin remodelling as well as regulating different downstream genes (Bultman *et al.*, 2000). Homozygous deletion of BRG1 is embryonic lethal whereas mice that lost both copies of Brm are still viable but interestingly they express very little or no CD44 (Banine *et al.*, 2005, Reyes *et al.*, 1998). The lack of strong phonotype in the Brm mutant may be due to the ability of Brg1 to compensate for Brm deficiency (Reyes *et al.*, 1998).

Previous studies of SWI/SNF chromatin remodelling complexes during male meiosis suggest that Brm and Brg1 may have complementary, non-redundant roles (Kim *et al.*, 2012). Contrary to this observation, Brm is unable to compensate for loss of conditionally deleted Brg1 allele in developing hematopoietic and endothelial cells questioning the functional

redundancy between Brm and Brg1 ATPases in vitro (Griffin *et al.,* 2008). Similarly, in vivo study of a retinoblastoma-induced growth arrest of human melanocytic nevi supports that notion. Cell culture studies of osteoblasts have also suggested the distinctive roles of those two ATPases as Brm negatively regulates osteoblast differentiation and in contrast Brg1 promotes this process (Flowers *et al.,* 2009).

It has been shown that both ATPase subunits of SWI/SNF complex Brm and Brg1 can have distinct roles in regulating transcription as they associate with different promoters as well as preferentially bind distinctive classes of transcription factors in response to signalling pathways. BRG1 binds zinc finger proteins via domain that is not present in BRM but BRM can uniquely interact with ankyrin repeats which results in differential promoter targeting (Kadam and Emerson 2003). Those two proteins that belong to the ankyrin family, ICD22 and CBF-1 play a crucial role in as regulators of Notch signalling pathway and therefore can inhibit differentiation, and thus alter fate of the proliferating cells.

Both, Brm and Brg1 proteins are involved in the regulation of cell cycle. In SW13 cell line expression of either of proteins induces growth arrest (Dunaief *et al.,* 1994, Shanahan *et al.,* 1999, Strober *et al.,* 1996) which has been indicated as an effect of the interaction between those ATPases and tumour suppressor and cell cycle control Rb (retinoblastoma) protein (Asp *et al.,* 2002). Functional Brm protein is necessary for formation of Rb/HP1β complex and binding of Rb protein to chromatin during cellular senescence in vivo.

Brm and Brg1 are also capable of inducing the changes in DNA methylation at the promoter sites of CD44 and E-cadherin genes in order to promote transcriptional activation. Hypermethylation of those two promoters is observed in cells that have lost Brm or Brg1 but restoration of ATPase activity by transfection with either Brm or Brg1 induces loss of methylation, activation of transcription and CD44 and E-cadherin expression in those cells. Proposed mechanism by which Brm and Brg1 could influence the methylation of the promoters may involve recruitment of demethylase to those promoter sequences or by blocking the methyltransferases (Banine *et al.,* 2005). Previous studies have shown that Brm and Brg1 proteins possess the ability to enhance transcription mediated by the glucocorticoid receptor (Muchardt *et al.,* 1993, Wang *et al.,* 1996), the estrogen receptor (Chiba 1994) and retinoic acid receptor (Chiba 1994).

1.3.4 Physiological functions of Brm

Murine studies of spermatogenesis and oogenesis demonstrated that a decrease in the methylation of CpG islands within Brm promoter correlates with an increase in expression of Brm (Nagrani *et al.,* 2011) which facilitates its transcription. Brm is actively recruited to cyclin A promoter by cyclin A bipartite repressor sequence and consequently maintains the state in which cyclin A promoter is tightly wrapped around nucleosomes repressing cyclin A expression. Moreover quiescent cells that are deficient for Brm fail to repress this promoter suggesting that Brm is necessary for repression of cyclin A during early phases of cell cycle (Coisy *et al*. 2004).

In NB4 resistant cell line (retinoid-maturation-resistant NB4-LR1 subclone), CD44 expression is silence due to the methylation of CpG islands and underacetylation of H3 at CD44 promoter. The reversing CD44 gene silencing and therefore re-expression of functional CD44 signalling pathway is facilitated by cAMP which recruits Brm and c-jun to the sites at the CD44 proximal promoter where Brm is shown to be involved in the crosstalk between transcription and RNA polymerase II processing and also the binding of phosphorylated RNA Pol II to the proximal promoter region of CD44 (Abercassis *et al.,* 2008). In the same cell line, UV-irradiation induced apoptosis leads to the cleavage at carboxyl terminus of Brm by cathepsin G. The subsequent removal of bromodomain of Brm leads to the disruption of its association with nuclear matrix and inactivation of Brm protein as it cannot perform its functions in a same manner as full-length Brm. This rapid inactivation of Brm resulting indicates possible mechanism by which cells are becoming apoptotic is response to DNA damage (Biggs *et al.* 2001).

Brm has been reported to be contributing towards the crosstalk between transcription and RNA polymerase II processing of numerous genes such as CD44, E-cadherin and cyclin D1. Furthermore it is also found to be associated with elements of spliceosome and ERK-activated enhancer of variant exon inclusion Sam68 facilitating the recruitment of the splicing machinery and eventually inclusion of their variable exons of those genes (Abercassis *et al.* 2008, Batsche *et al.* 2006).

It has been found that formation of the complex between cEBP-α and Brm inhibits E2F-driven gene expression and therefore proliferation of hepatic progenitor cells leading to decline in regenerative capacity of aging liver (Conboy *et al.,* 2005). Similar interaction between cEBP-α and Brm has been observed in MCF-7 breast cancer cell line where the stimulation of hVDR transcription by binding between cEBP-α and Brm is inhibited by

mutation in Brm ATPase domain (Dhawan *et al.,* 2009). Brm has been also shown to form complex with MeCP2 in methylation-mediated gene silencing of gene promoters ABCB1 and THBS1 in cancer cell lines suggesting its ATPase activity is playing important role in co-repression mechanism. (Harikrishan *et al.,* 2005)

1.2.4.1 Brm interaction with Notch signalling

As previously mentioned in section 1.2.3 ChIP analysis of both ATPase subunits of SWI/SNF chromatin remodelling have detected an exclusive interaction of Brm but never Brg1 with ankyrin repeats domains which results in differential promoter targeting (Kadam and Emerson 2003). The two proteins identified belong to the ankyrin family, ICD22 and CBF-1 play a crucial role in as regulators of Notch signalling pathway and therefore can inhibit differentiation, and thus alter fate of the proliferating cells. This data suggest that manipulations of Brm levels may have an effect on Notch signalling which regulates multiple processes in the intestinal epithelium.

1.3.5 The role of Brm in mammalian development

Brg1 null animals similarly to SNF5-deficient mice are embryonic lethal whereas Brm null mice are viable suggesting a differential role of Brm and Brg1 in mouse development. In early development of murine embryo Brg1 is expressed during the pre-implantation development and Brm expression levels are detectable from blastocyst stage onward which also marks the first cell fate decision event. During this first differentiation event, cells within blastocyst so-called inner cell mass are destined to become a proper embryo and external cells give rise to the trophectoderm that forms the embryonic part of placenta. Brm is uniquely restricted to inner cell mass however it becomes expressed in cell-type specific manner after the differentiation of embryonic stem cells (LeGouy 1998).

In adult animals, Brm is preferentially expressed in cell types such as brain or liver which do not undergo continuous self-renewal and proliferation. Brm is dispensable for thymic development, does not contributes towards the phenotype as well as being unable to compensate for loss of Brg1 in T cells (Chi *et al.,* 2003, Gebuhr *et al.,* 2003). Enzymes of SWI/SNF chromatin remodelling complex are necessary for activation of transcription of muscle-specific genes but are redundant for cell cycle arrest (de la Serna 2006). Previous data

on embryos deficient for both Brm and Brg1 showed no exacerbation of vascular phenotype over that seen in single Brg1 mutant (Griffin *et al.,* 2011).

1.3.6 The role of Brm as tumour suppressor

Consistent with the roles of both Brm and Brg1 in regulating transcription of numerous genes contributing towards processes involved in cell cycle, it implicates the importance of the presence as well as functioning of those ATPases on cancer development in *in vivo* and *in vitro* studies.

Furthermore, common point mutation in Brm has been detected in basal squamous carcinoma and basal cell carcinoma (de Zwaan *et al.,* 2010). Brm deficiency is shown to potentiate tumour development induced by lung-specific carcinogen ethyl carbamate leading to an increase in numbers of adenomas (Glaros *et al.,* 2007). Additionally, Brm expression is absent in approximately 15% of human tumours such as bladder, ovarian, esophageal, breast and lung (Glaros *et al.,* 2007). Further analysis of primary lung carcinoma cases revealed that independently of Brg1 status Brm low expression or loss correlates with poor prognosis suggesting that Brm loss may accelerate poorer cell differentiation and epithelial-mesenchymal transition (EMT) eventually leading to even more malignant phenotype (Matsubara *et al.,* 2013). Similarly Brm loss in mammary epithelial cells promotes the malignant phenotype by the induction of C/EBPβ-dependent transcription of α5 integrin (Damiano 2013). Expression levels of Brm but not Brg1 were significantly lower in primary hepatocellular carcinoma (HCC) and alike in lung carcinoma cases correlated with overall poor prognosis.

Previous studies conducted in our laboratory looking at Brg1 loss showed that upon the activation of Wnt pathway due to Apc loss, multiple adenomas form within small intestinal epithelium however Brg1-deficient cells are selected against leading to suppression of Wnt-driven tumorigenesis. In comparison, in Wnt-activated large intestine, Brg1 deficiency is tolerated in adenomas and Brm is overexpressed in Brg1 deficient tumour lesions.

Consistent with the data, similarly to Brg1 and BAF47 (SNF5), Brm is believed to function as tumour suppressor. Whereas many tumour suppressor genes are inactivated in cancer by mutations, Brm deficiency is caused by silencing and therefore its expression could be restored (Glaros *et al.,* 2007). Taken together, Brm re-expression may therefore be a valuable clinical target in many solid tumour types but regrettably interactions of Brm subunit with

signalling pathways such as Wnt, Notch or BMP pathway responsible for maintaining tissue homeostasis remain as yet unknown.

1.4 Aims and objectives

The main objective of this thesis is to explore the role of an active SWI/SNF chromatin remodelling complex containing Brm catalytic subunit in the small and large intestinal epithelium. The enzymatic activities of Brm towards nucleosome remodelling and therefore the role of Brm in the control of transcription of genes involved in cell cycle and differentiation implicates its function in the maintenance of normal homeostasis as well as during the cellular transformation during cancer development and progression. Strong evidence exists supporting the notion that aberrant activation of Wnt signalling is a key initiation step in intestinal tumorigenesis however no direct links between Brm and Wnt signalling have been identified in contrast to interactions between Brm and the Notch pathway (Kadam and Emerson 2003). This project aimed to further explore the possibility of modulation of phenotype observed in the small and large epithelium in the context of acutely activated Wnt signalling in context of Brm loss which might be possibly mediated by Brm effect on Notch pathway components or changes in the expression of Brm paralogue Brg1. Upregulation of Brm expression has been reported in Brg1-deficient human cancers, implying that a level of SWI/SNF chromatin remodelling is maintained, possibly through compensation mechanism between the Brm and Brg1 ATPases.

Initially, Brm null mouse model will be used to investigate the role of Brm ATPase subunit in the small and large intestine by assessment of effects of Brm deficiency on the maintenance of homeostasis within normal, non-neoplastic intestinal epithelium. This part of the project is outlined in Chapter 3. Furthermore, I will assess the consequences of Brm deficiency in the context of aberrant Wnt signalling on the epithelium of small and large intestine which are described in Chapter 4. Lastly, the consequences of combined deficiency in both Brm and Brg1 catalytic subunits will be analysed, with respect to normal homeostasis and acute Wnt signalling activation in small and large intestinal epithelial allowing for the differentiation between dependency on Brm-containing complexes, Brg1- containing complexes or synergistic effect of active SWI/SNF including both Brm and Brg1 on the intestinal phenotype in the epithelium. This part of the project is being addressed in Chapter 5 of this PhD thesis.

Chapter 2

Materials and Methods

2.1 Experimental animals

All the animal work conducted during this PhD studies have been carried out in accordance with UK Animal Scientific Procedures Act 1986 and UK Home Office regulations under valid personal (Joanna Krzystyniak 30/9673) and project licenses (Prof Alan R Clarke, years 2010-2015, 30/2737).

2.1.1 Transgenic constructs and animal models used in the project

A number of different transgenic mouse lines have been used for the needs of this project with all mice being maintained on the mixed background. Some of mice have not been carrying a Cre recombinase due to the *Brm* allele being constitutively knocked-out with no need for such a transgene. Mice carrying the *Tg(Cyp1a1-cre/ESR1)1Dwi* transgene (abbreviated in the text as AhCreER) are induced by combined injection of Tamoxifen and β-napthoflavone which drives the recombination in small intestine, esophagus, stomach, liver, gall bladder and bladder. *Tg(Cyp1a1-cre/ESR1)1Dwi* created by Douglas J Winton is a trangene insertion 1 of cytochrome 450 (*Cyp1a1*) rat promoter that drives the expression of cre recombinase fused with Estrogen receptor 1. The control over the Cre activity is greatly improved in comparison to *Tg(Cyp1a1-cre)1Dwi* transgene (abbreviated as AhCre) as it is regulated at two levels – by the transcriptional control of AhCre promoter and by the requirement for Tamoxifen binding to the fusion protein containing mutated oestrogen-binding domain. This type of dual control at the transcriptional and protein level ensures tightly regulated tissue-specific recombination (Kemp 2004). Animals used for the *ex vivo* studies were bearing *Tg(Vil-cre/ESR1)23Syr* transgene (abbreviated VillinCre) where fusion protein consisting of Cre recombinase and oestrogen receptor is transcriptionally controlled by *Villin1* promoter and requires a binding of synthetic ligand of Tamoxifen (el Marjou 2004). Animals carrying targeted disruption of *Brm* allele where the exon a has been replaced

by neomycin resistance cassette together with targeted *Brg1* allele with lox P sites are flanking exons 2 and 3 were provided by Christian Muchardt (Reyes 1998) (Figure 2.1a, 2.1 b). The targeted *Apc* allele bearing the lox P sites present in the intronic sequences on both sides of exon 14 was maintained in our laboratory (Shibata 1997) (Figure 2.1c).

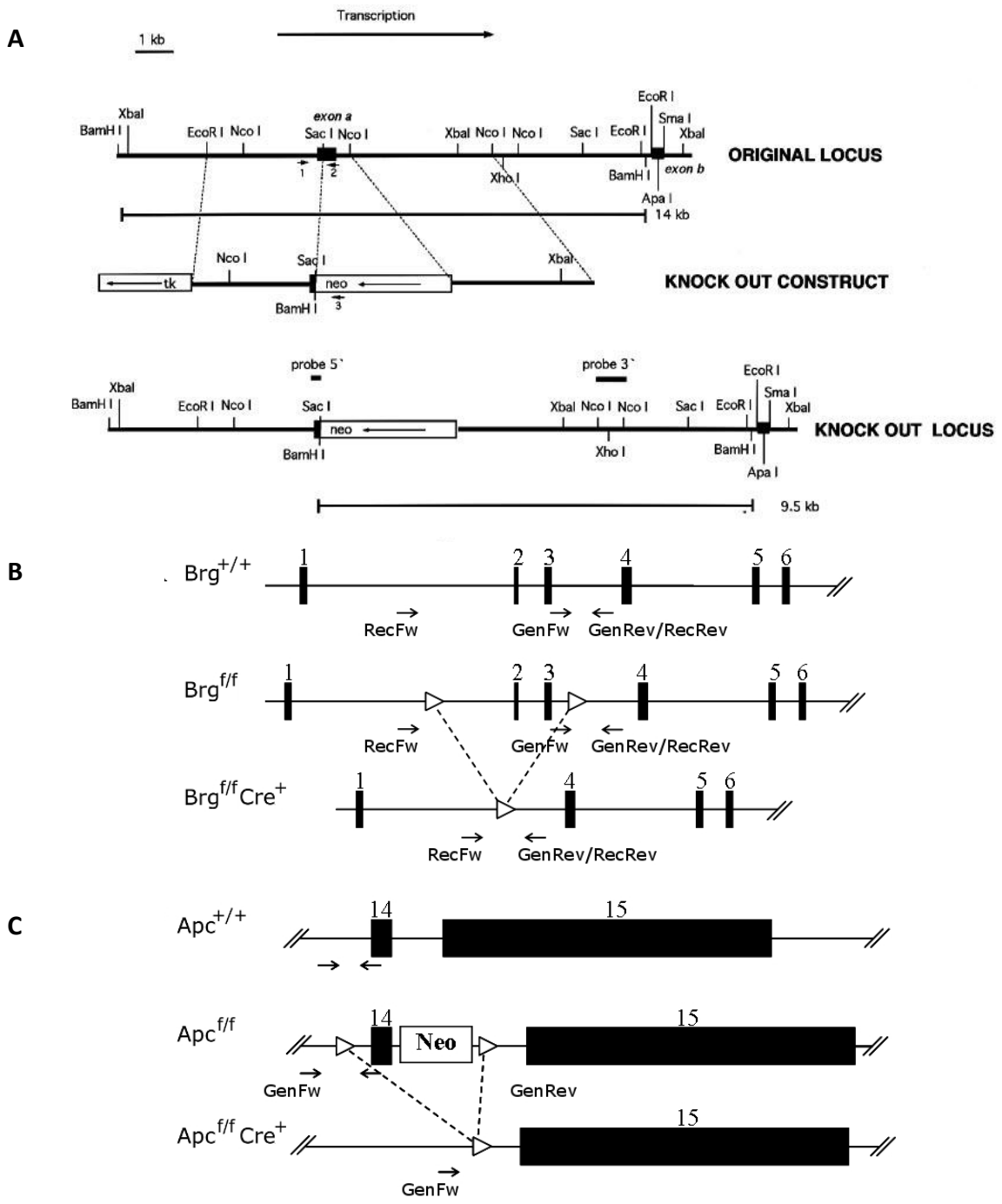

Figure 2.1 Schematic representation of the targeted disruption of *Brm* gene and loxP targeted *Brg1* and *Apc* alleles and their primer positions. (A) exon a of the endogenous *Brm* locus has been replaced by the targeting vector containing neomycin phosphotransferase (PGK-neo) gene and thymidine kinase (PGK-tk) gene both linked to the phosphoglycerate kinase (PGK) promoter placed in a reverse orientation relative to Brm transcription. Primers specific to the regions on the either side of exon a and within N*eo* gene are indicated as 1, 2 and 3 as the oligos used for genotyping of animals by PCR (B) Two loxP sites are placed in Brg1 gene in order to flank exons 2 and 3. Primers specific to regions either side of the second loxP site (GenFw-GenRev) are the oligos used for genotyping of animals by PCR. (Sumi-Ichinose et al., 1997). (C) Two loxP sites are placed in a way to flank either side of exon 14 of *Apc* gene. Primers specific to regions either side of the first loxP site (GenFw-GenRev) are the oligos used for genotyping of animals (Shibata et al.,1997).

2.1.2 Animal husbandry

2.1.2.1 Colony maintenance

All animals were housed in the semi-barriered facility and have been fed the Harlan standard diet (Scientific Diet Services, RM3(E)) and water.

2.1.2.2 Breeding

All animals were maintained as outbred. Adult animals (6-8 weeks old) of a known genotype were bred mainly as pairs (one male and one female), rarely in trios (one male and two females). Pups were left with their mother until they were capable of feeding independently. Those pups were usually weaned at 4 weeks of age unless they were too small which meant the risk of post-weaning mortality was high.

2.1.2.3 Identification by ear biopsy

At the time that pups were weaned, the male and female littermates were sexed and separated accordingly. The method of animal identification involved ear clipping and the tissue sample obtained through this procedure was used for DNA extraction and genotyping.

2.1.3 Experimental procedures

All experimental animals were aged until 70 days of age (10 weeks) before being subjected to any procedures. Intraperitoneal injections were performed using 1 ml syringe (BD Plastipak) and 26G needle (BD Microlance).

2.1.3.1 Injection of Tamoxifen

Animals carrying the VillinCre transgene were induced by administration of Tamoxifen (Sigma) in corn oil according to the high dose protocol of four daily IP injections of 80 mg/kg. Tamoxifen in the powder form was measured out and added to amber glass bottle containing corn oil to the final concentration of 10 mg/ml. The solution was then heated up to 80 °C with continuous stirring of the in order to aid the Tamoxifen to dissolve and finally aliquoted appropriately and stored at -20 °C. At the time of the procedure, the solution was briefly defrosted and heated up to 80 °C in the water bath and kept at that temperature until

immediately prior to the injection. At the end of the procedure, the remaining solution of Tamoxifen was re-frozen and was further defrosted and used up to 3 times to minimize the risk of Tamoxifen degradation.

2.1.3.2 Injection of Tamoxifen and β-napthoflavone

Animals expressing the AhCreER transgene were inducted by administration of Tamoxifen and β-napthoflavone solution. Cre recombinase activity and expression was achieved by five bi-daily IP injections of 80 mg/kg β-napthoflavone combined with 80 mg/kg Tamoxifen at the interval of 12 hours between each injection. Both, powdered β-napthoflavone and Tamoxifen were dissolved in corn oil to obtain final concentrations of 10 mg/ml. The solution was then heated up to 80 °C in the water bath and further stirred on the heated magnetic stirrer until complete dissolution of both components. Obtained solution was stored at -20 °C and a single batch was used during the bi-daily induction protocol which included repeated cycles of defrosting and re-freezing.

2.1.3.3 Injection of 5'-bromo-2-deoxyuridine

Selected experimental animals were administered with a single IP injection of 0.25 ml of 5'-bromo-2-deoxyuridine at the concentration of 10 mg/ml (BrdU, Amersham Biosciences). This procedure was conducted 2 hours or 24 hours prior to the dissection of the animal in order as a means to labelling all of the cells in the S-phase of the cell cycle at that discrete point of time.

2.1.4 PCR genotyping

All animals were genotyped by PCR using DNA extracted from the ear biopsies at the weaning age of four weeks and furthermore all experimental animals were genotyped again upon their death to confirm the genotype. Majority of the primers were provided by previous publications however if this was not the case they were designed using primer3 software at http://fokker.wi.mit.edu/primer3/input.htm, checked for specificity using BLAST engine against Ensembl database (http://www.ensembl.-org/Multi/blastview) and synthesised by Sigma Genosys.

2.1.4.1 DNA purification

At the time of the ear biopsy, the tissue sample taken was placed in a 1.5 ml eppendorf tube and stored at -20 °C until analysis. DNA isolation was performed using 250 µl of Cell Lysis Solution (Gentra) and 5 µl of 20mg/ml Proteinase K (Roche) which were both added to the tissue and incubated with agitation at 37 °C overnight. The following day the tube contests were cooled to room temperature, then mixed with 100 µl of Protein Precipitation Solution (Gentra) and centrifuged at 13000 RPM for 10 min in a microcentrifuge. The supernatant was collected and placed in a fresh 1.5 ml eppendorf, then mixed with 250 µl of isopropanol and centrifuged at 13000 RPM for 15 min. Resulting supernatant was carefully removed and discarded leaving the tubes to air-dry for 1 hour. Purified DNA was dissolved in 250 µl of PCR-grade water (Sigma) and 2.5 µl of the solution obtained was used to perform PCR reactions.

2.1.4.2 Generic protocol for PCR genotyping

PCR reactions were performed in a thin-wall 0.2 ml strip tubes (Greiner Bio-One) or thin-wall 96-well plate and run using GS1 (G-Storm) thermal cycler. All the pipetting of the reagents and DNA samples was carried out using filtered pipette tips to avoid aerosol contamination.

2.5 µl of genomic DNA extracted from ear biopsy was loaded into wells using a multi-channel pipette followed by the addition of 47.5 µl of prepared master-mix (Table 2.1) containing all the remaining components of the reaction (distilled water, GOTaq 5X PCR buffer (Promega), 25 mM Magnesium Chloride (Promega), 25 mM dNTPs (Bioline), Primers (Sigma-Genosys) and either GOTaq (Promega) or Dream-Taq (Fermentas) DNA Polymerase). Strip-tubes were closed using caps (Greiner Bio-One) whereas 96-well plates were sealed with aluminium foil tape ensuring that no air bubbles were present in the mixture.

Reactions were run using cycle conditions outlined in Table 2.1.
The primer sequences used for genotyping of the particular transgenes and the size of respective products are provided in Table 2.2.

2.1.4.3 Visualization of PCR products

After the completion of PCR reactions the products were visualised using agarose gel elecrophoresis. The reactions using colourless 5X PCR buffer (Promega) were mixed with 5 µl of DNA loading dye (50% Glycerol (Sigma), 50% distilled water, 0.1% (w/v) Bromophenol Blue (Sigma)) while the reactions using 5X Green PCR buffer (Promega) were loaded without the addition of loading dye. All samples along with an appropriate marker (e.g. 100 bp ladder (Promega)) were loaded onto 2% agarose gel (4 g agarose (Eurogentech), 200 ml 1X Tris-Borate-EDTA (TBE) buffer (Sigma), 10 µl of 10 mg/ml ethidium bromide (Sigma) or 10 µl Safeview (NBS Biologicals)). Gels were run in 1X TBE buffer at 120 V for 30 min. Products were visualised in UV light using ChemiDoc MP apparatus (BioRad).

Table 2.1 Genotyping PCR reaction components and cyclin conditions

	Cre/LacZ	**Responder**	**ApcLoxP**	**Brg1LoxP**	**Brm null**
PCR Reaction Components:					
DNA extract (See section 2.1.4.1)	2.5 µl	2.5 µl	2.5 µl	2.5 µl	2.5 µl
Master Mix:					
PCR-grade H2o (Sigma)	31.5 µl	31.7 µl	31.7 µl	31.7 µl	31.6 µl
GOTaq PCR Buffer (5X, Promega)	10 µl	10 µl	10 µl	10 µl	10 µl
Magnesium Cloride (25 mM, Promega)	5 µl	5 µl	5 µl	5 µl	5 µl
dNTPs (25 mM, Bioline)	0.4 µl	0.4 µl	0.4 µl	0.4 µl	0.4 µl
Forward Primer (100 mM, Sigma Genosys)	2 x 0.1 µl	0.1 µl	0.1 µl	0.1 µl	0.1 µl
Reverse Primer (100 mM, Sigma Genosys)	2 x 0.1 µl	0.1 µl	0.1 µl	0.1 µl	2 x 0.1 µl
Taq Polymerase	0.2 µl	0.2 µl	0.2 µl	0.2 µl	0.2 µl
Taq Polymerase Brand	GOTaq	DreamTaq	DreamTaq	GOTaq	DreamTaq
Total Reaction Volume:	50 µl	50 µl	50 µl	50 µl	50 µl

Cycling conditions (Time; Temperature)	**Cre/LacZ**	**Responder**	**ApcLoxP**	**Brg1LoxP**	**Brm null**
Initial denaturation	3 min; 94 °C	5 min; 94 °C	2.5 min; 95 °C	2.5 min; 95 °C	2.5 min; 95 °C
Cycle number	30	30	30	35	35
Step 1 (Denaturation)	30 sec; 95 °C	20 sec; 94 °C	30 sec; 95 °C	30 sec; 94 °C	30 sec; 94 °C
Step 2 (Annealing)	30 sec; 55 °C	20 sec; 57 °C	30 sec; 60 °C	30 sec; 60 °C	30 sec; 61°C
Step 3 (Elongation)	1 min; 72 °C	30 sec; 72 °C	1 min; 72 °C	1 min; 72 °C	1 min; 72 °C
Final Extension	5 min; 72 °C	5 min; 72 °C	5 min; 72 °C	5 min; 72 °C	5 min; 72 °C
Hold	1; 15 °C	1; 15 °C	1; 15 °C	1; 15 °C	1; 15 °C

Table 2.2 Primer sequences and size of products of genotyping PCR reaction

Name	Forward primer	Reverse primer	Product size
Cre specific	TGACCGTACACCAAAATTTG	ATTGCCCCTGTTTCACTATC	1000 bp
ROSA26:LacZ	CTGGCGTTACCCAACTTAAT	ATAACTGCCGTCACTCCAAC	500 bp
ApcLoxP	GTTCTGTATCATGGAAAGATAGGTGGTC	CACTCAAAACGCTTTTGAGGGTTGATTC	WT at 226 bp; Targeted at 314 bp
Brg1LoxP	CCAAGGTAGCGTGTCCTCAT	CACTGCTCAGCTTCACTTGC	WT at 407 bp; Targeted at 500 bp
Brm$^-$	CCTGAGTCATTTGCTATAGCCTGTG	CTGGACTGCCAGCTGCAGAG; CATCGCCTTCTATCGCCTTC	WT at 310 bp; Targeted at 700 bp

2.2 Tissue harvesting and processing

2.2.1 Tissue harvesting

All experimental animals were culled by cervical dislocation which was chosen amongst schedule 1 approved methods of culling mice. The animals were dissected in the designated surgery room using a student micro-dissection kit. The fur along the ventral axis of the animal was sprayed using 70% ethanol and incisions were made along the mid-line of the abdomen, initially through the skin, then through peritoneal wall followed by two horizontal incisions on both sides of the mid-line in order to expose all contents of abdominal cavity. The standard protocol of intestinal tissue harvesting was applied to all animals in exception to animals harvested for *ex vivo* studies. Stomach together with about 0.5 cm of esophagus was separated from the remainder of gastrointestinal tract. It was cut open in the middle with its contents flushed away with running cold tap water. Once empty, the forestomach was folded over the glandular stomach along the ridge separating respective parts and together with esophagus they were fixed using surgical microtape. The small intestine from the pylorus junction to the caecum was separated and it contents flushed away using syringe filled up with ice cold 1X PBS (Invitrogen). The first 9 cm of the small intestine were assembled as a "swiss roll" where the all 9 cm were cut open longitudinally, spread on the flat surface with the intestinal epithelium side-up, rolled from the pylorus junction down using the forceps and securing this conformation by piercing it through with 23G syringe needle (BD Microlance). Following 8 cm of the small intestine were cut into 4 equal-size pieces and bundled together with surgical microtape. The tissue for RNA and protein extraction was taken from the next 5 cm of the intestinal epithelium which were cut into 2-3 mm pieces, placed in an eppendorf and snap frozen in liquid nitrogen. Following 6 cm of the small intestine were cut into 3 equal pieces and bundled using microtape. The remainder of the small intestine down to caecum was "swiss rolled". The entire length of the large intestine was "swiss rolled" expect from the first 5 mm of the caecum and last 5 mm of rectum that were cut into half, the tissue placed in an eppendorf and snap frozen in liquid nitrogen for RNA and protein extraction.

The samples from other abdominal cavity tissues such as liver, pancreas, spleen, kidney and bladder were taken for histological analysis as well as snap frozen in liquid nitrogen.

2.2.2 Tissue fixation

All the tissue samples collected for histological analysis were immersed in the ice cold formalin (4% neutral buffered formaldehyde in saline, Sigma) and quick fixed for 24 hours at 4 °C. In case of samples that could not be processed straight away after fixation, the tissues were transferred into 70% ethanol and stored at 4 °C until processed.

2.2.3 Tissue processing for light microscopy

2.2.3.1 Tissue dehydration

All the tissue samples collected during dissection were appropriately arranged in the histocassettes and processed by automatic processor (Leica TP1050). The dehydration of the samples occurred as a sequential process involving increasing concentrations of ethanol (70% for 1 hour, 95% for 1 hour, 100% 2 x 1 hour 30 min, 100% for 2 hours), xylene 2 x 1 hour and eventually paraffin 1 x 1 hour and 2 x 2 hours. Once the dehydration process was completed, tissue samples were embedded in paraffin wax.

2.2.3.2 Tissue sectioning

5 µm thick sections were cut from paraffin blocks using microtome (Leica RM2135). Those pre-cut section were then floated on slides coated with poly-L-lysine (PLL) and baked at 58 °C for 24 hours.

2.2.4 Tissue preservation for DNA, RNA and protein

2.2.4.1 Tissue collected for DNA extraction

The tissues collected for DNA extraction were placed in 1.5 ml eppendorf, transported on ice into laboratory and stored at -20 °C until required for DNA extraction.

2.2.4.2 Tissue collected for RNA and protein extraction

As previously briefly explained in section 2.2.1 tissue samples collected for RNA and protein extraction were removed, cut into small pieces and transferred into a clean 1.5 ml eppendorf. The tissue was arranged around the walls of an eppendorf in a way to avoid the single pieces touching one another. This method was implied in order to enable the transfer of single pieces of tissue once required for extraction without the need of defrosting whole block of tissue

collected. The eppendorf was immersed in the liquid nitrogen as quickly as possible, later on transferred onto the dry ice to be transported between semi-barriered animal facility and laboratory and eventually stored at -80 °C until needed.

2.3 Histological analysis

2.3.1 Haematoxylin and Eosin staining (H&E)

Tissue sections have undergone the dewaxing and rehydration step as described in section 2.4.1 and were immersed in Mayer's Haemalum (R.A. Lamb) for 5 min. Stained slides were then washed under the running tap water for 5 min followed by staining in 1% aqueous Eosin solution (R.A. Lamb). The excess of Eosin stain was briefly washed off using water by 15 second washes. Stained sections were subsequently dehydrated and mounted as described in section 2.4.9.

2.3.2 Quantitative histological analysis of H&E sections

Histological quantification of stained sections of tissue was carried out using an Olympus BX43. The images representing histological traits analysed were taken using Moticam 5000 (5 megapixel, Motic Instruments) aided with Motic Images Advanced software (version 3.2 Motic China Group).

2.3.2.1 Scoring of crypt length

The crypt length was scored by counting the number of cells from the base of the intestinal crypt up to the crypt-villus junction where the bottom-most cell was indicated as #1. Crypt length was counted per half crypt-villus and minimum of 50 crypts were scored per animal. In order to maintain the consistency of the epithelium scored, the proximal ends of both small and large intestine were chosen for the analysis.

2.3.2.2 Scoring of villus length

The villus length was determined by counting the number of cells from the crypt-villus junction all the way up to the tip of the villus. Similarly to crypt scoring, villus scoring was conducted on half crypt-villus axis and minimum of 50 villi were scored per animal. Parallel

to crypt length scoring mentioned above, villus length was scored for the epithelium at the proximal end of small intestine.

2.3.3 Quantitative of histological traits using specific stains and markers

2.3.3.1 Alkaline phosphatase staining

The combined microvilli on the entire epithelial surface form the brush border. Alkaline phosphatase is a brush border-specific stain used as a differentiation marker to measure the abundance of mature enterocytes. Slides with tissue were dewaxed and rehydrated as described in section 2.4.1 and placed in the humidified chamber. Tissue sections were then covered with Liquid Permanent Red solution (DAKO) (1 drop of Liquid Permanent Red Chromogen in 3 ml of Liquid Permanent Red Substrate Buffer) and incubated for 20 min at the room temperature. The excess of staining solution was removed and tissue sections were washed in dH_2O for 5 min. The slides were counterstained in Mayer's Haemalum for 30 seconds, washed for 5 min under running tap water and mounted using glycerol (Sigma).
The localisation and intensity of staining as well as the thickness of the brush border were visually assessed using light microscopy and representative photograph of appropriate structures were taken.

2.3.3.2 Lysozyme staining

Lysozyme is one of Paneth cells-specific secretions therefore anti-lysozyme immunohistochemistry (section 2.4) was used to detect those cells. Cell numbers as well as cell position were scored within the small intestinal epithelium. The Paneth cell quantification was assessed as number of cells displaying positive lysozyme staining scored in 50 half crypt-villi per tissue section. Furthermore the average number of Paneth cells across those 50 crypt-villi was calculated for each animal in that cohort and analysed as described in section 2.7. Paneth cell position was counted from the base of the intestinal crypt up all the way up to the villus tip where the bottom-most cell was indicated as #1. Paneth cells positions from all animals belonging to the same experimental cohort were pooled together and analysed as described in section 2.7.

2.3.3.3 Alcian Blue staining

Mucin-secreting goblet cells have been identified using Alcian Blue staining. Slides with tissue were dewaxed and rehydrated as described in section 2.4.1 and immersed in Alcian Blue solution (1% (w/v) Alcian Blue (Sigma) in 3% (v/v) Acetic acid (Fisher Scientific)) for 30 seconds. Stained slides were washed under running tap water for 5 min and counterstained with 0.1% Nuclear fast red (Sigma) for 5 min. The excess of counterstain was washed off under running tap water for 5 min and sections were subsequently dehydrated and mounted as described in section 2.4.9.

Tissue sections were assessed for the presence of positive staining and the number of goblet cells was scored in 50 crypt-villi for each animal. The average number of goblet cells per half crypt-villus axis was calculated for each animal and further analysed as described in section 2.7.

2.3.3.4 Grimelius staining

Enteroendocrine cells have been identified within the intestinal epithelium using Grimelius staining which detects argyrophilic cells. Prior to the beginning of staining, all glassware to be used was carefully rinsed 3 times in ultrapure double-distilled (dd) H_2O. Slides with tissue were dewaxed and rehydrated as described in section 2.4.1. The silver solution was prepared by dissolving 1% (w/v) silver nitrate (Sigma) in Acetate buffer pH5.6 (0.02M Acetic acid (Fisher Scientific), 0.02M sodium acetate (Sigma) in ddH_2O) and heated to 65°C in a Coplin jar in the water bath. Tissue sections were subsequently inserted, Coplin jar was sealed and wrapped in tin foil to avoid any exposure to light, water or steam. Slides were incubated at 65 °C for 3 hours and then transferred into freshly prepared reducing solution (0.04M sodium sulphite (Fisher Scientific), 0.1g hydroquinone (Sigma) in ddH_2O) preheated to 45 °C in the water bath. Sections were incubated for 5 min or until the tissue developed intensive yellow colour. Tissue sections were subsequently dehydrated and mounted as described in section 2.4.9.

Grimelius stained tissue sections were examined to identify enteroendocrine cells and the number of those cells was scored in 50 half crypt-villi for each animal. The average number of enteroendocrine cells per half crypt-villus axis was calculated for each animal and further analysed as described in section 2.7.

2.3.3.5 Ki67 staining

Proliferating cells within the tissue have been identified using anti-Ki67 immunohistochemistry (section 2.4). The numbers as well as position of Ki67 positive cells were scored within the intestinal epithelium where the cell position of those cells was indicative of the localization and size of proliferative compartment within this tissue. The number of proliferating cells was assessed and scored in 50 half crypt-villi per tissue section. Furthermore the average number of Ki67 positive cells across those 50 crypt-villi was calculated for each animal in that cohort and analysed as described in section 2.7. Position of those proliferating cells was counted from the base of the intestinal crypt up all the way up to the villus tip where the bottom-most cell was indicated as #1. Ki67 positive cell positions from all animals belonging to the same experimental cohort were pooled together and analysed as described in section 2.7.

2.3.3.6 BrdU staining

5-bromo-2'-deoxyuridine (BrdU) can be incorporated into the newly synthesized DNA of replicating cells during the S phase of the cell cycle, substituting for thymidine. By performing anti-BrdU immunohistochemistry we are capable of detecting all cells that have been actively replicating their DNA. Therefore BrdU as well as Ki67 is a marker of proliferating cells however due to being limited to S phase, it is more specific.

Experimental mice were injected with BrdU at 2 or 24 hours prior to dissection and tissue harvest. Staining with anti-BrdU antibody was conducted according to generic protocol described in section 2.4. The numbers as well as position of BrdU positive cells at both 2 hour and 24 hour time point were scored within the intestinal epithelium. This quantification allowed for evaluation of overall proliferation activity as well as cell migration within the tissue. The number of proliferating cells was assessed and scored in 50 half crypt-villi per tissue section. The average number of BrdU positive cells per 50 crypt-villi was calculated for each animal in that cohort and analysed as described in section 2.7. Position of those proliferating cells was counted from the base of the intestinal crypt up all the way up to the villus tip where the bottom-most cell was indicated as #1. BrdU positive cell positions from all animals belonging to the same experimental cohort were pooled together and analysed as described in section 2.7.

2.3.3.7 Cleaved-Caspase-3 staining

Immunohistochemistry against cleaved caspase 3 was used to identify apoptotic cells in which caspase 3 is activated. Staining with anti-cleaved caspase 3 antibody was conducted according to generic protocol described in section 2.4. The number of cells in which positive staining was detected was scored in 50 half crypt-villi per tissue slide. The average number of apoptotic cells per half crypt-villus axis was calculated for each animal and further analysed as described in section 2.7.

2.4 Immunochistochemical staining (IHC)

2.4.1 Dewaxing and rehydrating of tissue sections

The tissue sections were dewaxed by the immersion 2 x 5 min in the xylene (Fisher Scientific) followed by the series of rehydration steps in decreasing concentration of ethanol (Fisher Scientific): two 3 min immersions in 100%, one 3 min immersion in 95% and one 3 min immersion in 70% ethanol. After the slides have reached 70% ethanol they were transferred into dH_2O prior to antigen retrieval step.

2.4.2 Antigen retrieval

Depending upon the primary antibody used as well as how long time ago the sections were cut, different methods of antigen retrieval were applied. All of those have involved using citrate buffer: either 1X Citrate Buffer (LabVision) or custom-made citrate buffer (10 mM sodium Citrate (Sigma) at pH 6.0). Most commonly applied method of antigen retrieval involved boiling water bath where the Coplin jar (R.A. Lamb) filled up with citrate buffer was placed in cold water bath and then gradually heated up to 100 °C. Once this temperature was reached the dewaxed and rehydrated sections were immersed in the pre-heated buffer and incubated at this temperature for a time specified in the protocol (Table 2.3). Another method involved using microwave either using a plastic box or pressure cooker to pre-heat the citrate buffer for 5 min at 900 W. Once pre-heated the slides were submerged in the buffer and incubated for 3 cycles of 5 min at 300 W with occasional shaking of the rack containing sections. For the pressure cooker, after the slides were immersed in the heated buffer, the pressure cooker lid was firmly closed and short cycle of 2 min at 900 W was applied until we have observed the rise in pressure in the pressure cooker, followed by

decrease in the power to 300 W for the remaining 15 min of the antigen retrieval cycle. After the antigen retrieval process was complete, the slides were left in the citrate buffer to cool down for minimum 30 min. Slides were briefly washed in dH_2O followed by 3 x 5 min washes in wash buffer: either 1X TBS (Sigma) or 1X PBS (Invitrogen) in dH_2O with 0.1% (v/v) TWEEN-20 (Sigma) according to the protocol (Table 2.3).

2.4.3 Endogenous peroxidise activity block

The activity of endogenous peroxidises was blocked by incubating tissue sections with hydrogen peroxide. Depending upon the particular primary antibody used, different concentrations and incubation times have been used indicated in Table 2.3. Either commercial peroxidise block solution (Envision+Kit, DAKO) or 30% hydrogen peroxide (Sigma) diluted to an appropriate concentration in distilled water. In cases when ready-made peroxidise block was used, the excess of wash buffer was removed by tapping dry, tissue area is circled with water-resistant pen and placed in the humidified slide chamber and tissue was overlaid with enough solution. Otherwise when using hydrogen peroxide made up from 30% stock solution, slides were placed in the Coplin jars containing enough solution to fully cover the tissue. After slides were incubated for required amount of time with blocking solution, the solution was removed and washed 3 x 5 min in wash buffer.

2.4.4 Non-specific antibody binding block

In order to reduce the non-specific antibody binding, tissue sections were incubated with normal serum (DAKO) or BSA (Sigma) which was diluted to a correct concentration in wash buffer. The specific blocking agent, its concentration and incubation time in regards to particular primary antibody is detailed in Table 2.3.

Generally, the serum from the species that secondary antibody was raised is used prior to primary antibody incubation (i.e. if a secondary antibody was raised in goat, normal goat serum is used as block against non-specific binding). In cases when peroxidise block was performed using 30% stock solution, the tissue sections were circled with water-resistant pen prior to covering the slide surface with 200 µl of blocking solution and incubating for time indicated in Table 2.3.

2.4.5 Primary antibody

Subsequent step after incubation is the removal of blocking serum and 200 µl of primary antibody diluted in the blocking serum solution was directly overlaid without washing sections in wash buffer. The dilution and incubation time and temperature for particular antibodies are outlined in Table 2.3. After the incubation, the tissue sections were washed 3 x 5 min in wash buffer.

2.4.6 Secondary antibody

The slides were removed from Coplin jars and placed in the humidified chamber and 200µl of an appropriate secondary was applied.

Depending whether the signal amplification was necessary for the specific protocol, different types of secondary antibodies were used. When signal amplification was needed, an appropriate biotinylated secondary antibody (DAKO) was diluted 1:200 in blocking serum solution. Otherwise, an appropriate Horseradish peroxidase (HRP) conjugated secondary antibody (Envision+Kit, DAKO) was applied directly onto the slides.

Detailed information about secondary antibodies applied and their incubation times is provided in Table 2.3. After the incubation, slides were washed 3 x 5 min in wash buffer.

2.4.7 Signal amplification

For those primary antibodies where Envision+Kit (DAKO) could not be used additional step including signal amplification was introduced into the protocol. The Avidin-Biotin Complex reagent (Vectastain ABC kit, Vector labs) was prepared as indicated by the manufacturer's instructions 30 min prior to application and stored at room temperature. Tissue was then covered with 200 µl of ABC reagent and left for 30 min incubation at room temperature, followed by 3 x 5 min washes in wash buffer.

2.4.8 Signal visualisation using DAB

Primary antibody binding was visualised by colourimetric detection with 3,3'-diaminobenzidine (DAB). Tissue sections were removed from humidified chamber and placed on the blue tissue roll and then covered with 200 µl of DAB solution (2 drops of DAB chromogen in 1 ml of DAB substrate (Envision+ Kit, DAKO)). Slides were incubated for 5-10 min until a sufficient level of staining was obtained followed by a 5 min wash in dH_2O.

2.4.9 Counterstaining, dehydration and tissue mounting

Tissue sections were placed in the slide wrack and counterstained in Mayers Haemalum (R.A. Lamb) for 1 min and subsequently washed under running tap water for 5 min. Slides were then transferred into 70% ethanol and dehydrated by consecutive washes in increasing concentrations of ethanol (1 x 3 min 70%, 1 x 3 min 95%, 2 x 3 min 100%) and 2 x 5 min washes in xylene until the tissue was mounted using DPX (R.A. Lamb).

Table 2.3 Antibody-specific conditions for immunohistochemical staining

Primary antibody	Manufacturer	Antigen retrieval	Non-specific staining block	Wash Buffer	Primary antibody incubation	Secondary antibody	Signal amplification
Anti-β-catenin	BD Transduction Labs #610154	20 min, 100°C, WB, citrate buffer (Thermo)	Peroxidase block (DAKO) 5 min, RT; 10% NRS, 30 min, RT	3 x 5 min TBS/T	1:300 in 10% NRS o/n, 4°C	Envision + HRP-conjugated anti-mouse (DAKO), 30 min, RT	N/A
Anti-BrdU	BD Biosciences #347580	20 min, 100°C, WB, citrate buffer (Thermo)	Peroxidase block (DAKO) 5 min, RT; 1% BSA, 30 min, RT	3 x 5 min PBS/T	1:150 in 1% BSA, 1h, RT	Envision + HRP-conjugated anti-mouse (DAKO), 30 min, RT	N/A
Anti-Brg1	Santa Cruz (G-7): sc-17796	20 min, 100°C, WB, citrate buffer (Thermo)	Peroxidase block (DAKO) 5 min, RT; 10% NRS, 30 min, RT	3 x 5 min TBS/T	1:200 in 10% NRS o/n, 4°C	Envision + HRP-conjugated anti-mouse (DAKO), 30 min, RT	N/A
Anti-Brm	Santa Cruz (N-19): sc-6450	20 min, 100°C, WB, citrate buffer (Thermo)	Peroxidase block (DAKO) 5 min, RT; 5% NRS, 30 min, RT	3 x 5 min TBS/T	1:200 in 10% NRS o/n, 4°C	Biotinylated anti-goat (DAKO), 1:200 in 10% NRS, 30 min, RT	ABC Kit (Vector Labs)
Anti-CD44	BD Pharmigen #550538	20 min, 100°C, WB, citrate buffer (Thermo)	1.5% H_2O_2, 15 min, RT; 10% NRS, 30 min, RT	3 x 5 min TBS/T	1:50 in 10% NRS, 1h, RT	Biotinylated anti-rat (DAKO), 1:200 in 10% NRS, 30 min, RT	ABC Kit (Vector Labs)
Anti-Cleaved Caspase 3	Cell Signalling Technology #9661	Boil in PC, 15 min under pressure, citrate buffer (Thermo)	3% H_2O_2, 10 min, RT; 5% NGS, 1h, RT	3 x 5 min TBS/T	1:200 in 5% NGS, 2 days, 4°C	Biotinylated anti-rabbit (DAKO), 1:200 in 5% NGS, 30 min, RT	ABC Kit (Vector Labs)
Anti-Hes5	Millipore: AB5708	20 min, 100°C, WB, citrate buffer (Thermo)	Peroxidase Block (DAKO) 5 min, RT; 5% NGS, 30 min, RT	3 x 5 min TBS/T	1:200 in 5% NGS, o/n, 4°C	Envision + HRP-conjugated anti-rabbit (DAKO), 1h, RT	N/A
Anti-Ki67	Vector Labs #VPK452	20 min, 100°C, WB, citrate buffer (Thermo)	0.5% H_2O_2, 20 min, RT; 20% NGS, 30 min, RT	3 x 5 min TBS/T	1:20 in 20% NRS o/n, 4°C	Biotinylated anti-mouse (DAKO), 1:200 in 20% NGS, 30 min, RT	ABC Kit (Vector Labs)
Anti-Lysozyme	Neomarkers #RB-372-A	20 min, 100°C, WB, citrate buffer (Thermo)	1.5% H_2O_2, 15 min, RT; 10% NGS, 30 min, RT	3 x 5 min TBS/T	1:100 in 10% NGS, 1 hour, 4°C	Envision + HRP-conjugated anti-rabbit (DAKO), 30 min, RT	N/A

2.5 Gene expression analysis

During all procedures involving RNA handling and processing additional care was taken to ensure that all plasticware and glassware was RNA free. All solutions used within the protocol were prepared using RNAse free water (Sigma) and sterile filter-tips were used throughout.

2.5.1 RNA extraction from tissue

2.5.1.1 Homogenisation of tissue

Frozen at -80 °C tissue samples were removed and adequate amount was placed in screw-cap tubes containing 1.4 mm ceramic beads (Lysing matrix D tubes, MP Biomedical) overlaid with 1 ml Trizol (Invitrogen). Prepared samples were homogenised in the Precellys24 homogeniser (Bertin Technologies) at 6500 RPM for 2 x 45 second cycles followed by the centrifuging of tubes at 11000 x g for 10 min at 4 °C. The centrifugation step is necessary in order to pellet the ceramic beads and tissue debris created during homogenisation.

2.5.1.2 RNA extraction

The supernatant created after centrifugation was carefully transferred without disturbing ceramic beads into a fresh 1.5 ml eppendorf tubes and 200 µl of pre-cooled on ice chloroform (Fisher Scientific) was added. The contents of tubes were shaken vigorously for 30 seconds and allowed to stand at room temperature for 3 min. All eppendorf tubes were centrifuged at 11000 x g for 15 min at 4 °C. The top, aqueous phase (approximately 500 µl) containing RNA was transferred into fresh eppendorf tubes containing 500 µl of isopropanol. Tubes were gently inverted until all contents mixed well and incubated at 4 °C over night. The following day tubes were centrifuged at the maximum speed for 15 min at room temperature. The supernatant was carefully discarded and the pellet was washed with 500 µl pre-cooled 70% ethanol. The tube contents were centrifuged at the maximum speed for 5 min at room temperature and the resulting supernatant was removed leaving the pellet to air dry for 5-10 min. The pellet was then dissolved in 20 µl of RNAse free H_2O (Sigma), placed on the heat block at 65 °C for 10 min followed by quenching on ice. While sample were on the ice, the purity and concentration of extracted RNA was determined using NanoVue Plus (GE

Healthcare). RNA samples were stored at -80 °C with exception of 10 µg of RNA which underwent further DNase treatment.

2.5.1.3 DNase treatment of RNA samples

DNase treatment of extracted RNA was performed using RQ1 RNase-Free DNase (Promega) according to the protocol described at: http://www.promega.co.uk/~/media/Files/Resources/Protocols/Product%20Information%20Sheets/G/RQ1%20RNase-Free%20DNase%20Protocol.pdf.

For each digestion reaction 10 µg of extracted RNA was used and mixed with 10 µl of RQ1 RNase-Free DNase, 5 µl of RQ1 RNase-Free DNase 10X Reaction Buffer and made up to 50 µl with RNAse free H_2O (Sigma). The contents of tubes were placed on the heating block at 37 °C for 30 min followed by addition of 5 µl of RQ1 DNase STOP Solution to terminate the DNAse digestion reaction. Tubes were incubated on the heating block at 65 °C for 10 min in order to inactivate the DNase. All samples were quenched on ice and the purity and concentration of DNAse-treated RNA was determined using NanoVue Plus (GE Healthcare). RNA samples were stored at -80 °C until needed.

2.5.1.4 Determining of RNA quality

The quality of total RNA extracted – its integrity and some initial information about the yield was assessed by elecrophoresis on a denaturing agarose gel as described in Qiagen Bench Guide (Qiagen). The aliquot of RNA samples containing 2 µg of RNA were mixed with an appropriate amount of RNA 5X buffer (0.25% Bromophenol blue (Sigma), 4 mM EDTA (Sigma), 0.9 M formaldehyde (Sigma), 20% glycerol (Sigma), 30.1 % formamide (Sigma), 4X FA gel buffer (instructions bellow)). Samples were incubated at 65 °C for 3-5 min, quenched on ice, followed by loading onto a denaturing agarose gel (1% agarose (Eurogentech), in 1X FA gel buffer (20 mM 3-(N-Morpholino) propanesulfonic acid (MOPS, Sigma), 5 mM sodium acetate (Sigma), 1 mM EDTA (Sigma), 0.22 M formaldehyde (Sigma), 0.1 µg/ml Ethidium bromide (Sigma) in dH2O)). Prepared gel was run in FA gel running buffer (20 mM 3-(N-Morpholino)propanesulfonic acid (MOPS, Sigma), 5 mM sodium acetate (Sigma), 1 mM EDTA (Sigma), 0.25 M formaldehyde (Sigma) in dH_2O) at 50 V for 1 hour. RNA products were visualised in UV light using ChemiDoc MP apparatus (BioRad). Intact total RNA run on a denaturing gel should result in clear and sharp 28S and

18S ribosomal RNA bands therefore the gel was carefully assessed for the presence of appropriate ratio between 28S rRNA band and 18S rRNA band intensiveness and lack of any smeared RNA bands.

2.5.2 Preparation of cDNA

cDNA synthesis was performed using Superscript III Reverse Transcriptase (Invitrogen) according to the protocol described at http://tools.lifetechnologies.com/content/sfs/manuals/superscriptIII_man.pdf

First-strand cDNA synthesis was done in strip tubes where 2 µg of total RNA was mixed with 0.5 µl of 500 ng/µl random primers (Promega), 1 µl of 10 mM dNTPs (Bioline) and made up to 13 µl with DNAse free H_2O (Sigma). Prepared reaction volume was incubated at 65 °C for 5 min and then quenched on ice for at least 1 min. The contents of tubes were briefly centrifuged to collect all the volume to which 7 µl enzyme mix was added (4 µl 5X First Strand Buffer, 1 µl 0.1 M DTT, 1 µl RNAse-free H_2O (Sigma), 1 µl SuperScript III RT (200 units/µl) per each reaction strip tube. All contents of tubes were gently mixed by pipetting and incubated at 25 °C for 10 min, 50 °C for 1 hour, 70 °C for 15 min and held at 4 °C. At the end of the incubation 20 µl of DNAse free dH2O was added to 20 µl volume of reaction and 1 µl of the resulting cDNA was used per reaction in quantitative RT-PCR. Negative control cDNA samples were synthesised in the same manner as mentioned above however no Superscript III enzyme was added to the enzyme mix.

2.5.3 Quantitative real-time PCR analysis

2.5.3.1 Primer design

Primers used for qRT-PCR analysis that have not been previously published were designed using Primer3 software (http://fokker.wi.mit.edu/primer3/input.htm). Moreover BLAST engine (http://www.ensembl.org/Multi/blastview) was used to check for any mispriming of those primers followed by primer synthesis by Sigma Genosys. Therefore while designing and selecting for sets of primers some general guidelines were followed. The primers have to be specific to the target gene with no amplification of pseudogenes or other related genes. The primer should span one or more introns to avoid amplification of sequences in genomic DNA. In order to obtain the most efficient and the most consistent results amplicons were

designed to yield PCR products of 100 – 200 bp. The annealing temperature should be between 58–60°C.

All primers designed should be tested to select the ones that have the highest signal-to-noise ratio. The primer and probe sequences used for qRT-PCR are listed in Table 2.4.

Table 2.4 Primer and probe sequences for qRT-PCR analysis

Name	Forward primer	Reverse primer
Brm	CGGGATGTGGACTACAGTGA	AGCCGTACCTCCTCTTCCAT
Brg1	Probe pre-designed cat n: 4331182	Probe pre-designed cat n: 4331182
β-catenin	AGTCCTTTATGAATGGGAGCAA	TCTGAGCCCTAGTCATTGCATA
c-Myc	CTAGTGCTGCATGAGGAGACAC	GTAGTTGTGCTGGTGAGTGGAG
CD44	ATCGCGGTCAATAGTAGGAGAA	AAATGCACCATTTCCTGAGACT
Cyclin D1	ACGATTTCATCGAACACTTCCT	GGTCACACTTGATGACTCTGGA
E-cadherin	CAGATGATGATACCCGGGACAA	GGAGCCACATCATTTCGAGTCA
Hes1	TCATGGAGAAGAGGCGAAGG	GGTTCCGGAGGTGCTTCAC
Hes5	TCAGCTACCTGAAACACAGCA	TAGTCCTGGTGCAGGCTCTT
Math1	ATGCACGGGCTGAACCA	TCGTTGTTGAAGGACGGGATA

2.5.3.2 Setting up of qRT-PCR reaction

Reactions set up in the 96-well plate were run on StepOnePlus real-time PCR system supplemented with StepOne software version 2.2.2 (Applied Biosystems) whereas reactions loaded onto 384-well plate were run on QuantStudio 7 Flex aided with QuantStudio 6 and 7 Flex Real-Time PCR System Software version 1.0. All reactions were run as triplicates and minimum of four biological replicates were run per each qRT-PCR. Samples lacking cDNA were set up as negative controls in order to be able to detect possible contamination or non-specific amplicon in the reaction. β-actin housekeeping gene was used as a reference gene for each qRT-PCR run.

All qRT-PCR reactions were run using either Fast SYBR Green Master Mix (Applied Biosystems) or TaqMan Universal PCR Master Mix (Applied Biosystems) according to the manufacturer's instructions in the 384-well PCR plate (Applied Biosystems). TaqMan assay was specifically used for intestinal stem cell markers such as Ascl2, Lgr5 and Olfm4 where instead of primers, custom designed TaqMan probes for those stem cell markers were used. Each TaqMan probe comprises oligonucleotide with a reporter dye at its 5' end and a

quencher dye at its 3' end. During the reaction, TaqMan probe undergoes cleavage by AmpliTaq Gold DNA Polymerase which results in separation of dyes at their respective ends of the probe and consequently increases the fluorescence of the reporter. This increase in reporter florescence is recorded as it is a direct indication of the amount of PCR product that becomes accumulated (Figure 2.2). In contrast, the SYBR Green assay takes advantage of the chemistry of SYBR Green I dye as a way of detecting the PCR product due to the binding of this dye to the newly generated double-stranded DNA (Figure 2.2). The primer sequences and probes used for qRT-PCR reactions using SYBR Green and TaqMan assay are indicated in Table 2.4. For all reactions using SYBR Green assay, appropriate forward and reverse primers (100 mM) were mixed in equal quantities and further diluted to concentration of 10 mM with 0.5 µl of this primer mix used for each reaction within the assay.

Master mix containing 5 µl of either SYBR Green Mix or TaqMan Mix, 4 µl of RNAse-free H_2O and 0.5 µl of appropriate primer mix (10 mM) or TaqMan probes(10 mM) was prepared and each reaction well on the 384-well PCR plate was loaded with 9 µl of this mix. Subsequently 1 µl of cDNA was loaded to individual wells and plate was sealed with optically clear sealing film (Applied Biosystems). Plate was centrifuged at 8000 RPM for 1 min.

All reactions using SYBR Green were run under following thermocycler conditions: 95 °C for 10 min followed by 40 cycles (95 °C for 15 seconds, 60 °C for 30 seconds, 72 °C for 30 seconds). In case of running TaqMan reactions, the cycling conditions were following: 50 °C for 2 min, 95 °C for 10 min followed by 40 cycles (95 °C for 15 seconds, 60 °C for 1 min).

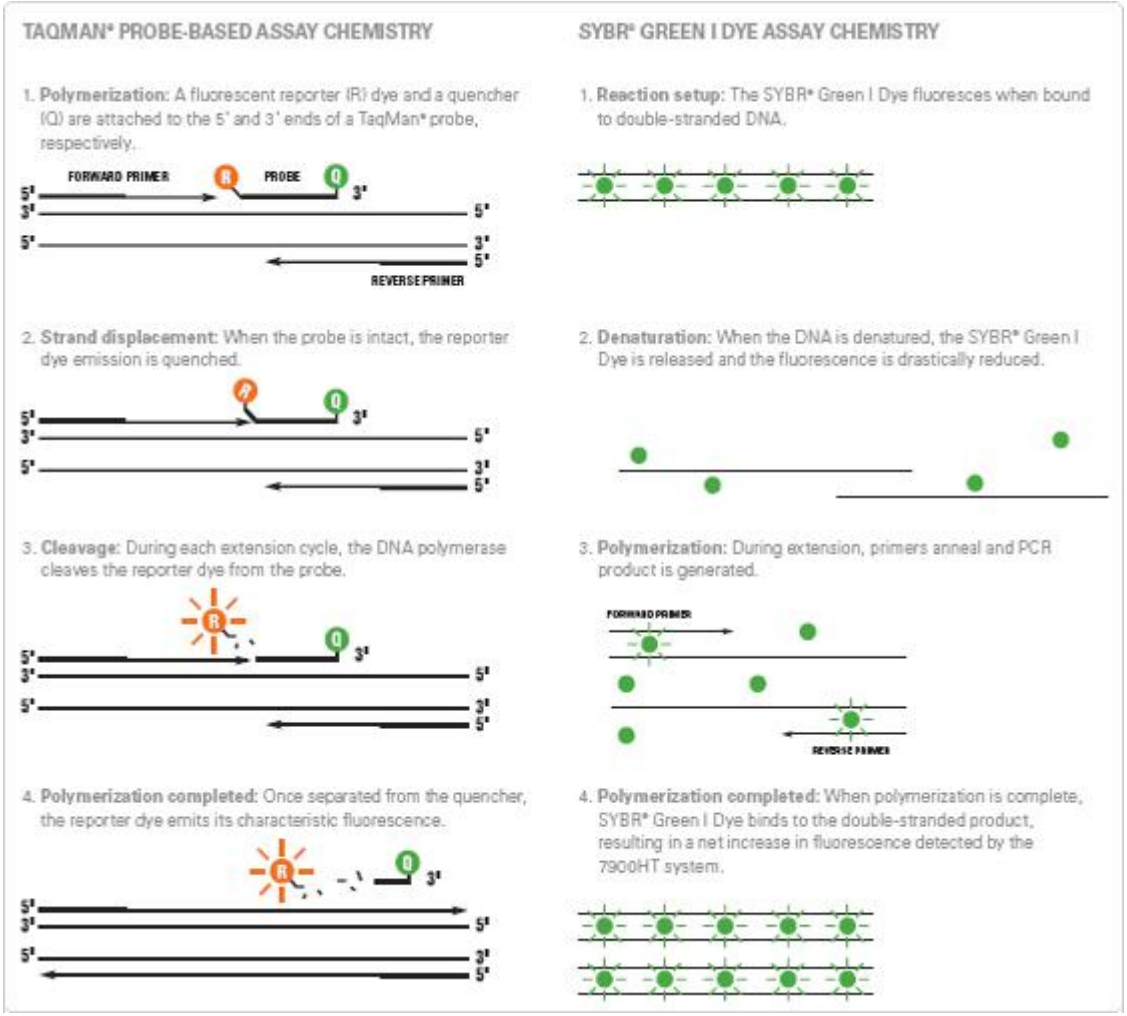

Figure 2.2 The differences between SYBR Green-based and TaqMan-based qRT-PCR reactions. The diagram was taken from http://www.lifetechnologies.com/uk/en/home/life-science/pcr/real-time-pcr/qpcr-education/taqman-assays-vs-sybr-green-dye-for-qpcr.html

2.5.3.3 Analysis of qRT-PCR data

The data collected automatically by StepOne Software from samples with reproducible cycle time (C_t) values were analysed.

For the data analysis, all C_t values were examined manually from raw data to ensure all replicates of the reaction can be used. The difference in the cycle time ΔC_t values were calculated between cohorts of experimental animals by normalising each reaction to β-actin C_t values for that reaction. β-actin was used as a reference gene for all reactions performed using either SYBR Green or TaqMan assay. The average ΔC_t values were calculated for each

cohort of experimental animals and those ΔC_t values were tested for significant differences using Mann-Whitney U test. In order to compare C_t values of a target gene to β-actin reference gene as a fold difference $\Delta\Delta C_t$ data for each biological group was further analysed using the formula: $2^{\Delta\Delta CT}$(Livak and Schmittgen, 2001). The data showing fold changes values were graphically represented as bar graphs using Microsoft Office Excel.

2.5.4 *In situ* hybridization

In situ hybridization method was used as a means of examining the expression of Wnt-independent intestinal stem cell marker *Olfm4* using anti-sense RNA probes for *Olfm4* which are complementary to the its mRNA sequence and labelled with digoxigenin (DIG). The binding of the probe visualised the presence of purple staining within the tissue was detected using anti-digoxigenin antibody conjugated to alkaline phosphatase. The probe for *Olfm4* was a gift from Hans Clevers's group (Hubrecht Institute, Netherlands). Due to the sensitivity of riboprobe all the glassware used in this protocol was treated at 200°C overnight in baking oven whereas dH_2O was treated with DEPC (Sigma).

2.5.4.1 Probe synthesis

The Olfm4 ribeprobe was synthesised through the process of linearisation of plasmid DNA, RNA polymerase reaction from the T7 promoter and DIG labelling of probes. 30 µg of plasmid DNA was linearised using NotI restriction enzyme (NEB) according to the manufacturer's protocol. Linear DNA required was then extracted using phenol-chloroform method (as described in section 2.5.1.2), the concentration was determined using NanoVue Plus (GE Healthcare) and dissolved at concentration of 1µg/µl in 10 Mm Tris (pH 8.0). Prepared linear plasmid DNA was as a template for probe transcription using T7 RNA polymerase (Roche) followed by the DIG labelling of riboprobes.

The labelling of riboprobes was performed for 2 hours at 37°C using components enlisted in Table 2.5. DNA template was DNase treated by incubation with 20 units of DNase I (Ambion) for 15 minutes at 37°C followed by the addition of 1µl of 0.5 M EDTA (ph 8.0). Ethanol precipitation was performed to purify riboprobes and 10 µl aliquots of those probes were stored at -80°C until needed.

Table 2.5 Components of probe-labelling reaction

Compound	Volume
RNase-free H_2O	12 µl
Transcription buffer 10X (Roche)	2 µl
DIG RNA labelling mix (Roche)	2 µl
RNA polymerase T7 (Roche)	2 µl
RNase inhibitor (Promega)	1 µl
DNA at 1 µg/µl	1 µl

2.5.4.2 Probe hybridization

Tissue slides were dewaxed in 2 x 10 min xylene followed by the rehydration step involving immersion in the decreasing concentrations of ethanol: 2 x 100% for 1 min, 95%, 85%, 75% 50% and 30% - all for 30 sec. The slides were transferred to 1X saline for 5 min and then washed in 1X PBS for 5 min. Endogenous alkaline phosphatase activity was blocked by the immersion of slides in 6% hydrogen peroxide solution in 1X PBS for 30 min followed by rinsing off in 1X PBS for 5 min. Ice-cold 4% RNase-free PFA (paraformaldehyde (Sigma), DEPC H_2O, 1 M NaOH in 1X PBS) was used for fixation followed by two washes in 1X PBS for 5 min. Next step involved incubation for 5 min in Proteinase K (Roche) (1 M Tris pH 8.0, 0.5 M EDTA, 20 µg/ml Proteinase K in DEPC H_2O) and subsequent two 5 min washes in 1X PBS. The disintegration of tissues on the glass slides was prevented by postfixing in ice-cold 4% PFA for 5 min. The slides were rinsed in DEPC dH_2O for 2 min and immersed into TEA HCl/acetic anhydrite solution (0.01 M acetic anhydrite (Sigma) in 0.1 M triethanolamine hydrochloride (Sigma)) for 10 min. Slides were then washed in 1X PBS for 5 min and 1X saline for 5 min followed by the dehydration in preparation for probing in increasing concentrations of ethanol: 30%, 50% for 30 sec, 75% for 5 min, 85%, 95% for 30 sec and finally twice in 100% for 30 sec. Slides were air-dried for 30-60 min and transferred to dark boxes in which overnight incubation of probe was performed. Those boxes were lines with 3 mm paper saturated with moisture buffer (5X saline sodium citrate buffer (SSC) (Sigma), 50% v/v formamide (Sigma) in dH_2O). The probe preparation included heating of probe at 80°C for 3 min followed by quenching on ice. Hybridization buffer (5X SCC, 50% formamide, 1% SDS, 0.05 mg/ml heparin (Sigma), 0.05 mg/ml calf liver tRNA (Merck) in dH_2O) was heated to 80°C and then mixed with probe at concentration of 1 µl of probe in 99 µl of hybridization buffer. Prepared mixture was then added to each slide and parafilm-

covered to avoid the evaporation. Dark boxes were then sealed with electrical tape and incubated at 65°C overnight in the water bath.

2.5.4.3 Post-hybridization treatment

Following overnight incubation with probe, tissue slides were incubated in the pre-warmed to 65°C 5X SSC buffer for 15 min and then immersed twice in pre-warmed solution I (50% formamide, 5X SSC, 1% (v/v) SDS(Sigma)) at 65°C for 15 min. Next step involved 3 washes at room temperature in solution II (0.5 M NaCl (Sigma), 0.01 Tris pH 7.5 (Sigma), 0.1% TWEEN-20 (Sigma)) and subsequent digestion of unhybridized probe by incubation with RNaseH (Roche) for 45 min at 37°C. A series of washes: two 5 min washes in warm solution II at 65 °C followed by another 2 x 30 min in solution III (50% formamide, 5X SSC) at 65°C and two 10 min washes in 1X PBS preceded application of DIG-labelled antibody. Slides were blocked using 10% heat-inactivated sheep serum (DAKO) in PBS/T for 3 hours. Anti-DIG antibody (Roche) was pre-absorbed in 1% sheep serum containing 3 mg/ml small intestinal powder for 3 hours at 4°C mixed using rotor. The antibody was then diluted to 1:2000 concentration in 1% sheep serum in PBS/T whereas slides were washed in PBS/T for 5 min followed by adding of 100 µl of prepared antibody on the top of tissue and overnight incubation at 4°C.

2.5.4.4 Signal detection

After probe binding and series of post-hybridization washes, the next step involved signal detection using BM Purple (Roche). Slides were washed 3 times in PBS/T for 5 min and then again washed in PBS/T twice for 30 min. Preconditioning of slides in NTMT (0.1 M sodium chloride, 0.1 M Tris pH 9.5, 0.05 M magnesium chloride (Sigma), 0.1% v/v TWEEN-20, 2 M Levamisole (Sigma)) by three 5 min washes proceeded applying of BM purple substrate (Roche) and incubation in the dark boxes for a required amount of time. Once the desired level of signal was detected, slides were washed in PBS/T for 10 min followed by wash in dH_2O for 30 min. Counterstaining using Eosin Y Solution (Sigma) for 5 seconds was followed by rinsing in dH_2O for 5 min, air-drying of slides for 30 min, immersion in xylene for 10 seconds and finally mounting using DPX mounting media (R.A. Lamb)

2.6 Protein analysis

2.6.1 Protein extraction from collected tissues

The samples of selected tissues: small intestine, large intestine and liver were removed from -80 °C storage and kept on dry ice until ready to be used to avoid defrosting and degradation of the tissue. Fresh cell lysis buffer consisting of 1 M Tris-HCl, pH 8.0, 0.5 M EDTA pH 8.0, 10% NP-40 (Sigma), ddH_2O with addition of protease inhibitors (cOmplete Mini Protease Inhibitor Cocktail Tablets, Roche) and phosphatase inhibitors (500 mM sodium β-glycerophosphate (Calbiochem), 0.5 M sodium fluoride (Sigma), 200 mM sodium pyrophosphate (Sigma), 20 μM Calyculin A from Discodermia calyx (Sigma)) was prepared prior to the extraction of the protein. 200 μl of ice cold lysis buffer were aliquoted into SpinLyse tubes placed on ice, tissue samples were briefly removed from dry ice and small pieces of frozen tissue were dropped into prepared tubes. All tubes were placed in Precellys homogeniser and span at maximum setting (2 cycles of 45 sec at 6500 RPM). Once the froth was settled out, the cell lysate was transferred into fresh eppendorf using 1 ml syringe and 23G needle and passed through needle 5-8 times. The tubes were briefly placed on ice prior to being centrifuged in the pre-cooled centrifuge at 13.3 x g for 10 min at 4 °C. The obtained supernatant was transferred into a fresh eppendorf and centrifuged at the same settings again in order to remove any insolubles. The collected supernatant was aliquoted into three separate 0.5 ml tubes: 10 μl for protein assay, 100 μl and all remaining volume of cell lysate which were snap frozen in liquid nitrogen and stored at -80 °C.

2.6.2 Quantification of protein concentration

To determine the protein concentration in the extracted tissue sample I have used Pierce BCA assay (Thermo Scientific). BSA was provided as a stock solution at 2 mg/ml and was further diluted to the concentration of 100 μg/ml in the cell lysis buffer. The serial dilutions of BSA (from 5 μg/ml to 35 μg/ml) in 1X PBS along with blank solutions containing 100 μl of 1X PBS were loaded in 96-well microtitre plate. 10 μl aliquot of the cell lysate was defrosted on ice and serial dilutions (1:100, 1:200, 1:400 in 1X PBS) of the protein were also prepared on the plate. All of the solutions: BSA, blanks and protein extracts were loaded in duplicates. BCA kit reagents A and B were mixed at the ratio 50:1 and 100 μl of obtained solution was added to each well and mixed well by pipetting. The plate was sealed and wrapped in

aluminium foil and incubated for 1 hour at 37 °C prior to the plate being read at 590 nm on a microplate reader (BioTek). All data were entered in Excel (Microsoft Office 2007) and standard curve was plotted on the basis of BSA serial dilutions. In respect to the standard curve, the protein concentrations of the extracted tissue samples were calculated together with respective volumes of the lysate to contain 30 µg of protein.

2.6.3 Analysis of protein levels by Western blotting

2.6.3.1 Preparation of protein samples

Previously frozen and stored at -80 °C protein extracts were placed on ice to defrost. The calculated volume of the protein extract to contain 30 µg of protein was removed and transferred into fresh 1.5 ml eppendorf. Appropriate amount of cell lysis buffer was added to the protein extract to the total volume of 15µl and further 15 µl of 2X Laemmli buffer (Sigma) were added. The samples together with molecular weight rainbow marker were heated to 95 °C on the heat block for 10 min and then quenched on ice prior to the loading.

2.6.3.2 Casting of SDS-PAGE gels

SDS-PAGE gels were casted in Mini-Protean III (BioRad) gel casting apparatus using 1.5 mm spacers. Prior to the gel casting, all casting plates were well washed to remove any remaining gel, wiped with 70% ethanol and left to air dry. Depending upon the expected molecular weight of the target protein, solutions for resolving gels at different concentrations were prepared along with solution for 5% stacking gels according to the Table 2.6. Once the gel casting apparatus was clean and assembles, the required amount of TEMED was added to resolving solution and the mixture was immediately poured using stripette in between the casting plates up to about 1.5 cm from the top of the short plate. The resolving gel solution was overlaid with 1 ml of ddH_2O to prevent the gel from drying. The gel was allowed to set and then the water was drained off onto a tissue paper. TEMED was added and mixed with stacking gel solution which was again immediately poured into the gel cast until it was overflowing the edge between two plates. The 1.5 mm 10-well comb was carefully inserted to avoid any bubbles to be formed and the gel was left to set. Once completely set, the plates containing gels were removed from the gel casting apparatus and kept wrapped in cling film to avoid drying and shrinking of gel.

Table 2.6 Gels and solutions used for quantitative protein analysis by Western blotting

10% resolving polyacrylamide gel (2 gels)	**5% stacking polyacrylamide gel (2 gels)**
6.8 ml dH_2O	6.9 ml dH_2O
8.4 ml 30% acrylamide/bisacrylamide (Sigma)	1.7 ml 30% acrylamide/bisacrylamide (Sigma)
9.4 ml 1 M Tris-HCl pH 8.8	1.3 ml 1 M Tris-HCl pH 6.8
250 µl 10% (w/v) SDS (Sigma)	100 µl 10% (w/v) SDS (Sigma)
72 µl 25% (w/v) Ammonium persulphate (Sigma)	66 µl 25% (w/v) Ammonium persulphate (Sigma)
13.2 µl N, N, N, N-tetramethylethylenediamine (TEMED, Sigma)	13.2 µl N, N, N, N-tetramethylethylenediamine (TEMED, Sigma)

5X Running Buffer	**1X Transfer Buffer**
950 ml dH_2O	800 ml dH_2O
15.1 g Tris base	2.9 g Tris base
94 g Glycine	14.5 g Glycine
50 ml 10% (w/v) SDS (Sigma)	100 ml Methanol (Fischer)

2.6.3.3 Protein separation using SDS-PAGE gels

The pre-casted gels were assembled onto the Mini-Protean III (BioRad) electrophoresis tank which was filled with 400 ml of 1X running buffer (Table 2.6). The combs were carefully removed from the gels and each well was rinsed with running buffer by repeated pipetting up and down to remove any unwanted pieces of the gel. Full-range Rainbow molecular weight marker (Amersham), cell lysate control and prepared protein samples were loaded into the appropriate wells. Gels containing 7% or 10% resolving gel were run at 130V and 15% gels – at 200V until the dye run out of the end of the gel.

2.6.3.4 Protein transfer onto nitrocellulose membrane

As soon as the protein elecrophoresis was completed the gels were released from the plates and submerged in the transfer buffer (Table 2.6). The wet electroblotting system (Flowgen Biosciences) was placed in the polystyrene box filled up with ice ready for the assembly. The blots were set up by placing a pre-soaked in transfer buffer elements on the top of plastic blot holder in the following order: sponge, 2 sheets of 3 MM blotting paper (Whatman) and the gel. The Amersham Hybond-ECL nitrocellulose membrane (GE Healthcare) was carefully placed on the top of the gel to avoid any air bubbles followed by another 2 sheets of blotting paper, sponge and plastic blot holder. All assembled blots were placed into the

electroblotting tank in a correct orientation and filled up with transfer buffer. The transfer was run at 100V for 1 hour for all target proteins with exception to Brg1 run for 18 hours at 65 mA.

2.6.3.5 Generic protocol for membrane probing

Once the transfer was completed, the membrane was removed from the sandwiched elements of blots and placed in the vessel to be blocked in 5% milk powder in TBS/T for a minimum of 1 hour at RT with agitation. Primary antibodies were diluted according to the manufacturer recommendations in 5% blocking buffer or 1-5% BSA in TBS/T and the membrane was incubated with the antibody with agitation in the conditions specified in the Table 2.7. At the end of incubation with primary antibody, the membrane was removed and washed 3 x 15 min in TBS/T. Remaining primary antibody was placed in the Falcon tube and frozen at -20°C to be re-used in future experiments. Secondary HRP-conjugated antibody was diluted in the blocking buffer (Table 2.7), applied on to the membrane and incubated with agitation. The secondary antibody was poured off and the membrane was washed 3 x 15 min in TBS/T. The membrane was drained off the excess TBS/T and appropriate ECL detection reagent kit (Amersham) was used according to manufacturer's instructions to develop the membrane depending on the abundance of the target protein and the specificity of primary antibody used. After the incubation with ECL reagents, the membrane was briefly drained and placed in the plastic pocket inside of the cassette ensuring no air bubbles formed between the membrane and the pocket.

Table 2.7 Outline of antibody-specific conditions for Western blotting

Primary antibody	Manufacturer	Primary Ab conditions	Secondary Ab conditions
Anti-active-β-catenin	Millipore clone 8E7; #05-665	1:2000 in 5% milk in TBS/T; o/n at 4°C	HRP-conjugated anti-mouse (GE Healthcare) 1:2000 in 5% milk in TBS/T, 1h at RT
Anti-total-β-catenin	Cell Signalling; #9562	1:3000 in 5% milk in TBS/T; o/n at 4°C	HRP-conjugated anti-rabbit (GE Healthcare) 1:2000 in 5% milk in TBS/T, 1h at RT
Anti-Brg1	Santa Cruz (G-7); #sc-17796	1:200 in 5% milk in TBS/T; o/n at 4°C	HRP-conjugated anti-mouse (GE Healthcare) 1:2000 in 5% milk in TBS/T, 1h at RT
Anti-Hes1	Millipore; #ab5702	1:1000 in 5% milk in TBS/T; o/n at 4°C	HRP-conjugated anti-rabbit (GE Healthcare) 1:2000 in 5% milk in TBS/T, 1h at RT
Anti-Hes5	Millipore; #ab5708	1:2000 in 5% milk in TBS/T; o/n at 4°C	HRP-conjugated anti-rabbit (GE Healthcare) 1:2000 in 5% milk in TBS/T, 1h at RT
Anti-Math1	Abcam; C-terminal #ab137534	1:1000 in 5% milk in TBS/T; o/n at 4°C	HRP-conjugated anti-rabbit (GE Healthcare) 1:2000 in 5% milk in TBS/T, 1h at RT
Anti-Notch1 ICD	Abcam; # ab8925	1:500 in 5% milk in TBS/T; o/n at 4°C	HRP-conjugated anti-rabbit (GE Healthcare) 1:2000 in 5% milk in TBS/T, 1h at RT
Anti-β-actin	Sigma; A5316	1:5000 in 5% milk in TBS/T; o/n at 4°C	HRP-conjugated anti-mouse (GE Healthcare) 1:2000 in 5% milk in TBS/T, 1h at RT

2.6.3.6 Signal detection

Enhanced chemiluminescent (ECL) signal produced by the secondary antibody-bound HRP enzyme was detected by radiograph exposure. The piece of X-ray film (FujiFilm Super RX blue background) was exposed to the blots in the dark room for various amounts of time until we obtained good quality images. The exposed film was fed into and processed by an automatic X-ray film processor (Xograph Compact X4). Processed films were placed back in the cassette containing the original blot as the identification of target protein is possible after correct labelling of the position of molecular weight markers on the film and comparing it to expected molecular weight described by the primary antibody manufacturer. The membrane was washed 3 x 15 min in TBS/T, placed in 50 ml Falcon tube of TBS/T and stored at 4 °C until needed again.

2.6.3.7 Evaluation of protein levels and densitometry analysis

Each membrane probed with specific target antibody was then re-probed with β-Actin antibody, a house keeping gene to ensure the equal loading of the extracted proteins. The processed film were scanned using GelDoc and assess by densitometry using ImageJ. The

amount of the target protein was normalized to the levels of β-Actin which ensures that any errors can be corrected for. The quantity of protein was represented as a percentage relative to control.

2.7 Statistical and quantitative analysis of data

2.7.1 Quantitative analysis of histological traits

Histological quantification of stained tissue sections was carried out using an Olympus BX43 light microscope. Initially the tissue of interest was assessed for sectioning artefacts and regions of epithelium to be scored were carefully selected as means to maintain consistency of quantification where proximal ends of both small and large intestine were chosen for the analysis. All histological traits that were quantifiable such as crypt length, villus length, number of proliferating and apoptotic cells, number of differentiated cells were scored on the appropriately stained tissue slides. Minimum of 50 crypts or 50 crypt-villi were assessed per mouse and at least 4 experimental animals of the same genotype were analysed. Individual scores for crypt or crypt-villus were totalled and averaged out to generate the values per mouse. Furthermore the scores from all animals of the same genotype were used to generate the score per experimental cohort and standard deviation for that experimental group. This data were represented as histograms where the average score for experimental cohort was plotted together with error bars representing standard deviation for that group. The values per mouse have been used to test the significance difference between the averages for particular experimental groups. Microsoft Office Excel 2007 was primary program used to graphically present the data.

2.7.2 Comparison of means

Initially all quantifiable data were tested for normal distribution using the R statistical software. Normally distributed data was then tested for significant difference between averages of experimental groups using One-Way ANOVA in SPSS software (IBM SPSS Statistics 20). In cases where more than two experimental cohorts were compared, in addition to One-Way ANOVA, Post-Hoc Tukey's test was used to make pair-wise comparisons between those cohorts.

Data that have been initially found not to be normally distributed were tested for significant difference using Mann-Whitney U test.

All mentioned above statistical tests were performed using SPSS software and a significant difference between the means was accepted if p value was equal or less than 0.05. Statistical significance of the data was indicated on the histograms representing that data by "*" symbol where p value was equal or less than 0.05.

2.7.3 Kolmogorov-Smirnov Z Test

Differences in the distribution between two data sets were tested using Kolmogorov-Smirnov Z test. Datasets tested included cell types such as distribution of Paneth cells as well as some histological traits like proliferation markers such as BrdU positive and Ki67 positive cells. Positions of the above mentioned cells were recorded in a specific manner in a Microsoft Office Excel spreadsheet where each half crypt-villus structure was represented as a single column of ascending numbers. Cells were counted from the base of the intestinal crypt with the bottom-most cell was indicated as #1, all the way up to the villus tip where each particular row meant cell position within half crypt-villus counted. Positive cells were recorded as 1 whereas negative cells were recorded as 0 for 50 half crypt-villi per experimental animal. For each row corresponding to cell position, the sum was calculated per mouse and then all those sums from animals belonging to the same experimental cohort were pooled together. The pooled data were used in SPSS (IBM SPSS Statistics 20) to construct graph of cumulative frequency of positive cells.

In order to be able to test for the difference in a distribution between different cohorts of experimental animals, data recorded and pooled in the Excel spreadsheet were transformed using KST (Kolmogorov-Smirnov Transformation) custom-designed program written by Aliaksei Holik (http://bio.bsu.by/t/temp/holik/KST/). The number of instances of positive cells at a position was transformed into a sequence of numbers corresponding to this particular position which in turn was tested using two-tailed Kolmogorov-Smirnov Z test. A significant difference between distributions was accepted if p value was equal or less than 0.05.

2.7.4 Kaplan-Meier survival analysis

Kaplan-Meier method was used for analysis of survival as well as generation of survival curves and was performed using SPPS software (IBM SPSS Statistics 20). Cohorts of experimental animals were tested for a statistical significance of survival time between groups of those animals using Log-Rank test. A significant difference in the survival possibility was accepted if p value was equal or less than 0.05.

Chapter 3

Investigating the effects of Brm loss in the epithelium of small and large intestine

3.1 Introduction

Subunits of the SWI/SNF chromatin remodelling complex have been implicated in regulating transcriptional activation and repression of genes controlling a variety of processes from embryonic development to cell apoptosis. Due to the very high sequence homology between Brm and Brg1 ATPases (~75%), it was speculated that those subunits might be redundant due to sharing of many cellular functions. However numerous studies conducted on both ATPases revealed that the catalytic subunits interact with different classes of transcription factors and bind different promoters, indicating they are recruited in response to specific signalling pathways by unique interactions with different protein domains (Kadam and Emerson 2003). As previously mentioned, Brg1 is involved in direct interaction with the Wnt pathway through its capacity of regulating Wnt target genes such as Cyclin D1 and CD44, whereas Brm exclusively interacts with the ICD22 and CBF-1 elements of Notch pathway (Baker *et al.* 2001, Kadam and Emerson 2002, 2003). This transcriptional specificity discriminating between Brm-containing SWI/SNF complexes and Brg1-containing SWI/SNF complexes in performing cellular functions has additionally been shown to be tissue-specific. Moreover, mouse model studies of loss of either ATPase revealed further differences with Brg1 emerging as a *bona fide* tumour suppressor gene whereas Brm loss not being capable of inducing tumorigenesis but rather potentiating tumour development when combined with a known carcinogen (Bultman *et al.* 2000, Bultman *et al.* 2008, Glaros *et al.* 2008). Specificity and often exclusivity of interactions between Brm and Brg1 together with an observation that Brg1 is ubiquitously expressed throughout development whereas Brm is expressed at high levels in differentiating cells may indicate the possibility that remodelling complexes containing a particular ATPase are preferentially recruited to a specific subpopulation of cells (Muchardt *et al.* 1998).

Considered as putative tumour suppressor genes, both Brm and Brg1 catalytic subunits of the SWI/SNF chromatin remodelling complex have been detected to frequently be lost in cancers

of the lung, esophagus, pancreas, skin, ovaries and breast (Reisman *et al.* 2009). However in contrast to Brg1, in many types of cancer Brm was found to be epigenetically silenced rather than mutated suggesting Brm as a potential therapeutic target (Glaros *et al.* 2007, Kahali *et al.* 2013). Moreover Brm loss has been correlated to poor prognosis in majority of those cancers suggesting that Brm expression may play an important role in modulation of cancer phenotypes.

The intestinal epithelium, due to its complex architecture and dynamic self-renewal, has been known to require a complex interplay between signalling pathways such as Wnt, Notch, Hedgehog and TGF β/BMP to maintain homeostasis (reviewed in Sancho 2004). More importantly, the maintenance of the stem cell niche is highly dependent upon the active signalling of Wnt and Notch pathways (Reya and Clevers 2005, K**ühl and** Kühl 2013) with Notch signalling in particular playing an important role in the regulation of cell fate and differentiation of intestinal epithelial cells (van Es *et al.* 2005). Moreover, mouse intestinal epithelium is the most commonly used model tissue to study human colorectal cancer.

In contrast to Brg1, due to the lack of evidence supporting interactions of Brm with the Wnt pathway, targeting Brm may have less adverse effects on those of tissues that in a great degree are dependent on the active Wnt signalling. To evaluate the capacity of Brm as a potential therapeutic target for cancer including colorectal cancer, it appears appropriate to investigate the consequences of Brm loss in the normal intestinal epithelium and therefore a possible role of Brm in maintenance of its homeostasis.

This chapter will aim to characterise the effects of Brm deficiency on the small and large intestinal epithelium.

3.2 Results

3.2.1 Brm null mice are viable and not prone to tumorigenesis

Mating of heterozygous mice yielded pups at the expected Mendelian ratio of wild-type, heterozygous and homozygous. Further crosses using Brm null mice have resulted in litters of normal size with no lethality – pre or post-weaning observed. The viability of Brm null mice contrasts to the respective knock-out mouse model of its paralogue, Brg1, as Brg1 null is embryonically lethal. However, some fertility issues have been encountered in Brm null mice

but this was only in the case of Brm null homozygous breeding couples. Moreover the sterility seems to affect males only as approximately 15% of those failed to produce a litter over a period of 3 months whereas the coupled Brm null females were successfully producing offspring once mated with other homozygous males. The genetic background does not seem to affect this partial sterility as all mice used in these studies are of the mixed background.

Similarly to Reyes *et al.* we have not observed any differences in the weight of homozygote animals in comparison to their wild-type littermates. Brm null mice have been also monitored for signs of illness or tumour formation, twice a week for a period of a year but no abnormalities were observed.

3.2.2 The complete loss of Brm in Brm null mice

Conversely to Brg1 which is expressed in tissues undergoing high cell turnover, Brm is actively expressed in low proliferating organs such as brain, liver, fibromuscular and endothelial cell. Additionally, in the cell line study by Muchardt *et al.* (1998) it has been observed that non-differentiated cells contain predominantly Brg1 whereas Brm accumulated upon *in vitro* differentiation. Furthermore as mentioned previously the loss of Brm in Brm null mice occurred without the need of induction of Cre recombinase as the Brm gene was constitutively inactivated (refer to Methods section 2.1.1). A LoxP flanked allele would have been preferable for this study, as combined with a Cre recombinase specific for the epithelium of the gastrointestinal tract, it would have alleviated any possible effects of Brm deficiency in other tissues and systems. However, such a strain does not exist. In order to overcome the issues resulting from the very low expression levels of Brm in the small intestinal epithelium, liver and spleen were chosen as internal controls of Brm loss in further investigation of the expression of Brm in the gastrointestinal tract.

Firstly, in order to investigate the pattern of expression of Brm in murine tissues, control ($Brm^{+/+}$) and Brm null ($Brm^{-/-}$) animals at 70 days of age were sacrificed and a number of different organs from the abdominal cavity were taken including stomach, small and large intestine, liver, spleen, kidney and bladder. The immunohistochemical analysis of Brm expression in various tissues confirmed its complete loss of expression in investigated tissues of Brm null animals (Figure 3.1). The presence of a minor population of cells characterized by a positive Brm staining in Brm null tissues is due to the cross-reactivity of anti-Brm antibody with Brg1. The same experiment showed different patterns of expression of Brm in individual organs with no detectable staining within the intestinal epithelium in control mice

cohort. The only Brm-positive cells in the small intestine of control animals were present in the lamina propria except from some non-specific staining of Goblet cells in both Brm null and controls (Figure 3.1d). The nuclear staining of cells of lamina propria was absent from tissue sections of Brm null animals. Co-immunofluorescence for Brm and its paralogue Brg1 in both control and Brm deficient animals further allowed the identification of Brm-expressing cells as well as the examination of co-distribution of those proteins in the same tissue slice (Figure 3.2). Due to the previously detected non-specific staining of some differentiated cell types within the epithelium of the small intestine, spleen samples present on the same tissue section were treated as internal controls for staining. The staining of spleen sections confirmed the presence of nuclear Brm expression in the lymphoid germinal centres and sinusoidal cells in red pulp in control animals; a staining pattern which was lost in Brm null (Figure 3.2b). As previously observed Brg1 was found to be ubiquitously expressed in all epithelial cells of small intestine in both control and Brm null animals (Holik A. unpublished observations) (Figure 3.2a). In comparison to Brg1, we have been able to detect Brm expression in the small intestinal epithelium of controls for the first time and found it to be expressed at very low levels. Brm expression appears to be stronger in stromal cells of the lamina propria than in epithelial cells however this positive staining disappeared in the Brm null animals with only some non-specific Goblet cell staining still present within the tissue samples (Figure 3.2a). Furthermore, no Brm-positive cells were found in the crypts of Lieberkühn with the expression being limited to low number of early differentiated or mature epithelial cell types.

Immunohistochemical staining of subsequent tissue sections with Brg1 confirmed the mosaic expression of both catalytic subunits of SWI/SNF in control animals (Figure 3.3). In the liver of control animals (Figure 3.3a) small neighbouring clusters of Brm and Brg1 positive cells were detected. Further immunofluorescence analysis detected very weak immunofluorescent signal for both Brm and Brg1 incapacitating the analysis of co-distribution of those proteins in the liver cells.

Brm null animals have an overall higher proportion of Brg1 positive cells than controls (Figure 3.3b) which is consistent with previous data (Reyes *et al.*, 1998) showing the upregulation of Brg1 in case of Brm loss. However not all of the liver cells are expressing Brg1 in case of Brm loss (Figure 3.3a) meaning there are some that are expressing neither of the ATPase catalytic subunits.

A

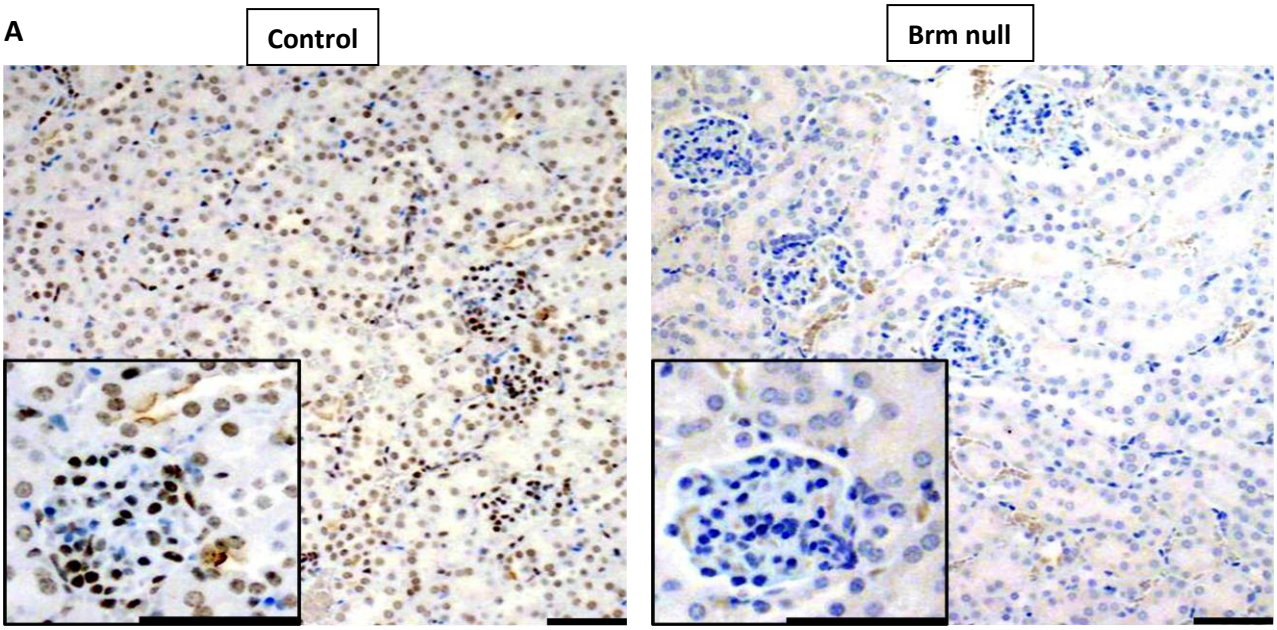

B

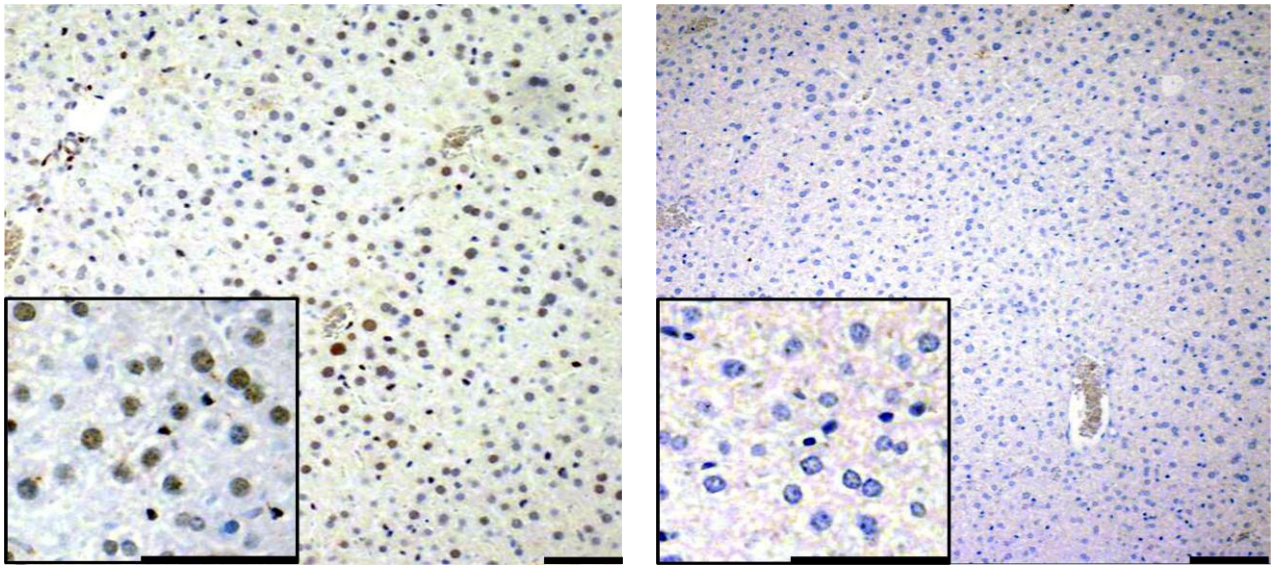

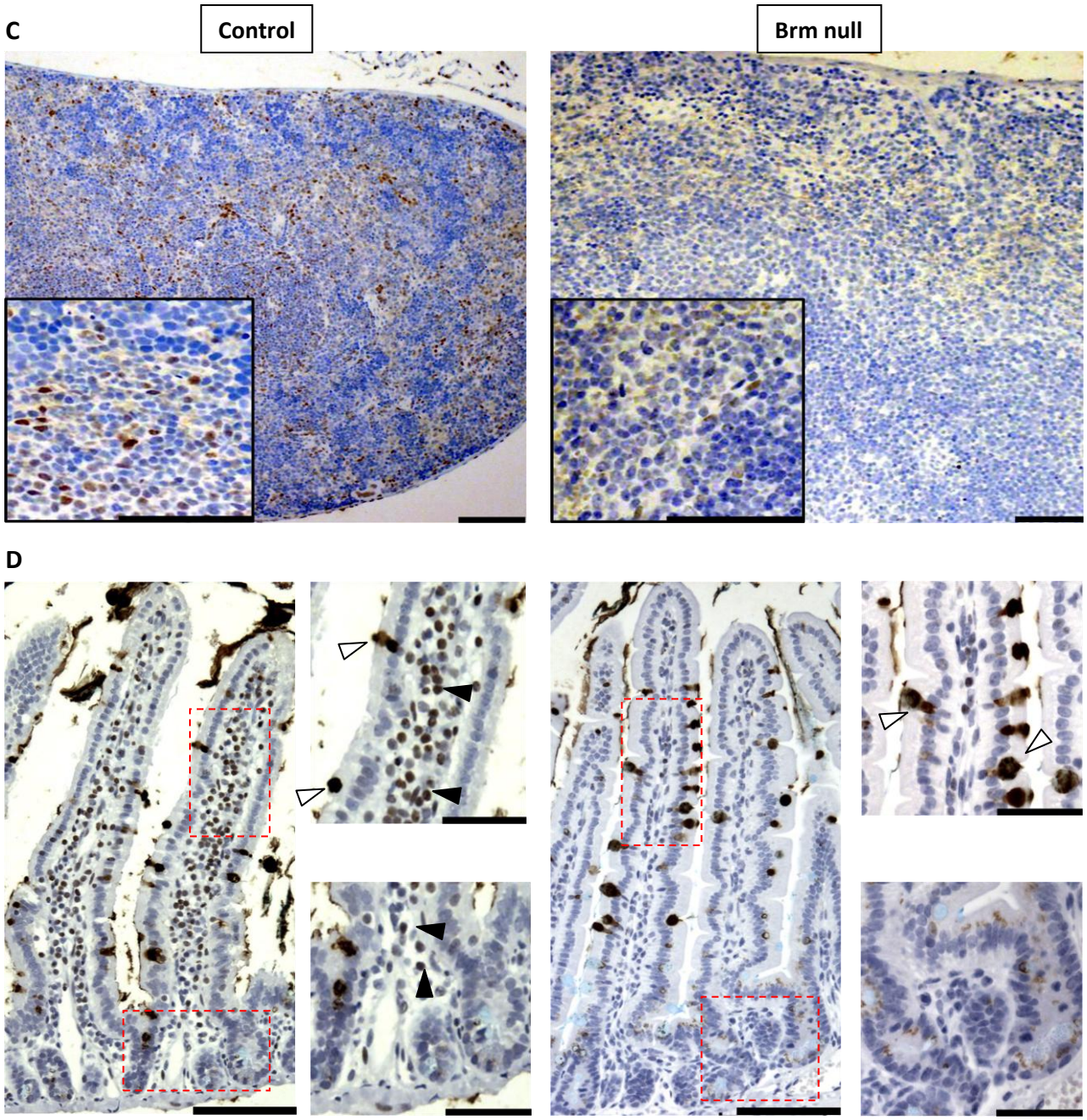

Figure 3.1 The complete loss of Brm in Brm null knock-out mice. Brm null animals along with Brm $^{+/+}$ controls were dissected at 70 days of age. Immunohistochemical analysis of Brm expression revealed 100% loss of Brm in all tissues investigated: (A) kidney, (B) liver, (C) spleen and (D) small intestine in comparison to normal expression levels of Brm in control cohort. White arrows mark non-specific positive staining of cells whereas black arrows positive Brm-specific-stained cells. Some positive non-specific staining was detected in cells of secretory lineage in small intestinal sections of both Brm null and control animals. No Brm-stained cells were detected in control animals. Scale bar represents 100µm except zoomed sections (x40 mag) (black and red box) where scale bar represents 50 µm.

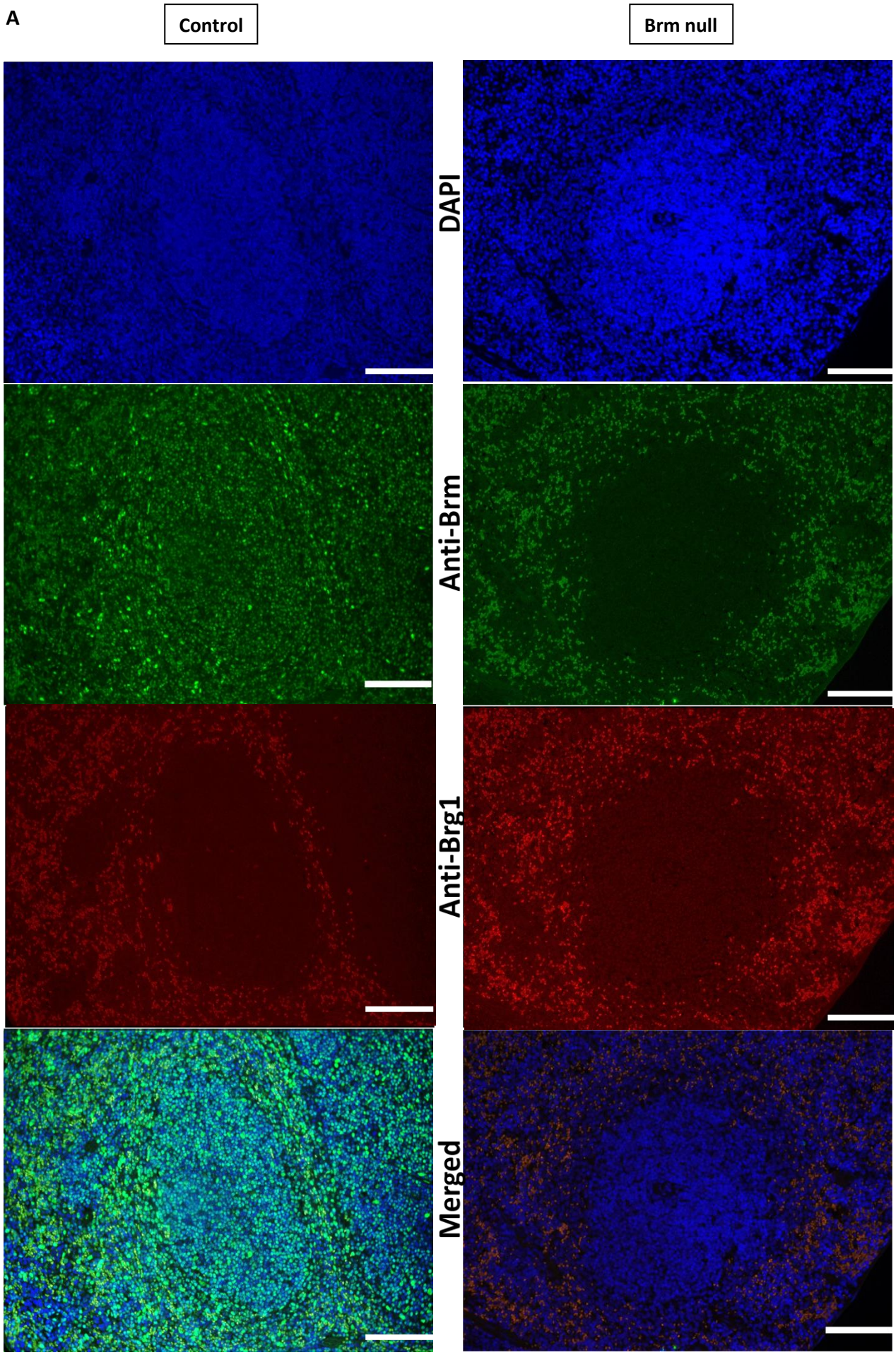
A
Control
Brm null
DAPI
Anti-Brm
Anti-Brg1
Merged

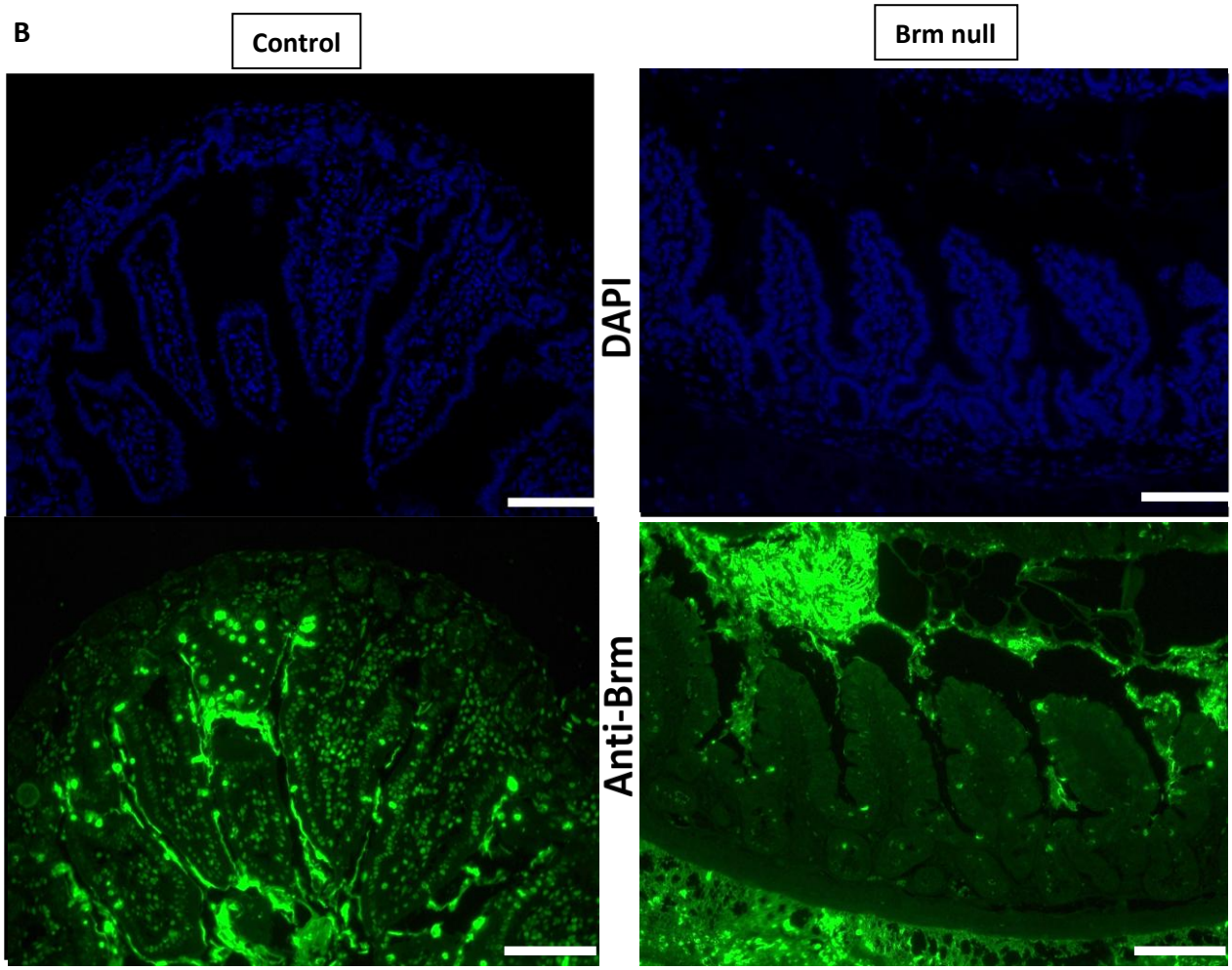

Figure 3.2 The expression pattern of Brm in the small intestinal epithelium. Brm null animals along with Brm $^{+/+}$ controls were dissected at 70 days of age and immunofluorescent staining was conducted on harvested tissue. Blue channel corresponds to DAPI nuclear staining, green channel to Brm staining and red channel to Brg1. (A) Immuflourescent analysis of Brm expression revealed 100% loss of Brm in control organ of spleen. However in contrast to the small intestinal epithelium, high levels of cross-reactivity between Brm and Brg1 have been detected in red pulp of spleen resulting in Brm-positive staining in Brm null tissue (B) Small intestine staining revealed lower levels of Brm expression in comparison to spleen. Brm expression levels were low in control cohort, limited to few cells and located outside of the crypt compartment. Some positive non-specific staining was detected in cells of secretory lineage in small intestinal sections of both Brm null and control animals. Scale bar represents 100μm.

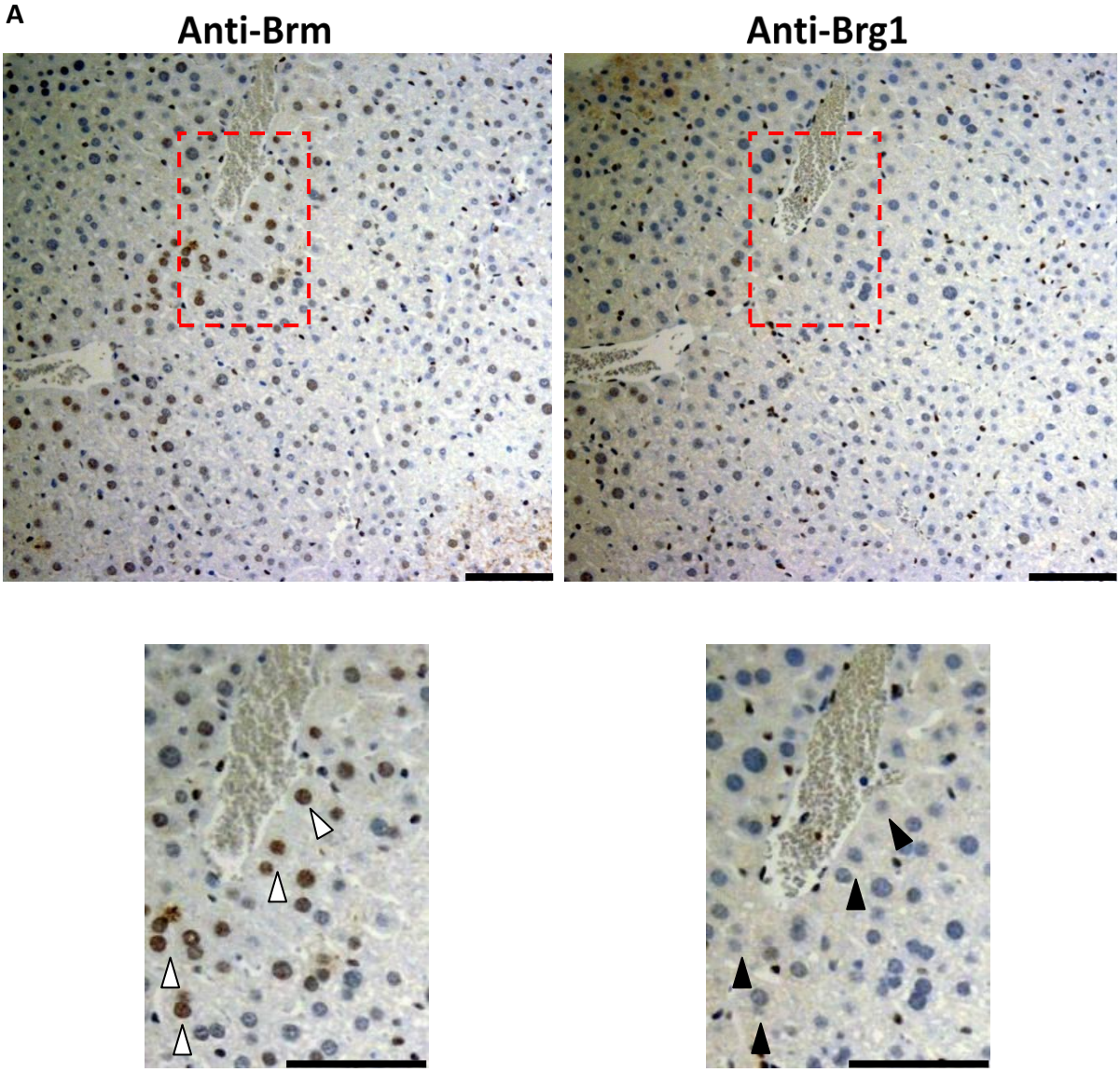
A
Anti-Brm
Anti-Brg1

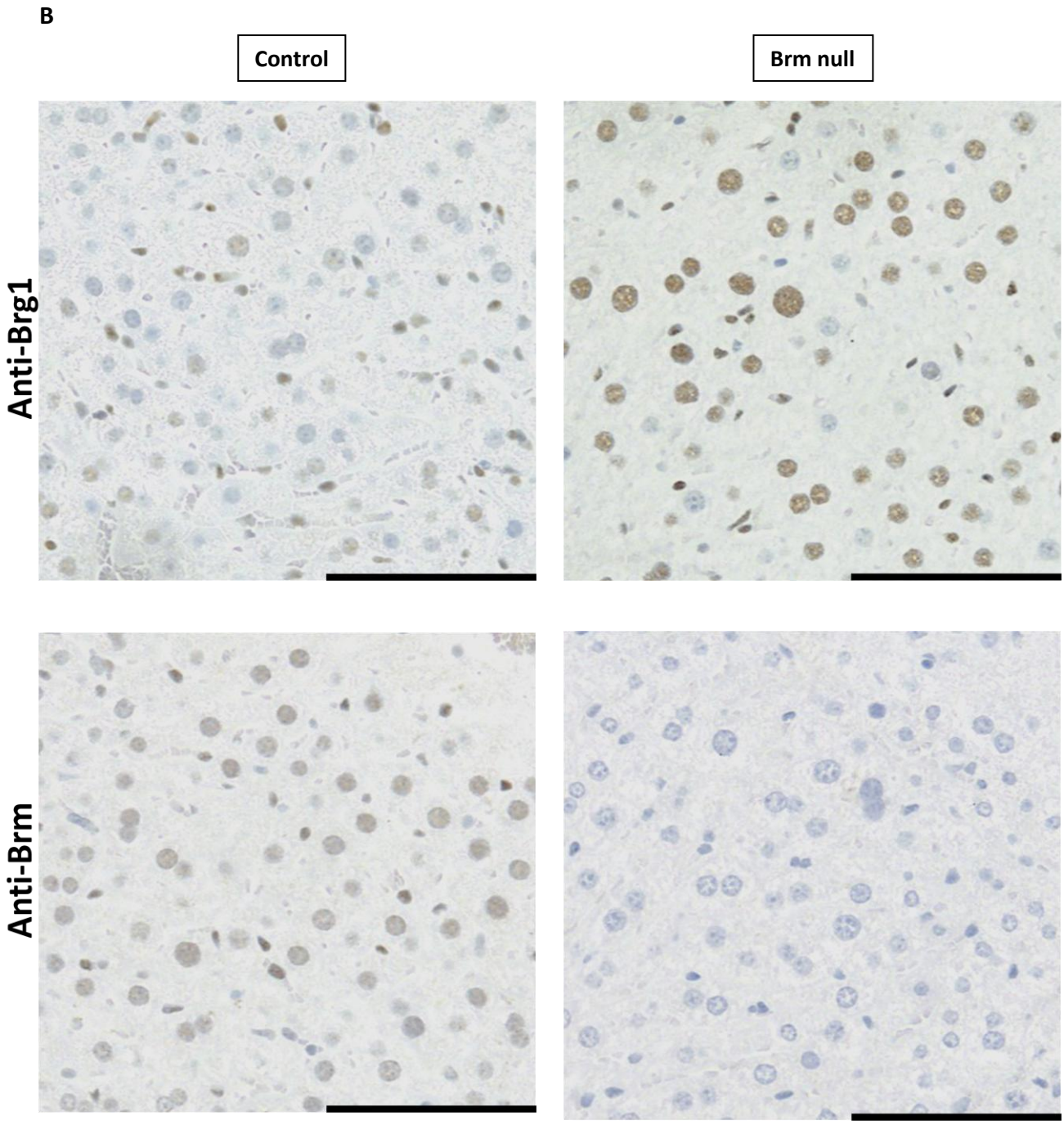

Figure 3.3 The mosaic expression of Brm and Brg1 in liver. (A) Immunohistochemical analysis of expression patterns of Brm and Brg1 on the sequential sections in Brm $^{+/+}$ animals at day 70 of age revealed a non-overlapping pattern of nuclear localisation of Brm and Brg1 subunits. White arrows mark individual cells stained with anti-Brm antibody whereas black arrows indicate the same cells stained with anti-Brg1 antibody present on the serial section of the same tissue (B) Immunohistochemical analysis of Brg1 and Brm in liver sections from Brm $^{+/+}$ control cohort and Brm null cohort shows a higher proportion of Brg1-positive cells in Brm null animals in comparison to controls. The scale bar represents 100 μm.

On the basis of the immunohistochemical data, I assessed whether the Brm loss affected the levels of Brg1 protein in the liver by a western blotting. Previously obtained tissue from the livers of control and Brm null mice (n=4) were used for protein extraction and Western blotting analysis (Figure 3.4a). Quantitative analysis of those protein samples further confirmed the higher levels of Brg1 in Brm null animals in comparison to controls (p=0.03, n=8, Figure 3.4b).

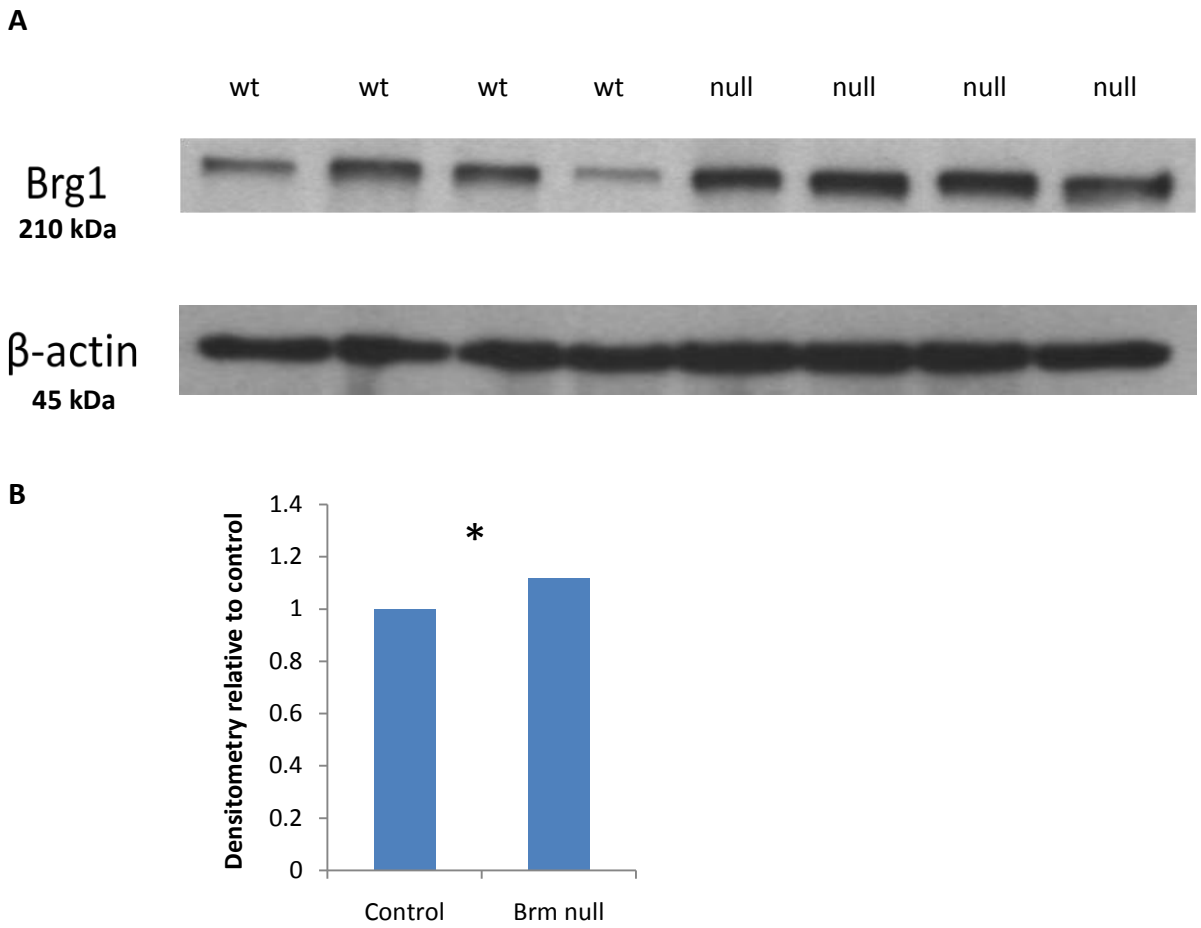

Figure 3.4 Brm loss affects the expression levels of Brg1. (A) Western blotting analysis for Brg1 confirmed the presence of upregulated levels of Brg1 in Brm null animals in comparison to controls (B) Densitometry was carried out to quantify the differences observed. The results were normalised to β-actin loading control and represented as a value relative to controls (p=0.03, n=4, Mann Whitney U Test)

3.2.3 Brm loss has mild effects on the small intestinal homeostasis

Although Brm null intestinal epithelium did not show any obvious morphological abnormalities that could be assessed on H&E sections, quantitative analysis of histological and some basic functional parameters detected some subtle differences between Brm null and control animals. The results of quantitative analysis of those histological parameters are summarized in Table 3.1.

Crypt and villus lengths have been assessed on H&E stained sections as the average number of cells (± standard deviation) from the bottom of the crypt of Lieberkühn till the crypt-villus junction and from the crypt-villus junction till the very top of the villus where the cell shedding occurs respectively. Both, crypt and villus size are found to be altered in the Brm null small intestinal epithelium with a small increase in crypt length in experimental animals versus control (22.56±0.16 and 21.62±0.92, p=0.008, n=8, Figure 3.5a). Conversely, the quantification of the villus length showed a small decrease in the villus size (71.67±1.48 and 73.40±1.48, p=0.03, n=8, Figure 3.5b).

Both apoptosis and mitosis were scored on the basis of immunohistochemical staining using specific markers: Cleaved Caspase-3 for sequential caspase activation cascade in cell apoptosis and Ki67 protein expressed in all active phases of the cell cycle except G_0. Scoring of apoptosis detected a trend of lower apoptosis levels in Brm null mice in comparison to control animals. However, the trend was not significant (0.866±0.06 and 0.744±0.33, p=0.17, n=8, Figure 3.5c). Quantification of the cells scored as positive for Ki67 marker revealed no difference in the levels of proliferation between control and Brm null animals (13.51±0.70 and 13.40±0.76, p=0.74, n=8, Figure 3.5d).

A further marker of cell proliferation was used to quantify the number of cells in S-phase of the cell cycle. Brm null and control mice were injected with BrdU labelling reagent 2 hours and 24 hours prior to dissection and the obtained tissue sections were stained using an anti-BrdU antibody. In parallel to the previous levels of proliferation detected by Ki67, there was no difference between the numbers of BrdU-labelled cells in the half crypt-villus between controls and experimental animals at the 2 hour time point (5.07±1.61 and 6.06±0.95, p=0.40, n=4, Figure 3.5e). Further, scoring at the 24 hour time point showed the expected, approximate doubling of the number of cells in S-phase in comparison to 2 hour time point and detected a significant increase in the number of BrdU-positive cells in Brm null animals

in comparison to controls (10.15±1.82 and 14.31±2.13, p=0.026, n=4, Figure 3.5e) however this result should be considered with a great care due to the significant effect of Brm on the crypt length.

Therefore in the context of complete Brm loss, the quantitative analysis of basic functional and morphological factors detected some very mild effects including a small increase in crypt length, a decrease in villus length and subtle changes in the shape of the proliferative compartment within small intestinal epithelium. However, the intestinal homeostasis appears to be maintained and not affected by these small changes.

Parameter	Cohort	Mean	SD	p-value
Crypt length	Control	21.617	0.92	0.008
	Brm null	22.564	0.156	
Villus length	Control	73.402	1.478	0.029
	Brm null	71.669	1.476	
Caspase positive cells	Control	0.866	0.061	0.170
	Brm null	0.744	0.338	
Ki67 positive cells	Control	13.395	0.762	0.744
	Brm null	13.513	0.702	
BrdU positive cells				
2 hours	Control	5.070	1.605	0.400
	Brm null	6.064	0.950	
24 hours	Control	10.157	1.822	0.026
	Brm null	14.305	2.131	

Table 3.1 Quantitative analysis of the effects of Brm loss on the small intestinal histology. Epithelium from small intestine from Cre^{-} Brm $^{+/+}$ (marked as Control) and Cre^{-} Brm null (marked as Brm null) was harvested from animals at 70 days of age. Histological parameters including crypt and villus length, apoptosis, proliferation and BrdU incorporation were quantified and comparison between those two cohorts was conducted using statistical software.

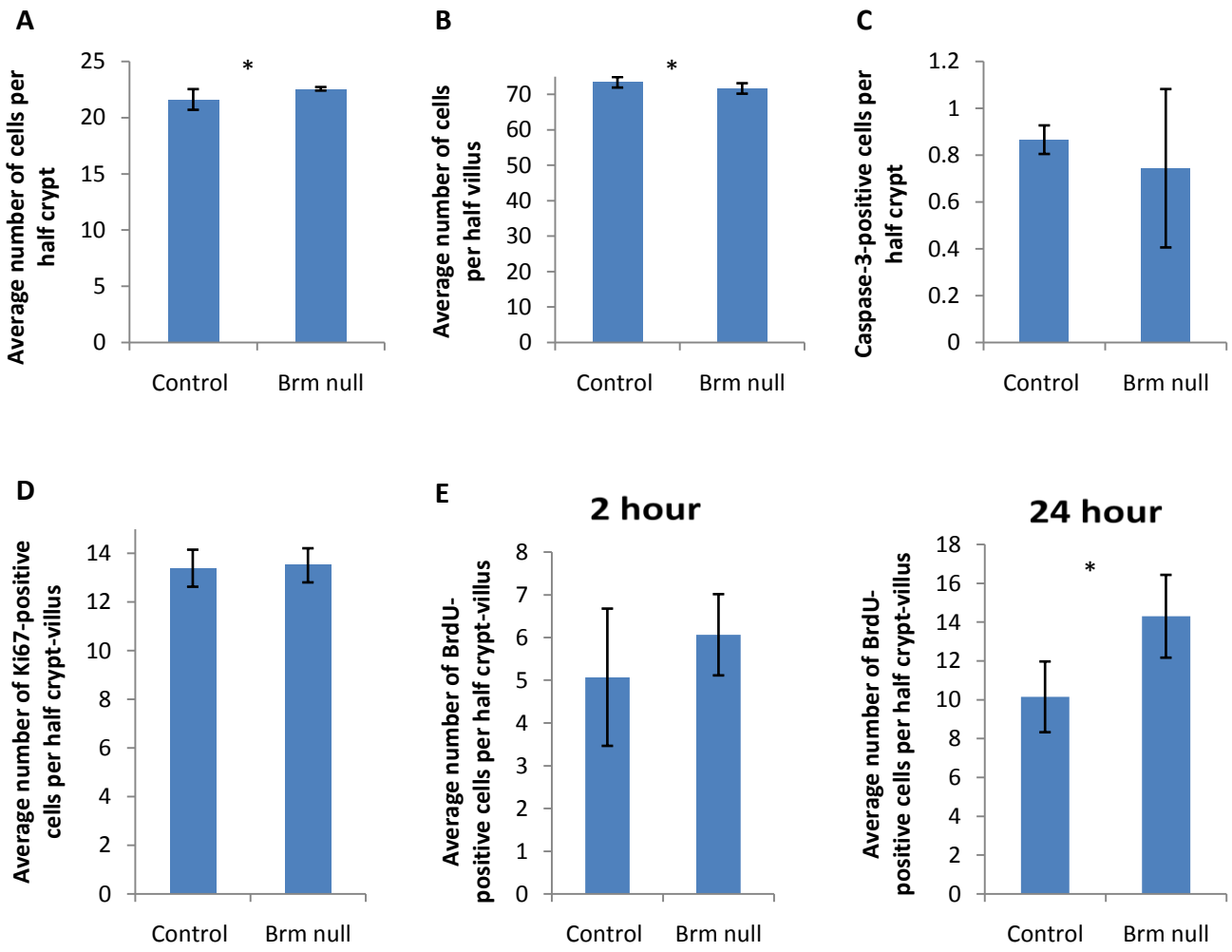

Figure 3.5 Histological analysis of the effects of constitutive Brm loss in the small intestinal epithelium. Control and experimental Brm null animals were harvested at day 70 of age. A-F histological parameters such as (A) crypt length (B) villus length were counted on H&E sections for control and Brm deficient animals. The average number of (C) Cleaved Caspase 3 (D) Ki67 (E) BrdU 2h and 24h -positive cells was scored on the corresponding immunostained sections. Error bars represent standard deviation and asterisk symbol indicates those histological parameters that showed a statistically significant difference (p value < 0.05) between cohorts of mice. Exact values, standard deviations, p values are provided in Table 3.1

3.2.4 Brm loss changes the shape of proliferative compartment in the epithelium of small intestine

The distribution of Ki67 positive cells was analysed to assess any possible changes in the shape of the proliferative compartment within epithelium of small intestine. Analysis of the cumulative frequency of Ki67 positive cells detected a significant change in the position of proliferating cells along the length of the intestinal crypt with a small but significant change in Ki67-labelled cells towards the top of the crypt suggesting an increase in activity within that region of the epithelium (Kolmogorov-Smirnov Z test, p=0.03, n=8, Figure 3.6).

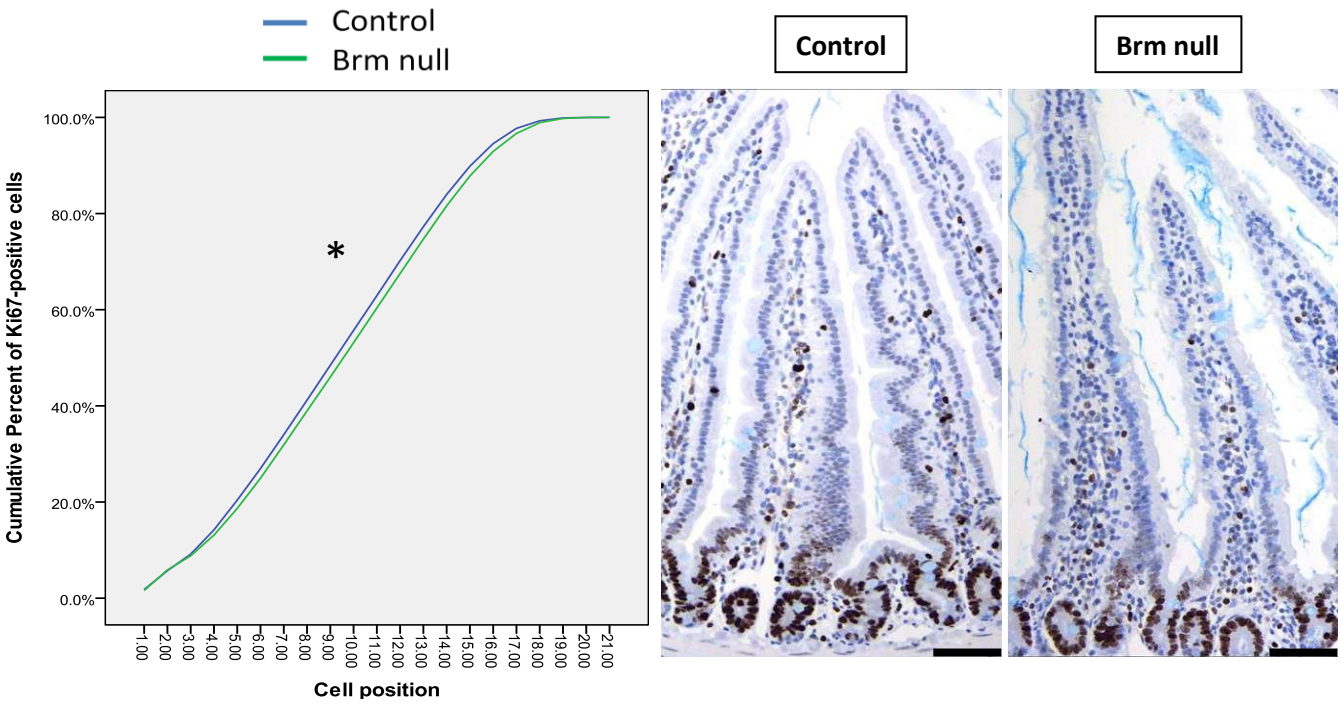

Figure 3.6 Immunohistochemical analysis of Ki67 staining of control and experimental animals at day 70 of age detected no gross differences in distribution of Ki67-positive cells within the epithelium. Cumulative frequency analysis of Ki67 positive cells revealed changes in the shape of proliferative compartment (Kolmogorov-Smirnov Z test p=0.03, n=8) with an expansion towards the top of the intestinal crypt. Scale car represents 100 µm.

3.2.5 Brm loss does not affect the cell migration in the small intestinal epithelium

BrdU labelling reagent is used not only as a cell cycle phase-specific proliferation marker in addition to Ki67, but also to visualise the migration of the cells within the crypt-villus axis of the small intestine. All Brm null and control animals at day 70 of age were administered with BrdU by intraperitoneal injection at either 2 hour or 24 hour prior to being sacrificed. Immunohistochemistry against BrdU was carried out and the position of all BrdU positive cells along a half crypt-villus axis was scored on the small intestinal sections in order to assess the effects of Brm loss on the migration capacity of epithelial cells of the small intestine.

The cumulative frequency of BrdU positive cell position at 2 hours prior to dissection showed that all of the BrdU labelled cells were confined within the intestinal crypt which is in agreement with the existence of proliferation zone. Although there is a trend of BrdU positive cells being present in the lower cell positions along the crypt-villus axis in small intestinal epithelium of Brm null mice this trend is not significant in comparison to control animals (Kolmogorov-Smirnov Z test, $p=0.619$, $n=4$, Figure 3.7a).

BrdU injection 24 hours prior to dissection showed an expansion of the migration area of labelled cells within crypt-villus axis outside of the intestinal crypt. Similarly to 2 hours experiment, the cumulative frequency of BrdU positive cells at 24 hours revealed a trend of BrdU labelled cells being positioned lower within the crypt-villus axis in Brm experimental mice compared to controls yet again this trend is not significant (Kolmogorov-Smirnov Z test, $p=0.281$, $n=4$, Figure 3.7b).

Although the cumulative frequency curve for both 2 hours and 24 hours appears to be shifted suggesting that the migration of the cells along crypt-villus axis is slower in the Brm null, this effect is not significant in comparison to control animals.

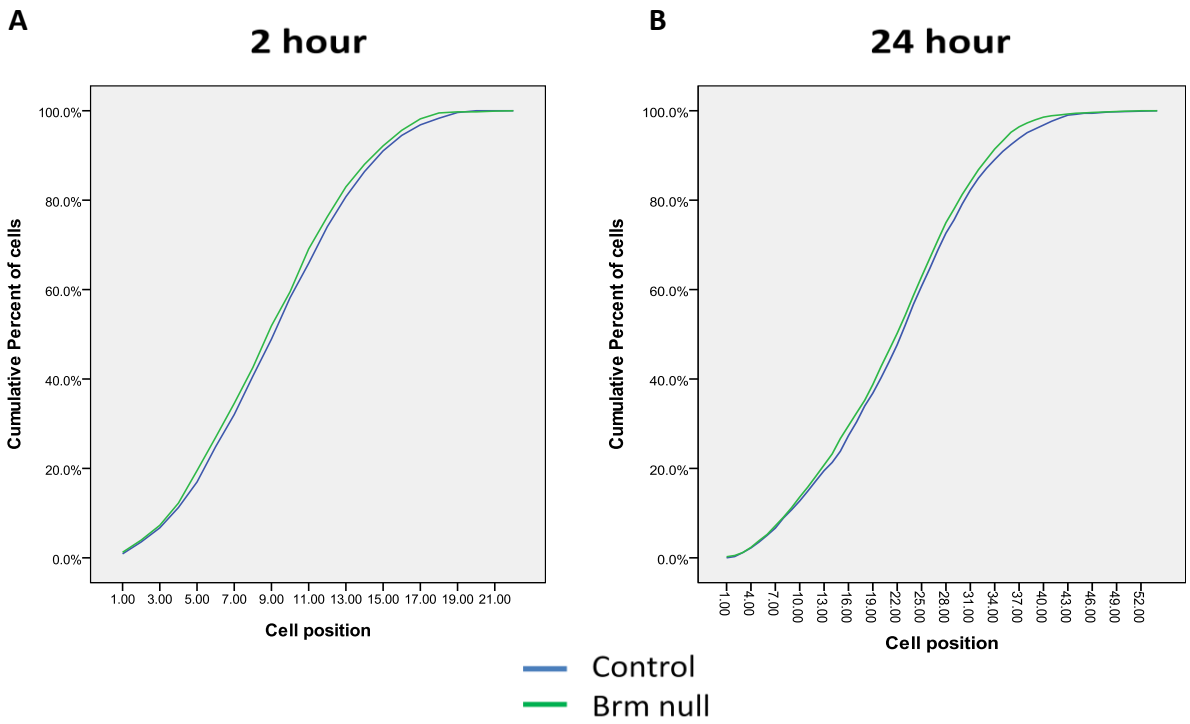

Figure 3.7 Brm deficiency does not affect the population of BrdU positive cells and the migration pattern of those cells remains unchanged. Cumulative frequency analysis of BrdU immunostaining 2 hours (A) and 24 hours (B) post labelling revealed no significant changes between Brm null and control animals (Kolmogorov-Smirnov Z test, p=0.619, n=4 and p=0.281, n=4, respectively).

3.2.6 Brm loss affects the differentiation of the certain intestinal epithelial cell types

The network of signalling pathways maintaining the homeostasis in the intestinal epithelium is also responsible for regulating cell proliferation and differentiation processes. As evidenced before, Brm loss has some effects on the crypt and villus length as well as the proliferative compartment in the epithelium. Accordingly, quantitative analysis of the four main differentiated cell types found in the small intestinal epithelium was conducted in Brm null and control mice at day 70 of age in order to further characterise the effects of Brm loss on the maintenance of small intestinal homeostasis.

Enterocytes are the only differentiated cell type of absorptive lineage nevertheless accounting for the majority of the cells present in the villus. To assess the abundance and the distribution of enterocytes in the Brm null epithelium, alkaline phosphatase staining was performed, which marks brush border of the enterocytes. No difference in the intensity or thickness of the staining was observed within the epithelium of Brm null and control animals (Figure 3.8)

The most abundant cell type of the secretory lineage in the small intestinal epithelium is a goblet cell. Alcian Blue staining was carried out to assess the frequency of goblet cells in the small intestine in Brm null and control animals (Figure 3.9). Scoring of the Alcian Blue stained cells showed the increase in the number of goblet cells in the experimental animals per half crypt-villus in comparison to controls (7.40±0.30 and 6.37±0.19, $p<0.0001$).

Another member of the secretory lineage, Paneth cells, are present only in the crypts of Lieberkühn. To quantify the numbers of this cell type, lysozyme staining was carried out on the sections of small intestinal epithelium (Figure 3.10). The quantification of the Paneth cells showed no difference in the number of cells present in the half-crypt between control and Brm null animals (1.84±0.26 and 1.73±0.15, $p=0.31$, $n=8$).

Enteroendocrine cells are the final differentiated cell type belonging to the secretory lineage. Those cells are identified within the small intestinal epithelium by Grimelius staining as enteroendocrine cells take up the silver ions present in the staining solution. Scoring of the enteroendocrine cells have detected an increase in the number of cells positively stained with Grimelius in Brm null mice compared to controls (2.24±0.05, 2.14±0.08, $p=0.009$, $n=8$) (Figure 3.11).

The quantification of differentiated cell types in the small intestinal epithelium revealed that Brm loss affects differentiation of two secretory lineages leading to an increase in the number of both goblet and enteroendocrine cells.

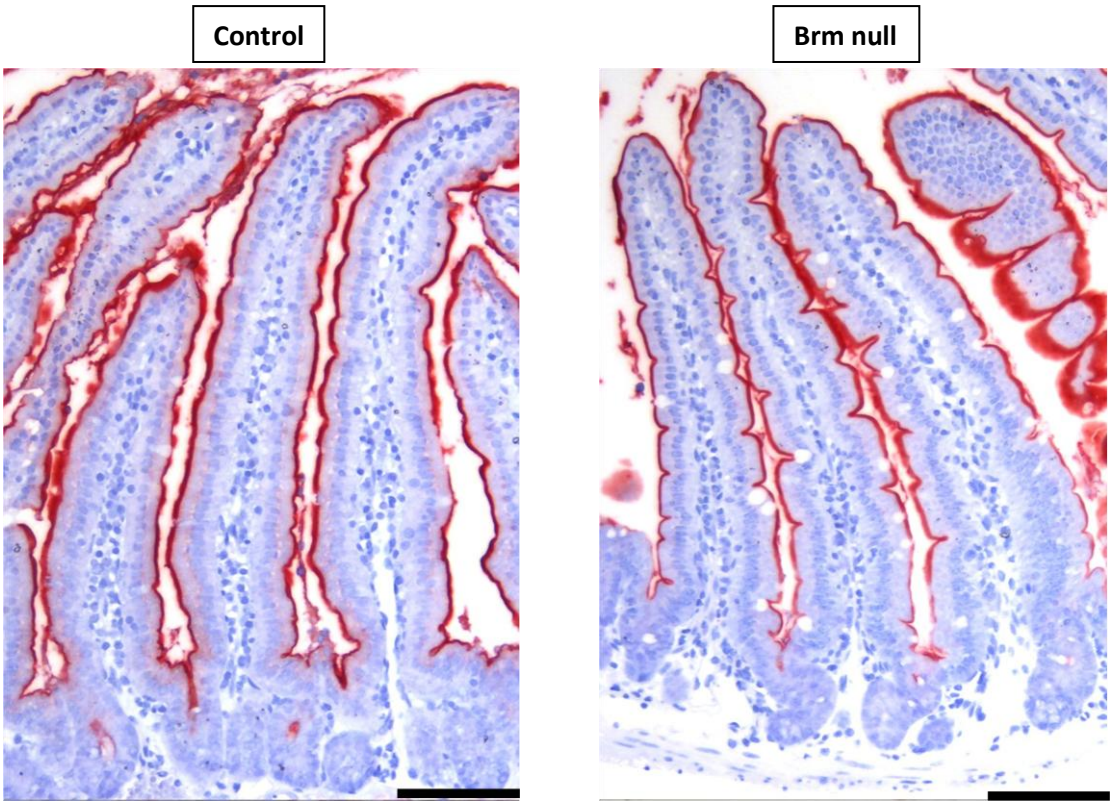

Figure 3.8 Alkaline phosphatase staining detected the normal brush border pattern corresponding to the membrane of differentiated enterocytes. The small intestinal sections of control and Brm null mice dissected at day 70 of age were stained with chromogen for alkaline phosphatase. Staining revealed no changes in the alkaline phosphatase expression in the small intestinal epithelium of control and Brm experimental animals. The localisation of differentiated enterocytes and therefore polarisation of the epithelium remains normal in control and Brm null cohort. The scale bar represents 100μm.

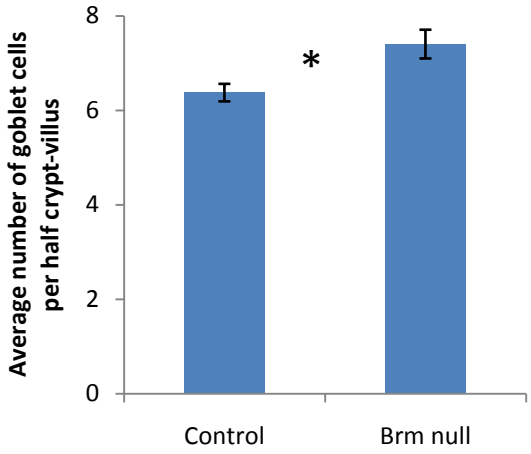

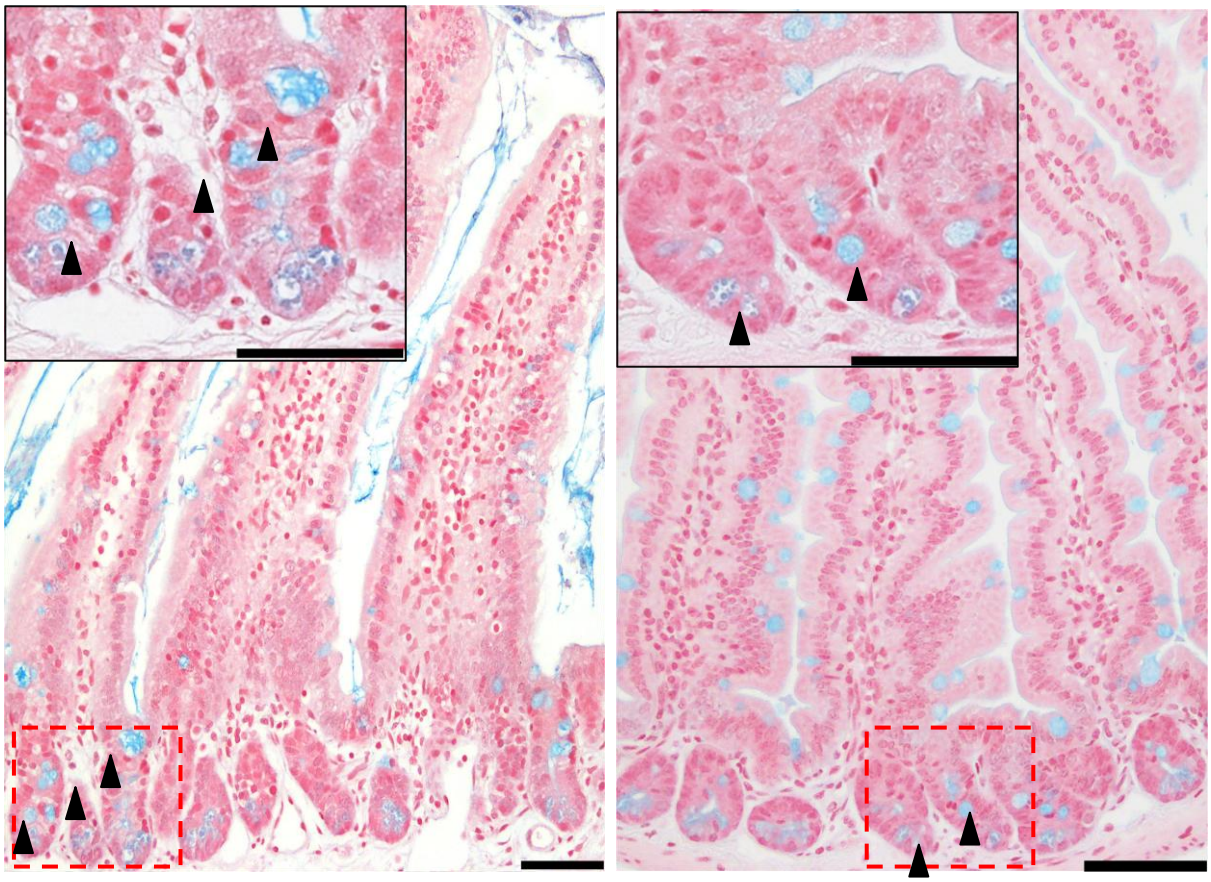

Figure 3.9 Alcian Blue staining was used in order to mark goblet cells within small intestinal epithelium. The small intestinal sections of control and Brm null mice dissected at day 70 of age and stained using cell specific stain detecting mucin secreting cells. Black arrows indicate individual goblet cells. Staining revealed no changes in the localisation of Alcian Blue stained cells in the small intestinal epithelium of control and Brm experimental animals. The number of Alcian Blue positive cells increased in Brm null animals in comparison with controls. The scale bar represents 100µm.

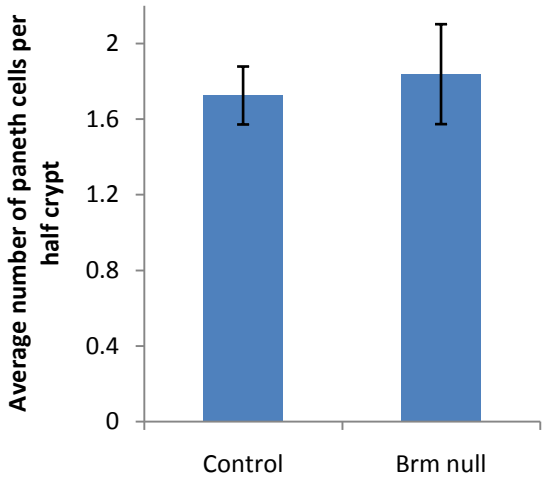

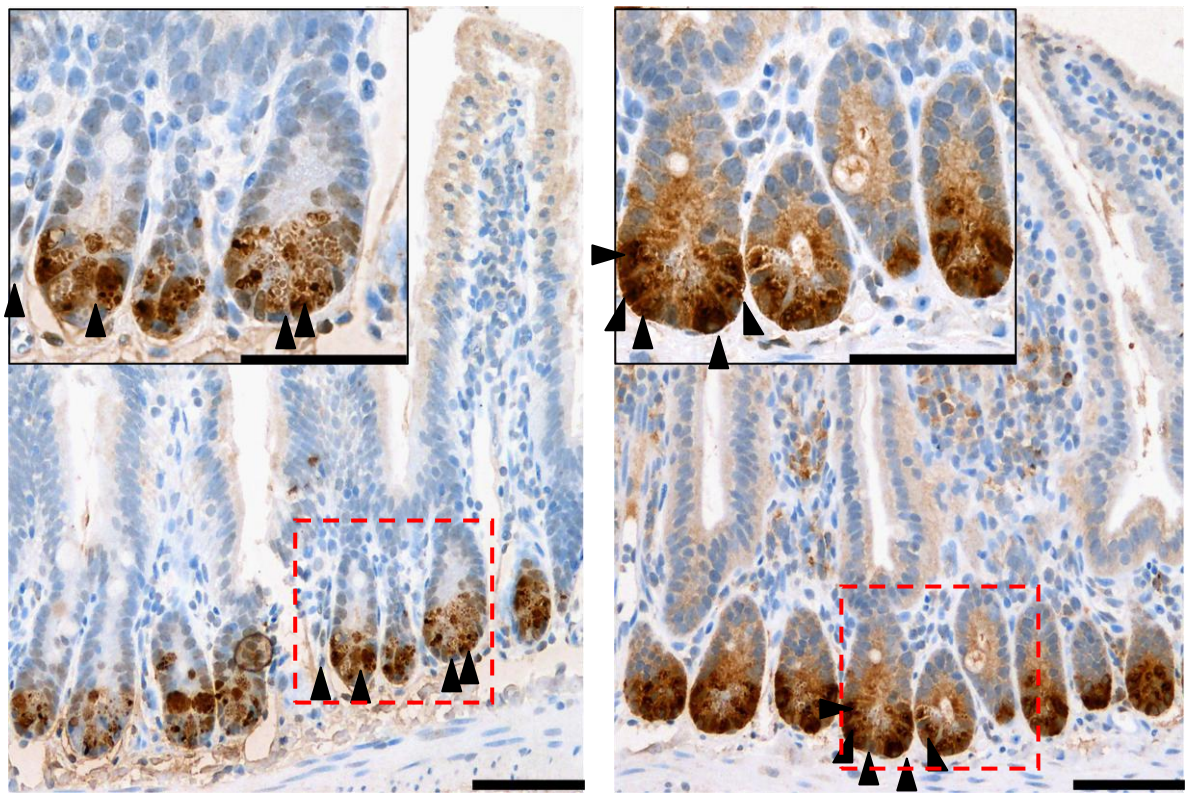

Figure 3.10 Immunohistochemistry against lysozyme was carried out in order to mark Paneth cells within small intestinal epithelium. The small intestinal sections of control and Brm null mice dissected at day 70 of age and stained using cell specific stain to reveal the number and localisation of Paneth cells. Black arrows indicate individual Paneth cells. Staining revealed no changes in the localisation of lysozyme positive cells in the small intestinal epithelium of control and Brm experimental animals. Subsequent scoring of Paneth cells showed no change in the number of lysozyme positive cells between Brm null and control animals. The scale bar represents 100µm.

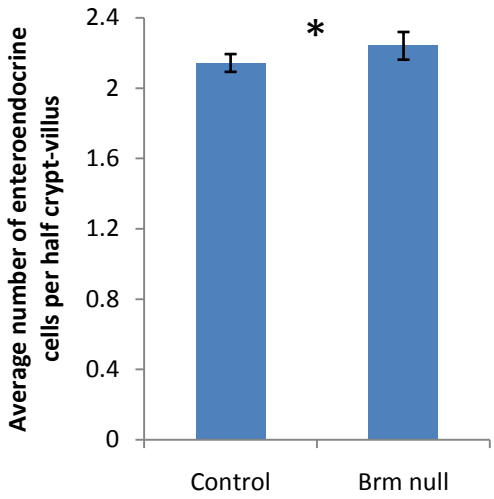

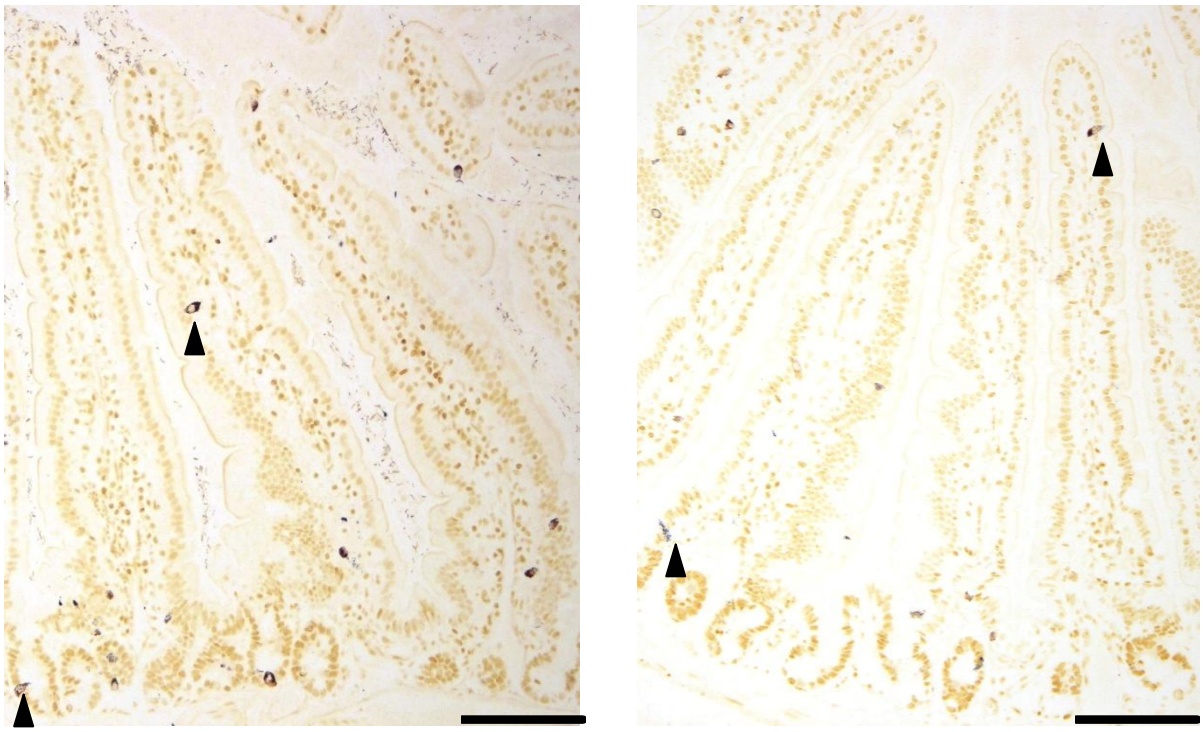

Figure 3.11 Grimelius staining of small intestinal sections was carried out to visualize the number of enteroendocrine cells on small intestinal sections of control and Brm null mice dissected at day 70 of age. Black arrows indicate individual enteroendocrine cells within the epithelium. Staining reveal normal localisation of enteroendocrine cells in Brm deficient animals in comparison with controls. The scoring of numbers of cells detected significant increase in numbers of enteroendocrine cells in Brm null in comparison to control animals. The scale bar represents 100µm.

3.2.7 Brm loss does not affect CD44 expression

Although complete loss of Brm does not have a tumorigenic effect on the small intestinal epithelium, immunohistochemical analysis of the Wnt target gene CD44 was conducted on the tissue sections from Brm null and control mice harvested when they were 70 days of age. Analysis of the CD44 staining in the small and large intestine detected no perceptible differences between Brm null and control animals (Figure 3.12a). In contrast, previous data from Reisman *et al.* (2002) showed that Brm loss leads to loss of expression of CD44 in multiple organs such as gut epithelium, lungs, brain and liver. The expression levels of CD44 were assessed by qRT-PCR. mRNA was extracted from small intestinal tissue samples of Brm null and control animals at day 70. qRT-PCR analysis of mRNA levels revealed no significant changes between Brm deficient and control mice ($p=0.29$, $n=8$, Figure 3.12b).

Given our data contrasted with published report, a collaboration was initiated with Prof Bernard E Weissman (Lineberger Comprehensive Cancer Center, University of North Carolina, Chapel Hill, North Carolina), co-author of Reisman *et al.* (2002), which resulted in immunofluorescent staining for CD44 of control and Brm null tissue sections sent by myself. The staining again showed no difference in CD44 expression in the small intestinal epithelium of control and Brm deficient cohorts confirming previously obtained data from immunohistochemical staining (Figure 3.13a). Similarly, no substantial differences in the expression of CD44 have been observed in the epithelium of stomach and lung tissue (Figure 3.13b, 3.13c). A decrease in the CD44 expression was detected in the liver of Brm null animals compared to control animals, however CD44-positive signal distribution was not even across the tissue sample with some areas characterized by high expression and other areas low or negative (Figure 3.13d).

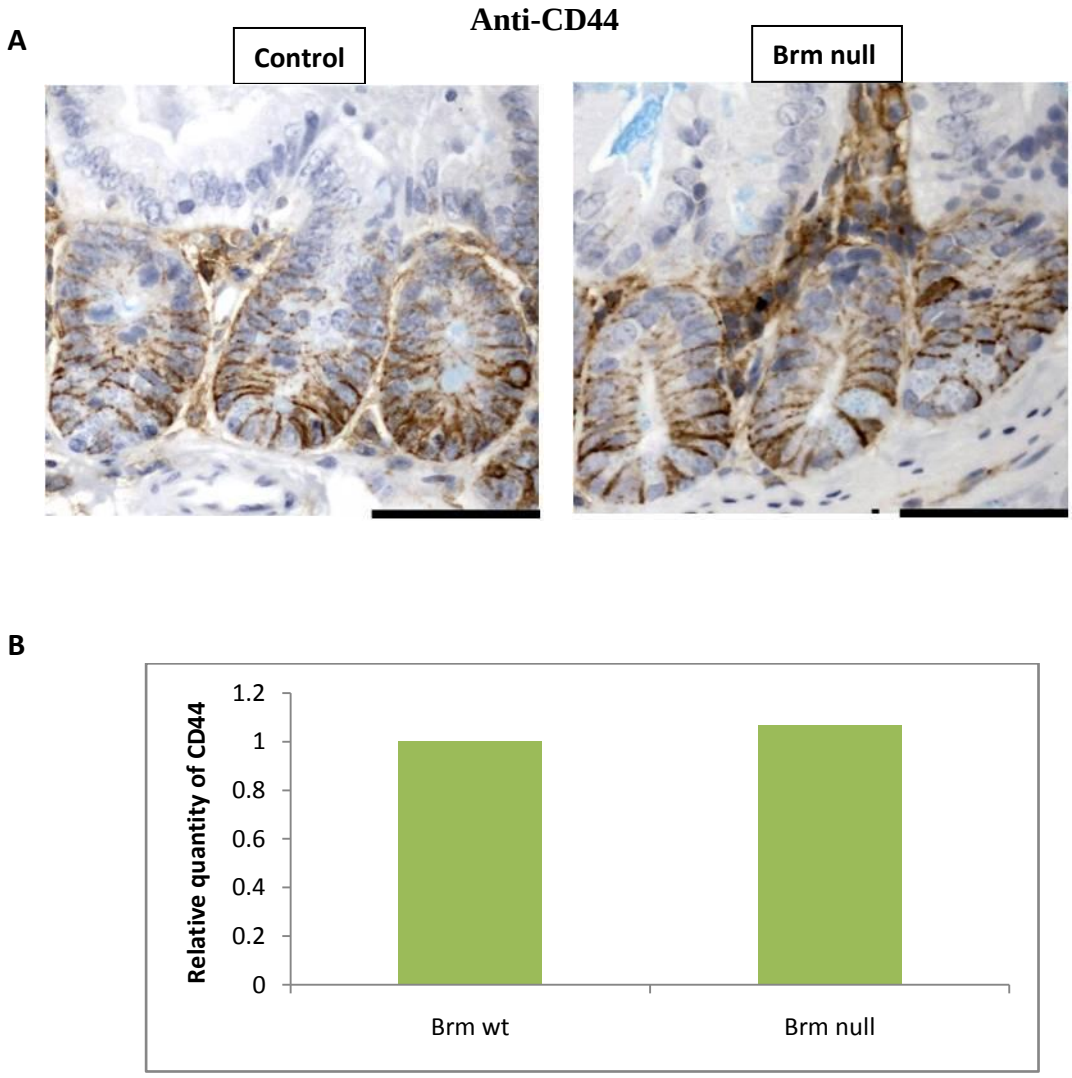

Figure 3.12 Analysis of the expression of CD44. Immunohistochemical staining against CD44 revealed no differences in expression of CD44 in the intestinal epithelium in Brm null in comparison to control animals. Scale bar represents 50 µm. (B) The transcriptional level of CD44 was quantified by quantitative real-time-PCR (qRT-PCR) as shown in bar graph form. The data from qRT-PCR are normalised with β-actin (n=8). Analysis of levels of CD44 mRNA further confirmed the lack of differences between control and experimental animals. The data is presented as a fold change (initial Ct values were plotted with error bars)

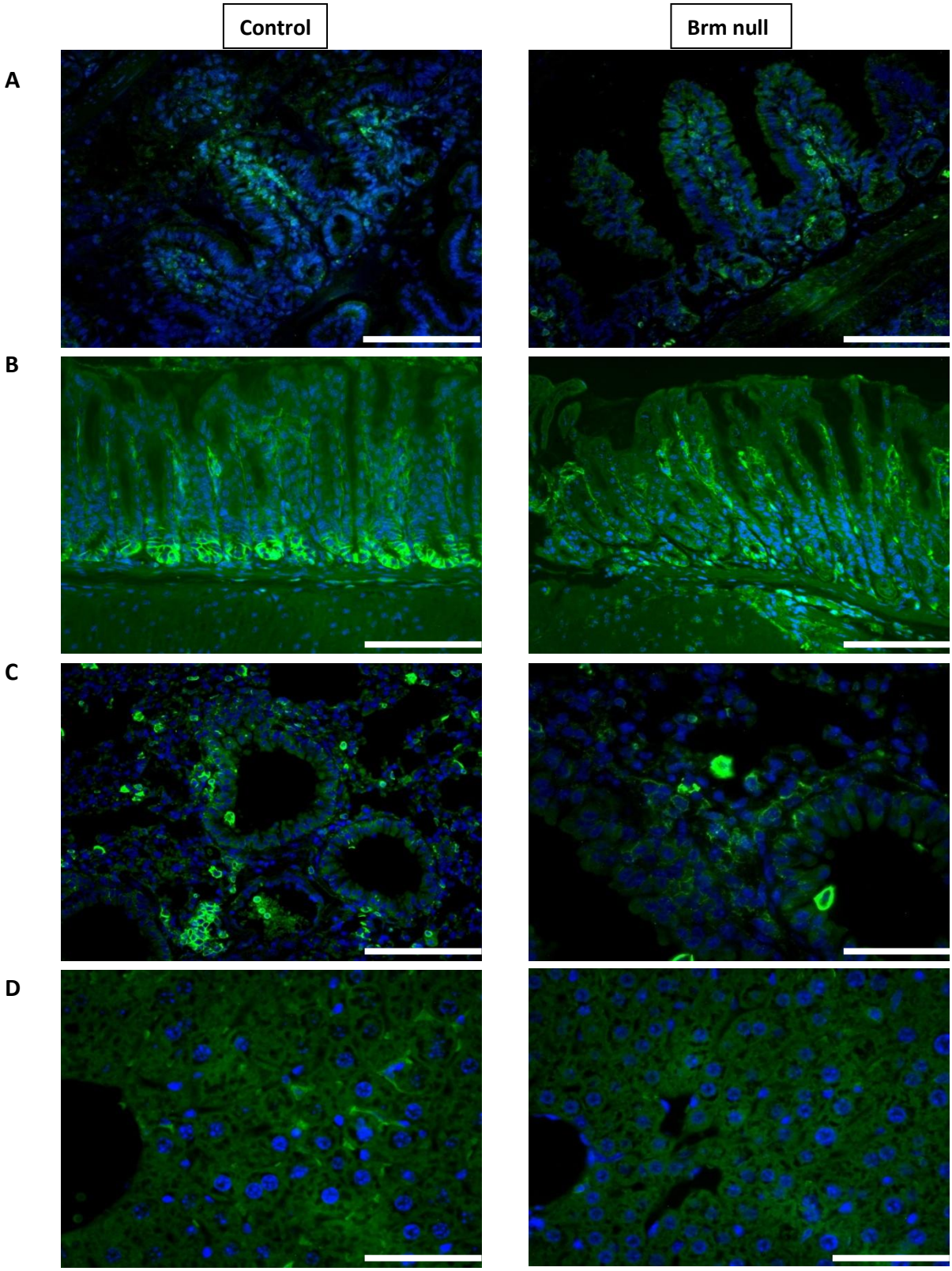

Figure 3.13 Immunofluorescent staining for CD44 for (A) small intestinal epithelium (B) stomach (C) lung (D) liver. The analysis of the CD44 expression revealed no differences in the small intestine, stomach or lung tissue between Brm null and controls harvested at 70 days of age. A decrease in the expression of CD44 was detected in the liver however the staining of whole tissue lacks the consistency of positive signal. Staining and CD44 expression analysis conducted by Prof B. E. Weissman (LCCC, Chapel Hill, USA). Scale bar represents 100 μm.

3.2.8 Brm loss does not directly interact with Wnt signalling

Brm null experimental animals did not show any signs of illness or tumour formation which confirms previously published data (Reyes *et al.,* 1998) but as its paralogue ATPase Brg1 is widely considered a tumour suppressor. Therefore I assessed levels of β-catenin in the epithelium to look for any evidence of a direct interaction between Brm and Wnt signalling.

Immunohistochemical analysis of β-catenin in 70 days old control and Brm null animals detected a significant difference in the expression levels of β-catenin in the small intestinal epithelium (Figure 3.14a). In both Brm deficient and control cohorts, β-catenin is observed at the cell membrane of intestinal epithelial cells, which is consistent with the role of β-catenin in cell-to-cell adhesion as adherens junction component however the staining was significantly stronger in control animals. Some nuclear β-catenin was detected within the bottom third of the crypts suggesting that some cells within the stem cell niche express nuclear β-catenin.

The observation of elevated levels of stabilized β-catenin in the cytoplasm and nucleus in following disruption of the β-catenin destruction complex is one of the first hallmarks of activated Wnt signalling. The validation of differences observed in β-catenin immunohistochemical staining between control and Brm null animals and therefore nuclear accumulation of β-catenin was investigated quantifiably by Western blotting in Brm null and control animals at day 70 (n=4) (Figure 3.14b). This analysis of levels of active (dephosphorylated) β-catenin detected no difference between control and experimental animals (p=0.355, n=4, Figure 3.14c). At the same time, I have also assessed the total levels of β-catenin including its endogenous expression. Once again, the levels of the total β-catenin showed no difference between control and Brm null animals (p=0.343, n=4, Figure 3.14c).

The data above show that complete Brm loss does not lead to changes in the downstream effector of Wnt signalling, β-catenin, further suggesting that any possible effects of Brm on Wnt signalling are not mediated at the level of β-catenin stabilization and accumulation but may occur somewhere downstream the pathway.

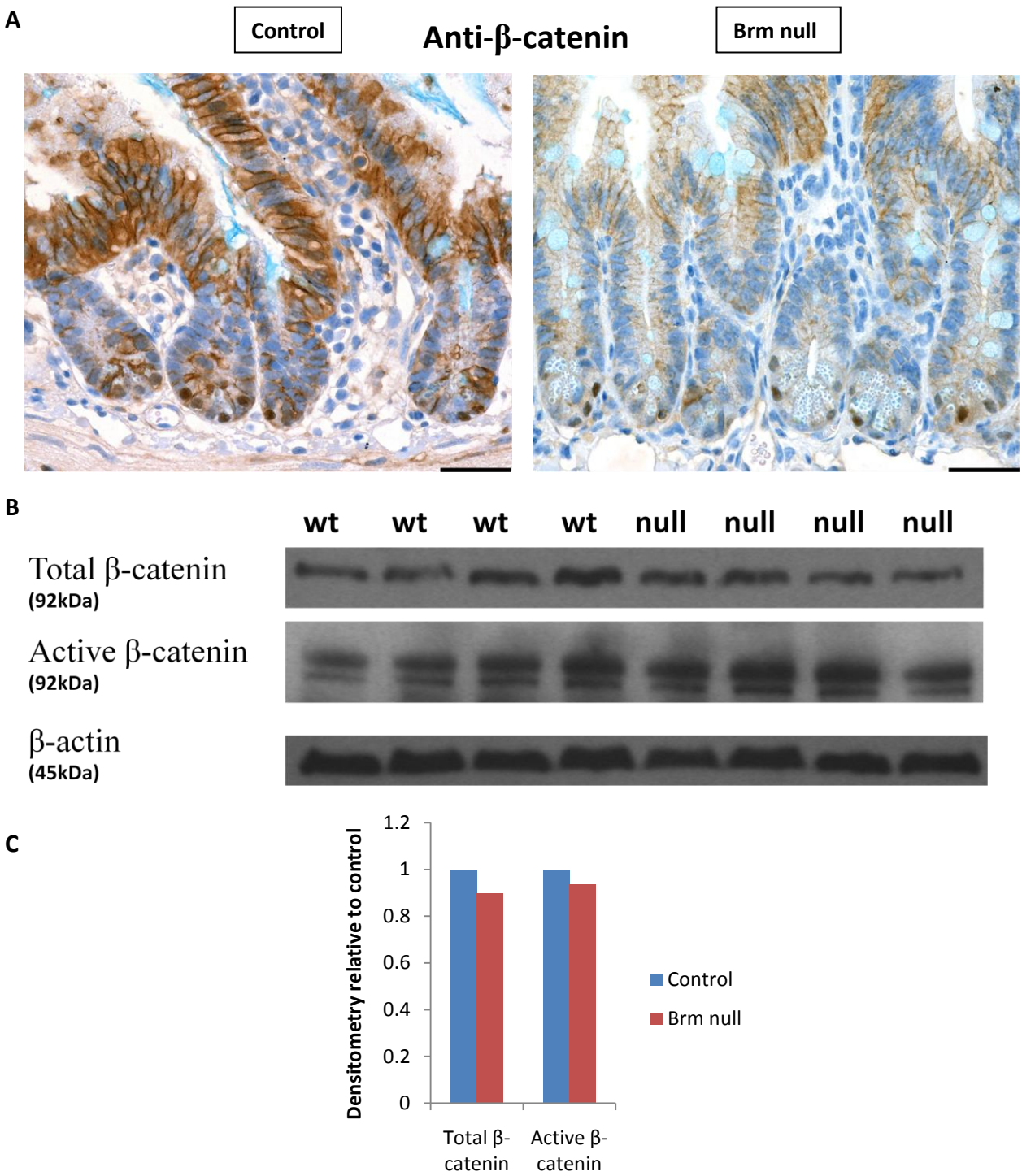

Figure 3.14 The analysis of expression of β-catenin in small intestinal epithelium in Brm null and Brm wild-type animals harvested at 70 days of age. (A) Immunohistochemical analysis of β-catenin revealed presence of staining within the membrane and decreased expression in Brm null in comparison to control animals. Nuclear β-catenin staining was detected in the certain cells within crypt compartment (B) Western blot for β-catenin forms: total endogenous β-catenin and dephoshorylated β-catenin. Previous immunohistochemical analysis does not allow for quantification of levels of β-catenin, protein levels of β-catenin were measured by Western blotting. (C) The analysis of blotting by densitometry revealed no differences in protein levels between Brm null and control animals indicating no effects of Brm loss on protein levels of main Wnt pathway effector, β-catenin. The results were normalised to the β-actin loading control and represented as a value relative to controls ($p= 0.355$, $n=4$ and $p=0.343$, $n=4$, Mann Whitney U Test). The scale bar represents 50μm.

3.2.9 Brm loss leads to changes in Notch signalling

Both Wnt and Notch signalling are responsible for controlling crypt cell proliferation, directing the differentiation of progenitor cells towards secretory or absorptive lineages and maintaining the intestinal stem cell niche. The immunohistochemical analysis reported changes in the number of identified differentiated cell types observed in Brm null animals suggest that the homeostasis between different signalling pathways maintaining the proliferation and migration of the cells within the small intestinal epithelium is somehow disturbed. The Notch pathway and its effectors belonging to the bHLH (basic helix-loop-helix) family of transcription factors play a crucial role in the progenitor cell fate determination. NICD (Notch intracellular domain) which is released upon the Notch ligand binding translocates into the nucleus to form an active complex with Rbp-j Notch mediator in order to stimulate the expression of Notch target genes. Hes1 is one of those target genes and it acts as a major effector of Notch signalling. During normal intestinal homeostasis Hes1 promotes the progression of progenitor cells into enterocytes whereas Hes1 loss shifts the differentiation and specification of progenitors from absorptive lineage cell type into a secretory Goblet cell fate. Other two hairy and enhancer of split (Hes) family members, Hes3 and Hes5, have been shown to act cooperatively with Hes1 in regulating the cell fate of intestinal progenitor cells and repressing the expression of epithelial cell fate determination genes such as Math1 (Ueo et al 2012, van Es et al 2005). Math1 is another member of the family of bHLH transcription factors which is essential for intestinal cell differentiation into secretory lineage (van Es 2010). Because of the crucial role of Notch signalling on the maintenance of intestinal homeostasis, the levels of “canonical” Notch signalling pathway elements such including Hes1, Hes5, Notch 1 ICD and Math1 were closely investigated by Western blotting. The target proteins have been specifically chosen as they are present in different parts within the signalling cascade to enable the step-wise analysis in determining whether any and which particular parts of the Notch signalling pathway are affected by Brm loss.

The analysis of Notch1 ICD protein levels which is a receptor for membrane-bound Notch ligands Jagged1, Jagged 2 and Delta1 showed no significant changes ($p=0.686$, $n=4$, Figure 3.15b). Similarly, the levels of main Notch signalling effector downstream of NICD binding, Hes1 did not detect any changes ($p=0.114$, $n=8$, Figure 3.15b).

Immunohistochemical analysis of Hes5 expression in the small intestinal epithelium of Brm null and control animals detected Hes5-positve cells to be localised predominantly at the crypt base neighbouring with Paneth cells with some rare positive cells present within the bottom two thirds of the crypt (Figure 3.16a). Therefore there is no difference in the localisation of the Hes5-positive cells between Brm deficient and control animals. Despite no changes detected in the pattern of expression of Hes5 within the small intestinal epithelium, notable changes in the level of expression of Hes5 were observed. In the control tissue, Hes5-positive cells were present in each crypt whereas in Brm null only a small percentage of small intestinal crypts contained Hes5-positive cells. Assessment of Hes5 protein levels conducted by Western blotting detected a significant reduction of Hes5 protein levels in Brm null tissue samples compared to controls ($p<0.05$, n=8, Figure 3.16b, 3.16c).

Finally, the levels of Math1 were investigated by Western blotting and revealed a slight increase in Math1 protein in Brm null samples in comparison to control tissue ($p<0.05$, n=4, Figure 3.15b).

In order to assess whether the observed changes are occurring at the transcriptional, protein level or both, the expression levels of Hes1 and Math1 were assessed by qRT-PCR. mRNA was extracted from small intestinal tissue samples of Brm null and control animals at day 70. qRT-PCR analysis of Hes5 mRNA levels revealed no significant changes between Brm deficient and control mice ($p=0.287$, n=6, Figure 3.17a). An increase in mRNA of Hes1 in Brm null animals was observed however this trend was not significant (Figure 3.17b, $p=0.054$, n=6). This was in contrast to Math1 mRNA, where we found a marked increase in Brm null in comparison to control cohort (Figure 3.17b, $p=0.031$, n=6).

Although Brm loss does not affect either the receptor Notch1 or the best-characterized effector of Notch signalling cascade Hes1, significant changes in Hes5 at the protein level and in Math1 at both transcriptional and protein level have been detected.

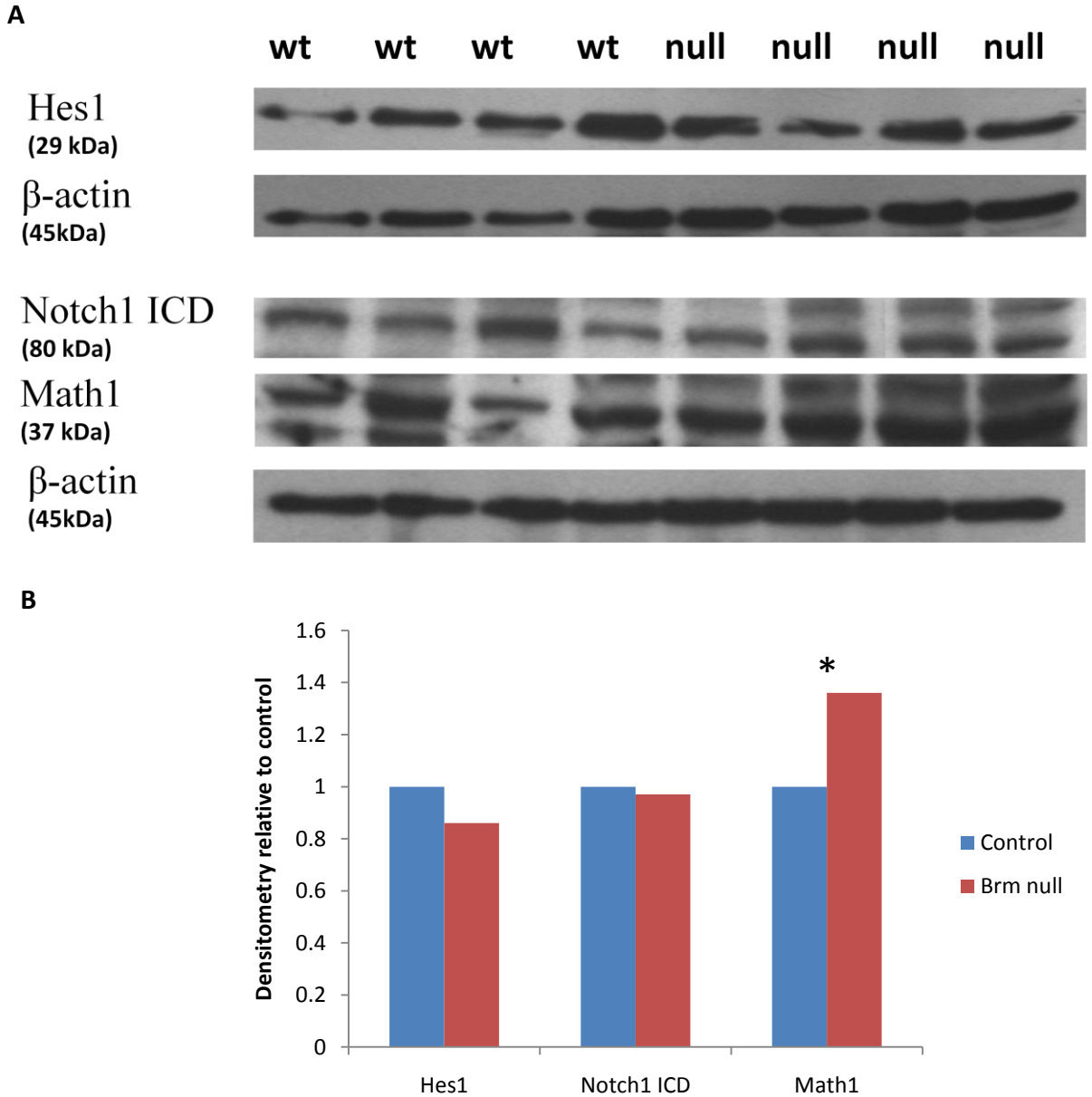

Figure 3.15 (A) Western blots for numerous elements of Notch signalling such as Hes1, Math1, Notch1 ICD. (B) Analysis of protein levels of Hes1 and Notch1 ICD revealed no changes due to Brm loss comparing Brm null and Brm wild-type animals ($p=0.114$, $n=8$ and $p=0.686$, $n=4$, respectively). However the increased protein levels of Math1 were found in Brm null animals in comparison to controls ($p<0.05$, $n=4$).

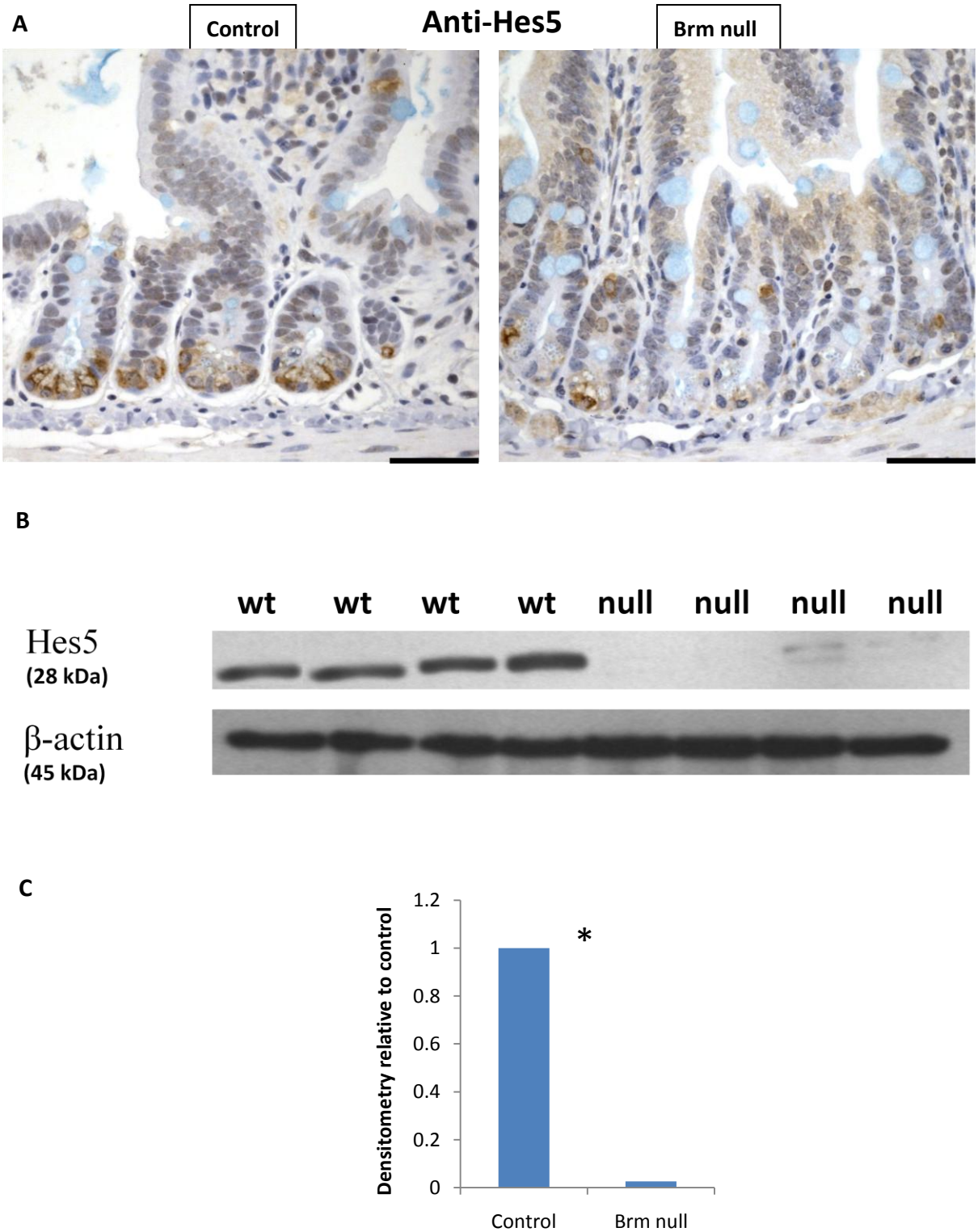

Figure 3.16 Analysis of Hes5 expression in the small intestinal epithelium. (A) Immunohistochemistry against Hes5 showed that Hes5 is expressed with intestinal crypt compartment and detected a decline in number of Hes5 positive cells in Brm null animals in comparison with controls (B) Western blot analysis was perform in order to confirm the observation from immunohistochemical staining of intestinal sections. (C) Analysis of protein levels of Hes5 by densitometry showed loss of Hes5 in Brm null animals in comparison to normal levels expressed in Brm wild-type animals ($p<0.05$, n=8, Mann Whitney U Test). Scale bar represents 50µm.

A

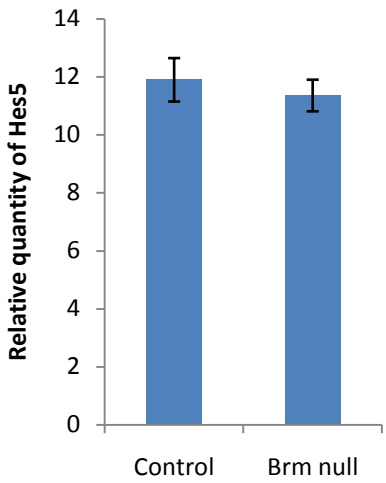

B

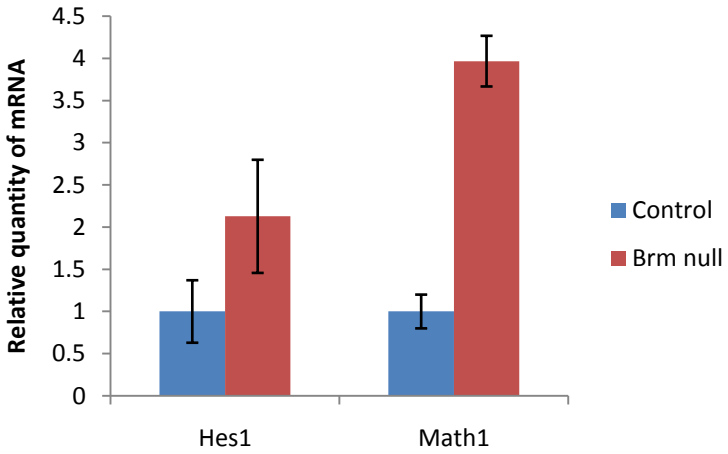

Figure 3.17 The transcriptional levels of Hes5, Hes1 and Math1 were quantified by quantitative real-time-PCR (qRT-PCR) as shown in bar graph form. The data from qRT-PCR are normalised with β-actin and presented as a mean ± S.D. (n=6). (A) Analysis of levels of Hes5 mRNA showed no differences between control and experimental animals (p=0.287, n=6). (B) Analysis of levels of Hes1 mRNA showed a trend of an increase in Brm null animals compared to controls (p=0.054, n=6) whereas a marked increase in Math1mRNA was detected (p=0.031, p=6)

3.2.10 Brm loss does not affect the stem cell compartment

To analyse potential changes in the stem cell compartment *in situ* hybridisation using a probe against *Olfm4*, a Wnt-independent gene and a marker of intestinal stem cells which revealed positive staining within the bottom third of the intestinal crypt of control animals whereas in Brm null animals the area where Olfm4 probe has bound extended approximately half way up the length of the crypt with some of Paneth cells showing positive staining with *Olfm4* ribo-probe. The intensity of staining also appeared to be higher in the Brm deficient cohort (Figure 3.18a). In order to further confirm the results obtained from *in situ* hybridization, we assessed the effects of Brm deficiency on the expression of stem cell marker Olfm4 at the transcriptional level. mRNA was extracted from the small intestinal tissue samples of Brm null and control animals at day 70 and used for qRT-PR. Expression analysis of the Olfm4 stem cell marker revealed a trend of decreased Olfm4 expression in Brm null animals however this result was not significant ($p=0.572$, $n=6$, Figure 3.18b).

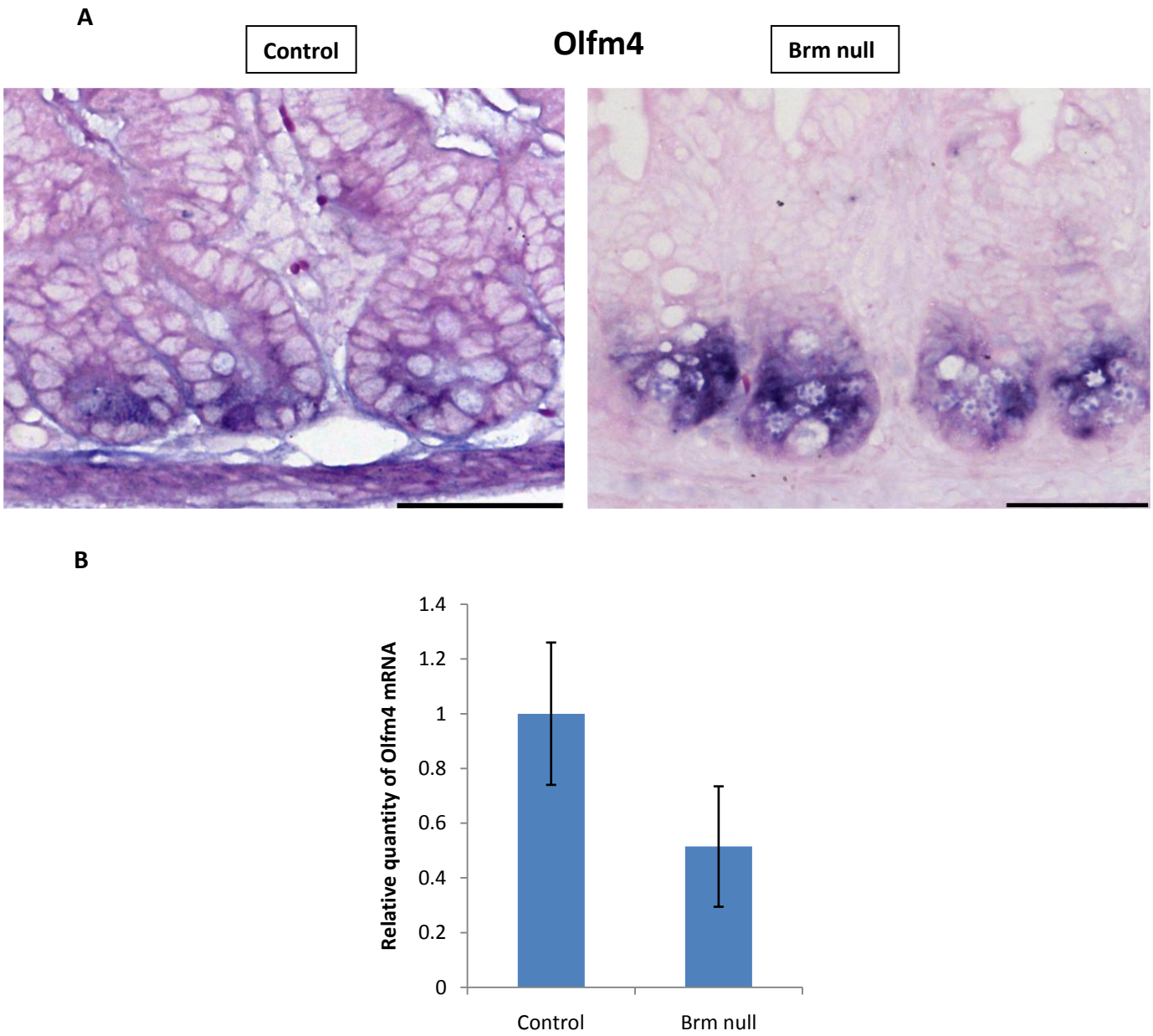

Figure 3.18 Analysis of intestinal stem cell niche in Brm null animals. (A) *In situ* hybridization against Olfm4 detected some differences in the amount of probe bound in the small intestinal epithelium of Brm null in comparison to control animals. The stained area is extended and the intensity of staining is higher in Brm null cohort. Scale bar represents 50 µm. (B) The transcriptional level of Olfm4 was quantified by quantitative real-time-PCR (qRT-PCR) as shown in bar graph form. The data from qRT-PCR are normalised with β-actin and presented as a mean (n=4). Analysis of levels of Olfm4 mRNA revealed a trend of decrease in Brm experimental animals in comparison to controls which was not significant (p=0.572, n=6).

3.2.11 The pattern of Brm expression in large intestinal epithelium

The expression of both Brm and Brg1 ATPase in normal human tissues have been described by Reisman *et al.,* (2005) indicating tissue-specific patterns of expression depending on whether particular cell types are engaged in constant proliferation and self-renewal. Brm was found to be expressed in the muscularis propria of small and large intestine however in the intestinal epithelium only Brg1 expression was detected. Contrary to this study, Yamamichi and his colleagues (2007) detected Brm-positive cells with a nuclear staining in human colonic mucosa. To investigate the pattern of expression of Brm in the colonic epithelium of our murine model, immunofluorescence staining against Brm was conducted (Figure 3.19). Staining of colonic epithelium revealed the presence of nuclear Brm-positive cells along the length of the colonic crypt. The vast majority of the cells within the epithelium were expressing Brm in contrast to results obtained in the small intestinal epithelium.

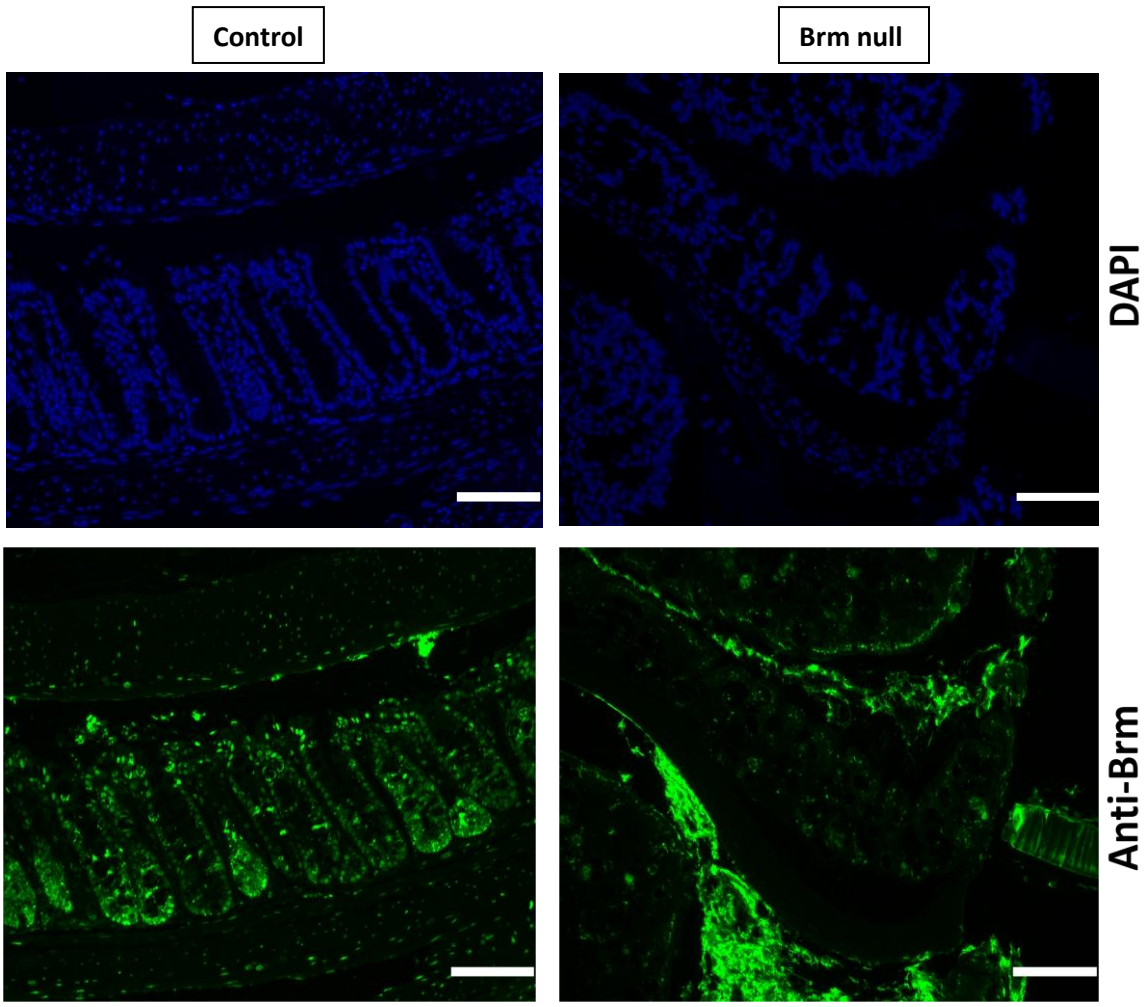

Figure 3.19 The expression pattern of Brm in the colonic epithelium. Brm null animals along with Brm $^{+/+}$ controls were dissected at 70 days of age and immunofluorescent staining was conducted on harvested tissue. Blue channel corresponds to DAPI nuclear staining and green channel to Brm staining. Immuflourescent analysis of Brm expression revealed Brm expression along the length of colonic crypt in control cohort. Some positive non-specific staining was detected in cells of secretory lineage of both Brm null and control animals. Scale bar represents 100μm.

3.2.12 Brm loss has a mild effects on the homeostasis of large intestinal epithelium

In the small intestinal epithelium no morphological abnormalities or tumorigenesis were observed in the cohort of Brm deficient animals. However a detailed quantitative analysis revealed significant changes in crypt and villus length as well as a shift in the differentiation of cells towards the secretory lineage in Brm null mice compared to controls. As a consequence of those observations and the fact that cells of the secretory lineages are the predominant cell population present in the colonic epithelium, the effects of Brm loss on the large intestinal epithelium were investigated in Brm null and control animals dissected at 70 days of age. A quantitative analysis performed on these tissue sections is summarized in Table 3.2.

Similarly to the results obtained from small intestinal epithelium, macroscopic analysis of colonic epithelium during tissue harvesting revealed no tissue abnormalities or tumorigenesis.

Crypt length was assessed on H&E stained sections as the average number of cells (± standard deviation) from the bottom of the crypt of Lieberkühn till the flat surface of the epithelium. Crypt size was found to be unaltered in Brm null colonic epithelium in comparison with control animals (24.50±0.43 and 24.31±0.32, p=0.476, n=8, Figure 3.20a).

Apoptosis within the epithelium was detected and scored by cleaved Caspase-3 immunohistochemical staining. The quantification of cleaved Caspase-3-positive cells showed a trend of increase in levels of apoptosis in Brm null mice versus control animals, however this increase was not significant (0.064±0.022 and 0.060±0.016, p=0.763, n=8, Figure 3.19b). The size and the shape of proliferative compartment in the colonic epithelium was assessed using immunohististochemical staining against proliferation marker, Ki67. Scoring of Ki67-positive cells revealed a trend of an increase in the average number of proliferating cells per crypt in Brm deficient cohort in comparison to controls, however this result was not significant (7.92±2.55 and 6.61±1.04, p=0.34, n=8, Figure 3.20c) similarly to the quantification of apoptosis by cleaved Caspase-3. The analysis of the cumulative frequency of Ki67-positive cells showed no difference between control and Brm null animals (Kolmogorov-Smirnov Z test p=0.978, n=8, Figure 3.20d). The distribution of proliferating cells and therefore the shape of proliferative compartment remained unaltered in the experimental mice in comparison with controls.

As in case of small intestine, BrdU incorporation was used as another marker for cell proliferation to specifically quantify number of cells in the S-phase of the cell cycle. Brm null and control mice were injected with BrdU labelling reagent 2 hours and 24 hours prior to dissection and the obtained tissue sections were stained using anti-BrdU antibody. However due to the low numbers of BrdU-positive cells detected the quantification and analysis of those cells would not prove beneficial towards histological analysis.

Therefore in the context of Brm deficiency within the colonic epithelium, the quantitative analysis of functional and morphological parameters detected no effect on the length of crypt and a trend in an increase in both apoptosis and proliferation but no changes in the shape of proliferative compartment. Thus homeostasis in the large intestinal epithelium appears to not be affected by constitutive loss of Brm.

Parameter	Cohort	Mean	SD	p-value
Crypt length	Control	24.31	0.32	0.476
	Brm null	24.50	0.43	
Caspase3 positive cells	Control	0.064	0.022	0.763
	Brm null	0.060	0.016	
Ki67 positive cells	Control	7.92	2.55	0.34
	Brm null	6.61	1.04	

Table 3.2 Quantitative analysis of the effects of Brm loss on the histology of colonic epithelium. Epithelium from large intestine from Cre^{-} Brm $^{+/+}$ (marked as Control) and Cre^{-} Brm null (marked as Brm null) was harvested from animals at 70 days of age. Histological parameters including crypt length, apoptosis and proliferation were quantified and comparison between those two cohorts was conducted using statistical software.

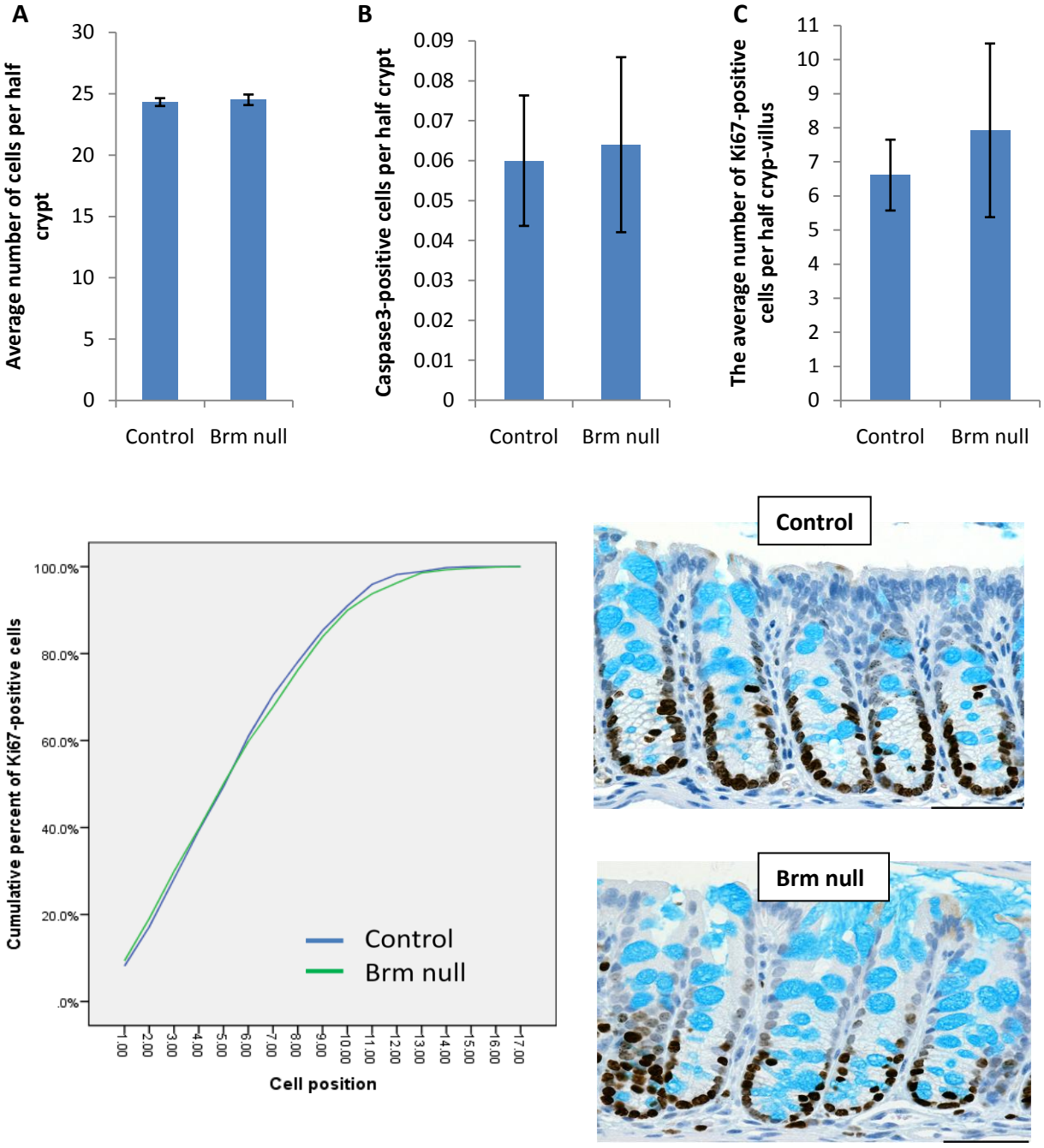

Figure 3.20 Histological analysis of the effects of constitutive Brm loss in the colonic epithelium. Control and experimental Brm null animals were harvested at day 70 of age. A-D histological parameters such as (A) crypt length was counted on H&E sections for control and Brm deficient animals. The average number of (B) Cleaved Caspase3 and (C) Ki67-positive cells was scored on the corresponding immunostained sections. (D) Cumulative frequency analysis detected no changes in the proliferation compartment between Brm null and control animals. Error bars represent standard deviation and asterisk symbol indicates those histological parameters that showed a statistically significant difference (p value <0.05) between cohorts of mice. Exact values, standard deviations, p values are provided in Table 3.2

3.2.13 Brm deficiency results in a shift in the differentiation pattern towards the secretory lineages

Although homeostasis of colonic epithelium appears to be maintained with no significant effects upon cell number or crypt size (as discussed in the previous section), quantification of the differentiated cell types within the colonic epithelium was carried out.

The most abundant cell type in the epithelium of the colon is the goblet cell. Alcian Blue staining was carried out to score the numbers of those secretory lineage cells in the colonic epithelium of Brm null and control animals (Figure 3.21). Quantification of the Alcian Blue stained cells showed a significant increase in the number of goblet cells per half crypt in the Brm deficient epithelium in comparison to controls (7.63±0.40 and 6.50±0.07, $p<0.0001$).

Enteroendocrine cells are another of secretory lineage present in the colonic crypts. Grimelius staining was used to identify these cells within the large intestinal epithelium. The scoring of cells per half crypt that have taken up the silver stain revealed a marked decrease in the numbers of enteroendocrine cells in the Brm null animals compared to control animals (1.47±0.07 and 1.61±0.05, $p=0.02$, $n=8$, Figure 3.22).

The quantification of the major differentiated cell types in the epithelium of the colon revealed a shift in the differentiation of secretory lineage with an increase in numbers of mucin-secreting cells and a decrease in enteroendocrine cells in the Brm deficient epithelium.

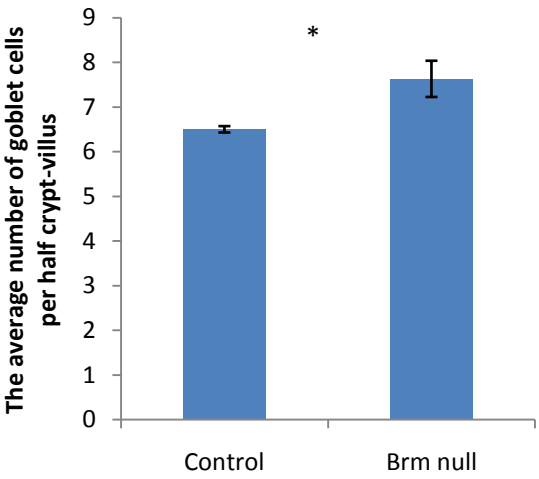

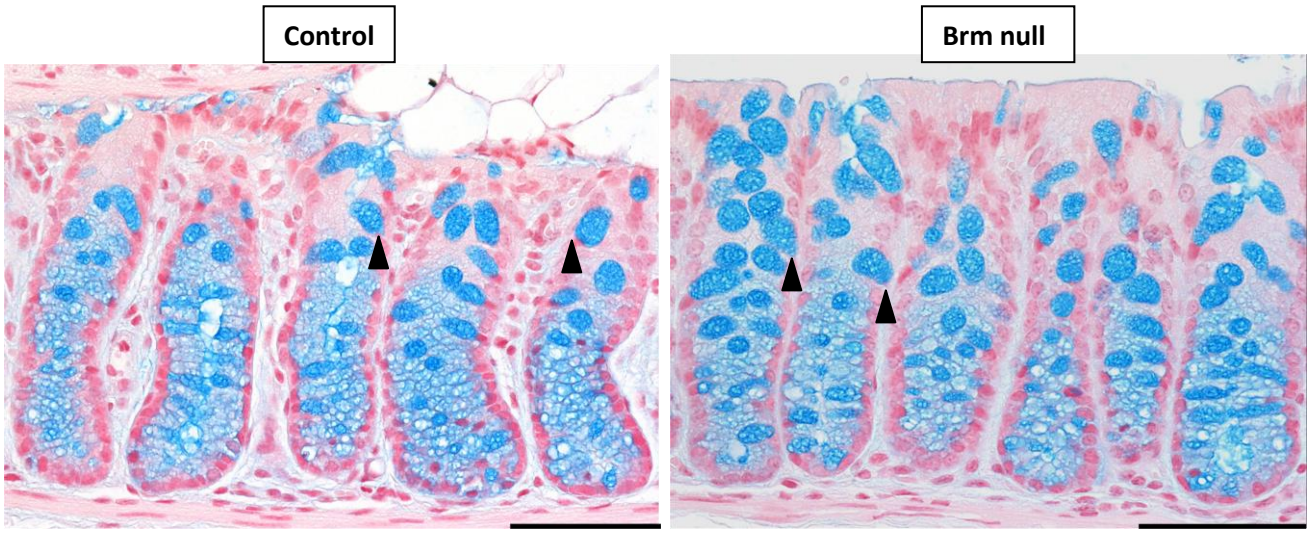

Figure 3.21 Alcian Blue staining was used in order to mark goblet cells within colonic epithelium. The colon sections of control and Brm null mice dissected at day 70 of age and stained using cell specific stain detecting mucin secreting cells. Black arrows indicate individual goblet cells. Staining revealed no changes in the localisation of Alcian Blue stained cells in the epithelium of control and Brm experimental animals. The number of Alcian Blue positive cells increased in Brm null animals in comparison with controls. The scale bar represents 50µm.

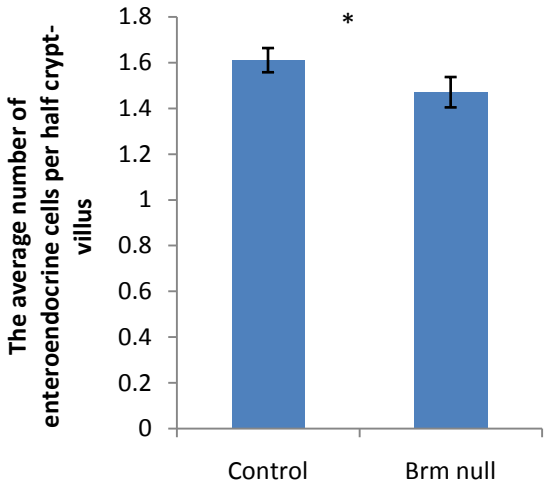

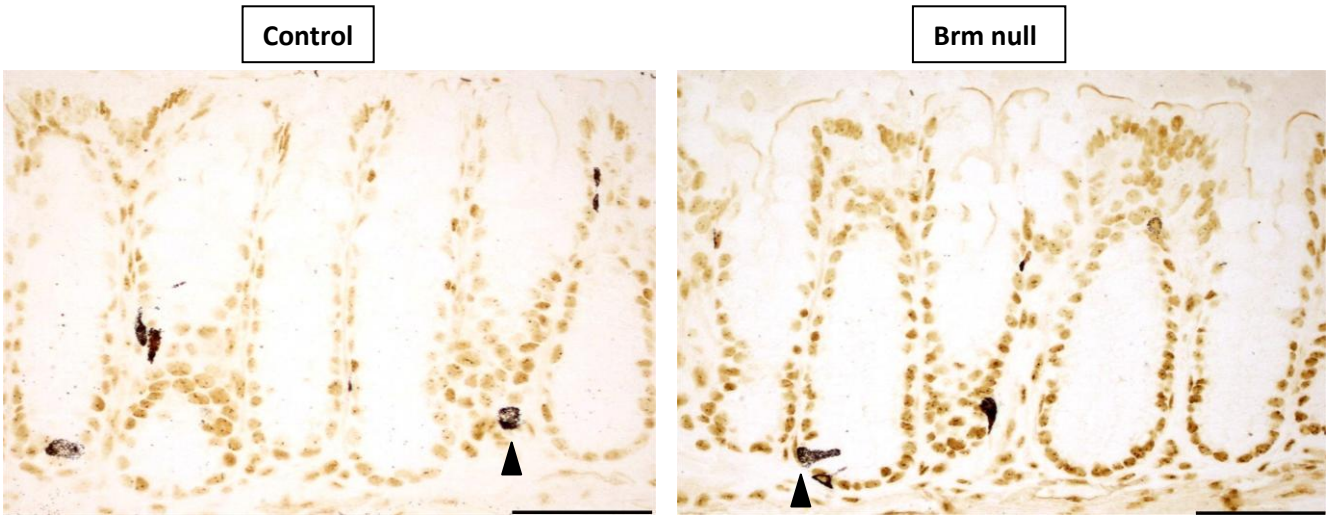

Figure 3.22 Grimelius staining of colonic sections was carried out to visualize the number of enteroendocrine cells on colonic epithelium sections of control and Brm null mice dissected at day 70 of age. Black arrows indicate individual enteroendocrine cells. Staining reveal normal localisation of enteroendocrine cells in Brm deficient animals in comparison with controls. The scoring of numbers of cells detected significant decrease in numbers of enteroendocrine cells in Brm null in comparison to control animals. The scale bar represents 50µm.

3.3 Discussion

The generation of constitutive knock-out through the replacement of the exon a by a Neomycin resistance cassette (Reyes *et al.,*1998) was the first and crucial step in providing important insights into the role of Brm as Brm null animals are viable and fertile, unlike its paralogue Brg1. This murine model has already provided some crucial insights into the physiological role of Brm with to date no spontaneous tumour formation being reported (Reyes *et al.,* 1998).

3.3.1 Mosaic pattern of expression of Brm in different tissues

Previous data on the pattern of Brm expression in normal tissues (non-dysplastic) have indicated that higher levels have been found in several slowly proliferating tissues such as brain, liver and spleen further suggesting that the levels of Brm within fast proliferating and high-turnover tissues like the intestine might be not discernible. I aimed to investigate the expression of Brm in a range of tissues from abdominal cavity: small and large intestine, liver, spleen and kidney collected from Brm null and control animals at day 70 days of age. Immunohistochemical analysis revealed nuclear localisation of Brm in liver, spleen and kidney whereas small and large intestine displayed very little or no nuclear Brm staining. The immunofluorescent analysis of Brm revealed a low level of Brm expression in the small intestinal epithelium in contrast to colon where nearly all epithelial cells were positive for Brm. Previous observations by Muchardt and Reyes (1998) indicated that non-differentiated cells contain predominantly Brg1 and Brm is accumulated upon *in vitro* differentiation. This could explain why the expression levels of Brm in intestinal and colonic crypts are lower than in other organs such as spleen. Nonetheless, in the small intestine Brm is limited to rare populations of early differentiating and mature epithelial cells whereas in the colon Brm is present in the crypt compartment. The expression levels of Brm could possibly be tissue-specific and depend upon the levels of Brg1 in a particular type of epithelium.

Similar to the data published by Reisman *et al.,* (2005), very specific cell types were observed to express nuclear Brm such as lymphoid germinal centers, sinusoidal cells in the red pulp and central artery of the spleen as well as in Bowman's capsule epithelium and mesangial cells of the kidney. In the liver of control animals only Brm expression was detected with no Brg1 expression in hepatocytes. However, in the liver of Brm deficient animals Brg1-positive cells with nuclear staining were present and some of those Brg1-expressing cells were hepatocytes.

Therefore we can conclude that although the level of Brm expression varies across numerous organs the presence of Brm is often limited to a particular subpopulation of cells.

3.3.2 Complete Brm loss has very mild effects on intestinal homeostasis

Due to the fact that Brm constitutive knockouts are viable, this model was the most suitable way of investigating the effects of Brm deficiency on homeostasis of the small intestinal and colonic epithelium.

General histological inspection of H&E sections of the intestinal epithelium of animals dissected at day 70 revealed no abnormal structures within the epithelium and the maintenance of general crypt-villus architecture in Brm null animals suggesting that complete loss of Brm expression does not lead to abrogation of intestinal organisation. Nevertheless, further quantitative analysis of the epithelium showed some subtle changes in the homeostasis.

In the small intestine, a slight increase in crypt length was detected together with a decrease in villus length which could implicate an expansion of the proliferative compartment of the epithelium. However as no differences in proliferation or apoptosis were observed this data suggests that rather than detecting an increasing pool of stem and progenitor cells we are detecting an increased pool cells that have already begun to differentiate towards the absorptive or secretory lineages. In contrast to the small intestine, there were no changes in the crypt length of the colonic epithelium and a trend of decrease in number of proliferating cells suggesting that small intestinal and colonic epithelium respond in a different manner to Brm deficiency.

Previous study by Reyes *et al.* (1998) detected a four-fold increase in proliferation in the liver of Brm null animals which was expressed as the increase in the number of BrdU-positive cells compared to control animals. In this study we have not quantified histological parameters such as proliferation in the liver, however our results from the small intestine revealed a marked increase in the number of BrdU-positive cells scored 24 hours after BrdU exposure additionally confirming the previously detected trend of an increase in the number of Ki67-positive cells in Brm null animals. As a result of the low numbers or indeed absence of BrdU-positive cells in the crypts of the colonic epithelium, quantification of BrdU incorporation did not reveal any differences yet the quantification of proliferation by Ki67

marker showed an opposite trend to the one observed in small intestine with a decrease in numbers of proliferating cells in the colon of Brm null mice.

The differences in effects and trends observed between small and large intestinal epithelium of Brm null animals indicates a tissue-specific role of Brm.

3.3.3 Complete Brm loss affects Notch signalling

Intestinal homeostasis is a finely controlled process of maintaining the balance between diverse cellular processes including proliferation, differentiation and apoptosis in order to ensure the continuous renewal of the intestinal epithelium. It involves different cell populations the most important of which are stem cells and immature progenitor cells both localised within the intestinal crypts. The Wnt pathway, specifically the canonical Wnt pathway is well known for playing a crucial role in regulating intestinal homeostasis. Recently, the Notch signalling pathway which comprises of a large family of bHLH (basic helix-loop-helix) transcription factors emerged as another of the central regulators of intestinal homeostasis and in particular regulation of the stem cells and progenitor compartments.

Hes1 is one of the best characterized target genes of Notch signalling and it is involved in the maintenance of hematopoietic and neural stem cells. In the intestinal epithelium, it is expressed by proliferating cells of the crypt and it represses the expression of *Math1* and *Ngn3*. *Math1* regulates the differentiation into all mature cell types of secretory lineage whilst *Ngn3* specifically directs the differentiation into enteroendocrine cell type. Hes1 knock-out animals display a phenotype characterised by overproduction of secretory cells and fewer enterocytes, which is consistent with the role of Notch-Hes1 signalling in regulating the proliferation within intestinal crypts and inhibiting Math1 and Ngn3 expression (Jensen *et al.*, 2000). Concurrently with the loss of Hes1 expression, two other members of the hairy and enhancer of split family, Hes3 and Hes5 are upregulated in the intestinal epithelium (Jensen *et al.*, 2000). The precise mechanism of action of the Hes genes and most of all the hierarchy of different members of this family of genes remains largely unclear. Hes1 phenotype is characterized by the increase in numbers of cleaved Caspase-3 positive cells, goblet and enteroendocrine cells at 2.5 days postnatal however none of these effects were observed in adult mice at 8 weeks. Furthermore, Hes1 was found to be expressed in the proliferating cells of the intestinal epithelium but not present in the Paneth cells in control animals and Hes5 is

expressed by Paneth cells (van Es 2005). In double of Hes3/5 knock-out mice, Hes1 was found to be expressed in the Paneth cells suggesting it compensates for Hes3 and Hes5 deficiency. The triple knock-out of Hes1/Hes3/Hes5 genes displayed a phenotype similar to that one found in Hes1 deficient mice at day 2.5 together with a premature Paneth cell differentiation and mislocalisation (Ueo *et al.,* 2012). No changes in Wnt or BMP pathways were reported in mutant Hes1/Hes3/Hes5 mice.

Previous studies investigating the role of the Notch signalling in the gut have found that all three Hes genes: Hes1, Hes3 and Hes5 negatively regulate the development of all types of secretory cells. Although the Hes genes are required for proliferation of intestinal progenitor cells they are not essential for the maintenance of the stem cells. This suggests that there are other Notch effectors that might be compensating for Hes genes in the maintenance of stem cells. Hes genes are essential for proliferation of transit-amplifying or progenitor cells and for the secretory versus absorptive cell fate decision ensuring normal intestinal development and homeostasis (Ueo *et al.,* 2012). The conditional removal of the Rbp-j transcription factor revealed undetectable levels of Hes1 and marked de-repression of Math1. The phenotype observed included a significant increase in goblet cell numbers and the arrest of all epithelial proliferation labelled by BrdU in both the small and large intestine of Rbp-j deficient mice. The marked differences in the phonotype observed in Rbp-j knock-out and Hes1 knock-out animals were accounted for by the presence of other genes belonging to the hairy and enhancer of split family, notably Hes5 and Hes6 (van Es *et al.,* 2005).

Western blot analysis performed on small intestinal tissue from Brm null mice revealed diminished protein levels of Hes5 expression in comparison to control animals. Further immunohistochemical analysis and scoring of Hes5-stained intestinal epithelium detected Hes5 positive cells localized exclusively within the crypt compartment however visibly reduced numbers of Hes5-posistive cells were observed suggesting that Hes5 expression is in some extent abrogated in the intestinal epithelium of Brm null animals. In contrast, no Hes5 expression was detected in the large intestinal epithelium. Further quantification of mRNA levels of Hes1, Hes5 and Math1 revealed no significant changes for Hes1 and Hes5. However, a significant decrease in Math1 mRNA was observed suggesting that Math1 is regulated at both transcriptional and protein levels in Brm deficient animals.

Chip analysis showed that CBF-1 recruits SWI/SNF Brm-containing complexes to Hes1 and Hes5 promoters through preferential interaction with Brm rather than Brg1. Promoter regions

of those two Notch target genes appear to be already remodelled prior to Notch signalling activation via Notch2, and therefore Hes1 and Hes5 promoters appear poised for transcription by CBF-1 binding, Brm recruitment and histone acetylation.

Taken together, previous data supports our results that in case of Brm loss and subsequent loss of Hes5 expression, Hes1 protein levels remain unchanged due to a compensatory mechanism between Hes family members as well as other elements of Notch signalling *nota bene* which have not been investigated by our study. Similarly as no changes in other signalling pathways have been observed in the Hes1/Hes3/Hes5 deficient mouse we can extrapolate that Hes5 deficiency induced by loss of Brm is likely to have little effect on other signalling pathways involved in the maintenance of intestinal homeostasis. This would explain the lack of change in β-catenin protein levels and would account for the very mild Brm phenotype we observe. As a result of morphological differences between small intestinal and colonic epithelium such as the absence of enterocytes, the balance between Hes1 and Math1 expression in the large intestine as well as the need for Hes5 expression appears to be different.

Furthermore, changes in cell numbers of goblet and enteroendocrine cells in both the small and large intestine seems to be driven by upregulation of Math1. Similarly to Rpbj deficient animals, in Brm null animals Math1 might become de-repressed as a result of Hes5 loss in small intestinal epithelium which however may be compensated for.

3.3.4 Brm loss does not compromise the expression levels of CD44

Previous data investigating the concomitant loss of Brm and Brg1 revealed that Brm null animals lack CD44 expression even in the presence of functional Brg1 regardless of upregulation of Brg1 expression. No positive CD44 staining was detected in tissues such as the liver, gut epithelium, brain and lungs suggesting that Brm loss alone results in the ablation of CD44 expression (Reisman *et al.,* 2002). In contrast to this data Strobeck *et al.* (2001) found that reintroduction of Brg1 only in the C33A cervical carcinoma cell line is capable of restoring CD44 expression.

The complete loss of CD44 expression was not confirmed for Brm null animals dissected at 70 days of age. The subtle trend of CD44 increase was observed but was not confirmed to be significant for the cohort of Brm null mice analysed during this PhD.

Analysis of Brm and Brg1 deficiency in a subset of human cancer cell lines has shown that combined lack of SWI/SNF results in loss of CD44 expression. Furthermore, in depth analysis of SW13 human adrenal carcinoma cell line revealed the existence of two subtypes of SWI/SNF complexes in the same cells: one that expresses both Brm and Brg1 and a second that expresses neither of two ATPases. No change in transcription activities between the subtypes was detected indicating the capacity of SW13 cell line to spontaneously transition between Brm Brg1 negative and Brm Brg1 positive subtype (Yamamichi *et al.*, 2003).

Taken together, as Brm loss does not compromise the expression levels of CD44 in the small intestinal epithelium at 70 day of age I hypothesise that the effect of Brm on CD44 observed by Reisman *et al.* was due to sampling at a different time point (timepoint not specified by Reisman *et al.* 2003). These observations correlate well with the mechanism of spontaneous transition suggested by Yamamichi *et al.* (2003) and therefore in case of re-expression of Brg1 restoring CD44 expression similarly to observations by Strobeck *et al.* (2001) providing us one possible explanation for the lack of change in CD44 expression in our experimental cohort.

Given the observation that Brm is not expressed in the stem cell compartment, but rather in the differentiating or mature epithelial cell types and further that the differentiation promoting genes Hes1, Hes5 and cyclin A are well-known Brm-specific target genes, we can conclude that Brm, in contrast to Brg1, has less severe effect on the epithelium of small and large intestine and is predominantly involved in the differentiation of progenitor cells into mature cell types.

Chapter 4

Investigating the effects of Brm loss in the Wnt activated epithelium of small and large intestine

4.1 Introduction

Subunits of SWI/SNF chromatin remodelling complex have been implicated in regulating numerous genes controlling a variety of processes from embryonic development to cell apoptosis. Some subunits have been detected to frequently be silenced in cancers of lungs, esophagus, ovaries and breast (Reisman *et al.* 2009). Similarly Brm loss has been correlated to poor prognosis in the majority of those cancers suggesting that Brm expression may play an important role in the modulation of cancer phenotype.

Over 80% of CRCs are caused by the aberrant activation of the Wnt pathway which has been proven to play a crucial role in normal homeostasis of intestinal epithelium (Korinek *et al.* 1998, Pinto *et al.* 2003, Kuhnert *et al.* 2004) as well as in colorectal tumorigenesis (Korinek *et al.* 1997, Morin *et al.* 1997, Polakis *et al.* 1999). The interplay between Wnt and Notch pathway is the most dominant force driving the stem cell/progenitor niche by controlling self-renewal and differentiation along the crypt-villus axis. Both pathways are frequently abnormally activated in CRC and despite the fact that there is no evidence supporting interactions of the Brm with Wnt pathways, Brm has been shown to be involved in interactions with the ICD22 and CBF-1 elements of the Notch signalling pathway indicating that Brm may contribute to colorectal tumorigenesis. Furthermore, together with the other ATPase subunit of SWI/SNF complex Brg1, Brm has been implicated in the transcriptional activation and repression of many genes and therefore in alteration of gene expression. One of those genes, CD44, is a major downstream target of β-catenin and it has been reported that its expression increases with a progression of the CRC (Wielenga *et al.* 1993, Zeilstra *et al.* 2008). Brm has been shown to associate with CD44 promoter (Strobeck *et al.* 2001, Reisman *et al.* 2002, Banine *et al.* 2005, Batsché *et al.* 2006) suggesting it may directly influence the levels of CD44 expression however no effect of Brm deficiency on CD44 expression was

observed (as described in Chapter 3.2.7). Moreover Brm has been reported to be necessary for Rb-mediated growth inhibition as Brm-deficient cancer cell lines are resistant to Rb-mediated cell cycle arrest (Strober *et al.* 1996, Reisman *et al.* 2003) and Brm can cooperate with Rb to repress cyclin A which is crucial in regulating the progression through the cell cycle (Dahiya *et al.* 2001).

Initiation of tumorigenesis by activating mutations in the Wnt cascade and subsequent neoplastic transformation makes targeting of components of the Wnt pathway downstream of β-catenin an interesting potential avenue for therapy. For the same reason, alterations in elements of SWI/SNF complex that are believed to function as *bona fide* specialized tumour suppressors such as Brm ATPase may result in modulation of phenotypes observed during CRC tumorigenesis.

This chapter will aim to characterise the effects of Brm deficiency on Wnt-driven tumorigenesis in the small intestinal and colonic epithelium as well as the potential of Brm to act as a modulator of CRC.

4.2 Results

4.2.1 Placing Brm in a context of aberrant Wnt signalling

In order to investigate the effects of Brm deficiency in the context of aberrant Wnt signalling specific to the intestinal epithelium, I exploited the Cre recombinase conditional knock-out system to inactivate *Apc*. Targeted *Apc* alleles contain loxP sites placed within introns on both sides of exon 14 and recombination between those loxP sites mediated by Cre recombinase results in a frame-shift mutation and the expression of a truncated version of Apc characterised by the loss of function (Shibata *et al*., 1997).

Animals carrying Brm null alleles were intercrossed with mice carrying *Tg(Cyp1a1-cre/ESR1)1Dwi* transgene (abbreviated here as AhCreER) (Kemp *et al*., 2004). AhCreER recombinase is expressed under the control of *Aryl hydrocarbon* (Ah) promoter element derived from the rat cytochrome *P4501A1* gene but additionally contains a modified hormone-binding domain of the estogen receptor (ER). Therefore the induction of AhCreER requires the administration of tamoxifen together with beta-naphthoflavone and recombination occurs in a range of tissues including the intestinal epithelium, liver and pancreas (Ireland et al., 2004). In the intestinal epithelium, expression of the AhCreER

transgene is restricted to the bottom of the crypt of Lieberkühn with stem cells and early progenitor cells being the only cell populations in which AhCreER is expressed. Cre mediated recombination driven by the AhCreER results in a lower recombination frequency in the intestinal epithelium in comparison to that delivered by AhCre recombinase. Due to the differences in the nature of constitutive (Brm null) and conditional (Apc floxed) alleles, loss of Brm and Apc alleles does not occur simultaneously.

The effects of the constitutive inactivation of Brm alleles in the intestinal epithelium have been previously described in Chapter 3.

4.2.2 Brm loss does not improve survival of Apc-deficient animals

A number of carcinogenesis studies reported that Brm is silenced in 10-25% of solid tumours whereas transgenic knock-out of Brm potentiates tumour development *in vivo*. Therefore, I aimed to examine whether Brm deficiency in the intestinal epithelium would alter Wnt-driven tumorigenesis accomplished by homozygous inactivation of Apc.

In order to investigate the long-term effects of Brm loss in the context of Wnt signalling activation and intestinal neoplasia, 70 day cohorts of AhCreER^{+}Apc$^{fl/fl}$Brm$^{+/+}$ and AhCreER^{+}Apc$^{fl/fl}$Brm null animals were induced with five bi-daily intraperitoneal injections of 80mg/kg β-naphthoflavone with Tamoxifen at 12 hour intervals. AhCreER^{-} control mice were induced alongside the above cohorts (n≥12 for all cohorts except AhCreER^{+}Apc$^{fl/fl}$Brm null n=7). Mice were then aged for a maximum of 100 days or until they developed signs of ill health and had to be sacrificed and appropriate tissues harvested. Whilst none of the animals from the control cohort became ill within the timeframe of the experiment, AhCreER^{+}Apc$^{fl/fl}$Brm$^{+/+}$ and AhCreER^{+}Apc$^{fl/fl}$Brm null animals started showing signs of ill health as early as 8 and 9 days post induction respectively. Survival analysis of AhCreER^{+}Apc$^{fl/fl}$Brm$^{+/+}$ and AhCreER^{+}Apc$^{fl/fl}$Brm null cohorts showed that all animals became ill and had to be sacrificed within less than 3 weeks of induction (Figure 4.1a, median survival of 9 and 12 days, respectively). Close observation of the induced experimental animals from the first day that they displayed early signs of ill health revealed that symptoms in the AhCreER^{+}Apc$^{fl/fl}$Brm null mice developed more rapidly and these mice had to be sacrificed within 24 hours, whereas in AhCreER^{+}Apc$^{fl/fl}$Brm$^{+/+}$ mice the progression of the symptoms was less rapid, allowing mice to be maintained for a further 2-3 days. The analysis of the overall survival probability revealed no statistically significant difference between the

AhCreER^{+}Apc$^{fl/fl}$Brm$^{+/+}$ and AhCreER^{+}Apc$^{fl/fl}$Brm null cohorts (Figure 4.1b, Log-Rank test p=0.144).

Histological analysis of H&E sections of small intestinal epithelium of AhCreER^{+}Apc$^{fl/fl}$Brm$^{+/+}$ and AhCreER^{+}Apc$^{fl/fl}$Brm null cohorts identified numerous mono-crypt adenomas and formation of early stage small adenomas with no perceptible differences in the tumour progression between those two cohorts of Apc-deficient animals (Figure 4.1c).

A

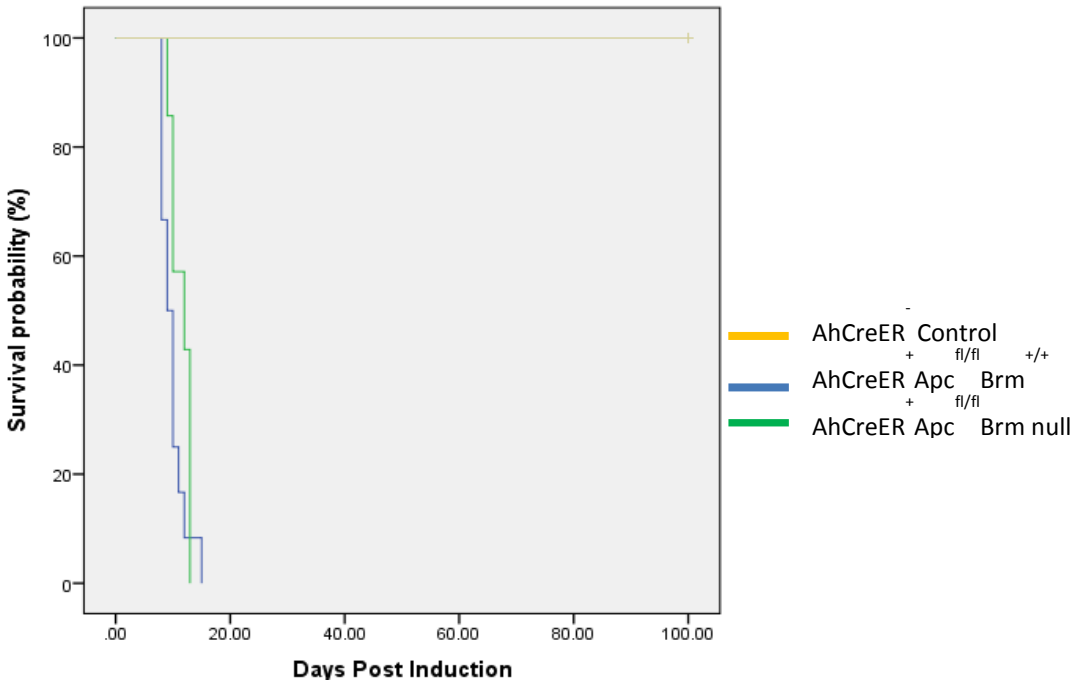

B

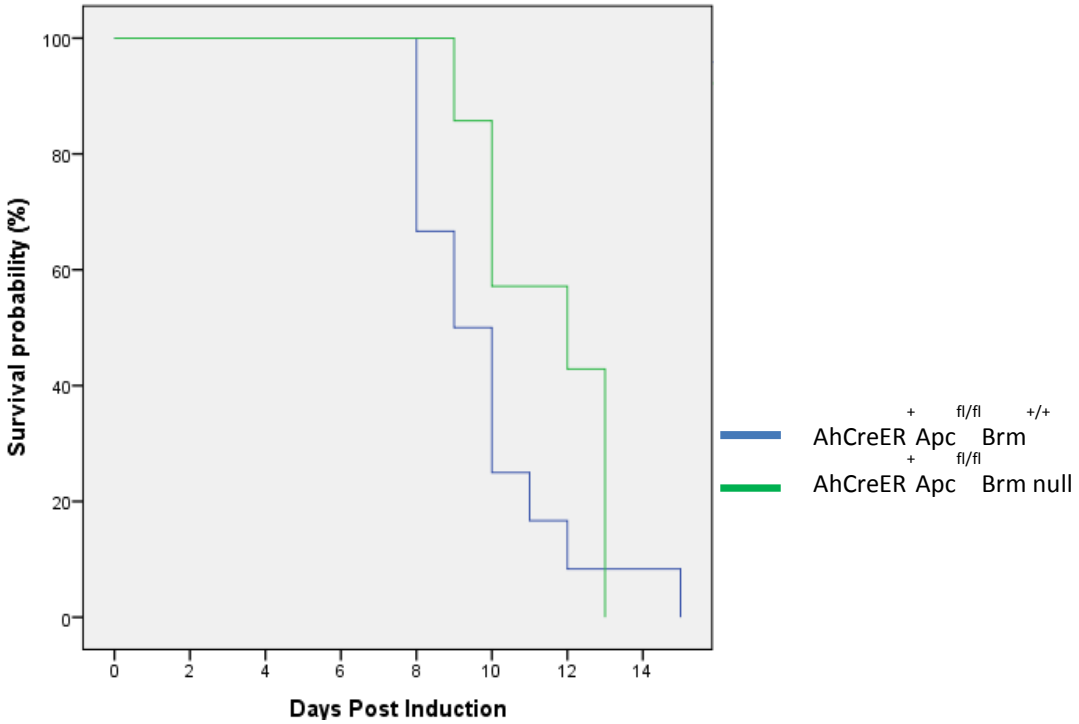

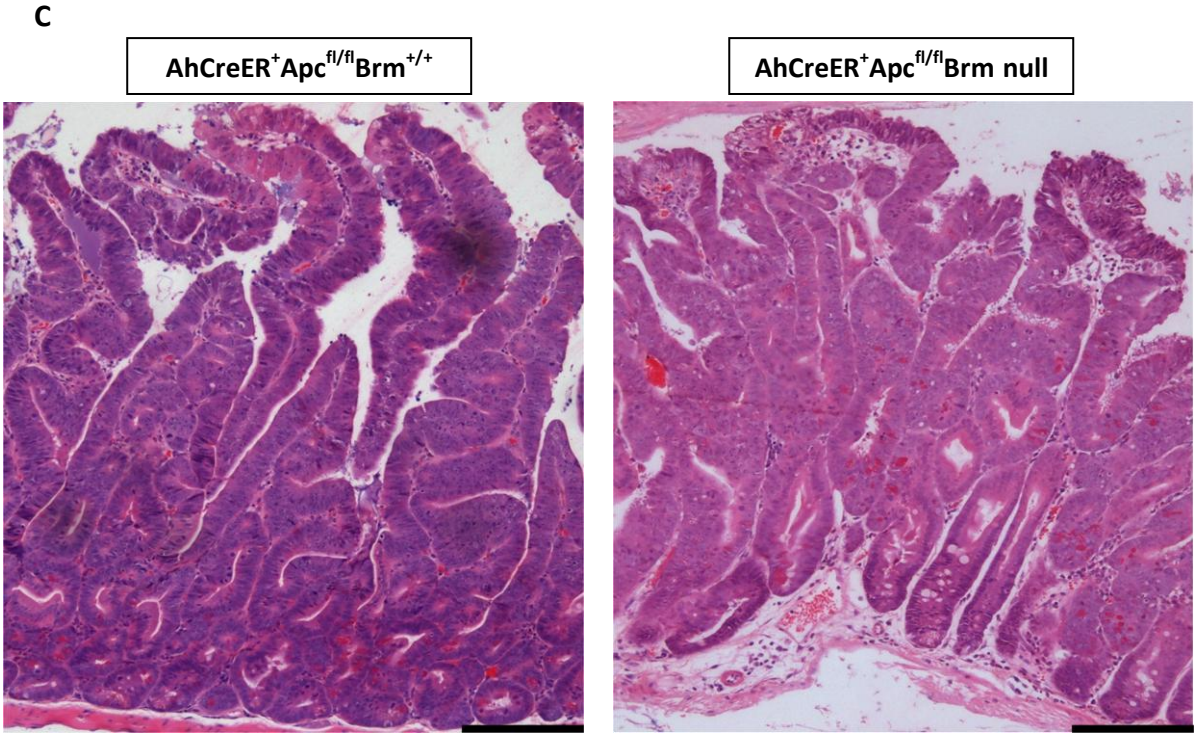

Figure 4.1 Brm deficiency does not alter the survival of animals with a homozygous inactivation of Apc. Cohorts of AhCreER^{+}Apc$^{fl/fl}$Brm$^{+/+}$ and AhCreER^{+}Apc$^{fl/fl}$Brm null were induced using an appropriate protocol along with AhCreER^{-} control mice ($n \geq 7$). Animals were aged for 100 days post induction or until they have developed signs of ill health. (A) Survival data was presented as a Kaplan-Meier plot and revealed a significant difference in the survival probability of both experimental cohorts in comparison to control animals (Log-Rank test $p<0.0001$, $n \geq 7$ for either cohort). (B) Analysis of survival probability between AhCreER^{+}Apc$^{fl/fl}$Brm$^{+/+}$ and AhCreER^{+}Apc$^{fl/fl}$Brm null revealed no significant difference (Log-Rank test $p=0.144$, $n \geq 7$). (C) H&E sections microscopic analysis identified numerous mono-crypt adenomas in the epithelium of both AhCreER^{+}Apc$^{fl/fl}$Brm$^{+/+}$ and AhCreER^{+}Apc$^{fl/fl}$Brm null animals with no perceptible differences between the dysplastic tissues.

4.2.3 Brm loss is compatible with nuclear β-catenin

In many studies focusing on Apc deficiency, β-catenin is used as a surrogate marker of Apc loss, as a specific change in the localization of β-catenin into the nucleus is a well-recognized immediate effect of dysregulated Wnt signalling (Sansom *et al.* 2004). Previous studies in our laboratory on the Brm paralogue Brg1 revealed that Brg1 loss is incompatible with Wnt-driven adenoma formation as in the small intestinal epithelium of AhCreER^{+}Apc$^{fl/fl}$Brg1$^{fl/fl}$ mice at 30 and 100 days post induction all mono-crypt adenomas characterised by nuclear β-catenin were also found to express Brg1. Immunohistochemical analysis of β-catenin expression in the small intestine of AhCreER^{+}Apc$^{fl/fl}$Brm null revealed numerous dysplastic aberrant crypt foci (ACF) and small lesions with nuclear localisation of β-catenin (Figure 4.2). This pattern of expression was similar to that observed in AhCreER^{+}Apc$^{fl/fl}$Brm$^{+/+}$ indicating that Wnt signalling activation does occur in AhCreER^{+}Apc$^{fl/fl}$Brm null mice. Due to the very short survival of both AhCreER^{+}Apc$^{fl/fl}$Brm$^{+/+}$ and AhCreER^{+}Apc$^{fl/fl}$Brm null mice, only multiple intestinal lesions and small tumours were observed in Apc experimental cohorts.

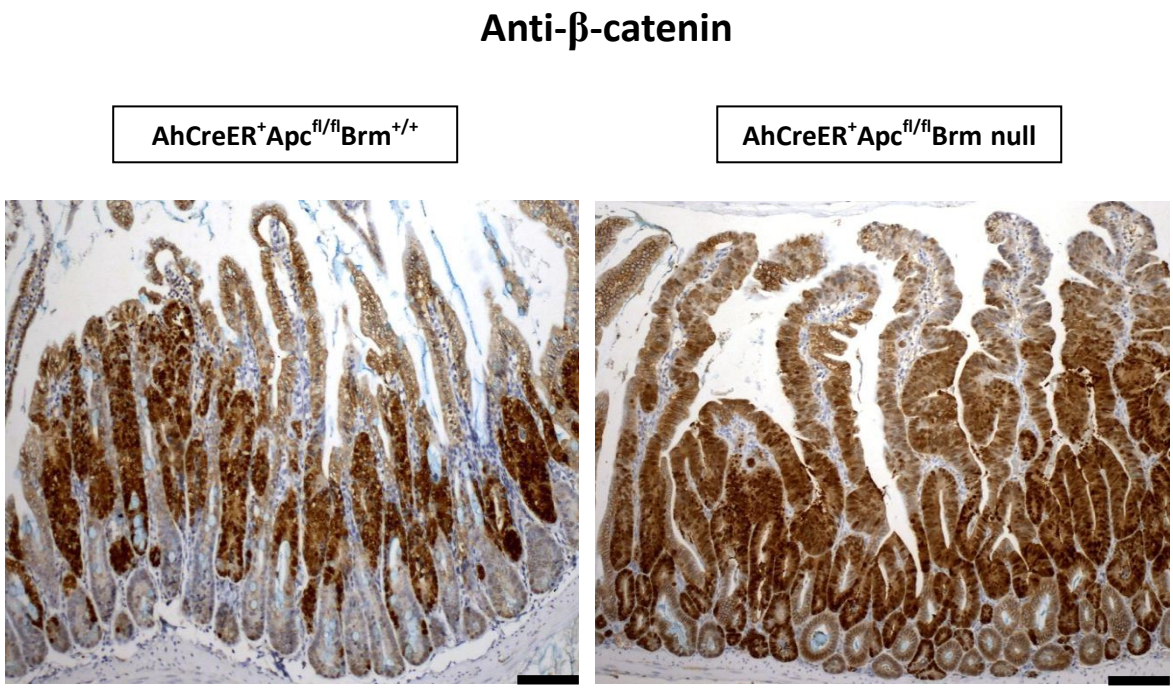

Figure 4.2 Brm deficiency is compatible with Wnt pathway activation in the stem cells and progenitors cells of small intestinal epithelium. Immunohistochemical analysis of β-catenin expression in AhCreER^{+}Apc$^{fl/fl}$Brm$^{+/+}$ and AhCreER^{+}Apc$^{fl/fl}$Brm null cohorts at days 10-12 post-induction showed multiple intestinal lesions with nuclear β-catenin. The constitutive nature of Brm loss ensured that the observed pattern of β-catenin localisation was consistent across the small intestinal epithelium. Scale bar represents 100μm.

4.2.4 Brm deficiency is permissive of Apc loss and accentuates some of the manifestations associated with Wnt signalling activation

No previous direct links between the Brm chromatin remodelling factor and the Wnt signalling pathway have been reported, however due to the more rapid and severe progression of symptoms of ill health in AhCreER^{+}Apc$^{fl/fl}$Brm null mice in comparison to the AhCreER^{+}Apc$^{fl/fl}$Brm$^{+/+}$ mice and a non-tumour morbidity, I investigated whether Brm loss may amplify the effects of aberrant Wnt activation in the small intestinal epithelium. Due to the lower efficiency of the AhCreER-driven recombination in comparison to that observed by other recombinases (such as AhCre), tissue sections showing similar ratios of unfloxed to floxed tissues were selected for further histological analysis. Initially, the morphology of tissue sections was assessed revealing some of previously published histological features of Wnt activated intestinal epithelium, such as elongated crypts (Sansom *et al.*, 2004). The analysis of histological and functional parameters (crypt length, villus length, levels of apoptosis and proliferation) of AhCreER^{+}Apc$^{fl/fl}$Brm$^{+/+}$ and AhCreER^{+}Apc$^{fl/fl}$Brm null revealed differences between those cohorts. The results of quantitative analysis of those histological parameters are summarized in Table 4.1 and Figure 4.3.

Initial morphological analysis of small intestinal H&E sections of control AhCreER^{-}, AhCreER^{+}Apc$^{fl/fl}$Brm$^{+/+}$ and AhCreER^{+}Apc$^{fl/fl}$Brm null animals revealed altered crypt-villus architecture in both Apc-deficient cohorts characterized by an elongated crypt extending towards the crypt-villus axis and an absence of distinct crypt compartment compared to the epithelium of control animals. Furthermore, both crypt and villus lengths were assessed on H&E stained tissue sections as the average number of cells (± standard deviation) from the bottom of the crypt of Lieberkühn till the crypt-villus junction and from the crypt-villus junction to the top of the villus. Small intestinal epithelium crypts of the AhCreER^{+}Apc$^{fl/fl}$Brm$^{+/+}$ mice and DKO mice were found to be significantly increased in comparison to the control animals (42.090±0.082 and 43.545±0.940 compared to 21.617±0.92, p values for either comparison $p<0.001$, $n\geq4$) and furthermore crypts of DKO animals are more elongated than those found in Apc deficient epithelium ($p=0.022$, $n=4$, Figure 4.3a). The quantification of villus length revealed a significant difference between control animals and both AhCreER^{+}Apc$^{fl/fl}$Brm$^{+/+}$ and DKO animals with a marked decrease in length of the villus in both Apc deficient cohorts (73.402±1.478, 48.003±1.871 and

51.59±3.108, p values for either comparison $p<0.001$, $n\geq4$). No difference in the villus length between AhCreER^{+}Apc$^{fl/fl}$Brm$^{+/+}$ and DKO was detected (p value=0.095, n=4, Figure 4.3b).

Both apoptosis and mitosis have been detected and scored on the basis of immunohistochemical staining using specific markers: Cleaved Caspase-3 for sequential caspase activation cascade in cell apoptosis and Ki67 protein expressed in all active phases of the cell cycle except G_0. Scoring of apoptosis revealed a significant increase in apoptosis levels in both AhCreER^{+}Apc$^{fl/fl}$Brm$^{+/+}$ and DKO mice in comparison to control animals (0.866±0.06, 3.505±0.142 and 4.905±0.347, p values for either comparison $p<0.001$, $n\geq4$). Notably, a significant increase in the number of Cleaved Caspase-3-posistive cells scored was revealed in the epithelium of DKO animals compared to AhCreER^{+}Apc$^{fl/fl}$Brm$^{+/+}$ (p=0.015, n=4, Figure 4.3c). Similarly to Caspase 3 staining, the quantification of the cells scored as positive for Ki67 proliferation marker revealed a marked increase in the levels of proliferation between control and AhCreER^{+}Apc$^{fl/fl}$Brm$^{+/+}$ and DKO animals (13.51±0.70, 56.53±6.242 and 64.83±5.720, p values for either comparison $p<0.001$, $n\geq4$). No difference in the number of Ki67-positive cells in the small intestinal epithelium was detected between DKO and AhCreER^{+}Apc$^{fl/fl}$Brm$^{+/+}$ (p=0.098, n=4, Figure 4.3d).

Therefore in the context of conditional deletion of Apc, Brm loss has further amplified some of the effects of aberrant Wnt signalling activation such as an increase in crypt length and apoptosis levels however only an non-significant trend of an increase in the size of the proliferative compartment was detected in the small intestinal epithelium of AhCreER^{+}Apc$^{fl/fl}$Brm null animals in comparison to the AhCreER^{+}Apc$^{fl/fl}$Brm$^{+/+}$ cohort.

Parameter	Cohort	Mean	SD	p-values		
				Control vs Apc KO	Control vs DKO	Apc KO vs DKO
Crypt length	Control	21.617	0.92	0.000	0.000	0.022
	Apc KO	42.09	0.082			
	DKO	43.545	0.940			
Villus length	Control	73.402	1.478	0.000	0.000	0.095
	Apc KO	48.003	1.871			
	DKO	51.59	3.108			
Caspase positive cells	Control	0.866	0.060	0.000	0.000	0.015
	Apc KO	3.505	0.142			
	DKO	4.904	0.347			
Ki67 positive cells	Control	13.395	0.762	0.000	0.000	0.098
	Apc KO	56.53	6.242			
	DKO	64.83	5.720			

Table 4.3 Quantitative analysis of the effects of Brm loss on the histology of Wnt-activated small intestinal epithelium. Epithelium from small intestine from Cre^{-} $Brm^{+/+}$ (marked as Control), $AhCreER^{+}Apc^{fl/fl}Brm^{+/+}$ (marked as Apc KO) and $AhCreER^{+}Apc^{fl/fl}$Brm null (marked DKO) was harvested from animals at days 10-12 post induction. Histological parameters including crypt and villus length, apoptosis and proliferation were quantified and comparison between those two cohorts was conducted using statistical software.

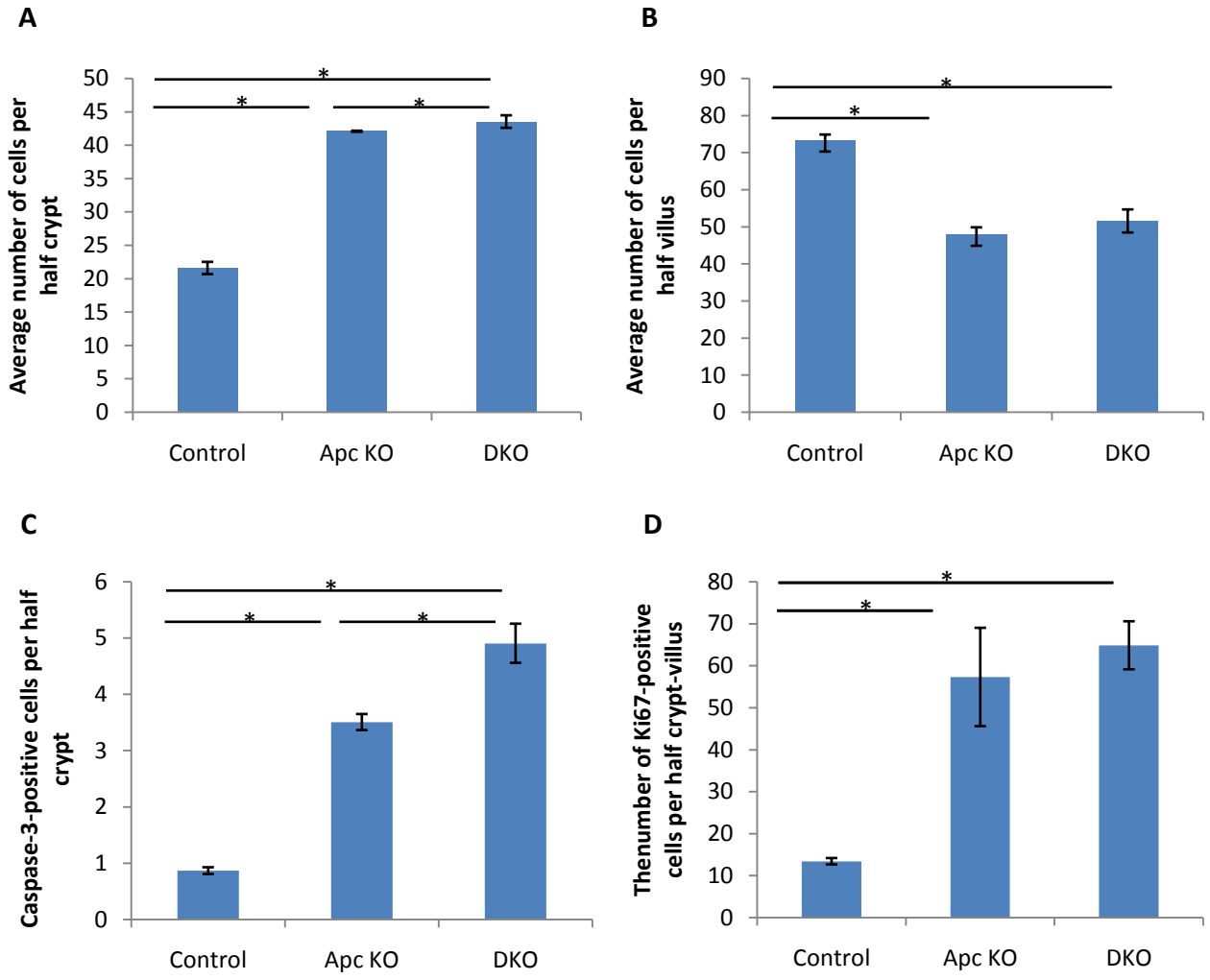

Figure 4.3 Histological analysis of the effects of Brm loss in the Wnt-activated small intestinal epithelium. Control AhCreER^{-} and experimental AhCreER^{+}Apc$^{fl/fl}$Brm$^{+/+}$ (marked as Apc KO) and AhCreER^{+}Apc$^{fl/fl}$Brm null (marked DKO) was harvested from animals at days 10-12 post induction. A-D histological parameters such as (A) crypt length (B) villus length were counted on H&E sections. The average number of (C) Caspase 3 (D) Ki67-positive cells was scored on the corresponding immunostained sections. Error bars represent standard deviation and asterisk symbol indicates those histological parameters that showed a statistically significant difference (p value <0.05) between cohorts of mice. Exact values, standard deviations, p values are provided in Table 4.1.

4.2.5 Brm loss leads to a change in distribution pattern of proliferating cells in the Wnt-activated epithelium of small intestine

The position of the Ki67 positive cells was analysed to assess the changes in the distribution of proliferating cells and furthermore the distribution of the proliferative compartment within the epithelium of the small intestine. Analysis of cumulative frequency of Ki67 positive cells revealed a significant increase in the number of Ki67-labelled cells along the length of the intestinal crypt-villus axis in Apc deficient cohorts in comparison to controls (p values for either comparison $p<0.001$, $n\geq4$). Furthermore, a change in the distribution of proliferating cells marked by Ki67-positivity was observed in DKO animals in comparison to $AhCreER^{+}Apc^{fl/fl}Brm^{+/+}$ animals suggesting Brm deficiency permitted for a differential pattern of proliferating cells distribution along the crypt-villus axis of the small intestinal epithelium (Kolmogorov-Smirnov Z test, $p<0.001$, $n\geq4$, Figure 4.4).

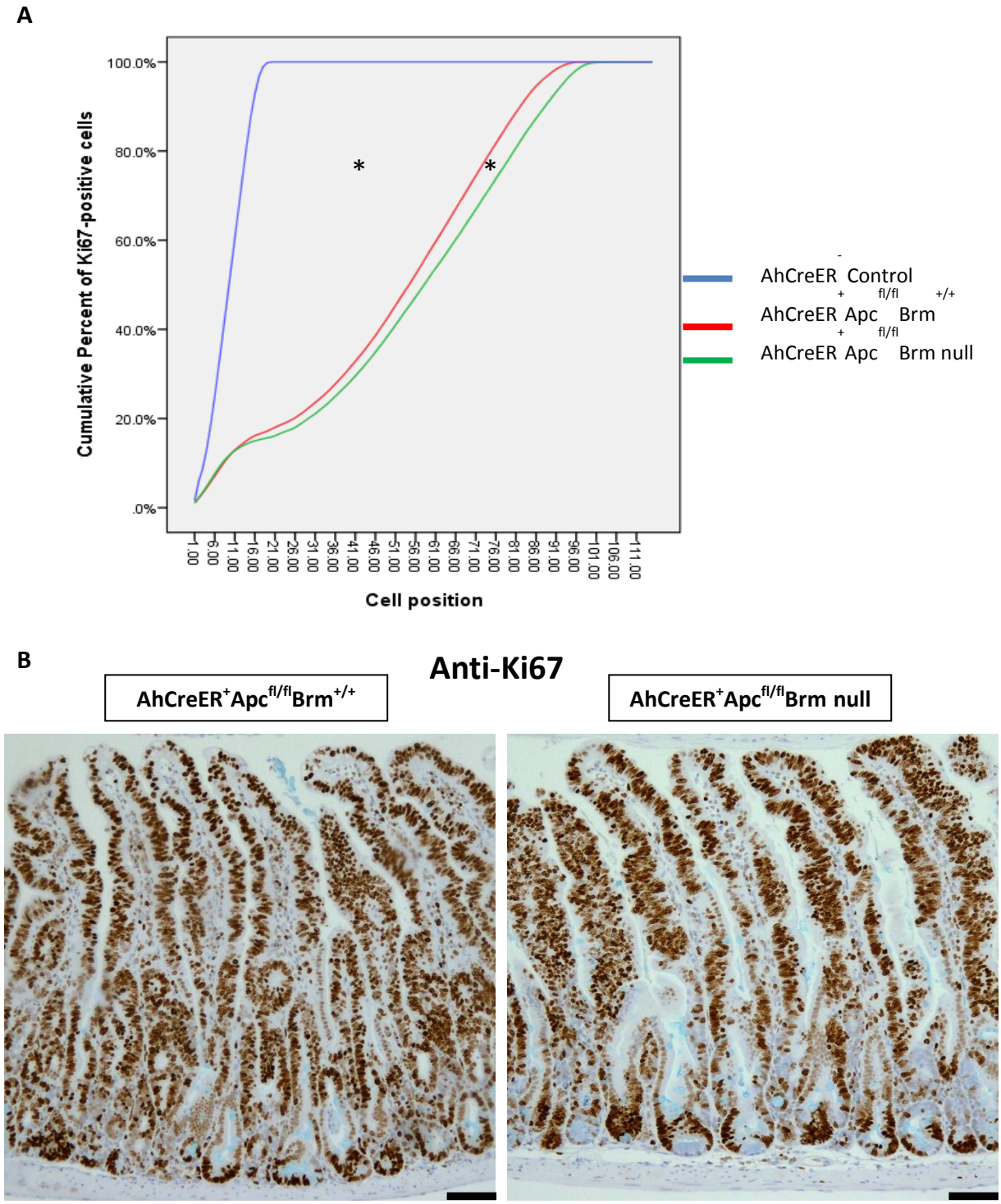

Figure 4.4 Analysis of proliferative compartment by Ki67 staining of control and experimental Apc-deficient animals at day 10-12 post induction. (A) Cumulative frequency analysis of Ki67-positive cells revealed a significant enlargement of the proliferative compartment in AhCreER^{+}Apc$^{fl/fl}$Brm$^{+/+}$ and AhCreER^{+}Apc$^{fl/fl}$Brm null animals in comparison to control mice (Kolmogorov- Smirnov Z test $p<0.0001$, $n\geq4$). Comparison of the distribution of proliferating cells between AhCreER^{+}Apc$^{fl/fl}$Brm$^{+/+}$ and AhCreER^{+}Apc$^{fl/fl}$Brm null animals revealed a significantly more expanded proliferative compartment in AhCreER^{+}Apc$^{fl/fl}$Brm null mice (Kolmogorov-Smirnov Z test, $p<0.001$, $n\geq4$). (B) Immunohistochemical analysis of Ki67 staining confirmed the enlargement of proliferative compartment in the small intestinal epithelium of AhCreER^{+}Apc$^{fl/fl}$Brm null. Scale bar represents 100 µm.

4.2.6 Brm loss affects the differentiation of the certain intestinal epithelial cell types

The interactions between Wnt and Notch signalling pathways play a crucial role in maintaining the homeostasis of the intestinal epithelium as well as being responsible for cell fate decisions of immature progenitor cells undergoing differentiation towards distinct populations of mature cells belonging to either the absorptive or secretory lineages. Previous studies of conditional deletion of Apc indicated that Wnt activation promotes proliferation and simultaneously leads to perturbation of the differentiation process. As evidenced before, in the context of Apc loss and subsequent aberrant Wnt signalling, Brm loss has shown to amplify some of the effects of Wnt activation on the crypt length and proliferative compartment in the epithelium of small intestine. Accordingly, the quantitative analysis of four main mature epithelial cell types found in the small intestine was conducted in AhCreER^{+}Apc$^{fl/fl}$Brm$^{+/+}$ and AhCreER^{+}Apc$^{fl/fl}$Brm null animals at day 10-12 post induction in order to characterise the effects of Brm loss on the cell differentiation in context of activated Wnt signalling.

To assess the abundance and the distribution of enterocytes belonging to the absorptive lineage in the small intestinal epithelium, alkaline phosphatase staining was carried out marking the brush border of the enterocytes. A marked decrease in the intensity and the thickness of the staining was observed within the epithelium of Apc-deficient mice in comparison to the normal epithelium of control animals (Figure 4.5). A pronounced reduction in the brush border staining was detected in DKO animals compared to AhCreER^{+}Apc$^{fl/fl}$Brm$^{+/+}$.

Alcian Blue staining was performed to assess the frequency of goblet cells in the small intestine in experimental and control animals. Scoring of the positively stained cells showed a significant reduction in the number of goblet cells in both AhCreER^{+}Apc$^{fl/fl}$Brm$^{+/+}$ and DKO animals per half crypt-villus compared to controls (6.37±0.185, 3.59±0.120 and 4.42±0.224, p values for all comparisons $p<0.001$, $n\geq4$). Consistent with previous observations in small intestine in context of homeostasis, a significant increase in the number of Alcian Blue-stained cells was detected in Brm deficient animals in the context of Apc loss in comparison to AhCreER^{+}Apc$^{fl/fl}$Brm$^{+/+}$ mice ($p<0.001$, $n\geq4$, Figure 4.6) with the frequency of goblet cells being intermediary between normal and Wnt activated epithelium.

Paneth cells numbers and positions were scored by carrying out lysozyme immunohistochemical staining. The quantification of Paneth cells showed a significant increase in the number of cells present in the half-crypt between control and both cohorts of experimental animals (4.48±0.262 and 4.4±0.205 compared to 1.73±0.153, p values for all comparisons $p<0.001$, $n\geq4$). Scoring of lysozyme-positive cells in the small intestinal epithelium of DKO revealed no difference from AhCreER^{+}Apc$^{fl/fl}$Brm$^{+/+}$ mice ($p=0.678$, $n\geq4$, Figure 4.7a). As normal levels of Wnt signalling are responsible for the positioning of Paneth cells within the crypt, the distribution of Paneth cells along the half crypt axis was scored in control, AhCreER^{+}Apc$^{fl/fl}$Brm$^{+/+}$ and AhCreER^{+}Apc$^{fl/fl}$Brm null animals. The analysis of cumulative frequency of lysozyme-positive cells revealed a significant expansion of Paneth cells in both Apc-deficient cohorts in comparison to controls (for either comparison, $p<0.001$, $n\geq4$) as in the intestinal epithelium of control mice, Paneth cells were restricted to the base of the crypt whereas animals from both Apc-deficient cohorts showed a wider distribution of lysozyme-positive cells throughout the crypt compartment. The analysis of Paneth cell distribution revealed no differences between AhCreER^{+}Apc$^{fl/fl}$Brm$^{+/+}$ and AhCreER^{+}Apc$^{fl/fl}$Brm null small intestinal epithelium ($p=0.283$, $n\geq4$, Figure 4.7b).

Grimelius staining was used to identify another mature cell type belonging to the secretory lineage, namely enteroendocrine cells. The quantification of positively stained cells revealed a significant reduction in the number of cells with Grimelius staining in both Apc deficient and the DKO cohort in comparison to controls (0.37±0.033, 0.39±0.027 and 2.14±0.05 respectively, p values for all comparisons $p<0.0001$, $n\geq4$). The number of enteroendocrine cells in the small epithelium of DKO did not differ significantly from AhCreER^{+}Apc$^{fl/fl}$Brm$^{+/+}$ epithelium ($p=0.274$, $n\geq4$, Figure 4.8).

The expression of Hes1 and Math1 the Notch effector genes is a key factor in the regulation of cell fate between absorptive and secretory lineages therefore expression levels of Hes1, Math1 and Muc2 were assessed by qRT-PCR allowing an assessment at the transcriptional level. mRNA was extracted from small intestinal samples of controls, AhCreER^{+}Apc$^{fl/fl}$Brm$^{+/+}$ and AhCreER^{+}Apc$^{fl/fl}$Brm null and control animals at the day 10-12 post induction. qRT-PCR analysis of Hes1 revealed no changes between control and Apc-deficient mice ($p=0.487$, $n=6$, Figure 4.9) with a marked decrease observed in DKO animals ($p=0.022$ and $p=0.028$ respectively, $n=6$). A significant increase in mRNA of Math1 in both Apc experimental cohorts was observed in comparison to controls (Figure 4.9, $p=0.034$ and

p=0.042, n=6). In contrast Muc2 expression remained unaltered in all but Apc-deficient cohort (Figure 4.9, p=0.039, n=6).

Overall, the quantification of mature cell types in Wnt activated small intestinal epithelium revealed that Brm deficiency affects the differentiation of both absorptive and secretory lineage by leading to a marked reduction in the brush border enterocytes and a significant increase in the number of goblet cells.

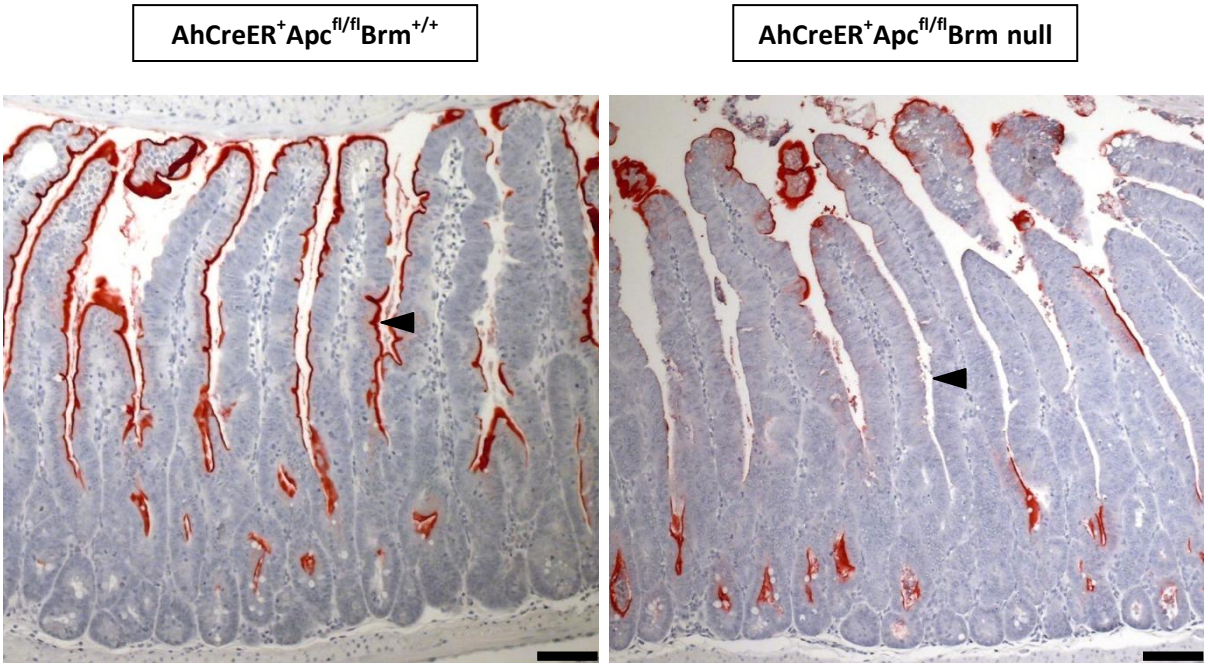

Figure 4.5 Alkaline phosphatase staining detected a decreased brush border enterocytes in the epithelium of Apc deficient animals. The small intestinal sections of control, AhCreER^{+}Apc$^{fl/fl}$Brm$^{+/+}$ and AhCreER^{+}Apc$^{fl/fl}$Brm null animals harvested at days 10-12 post induction were stained for alkaline phosphatase. Staining with chromogen revealed a marked decrease in the alkaline phosphatase expression in the small intestinal epithelium of both experimental cohorts compared to control mice. Visual inspection of the epithelium of AhCreER^{+}Apc$^{fl/fl}$Brm$^{+/+}$ and AhCreER^{+}Apc$^{fl/fl}$Brm null animals revealed a difference between those two cohorts with further reduction in brush border staining in Brm deficient animals. The scale bar represents 100μm.

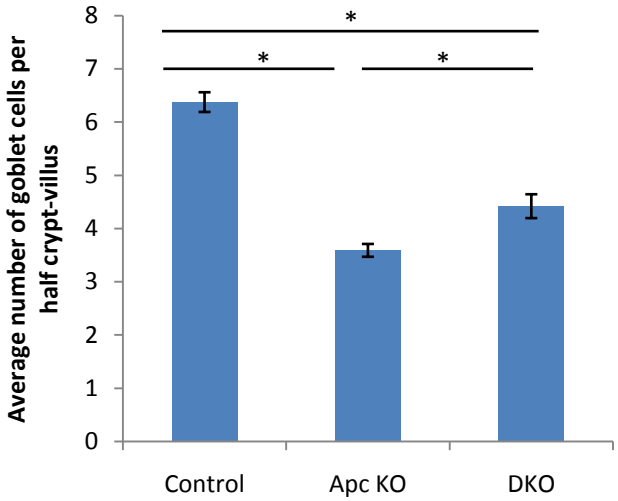

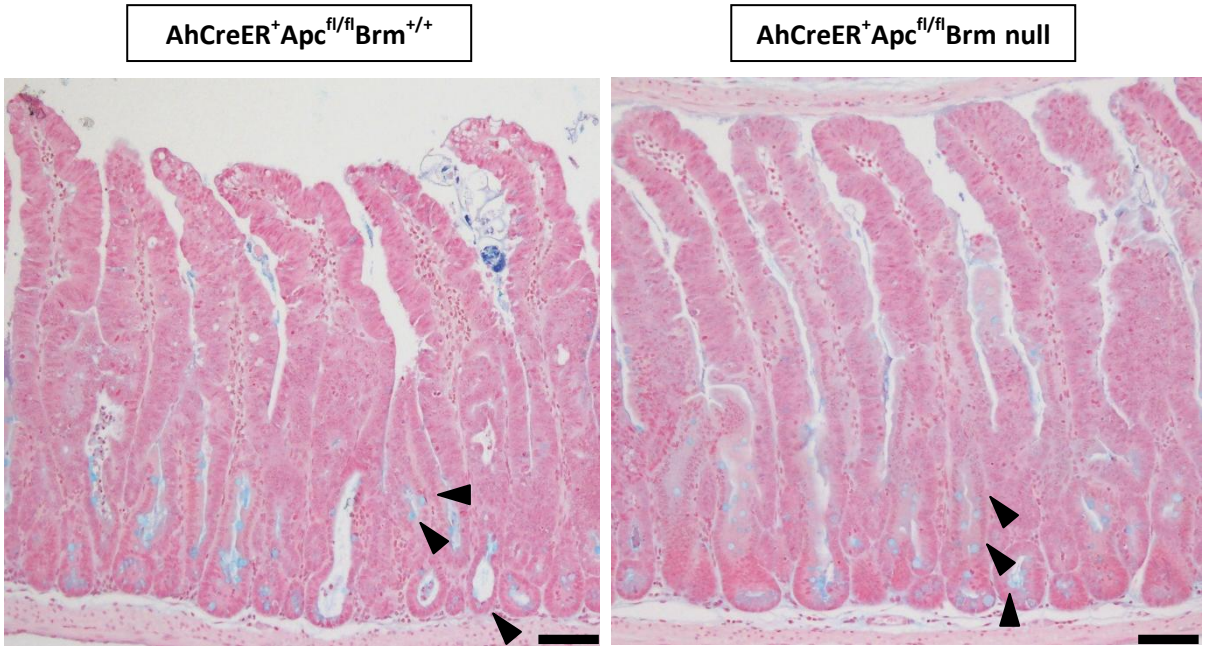

Figure 4.6 Alcian Blue staining was used to identify goblet cells within small intestinal epithelium. The small intestinal sections of control, AhCreER^{+}Apc$^{fl/fl}$Brm$^{+/+}$ and AhCreER^{+}Apc$^{fl/fl}$Brm null animals dissected at days 10-12 post induction were stained to detect mucin secreting cells. Alcian Blue staining revealed a significant reduction in the number of stained cells in the small intestinal epithelium of both Apc-deficient cohorts (for either comparison $p<0.001$, $n\geq4$). The quantification of Alcian Blue-positive cells detected a significant increase in goblet cells in DKO epithelium in comparison to AhCreER^{+}Apc$^{fl/fl}$Brm$^{+/+}$ epithelium ($p<0.001$, $n\geq4$). The scale bar represents 100µm.

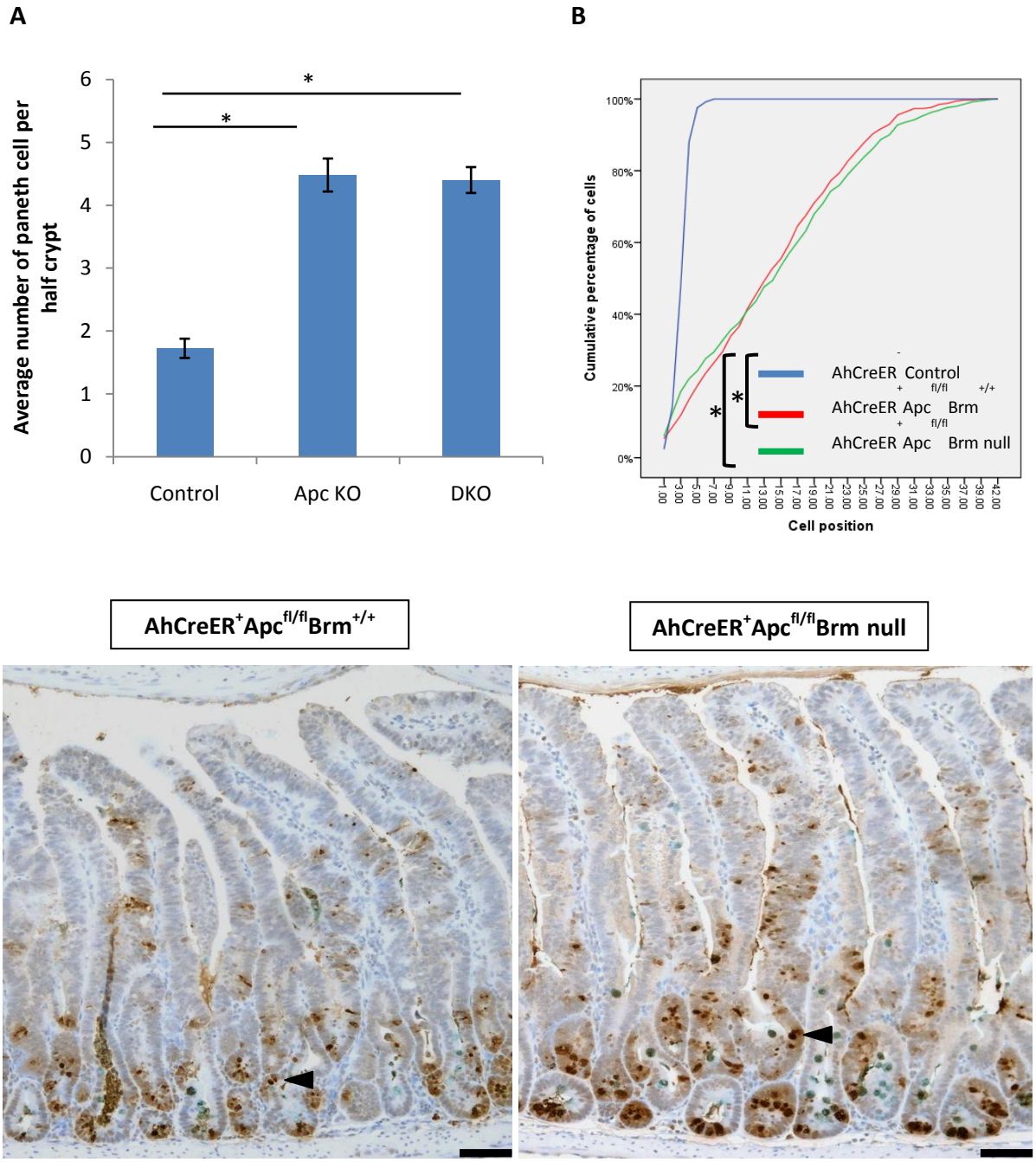

Figure 4.7 Immunohistochemistry against lysozyme was carried out to visualize Paneth cells within small intestinal epithelium. The small intestinal sections of control, AhCreER^{+}Apc$^{fl/fl}$Brm$^{+/+}$ and AhCreER^{+}Apc$^{fl/fl}$Brm null animals dissected at days 10-12 post induction were stained to reveal the number and localisation of Paneth cells. (A) Lysozyme staining detected a significant increase in number of Paneth cells in both experimental cohorts in comparison to controls (for either comparison $p<0.001$, $n\geq4$). No changes in the numbers of Paneth cells were observed between DKO and Apc-deficient animals ($p=0.678$, $n\geq4$). (B) Subsequent Cumulative frequency analysis of Paneth cell distribution revealed a significant expansion of Paneth cells throughout the crypt in AhCreER^{+}Apc$^{fl/fl}$Brm$^{+/+}$ and AhCreER^{+}Apc$^{fl/fl}$Brm null small intestine compared to control animals (for either comparison Kolmogorov-Smirnov Z test $p<0.001$, $n\geq4$) with no difference observed between DKO and Apc-deficient cohorts (Kolmogorov-Smirnov Z test $p=0.283$, $n=4$).. The scale bar represents 100µm.

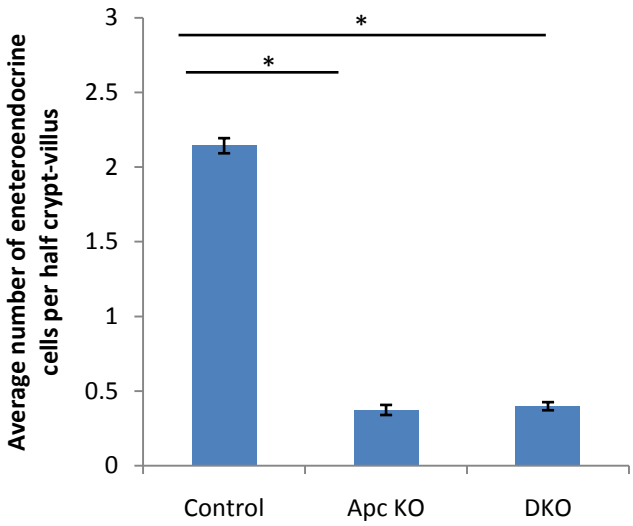

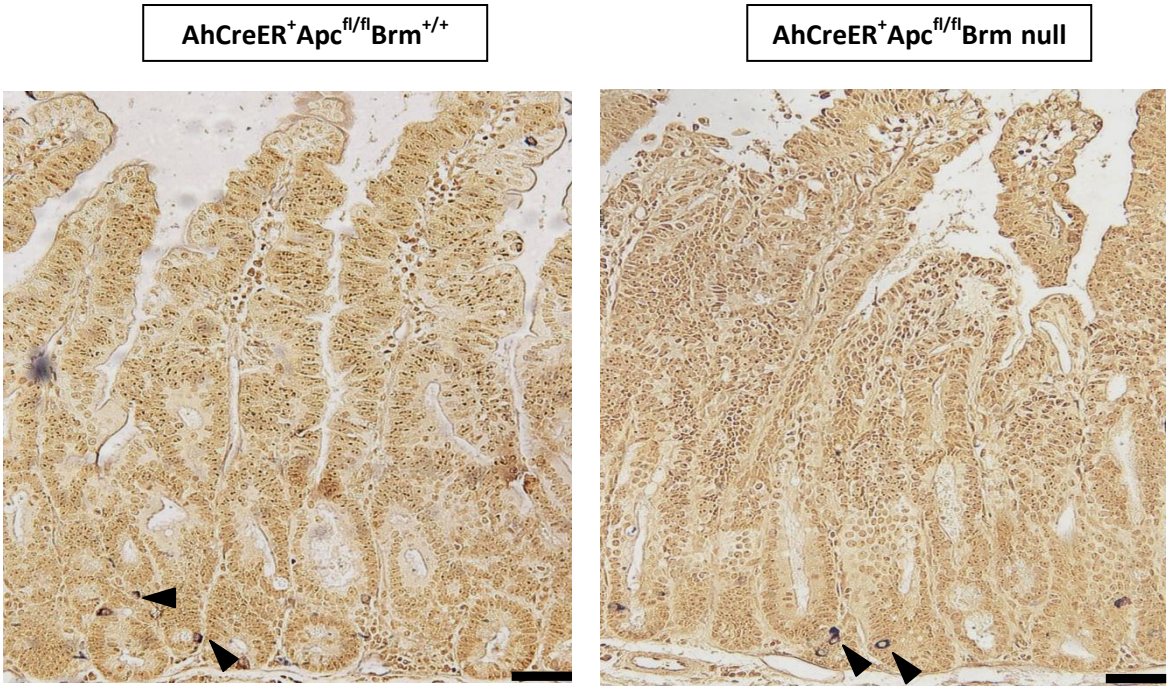

Figure 4.8 Grimelius staining of small intestinal sections was carried out to label enteroendocrine cells. The small intestinal sections of control, AhCreER^{+}Apc$^{fl/fl}$Brm$^{+/+}$ and AhCreER^{+}Apc$^{fl/fl}$Brm null animals dissected at days 10-12 post induction were stained to identify enteroendocrine cells. This cell-specific staining revealed a significant decrease in the number of enteroendocrine cells in Apc-deficient animals in comparison with controls (for either comparison, $p<0.001$, $n\geq4$). The quantification of positively stained cells detected no difference in the enteroendocrine cell numbers between DKO and AhCreER^{+}Apc$^{fl/fl}$Brm$^{+/+}$ animals. The scale bar represents 100µm.

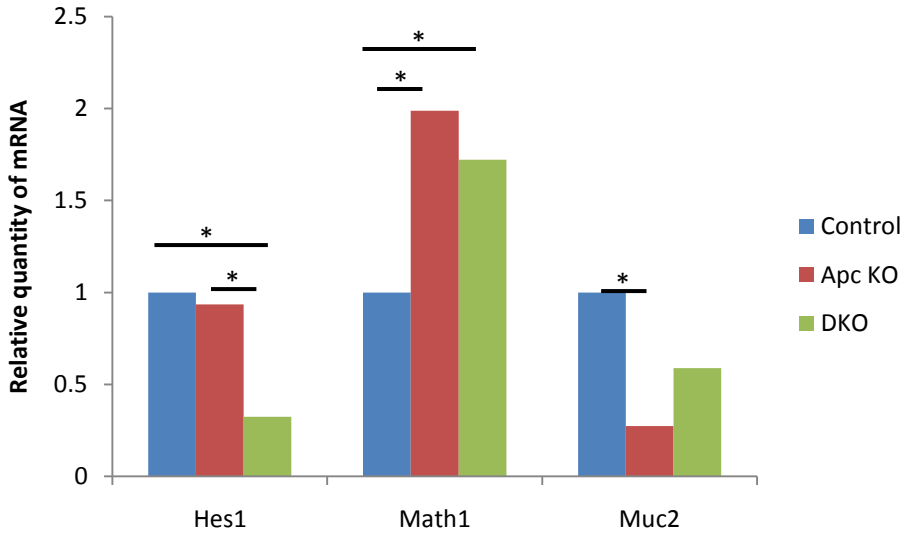

Figure 4.9 The transcriptional levels of Hes1, Math1 and Muc2 were assessed by quantitative real-time-PCR (qRT-PCR) as shown in bar graph form. The data from qRT-PCR are normalised with β-actin (n=6). Analysis of levels of Hes1 mRNA showed a significant downregulation of expression in the epithelium of DKO animals in comparison to both control and Apc-deficient animals (p=0.022 and p=0.028 respectively, n=6). The levels of Math1 mRNA were significantly upregulated from those observed in controls (p=0.034 and p=0.042, n=6) whereas no changes in the Muc2 expression was observed between Apc-deficient epithelium with or without functional Brm (p=0.039, p=6)

4.2.7 Brm loss does not modulate β-catenin levels and localisation following loss of Apc

Histological analysis of proliferation, apoptosis and cell differentiation in AhCreER^{+}Apc$^{fl/fl}$Brm$^{+/+}$ and AhCreER^{+}Apc$^{fl/fl}$Brm null epithelium suggested that Brm deficiency does modulate some of the phenotypes observed following Wnt activation in Apc-deficient animals.

In order to investigate whether the apparent accentuation of the Wnt-driven phenotype by Brm deficiency is caused by modulation of Wnt signalling I initially assessed the levels of stabilised β-catenin in the small intestinal epithelium. One of the immediate effects of loss of Apc is the disruption of β-catenin destruction complex in the cytoplasm subsequently allowing the accumulation of non-phosphorylated and therefore stabilized β-catenin. The accumulation of β-catenin in the nucleus results in the activation of Wnt-driven transcription of genes (Waterman *et al.* 2002) hence it is one of the hallmarks of activated Wnt signalling upon Apc loss. Therefore I aimed to examine the levels of stabilised β-catenin in the small intestinal epithelium of AhCreER^{+}Apc$^{fl/fl}$Brm$^{+/+}$ and AhCreER^{+}Apc$^{fl/fl}$Brm null animals at day 10-12 post induction.

As previously described in section 2.2.3, immunohistochemical analysis of β-catenin expression at day 10-12 post induction in AhCreER^{+}Apc$^{fl/fl}$Brm$^{+/+}$ and AhCreER^{+}Apc$^{fl/fl}$Brm null animals identified nuclear localisation of β-catenin in the floxed areas of epithelium in both experimental cohorts. However no discernible difference in the expression levels of stabilized β-catenin was detected between Apc-deficient and DKO mice.

The levels of β-catenin stabilization were quantified by Western blotting in AhCreER^{+}Apc$^{fl/fl}$Brm$^{+/+}$ and AhCreER^{+}Apc$^{fl/fl}$Brm null animals at the day 10-12 post induction (n=4). The analysis of the levels of protein detected significantly higher levels of activated β-catenin in both Apc-deficient cohorts in comparison to controls (Figure 4.10a) however the analysis of the levels of nuclear β-catenin between AhCreER^{+}Apc$^{fl/fl}$Brm$^{+/+}$ and AhCreER^{+}Apc$^{fl/fl}$Brm null animals revealed no difference in the expression of this protein in the intestinal epithelium samples (Figure 4.10b).

Therefore the effects of Brm loss on the phenotype of Apc-deficient small intestinal epithelium are not directly mediated at the level of major downstream effector of Wnt signalling β-catenin further suggesting that modulations of Wnt-driven tumorigenesis in AhCreER^{+}Apc$^{fl/fl}$Brm null epithelium may occur somewhere downstream of β-catenin.

A

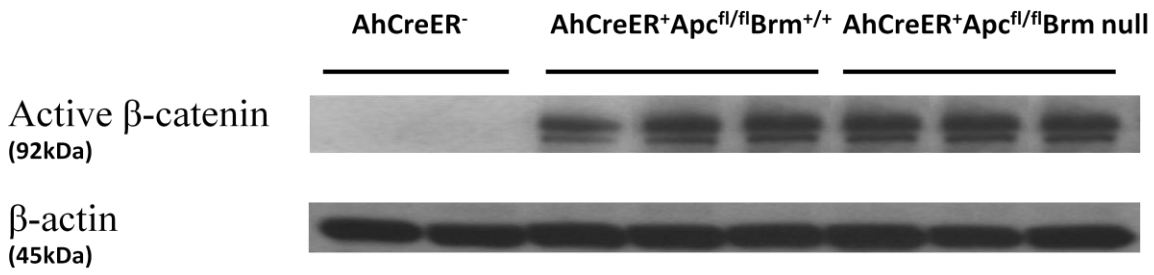

B

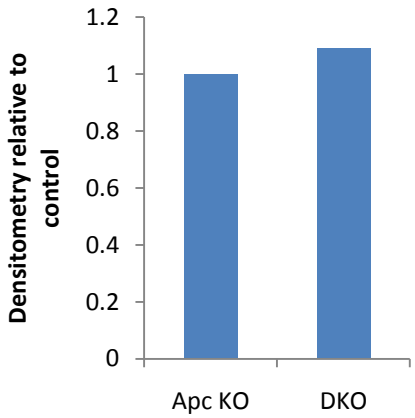

Figure 4.10 Brm loss does not affect the levels of stabilized β-catenin in the small intestinal epithelium of Apc-deficient animals. (A) Western blotting analysis of samples from AhCreER^{-}, AhCreER^{+}Apc$^{fl/fl}$Brm$^{+/+}$ and AhCreER^{+}Apc$^{fl/fl}$Brm null animals harvested at day 10-12 post induction showed a marked increase in the levels of activated β-catenin in Apc-deficient animals in comparison to controls. β-actin represents a loading control for the blot. (B) The analysis of β-catenin levels by densitometry revealed no differences in protein levels between DKO and Apc-deficient animals ($p=0.318$, $n\geq4$, Mann Whitney U Test).

4.2.8 Brm deficiency modulates the expression of genes crucial to the development and progression of CRC

No direct interactions between Brm chromatin remodelling factor and the Wnt pathway have been reported to date however Brm has been reported to associate with one of the major downstream targets of β-catenin, namely CD44 (Reisman *et al.* 2002, Banine *et al.* 2005, Batsché *et al.* 2006) as well as with the transmembrane glycoprotein E-cadherin whose expression is associated with size, differentiation and invasive potential of CRCs. These observations may suggest that whereas there is no association between Brm and the major effector of Wnt signalling (β-catenin), Brm may indirectly influence the levels of Wnt target genes such as CD44 and c Myc and other genes crucial in CRC tumorigenesis such as E-cadherin. Therefore I aimed to investigate whether Brm loss modulated the transcriptional program activated via mutation of *Apc* gene by performing a qRT-PCR analysis of expression levels of a subset of Wnt target genes and genes involved in the development and progression of CRC. mRNA was extracted from small intestinal tissue samples of control, AhCreER^{+}Apc$^{fl/fl}$Brm$^{+/+}$ and AhCreER^{+}Apc$^{fl/fl}$Brm null animals dissected at day 10-12 post induction.

The assessment of mRNA levels of *CD44*, *c-Myc* and *Cyclin D1* and *E-cadherin* revealed a significantly higher expression of these genes in the epithelium of AhCreER^{+}Apc$^{fl/fl}$Brm$^{+/+}$ animals compared to controls (for all comparisons $p<0.05$, $n\geq4$, Figure 4.11). Remarkably, the up-regulation of those genes in the epithelium of AhCreER^{+}Apc$^{fl/fl}$Brm null animals was less pronounced with levels of *c-Myc* and *Cyclin D1* not different from those observed in the control small intestinal epithelium. Strikingly, *E-cadherin* was the only gene within the studied subset of genes whose mRNA levels displayed a trend of increase in DKO mice in comparison to Apc-deficient cohort however this trend was not proved to be significant ($p=0.073$, $n\geq4$). However, in the absence of an independent measure which would account for differences in the level of APC/β-catenin in the epithelium and therefore levels of Wnt activation, the above results could not be fully interpreted.

Furthermore, I assessed the influence of Brm deficiency on the expression of the CD44 Wnt target gene by immunohistochemical staining of AhCreER^{+}Apc$^{fl/fl}$Brm$^{+/+}$ and AhCreER^{+}Apc$^{fl/fl}$Brm null tissue sections of small intestine with an antibody against CD44 (Figure 4.12). Due to the AhCreER recombinase driving recombination of the targeted *Apc* allele at below 100% efficiency (Kemp 2004), the areas of unfloxed epithelium neighbouring with neoplastic tissue could be identified within the intestinal epithelium allowing inter- and

intra-comparison of CD44 expression. To further facilitate the analysis, I performed immunohistochemical staining against β-catenin which is well-known as a surrogate marker of Apc loss. Comparison of the non-neoplastic epithelium labelled by membranous β-catenin and Wnt-activated epithelium with nuclear β-catenin in both experimental cohorts revealed a marked increase in CD44 expression in the neoplastic areas of tissue. Moreover, analysis of the pattern of CD44 expression in the neoplastic epithelium between AhCreER^{+}Apc$^{fl/fl}$Brm$^{+/+}$ and AhCreER^{+}Apc$^{fl/fl}$Brm null cohort detected a noticeable decrease in the expression of CD44 in the DKO mice consistent with qRT-PCR results.

Taken together, these observations suggest that Brm loss is capable of suppressing β-catenin-mediated transcriptional activation of Wnt target genes and other crucial players in CRC tumorigenesis however this effect seems to be specific to a particular subset of genes.

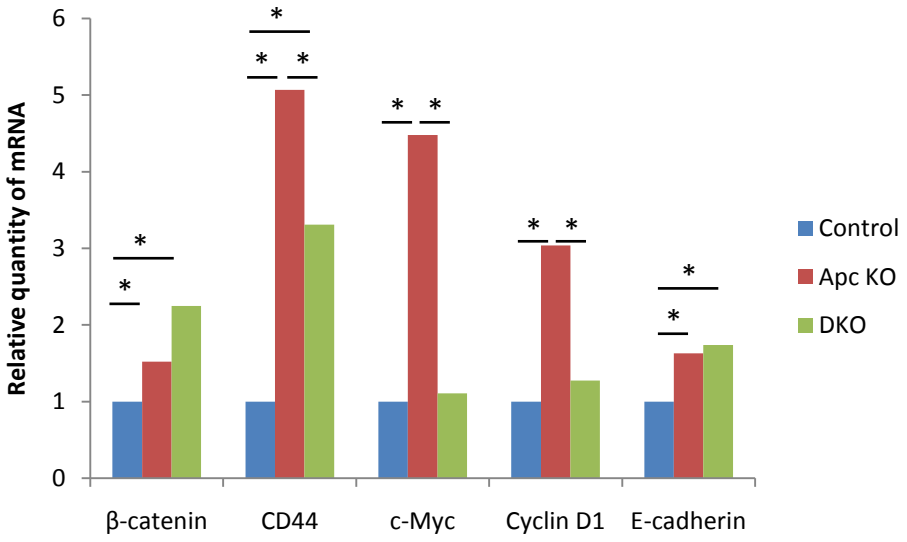

Figure 4.11 Brm loss suppresses the expression of the Wnt target genes and genes involved in development and progression of CRC. The transcriptional levels of Wnt targets *CD44* and *c-Myc* as well as *Cyclin D1* and *E-cadherin* genes was quantified by quantitative real-time-PCR (qRT-PCR) as shown in bar graph form. The data from qRT-PCR are normalised with *β-actin* and the asterisks indicate comparisons that were found to be significantly different ($p<0.05$, $n\geq4$). Analysis of levels of *CD44*, *c-Myc* and *Cyclin D1* mRNA displayed a significant decline in expression of those genes in the epithelium of AhCreER^{+}Apc$^{fl/fl}$Brm null in comparison to AhCreER^{+}Apc$^{fl/fl}$Brm$^{+/+}$ animals.

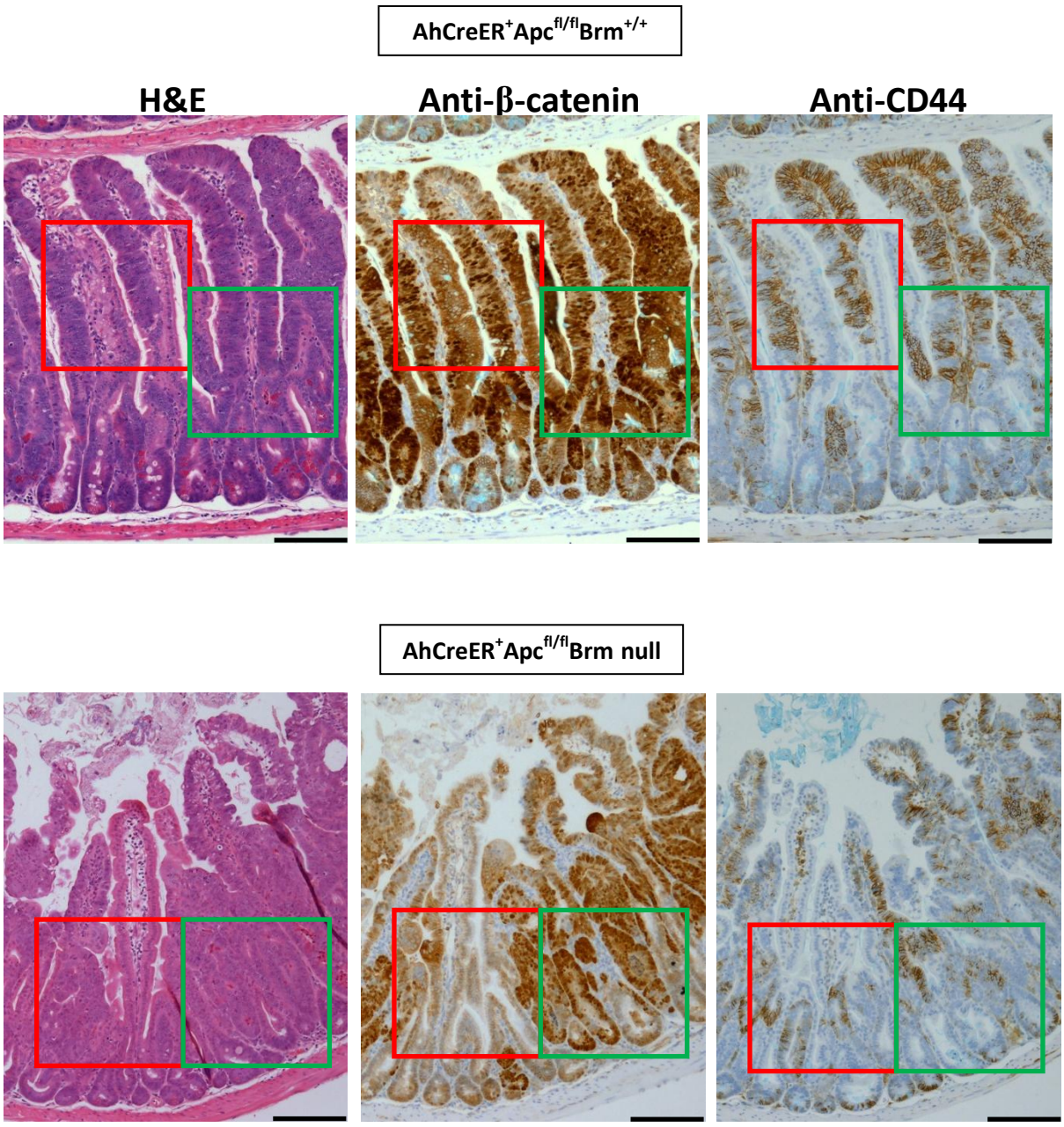

Figure 4.12 Brm deficiency results in the diminished expression of CD44 in context of aberrant Wnt signalling. Immunohistochemical staining against β-catenin and CD44 was performed on the serial sections of small intestinal epithelium of AhCreER^{+}Apc$^{fl/fl}$Brm$^{+/+}$ and AhCreER^{+}Apc$^{fl/fl}$Brm null animals. The analysis of β-catenin staining allowed for identification of Apc-deficient regions of epithelium (green box) and unfloxed areas (red box). The analysis of CD44 expression revealed a marked decrease in the CD44 expression in DKO cohort in comparison to Apc-deficient animals confirming the change in CD44 levels observed by qRT-PCR. The scale bar represents 100 μm.

4.2.9 Brm deficiency leads to the reduction of the Wnt-mediated expansion of stem cell population

Previous studies focusing on early stages of intestinal neoplasia found that many CRCs express high levels of intestinal stem cell-specific genes suggesting an expansion of intestinal stem cell population as a consequence of aberrant Wnt signalling (Sansom *et al.* 2004, Jubb *et al.* 2006, Merlos-Suarez *et al.* 2011). Taking into the account the significantly attenuated expression of Wnt target genes in Brm-deficient animals but similar phenotype and survival between both Apc-deficient experimental cohorts, I investigated whether the lack of improved phenotype might be due to Brm loss exacerbating the expansion of intestinal stem cell population in the Wnt activated epithelium of small intestine. To this end, mRNA was extracted from the tissue samples of AhCreER^{+}Apc$^{fl/fl}$Brm$^{+/+}$ and AhCreER^{+}Apc$^{fl/fl}$Brm null animals at day 10-12 post induction was used for qRT-PCR.

The expression levels of intestinal stem cell markers Ascl2, Lgr5 and Olfm4 revealed a trend of a decrease in both Ascl2 and Lgr5 expression in DKO animals in comparison with Apc-deficient animals however this result did not reach significance ($p=0.288$ and $p=0.425$ respectively, $n=6$, Figure 4.13a). Notably, a significant decrease in the expression levels of Olfm4 in the epithelium of AhCreER^{+}Apc$^{fl/fl}$Brm null animals was detected ($p=0.048$, $n=6$).

The diminished levels of these intestinal stem cell markers in the DKO cohort may simply reflect perturbation of Wnt signalling rather than changes in the actual stem cell compartment. Notably, Olfm4 is a Wnt independent stem cell marker and may therefore be used as a more direct assessment of changes in the stem cell compartment. Therefore to extend the qRT-PCR data above, *in situ* hybridisation against *Olfm4* was conducted on the small intestinal tissue from control, AhCreER^{+}Apc$^{fl/fl}$Brm$^{+/+}$ and AhCreER^{+}Apc$^{fl/fl}$Brm null animals harvested at day 10-12 post induction (Figure 4.13b). Analysis of *Olfm4* expression in the epithelium of control mice detected positive staining at the base of the intestinal crypt whereas in the epithelium of Apc-deficient animals *Olfm4* staining was present throughout the length of the Wnt activated crypt extending towards the crypt-villus axis. Conversely, DKO animals *Olfm4* expression in the area where Olfm4 probe has bound was limited to the base of the crypt similarly to the pattern observed in control animals. To conclude, these results suggest that in the context of aberrant Wnt signalling Brm loss attenuates the expression of the Wnt independent stem cell marker Olfm4.

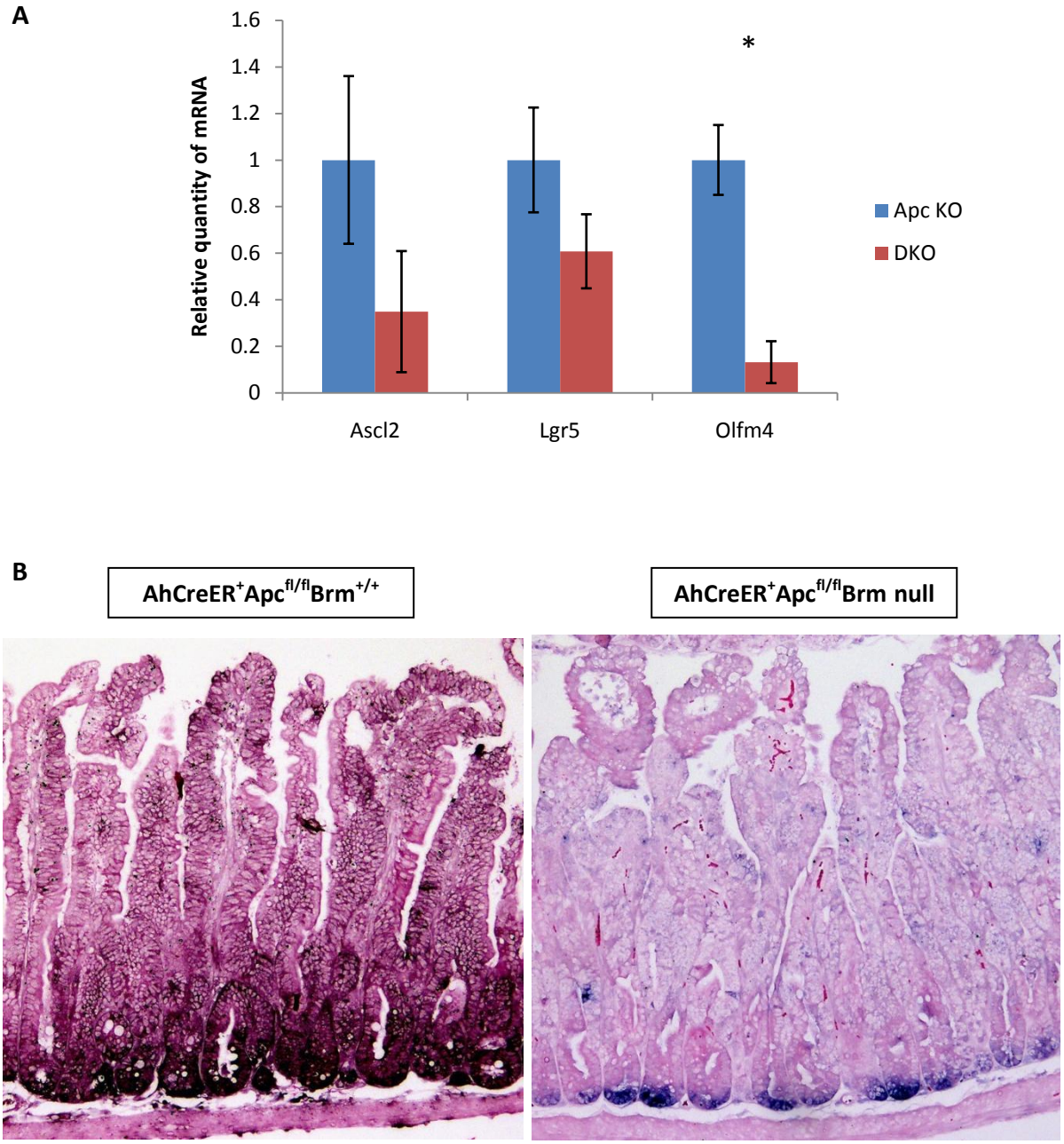

Figure 4.13 Analysis of intestinal stem cell niche in Brm null animals. (A) The transcriptional level of *Ascl2*, *Lgr5* and *Olfm4* was assessed by quantitative real-time-PCR (qRT-PCR) as shown in bar graph form. The data from qRT-PCR are normalised with *β-actin*. Analysis of levels of *Ascl2* and *Lgr5* mRNA revealed a trend of decrease in DKO experimental animals in comparison to AhCreER^{+}Apc$^{fl/fl}$Brm$^{+/+}$ animals which was not significant (p=0.288, p=0.425 respectively, n=6). A significant 7-fold decrease in the expression levels of *Olfm4* was observed in DKO cohort (p=0.048, n=6) (B) *In situ* hybridization against *Olfm4* detected a significant decrease in the amount of probe bound in the Wnt-activated small intestinal epithelium of DKO in comparison to AhCreER^{+}Apc$^{fl/fl}$Brm$^{+/+}$ animals. While a marked expansion of stem cell zone was observed in Apc-deficient animals compared to controls, the Olfm4 riboprobe-stained area was substantially lower in DKO cohort than in AhCreER^{+}Apc$^{fl/fl}$Brm$^{+/+}$ mice. Scale bar represents 100 μm.

4.2.10 Brm loss has mild effects on the homeostasis of large intestinal epithelium

As observed previously, in the Wnt-activated epithelium of small intestine Brm deficiency leads to the morphological abnormalities such as elongated crypt compartment and increase in apoptosis as well as some changes in the differentiation of mature epithelial cell types resulting in a marked decline in the brush border enterocytes and an increase in goblet cell population when compared to Apc-deficient animals. Due to the differences in the effects of Brm loss on the epithelium of small and large intestine (described in the chapter 3) together with the fact that colonic epithelium is also expressing AhCreER recombinase, I aimed to examine the effects of Brm deficiency on the colonic epithelium in AhCreER^{+}Apc$^{fl/fl}$Brm$^{+/+}$ and AhCreER^{+}Apc$^{fl/fl}$Brm null animals dissected at day 10-12 post induction. A quantitative analysis performed on this tissue sections is summarized in Table 4.2.

Similarly to the observations of Wnt-activated epithelium of small intestine, macroscopic analysis of colonic epithelium during tissue harvesting revealed no gross tissue abnormalities or perceptible tumours that could be assessed macroscopically.

Crypt length has been assessed on H&E stained sections as the average number of cells (± standard deviation) from the base of the crypt of Lieberkühn all the way to the flat surface of the colonic epithelium. Crypt size was found to be increased in colonic epithelium of both Apc-deficient and DKO animals compared to controls (30.66±1.33, 28.56±1.49 and 24.31±0.32, p=0.012 and p=0.002 respectively, n≥4, Figure 4.14a). There was no difference in the crypt length between AhCreER^{+}Apc$^{fl/fl}$Brm null and AhCreER^{+}Apc$^{fl/fl}$Brm$^{+/+}$ animals (p=0.096, n≥4).

Apoptosis within the epithelium was detected and scored by Cleaved Caspase-3 immunohistochemical staining. Similarly to the effects of Wnt activation of small intestinal epithelium, the quantitative analysis of Cleaved Caspase-3-positive cells revealed a significant increase in levels of apoptosis in Apc-deficient versus control mice (0.65±0.02 and 0.060±0.016, p=0.0001 n≥4, Figure 4.14b). A marked increase in the number of Caspase-3-positive cells was also detected in the epithelium of AhCreER^{+}Apc$^{fl/fl}$Brm null animals in comparison to control animals (1.17±0.14 and 0.060±0.016, p=0.0001 n≥4) and moreover the observed increase in the apoptosis in the colonic epithelium of DKO animals was significant compared to Apc-deficient cohort (p=0.001, n≥3, Figure 4.14b). The assessment of the size of proliferative compartment was performed using staining against Ki67 proliferation marker.

Quantification of Ki67-positive cells within the colonic epithelium showed that the average number of proliferating cells per crypt in Apc-deficient animals remains unaltered in comparison to control animals (7.57±0.67 and 6.61±1.04, p=0.196, n≥4, Figure 4.14c). In contrast, I detected a significant increase in the proliferation levels in DKO animals compared to control animals (11.35±1.59 and 6.61±1.04, p=0.001, n≥4). Furthermore, an increase in the number of Ki67-positive cells was observed in the epithelium of AhCreER^{+}Apc$^{fl/fl}$Brm null versus AhCreER^{+}Apc$^{fl/fl}$Brm$^{+/+}$ animals (p=0.004, n≥4, Figure 4.14b).

Therefore in the context of colonic epithelium and Wnt activation via mutation in *Apc* gene, the quantitative analysis of Brm-deficient tissue did not reveal any alteration in the length of crypt in contrast to marked increase in both apoptosis and proliferation levels when compared to Apc-deficient epithelium. Whereas the general morphology of Wnt-activated large intestine appears to not be affected by constitutive loss of Brm, the crucial cellular processes of apoptosis and proliferation are indeed altered.

Parameter	Cohort	Mean	SD	p-values		
				Control vs Apc KO	Control vs DKO	Apc KO vs DKO
Crypt length	Control	24.31	0.319	0.012	0.002	0.096
	Apc KO	30.66	1.331			
	DKO	28.56	1.492			
Caspase positive cells	Control	0.060	0.016	0.000	0.000	0.001
	Apc KO	0.650	0.025			
	DKO	1.172	0.148			
Ki67 positive cells	Control	6.609	1.039	0.196	0.001	0.004
	Apc KO	7.574	0.671			
	DKO	11.35	1.595			

Table 4.2 Quantitative analysis of the effects of Brm loss on the histology of Wnt-activated colonic epithelium. Epithelium from large intestine from Cre^{-} Brm$^{+/+}$ (marked as Control), AhCreER^{+}Apc$^{fl/fl}$Brm$^{+/+}$ (marked as Apc KO) and AhCreER^{+}Apc$^{fl/fl}$Brm null (marked DKO) was harvested from animals at days 10-12 post induction. Histological parameters including crypt length, apoptosis and proliferation were quantified and comparison between those two cohorts was conducted using statistical software.

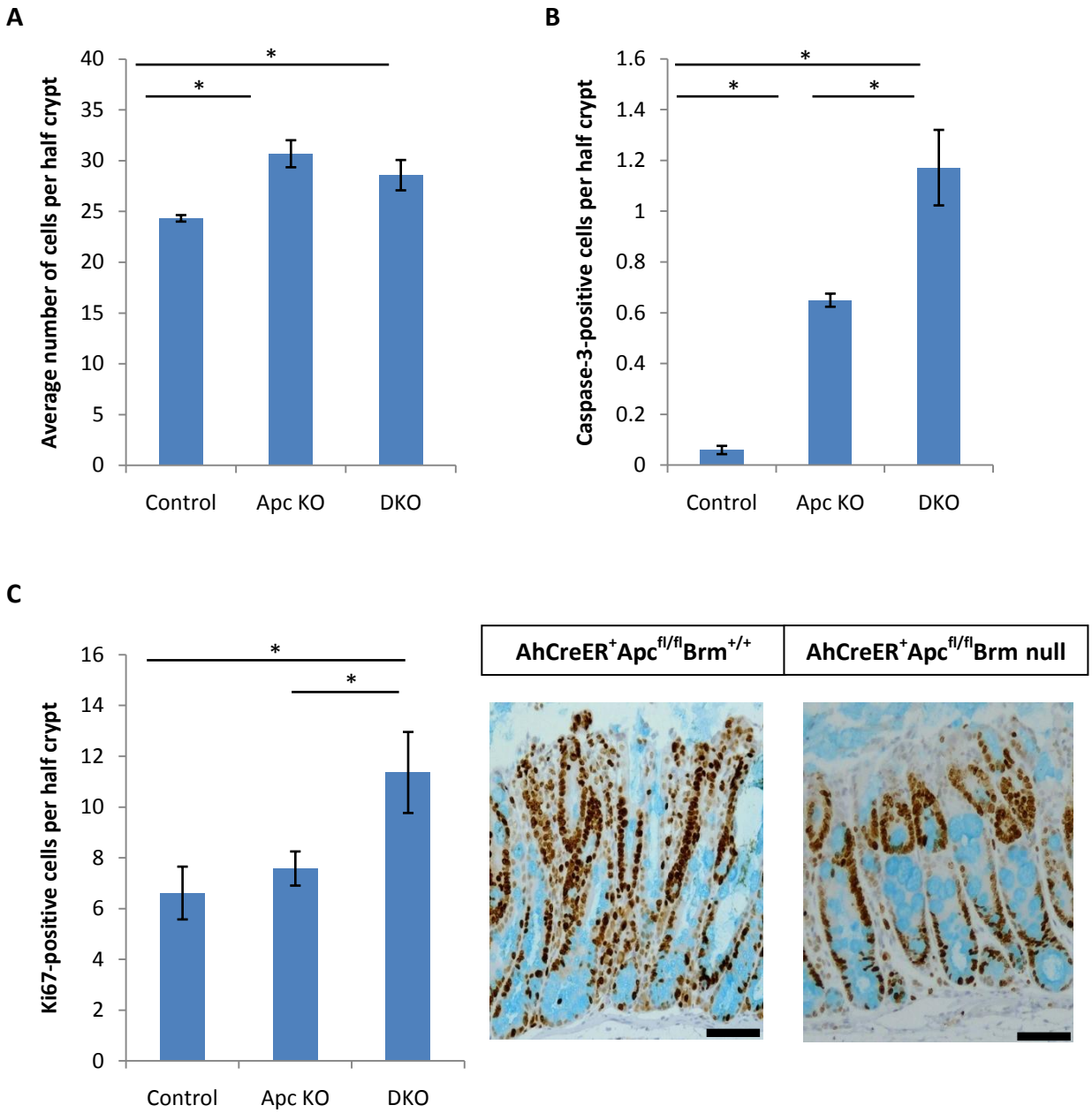

Figure 4.14 Histological analysis of the effects of Brm loss in the Wnt-activated colonic epithelium. Control AhCreER^{-} and experimental AhCreER^{+}Apc$^{fl/fl}$Brm$^{+/+}$ (marked as Apc KO) and AhCreER^{+}Apc$^{fl/fl}$Brm null (marked DKO) was harvested from animals at days 10-12 post induction. A-C histological parameters such as (A) crypt length were counted on H&E tissue sections. The average number of (B) Cleaved Caspase3 and (C) Ki67-positive cells was scored on the corresponding immunostained sections. Scale bar represents 100 µm. Error bars represent standard deviation and asterisk symbol indicates those histological parameters that showed a statistically significant difference (p value <0.05) between cohorts of mice. Exact values, standard deviations, p values are provided in Table 4.2

4.2.11 Brm loss results in a change in the distribution of proliferating cells in the Apc-deficient colonic epithelium

Immunohistochemical staining with Ki67 proliferation marker was also used to assess the shape of the proliferative compartment within the colonic epithelium of control, AhCreER^{+}Apc$^{fl/fl}$Brm$^{+/+}$ and AhCreER^{+}Apc$^{fl/fl}$Brm null animals.

The analysis of the cumulative frequency of Ki67-positive cells showed a significant expansion of the proliferative compartment in both AhCreER^{+}Apc$^{fl/fl}$Brm$^{+/+}$ and AhCreER^{+}Apc$^{fl/fl}$Brm null cohorts in comparison to controls (Kolmogorov-Smirnov Z test p=0.001, n≥4, Figure 4.15). Furthermore, the distribution of proliferating cells in the Apc-deficient experimental cohorts revealed a redistribution of Ki67-positive cells in the epithelium of Brm-proficient animals (Kolmogorov-Smirnov Z test p=0.001, n≥4) therefore suggesting that Brm loss alters the shape of the proliferative compartment in Wnt-activated epithelium.

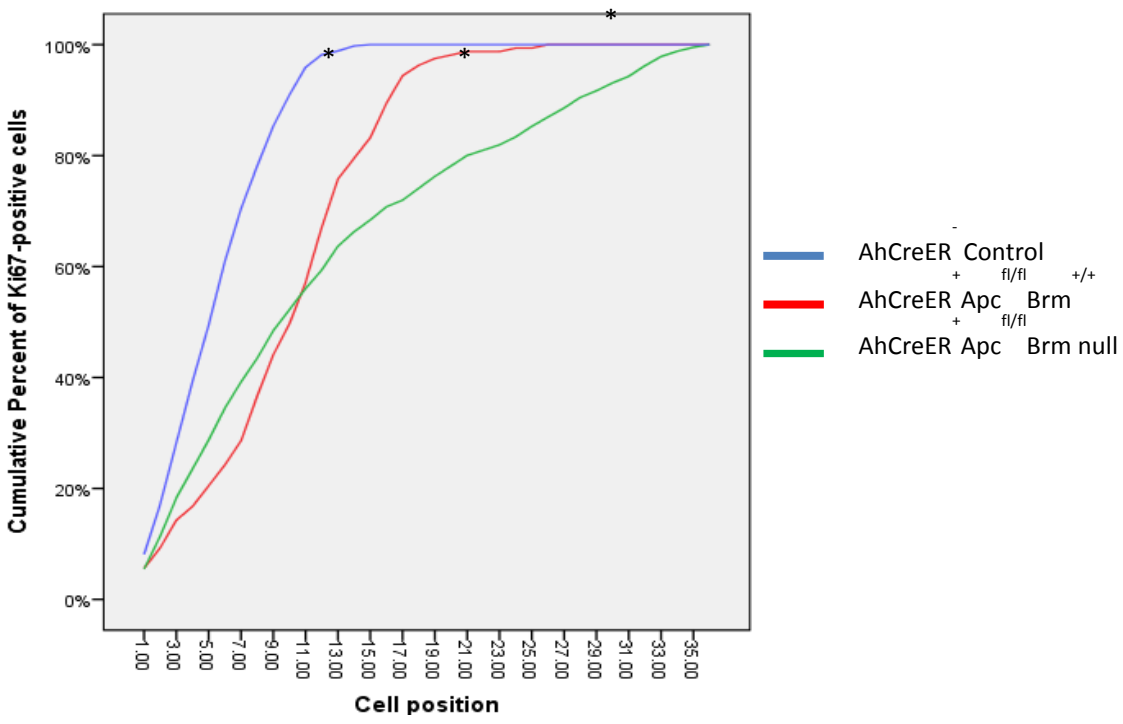

Figure 4.15 Analysis of proliferative compartment by Ki67 staining of AhCreER^{+}Apc$^{fl/fl}$Brm$^{+/+}$ and AhCreER^{+}Apc$^{fl/fl}$Brm null epithelium animals at day 10-12 post induction. Cumulative frequency analysis of Ki67-positive cells revealed a significant enlargement of the proliferative compartment in AhCreER^{+}Apc$^{fl/fl}$Brm$^{+/+}$ and AhCreER^{+}Apc$^{fl/fl}$Brm null animals in comparison to control mice (Kolmogorov-Smirnov Z test p<0.001, n≥4). Proliferative compartment is significantly shorter in AhCreER^{+}Apc$^{fl/fl}$Brm null in comparison to Apc-deficient colonic epithelium (Kolmogorov-Smirnov Z test, p<0.001, n≥4).

4.2.12 Brm deficiency does not alter differentiation status in Wnt-activated colonic epithelium

Consistent with the results from the previous section showing the alterations in both apoptosis and proliferation of Wnt-activated colonic epithelium, I aimed to examine whether the differentiation potential of progenitor cells within this epithelium was also affected by Brm deficiency. The analysis of populations of mature epithelial cells of secretory lineage was carried out on the tissue sections of AhCreER^{+}Apc$^{fl/fl}$Brm$^{+/+}$ and AhCreER^{+}Apc$^{fl/fl}$Brm null animals harvested at day 10-12 post induction.

Alcian Blue staining was performed to assess the population of goblet cells in the colonic epithelium of AhCreER^{+}Apc$^{fl/fl}$Brm$^{+/+}$ and AhCreER^{+}Apc$^{fl/fl}$Brm null animals (Figure 4.14). The quantification of positively stained cells revealed a significant decrease in the number of goblet cells per half crypt between control and Apc-deficient animals as well as between controls and DKO animals (6.50±0.07 versus 4.98±0.19 and 6.50±0.07 versus 5.00±0.34, $p=0.0001$ for either comparison, $n\geq4$). However no difference in the number of Alcian Blue-stained cells was detected in the crypts of DKO mice compared to Apc-deficient cohort ($p=0.905$, $n\geq4$, Figure 4.16).

The numbers of enteroendocrine cells present in the colonic crypts were determined using Grimelius staining. Identification and scoring of these cells per half crypt showed a marked decline in the numbers of Grimelius-stained cells in the Apc-deficient and DKO animals in comparison to control animals (0.47±0.06 versus 1.61±0.05 and 0.5±0.02 respectively, $p=0.0001$ for either comparison, $n\geq4$, Figure 4.17). The number of enteroendocrine cells in the colonic epithelium of AhCreER^{+}Apc$^{fl/fl}$Brm null mice was unaltered from that of AhCreER^{+}Apc$^{fl/fl}$Brm$^{+/+}$ cohort ($p=0.52$, $n\geq4$).

The quantification of the mature cell types that are predominant in the epithelium of large intestine revealed in the context of aberrant Wnt signalling, Brm-deficient animals display the general trend of diminished differentiation of epithelial cell types in comparison to the control cohort, however these changes are no different to those observed in the Apc-deficient, Brm proficient animals.

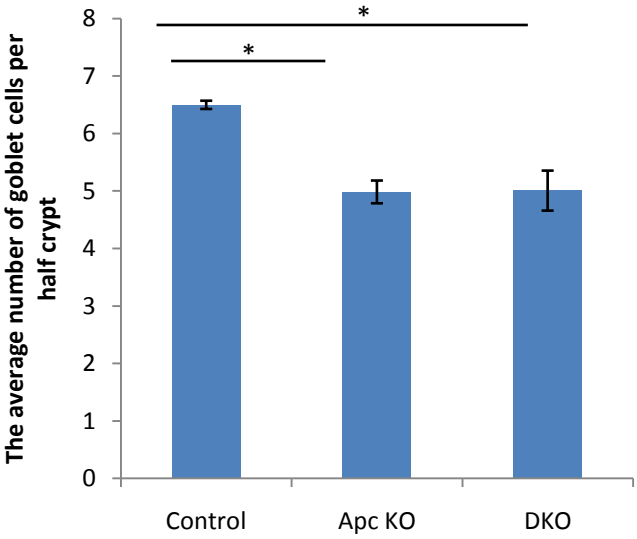

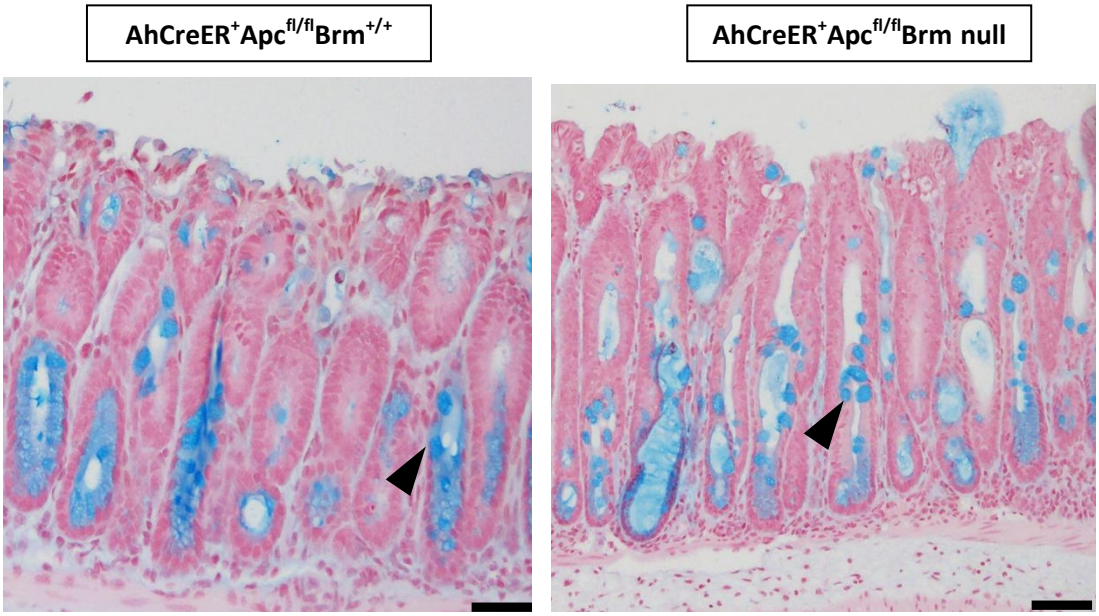

Figure 4.16 Alcian Blue staining was used in order to mark goblet cells within colonic epithelium. The colon sections of AhCreER^{+}Apc$^{fl/fl}$Brm$^{+/+}$ and AhCreER^{+}Apc$^{fl/fl}$Brm null animals were dissected at day 10-12 post induction and stained using cell specific stain detecting mucin secreting cells. Black arrows indicate individual goblet cells within the epithelium. Staining revealed no changes in the number of Alcian Blue-positive cells in DKO animals in comparison with Apc-deficient cohort. The scale bar represents 100µm.

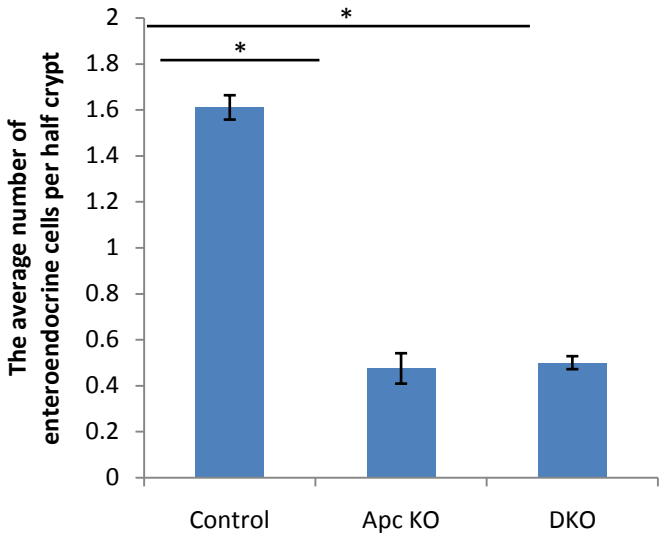

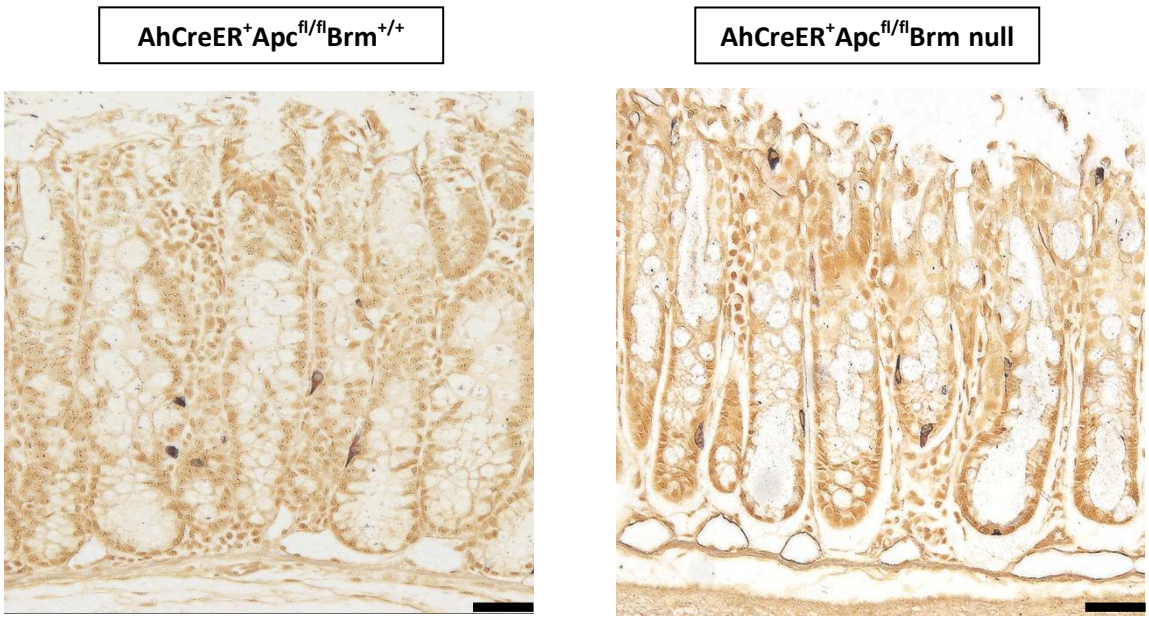

Figure 4.17 Grimelius staining of colonic sections was carried out to visualize the number of enteroendocrine cells on colonic epithelium sections of AhCreER^{+}Apc$^{fl/fl}$Brm$^{+/+}$ and AhCreER^{+}Apc$^{fl/fl}$Brm null animals dissected at day 10-12 post induction. Black arrow indicates individual enteroendocrine cell within the epithelium. The scoring of numbers of cells detected no difference in numbers of enteroendocrine cells between DKO and Apc-deficient epithelium. The scale bar represents 100μm.

4.2.13 Brm deficiency leads to the attenuation of the β-catenin-activated transcription of Wnt target genes

Previous observations indicating that Brm deficiency is capable suppression of the expression of Wnt target genes CD44 and c-Myc in the Wnt activated small intestinal epithelium (section 2.2.8). In order to compare the effects of Brm loss in the Wnt-driven tumorigenesis between small intestinal and colonic epithelium as well as to investigate whether Brm loss might also attenuate the Wnt-driven transcriptional program, I performed a qRT-PCR analysis of expression levels of some Wnt target genes and genes involved in the development and progression of CRC. mRNA was extracted from colon tissue samples of control, AhCreER^{+}Apc$^{fl/fl}$Brm$^{+/+}$ and AhCreER^{+}Apc$^{fl/fl}$Brm null animals dissected at day 10-12 post induction.

The expression analysis of mRNA levels of *CD44*, *c-Myc* and *Cyclin D1* revealed a significantly higher expression of these genes in the epithelium of Apc-deficient animals compared to controls (for all comparisons $p<0.05$, $n\geq4$, Figure 4.18). Similarly to the results obtained from small intestine, the up-regulation of both Wnt target genes in the epithelium of AhCreER^{+}Apc$^{fl/fl}$Brm null animals was less pronounced than in AhCreER^{+}Apc$^{fl/fl}$Brm$^{+/+}$ cohort. Expression levels of *CD44* in DKO animals were indifferent from those observed in the control small epithelium whereas *c-Myc* mRNA remained significantly higher. The levels of expression of *cyclin D1* were significantly higher in the AhCreER^{+}Apc$^{fl/fl}$Brm$^{+/+}$ and AhCreER^{+}Apc$^{fl/fl}$Brm null epithelium compared to controls ($p<0.05$, $n\geq4$) with no difference between both Apc-deficient cohorts ($p=0.265$, $n\geq4$).

As shown in the small intestinal epithelium, the presence of lesions with nuclear β-catenin in the colonic epithelium of AhCreER^{+}Apc$^{fl/fl}$Brm null animals indicated that Brm is dispensable for Wnt-driven CRC. Immunohistochemical analysis was used to further assess the effect of Brm deficiency on the tumorigenesis driven by the Apc loss. In particular, I aimed to examine whether the expression of the CD44 Wnt target gene was altered in the colonic lesions as CD44 upregulation is one of the well-described phenotype manifestations of aberrant Wnt signalling in colorectal tumorigensis. The staining of colonic AhCreER^{+}Apc$^{fl/fl}$Brm$^{+/+}$ and AhCreER^{+}Apc$^{fl/fl}$Brm null sections with antibody against CD44 was performed on tissue from animals dissected at day 10-12 post induction (Figure 4.19). Analysis of patterns of CD44 expression in the neoplastic epithelium labelled with nuclear β-catenin in both Apc-deficient cohorts revealed a marked decrease in CD44 expression in the

AhCreER^{+}Apc$^{fl/fl}$Brm null sections in comparison with AhCreER^{+}Apc$^{fl/fl}$Brm$^{+/+}$ sections which is consistent with the qRT-PCR results.

Taken together, these observations suggest that Brm loss is compatible with Wnt-driven tumorigenesis in the colonic epithelium. In the context of an activated Wnt pathway, Brm deficiency reduces transcriptional activation of Wnt target genes in particular CD44, however, deficiency failed to attenuate the expression of *cyclin D1* and *E-cadherin*, other key genes in CRC tumorigenesis. These results differ from those obtained from small intestinal epithelium suggesting that some modifications of Wnt-driven turmorigenesis by Brm appear be tissue- or cell type-specific.

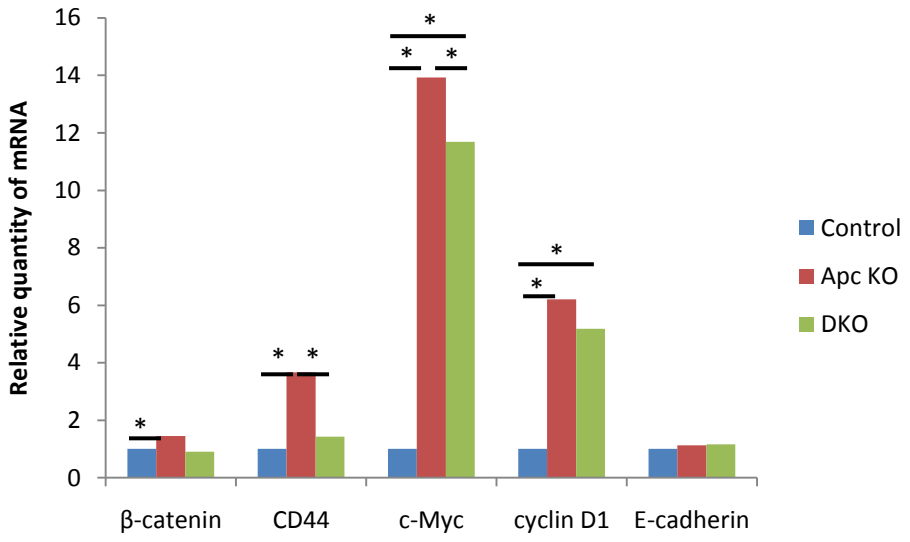

Figure 4.18 Brm loss suppresses the expression of the Wnt target genes. The transcriptional levels of Wnt targets *CD44* and *c-Myc* as well as *Cyclin D1* and *E-cadherin* genes was quantified by quantitative real-time-PCR (qRT-PCR) as shown in bar graph form. The data from qRT-PCR are normalised with *β-actin* and the asterisks indicate comparisons that were found to be significantly different ($p<0.05$, $n\geq4$). Analysis of levels of *CD44*, *c-Myc* revealed a significant decrease in the expression of those genes in the epithelium of AhCreER^{+}Apc$^{fl/fl}$Brm null in comparison to AhCreER^{+}Apc$^{fl/fl}$Brm$^{+/+}$ animals. The expression levels of two other key genes participating in the development and progression of CRC, *cyclin D1*and *E-cadherin* were found unaltered between those two Apc-deficient experimental cohorts.

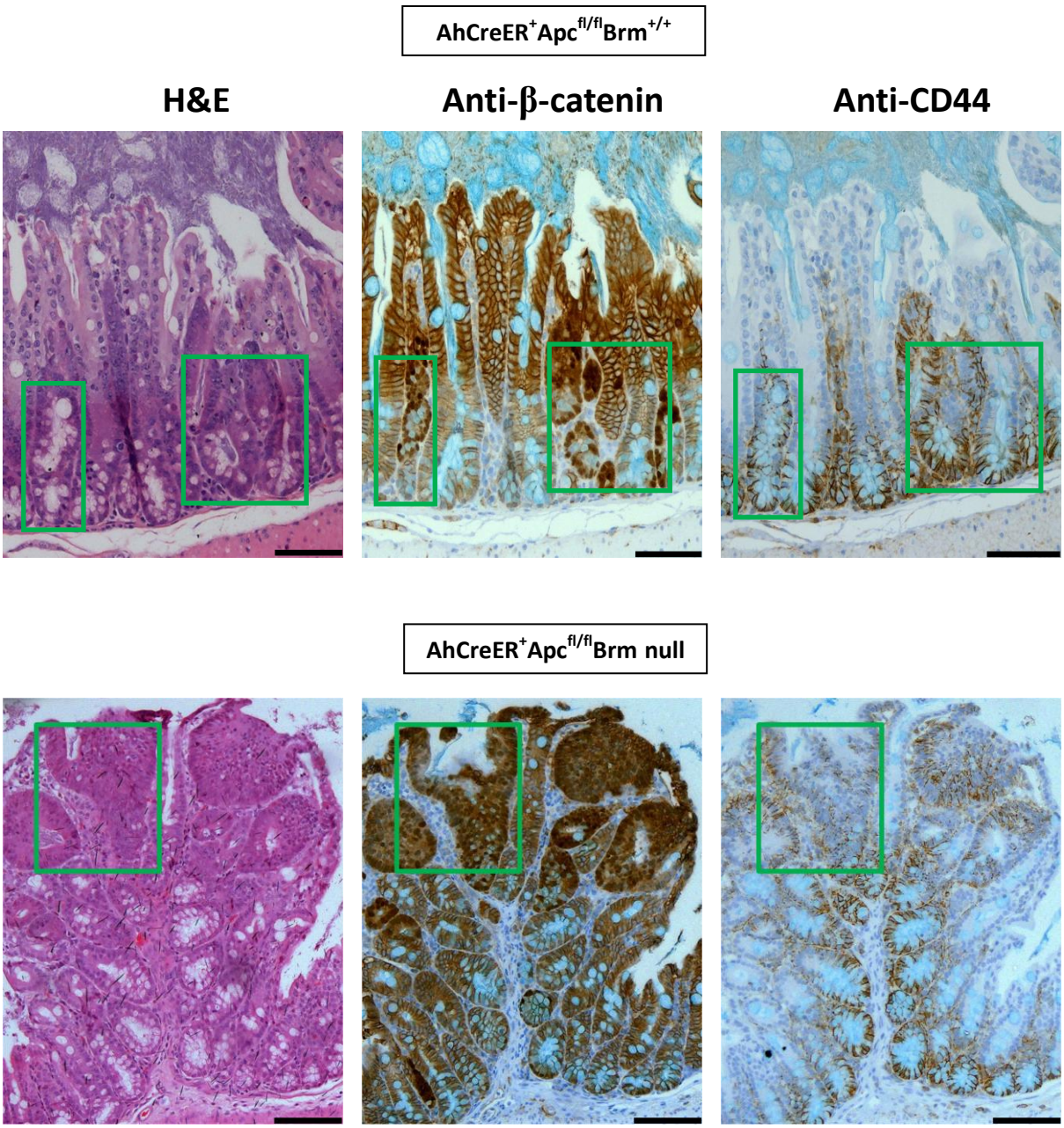

Figure 4.19 Brm deficiency leads to decrease in the expression of CD44 in context of activated Wnt pathway in the colonic epithelium. Immunohistochemical staining against β-catenin and CD44 was performed on the serial sections of colonic epithelium of AhCreER^{+}Apc$^{fl/fl}$Brm$^{+/+}$ and AhCreER^{+}Apc$^{fl/fl}$Brm null animals. The analysis of β-catenin staining allowed for identification of Apc-deficient regions of epithelium (green box) characterized by the presence of nuclear β-catenin. The comparative analysis of CD44 expression between the epithelia of AhCreER^{+}Apc$^{fl/fl}$Brm$^{+/+}$ and AhCreER^{+}Apc$^{fl/fl}$Brm null animals showed a perceptible decrease in the CD44 expression in DKO cohort in comparison to Apc-deficient animals. The scale bar represents 100 µm.

4.3 Discussion

In the previous chapter, I examined the impact of Brm deficiency in the homeostasis of epithelium of small and large intestine. In spite of numerous studies initially indicating SWI/SNF chromatin remodelling complex components as *bona fide* tumour suppressor genes, homozygous constitutive loss of Brm was not capable of inducing tumorigenesis in any of previously studied tissue type, nor in the small intestinal or colonic epithelium. In comparison to other transgenic murine models of SWI/SNF subunit deficiencies, both constitutive and conditional, loss of Brm ATPase did not lead to lethal phenotype. Brm deficiency resulted in the expansion of elongated crypts, unaffected proliferative compartment and significant upregulation of differentiation towards secretory lineages of mature epithelial cell type, however, stem cell function and intestinal homeostasis in general remained unaffected. To summarize, the results obtained indicated that deficiency in Brm chromatin remodelling factor is not capable of inducing tumorigenesis on its own which occurs in case of deficiency in SNF5 subunit of SWI/SNF chromatin remodelling complex. Histological analyses of human tumours suggested that alterations in SWI/SNF, in catalytic subunits such as Brm and Brg1 in particular, are frequently found in the gastric, leukemia, lung, prostate and skin cancers (reviewed in Weissman *et al.* 2009). The role of Brm as a component of the remodelling complex that is indispensable for Rb-mediated growth inhibition (Strober *et al.* 1996, Reisman *et al.* 2003) as well as being one of the key regulators of the expression of the Wnt target gene CD44 in cancer cell lines (Strobeck *et al.* 2001, Banine *et al.* 2005, Batsché *et al.* 2006) both implicated Brm as a potential factor contributing towards CRC tumorigenesis. Wnt signalling plays a critical role in the intestinal homeostasis and is dysregulated in almost all cases of intestinal neoplasia in both mice and humans. Therefore investigating whether Brm is capable of indirect interaction with the Wnt pathway and subsequently the effects of Brm deficiency in the context of aberrant Wnt signalling *in vivo*, is of a great importance for validation of Brm as a potential tumour suppressor gene in CRC tumorigenesis.

In this chapter, I investigated whether loss of Brm chromatin remodelling factor is capable of escalating Wnt-driven intestinal tumorigenesis caused by homozygous loss of Apc. The other aim of this study was to examine the modification of the activated Wnt pathway phenotype by Brm deficiency. In order to achieve this, I exploited a conditional Cre-loxP recombination system specific to intestinal epithelium to inactivate both alleles of *Apc* gene subsequently

leading to aberrantly activated Wnt pathway. Targeted Apc loss was put in the context of Brm loss by introduction of this allele to mice already bearing constitutive Brm null alleles. The results presented in this chapter show that Brm deficiency does not accelerate or suppress Wnt-driven tumorigenesis as both survival of animals and phenotype of Apc-deficient lesions are indifferent from those found in Apc KO animals. While Brm loss in the context of activated Wnt signalling leads to even further enlarged crypts, an increase in apoptosis, and an expansion of proliferative compartment at the cost of decline in differentiation, it also suppressed the expression of Wnt target genes and expansion of the stem cell population leading eventually to restoration of optimal level of Wnt activation in tumour cells similar to that seen in Apc-deficient intestinal epithelium.

4.3.1 Brm deficiency affects the survival of Apc-deficient animals

As shown in the previous chapter, constitutive loss of both alleles of Brm does not induce tumorigenesis in the small or large intestinal epithelium, therefore I aimed to investigate whether Brm deficiency would enhance the development of intestinal neoplasia in the context of targeted loss of *Apc* gene. By exploiting a mouse model of germline mutation in Apc^{580S} under the expression of intestinal-specific Cre recombinase (AhCreER) I have generated two cohorts of animals with homozygous Apc loss with and without Brm null alleles. Experimental $AhCreER^{+}Apc^{fl/fl}Brm^{+/+}$ and $AhCreER^{+}Apc^{fl/fl}$Brm null animals as well as $AhCreER^{-}$ controls were aged and the intestinal epithelium was harvested once mice became ill. All $AhCreER^{+}Apc^{fl/fl}Brm^{+/+}$ and $AhCreER^{+}Apc^{fl/fl}$Brm null had to sacrificed within the first 3 weeks following induction by Tamoxifen and β-napthoflavone. In contrast to other pan-intestinal recombinases, AhCreER expression is restricted to a relatively small population of intestinal stem cells and early intestinal progenitor cells. Exploiting this limited expression of AhCreER would possibly allow long-term activation of Wnt pathway as in order for cells carrying an induced loss of Apc to become detectable within the epithelium, numerous rounds of cell division must occur.

Despite the use of a tissue-specific Cre recombinase and a dually-controlled expression system, no long-term macroscopical tumour burden analysis was possible due to the overall short lifespan of experimental animals. Microscopic analysis of intestinal epithelium revealed numerous single crypt lesions and some larger lesions with highly dysplastic cells all featuring expression of stabilized β-catenin. In contrast in the colonic epithelium, the number of lesions expressing nuclear β-catenin as well as their size was lower than in small intestine

suggesting that the activation of Wnt-driven tumorigenesis lead to graduated neoplastic response within the intestinal epithelium. Furthermore, the analysis of survival probability detected no difference between Apc-deficient mice with or without Brm. Whereas the lack of effect on early stage dysplasia in Brm null animals has been previously well described (Reyes *et al.* 1998, Muchardt and Yaniv 1999), the observation that Brm deficiency is unable to accelerate the formation of tumours is in contrast with previous reports from lung and skin cancers suggesting that Brm contributes towards carcinogenesis. This disparity in results may indicate that Brm chromatin remodelling factor acts as a tumour suppressor in a tissue-specific manner or even more specifically, in a cell-type dependent manner. This tissue-specific requirement for SWI/SNF chromatin remodelling has been previously demonstrated by Holik *et al.* (PhD thesis 2011) showing that Brg1 loss is not compatible with Wnt activation and expression of nuclear β-catenin in the small intestinal epithelium subsequently implicating that only Brg1 proficient intestinal lesions have the capacity to develop towards more advanced forms of neoplasia.

Previous studies on murine models showed that the exposure of Brm-deficient animals to ethyl carbamate results in the increased development of lung adenomas (Glaros *et al.* 2007). Similarly the study of skin carcinogenesis showed that Brm null animals had an increased incidence of skin and ocular tumours once exposed to ultraviolet radiation compared to wild-type animals (Halliday 2012). Furthermore analysis of Brm expression in human cancers revealed that reduction of Brm expression in human gastric and prostate cancers correlates with poor prognosis whereas loss of heterozygosity at the Brm locus in the head and neck cancer is associated with poor prognosis in humans. However in this study I did not observe an acceleration of Wnt-driven tumorigenesis in the epithelium of small or large intestine suggesting that Brm might not function as *bona fide* tumour suppressor gene in the intestinal neoplasia. Notably, a transgenic model of skin cancer exploiting p53 deficiency combined with a loss of Brm failed to detect higher tumour number than that of $p53^{+/-}$ however the growth rate of the tumours was significantly higher in $Brm^{-/-}$ $p53^{+/-}$ compared to $p53^{+/-}$ (Halliday *et al.* 2012). Loss of p53 is known as one of the earliest events in UV-induced skin carcinogenesis, similar to the mutations in Apc in colorectal cancers, indicating that whereas Brm does not influence overall tumour burden, there might be a requirement for Brm expression for tumour suppression in a cell type-specific manner.

Taken together, the results obtained from normal intestinal epithelium as well as Wnt-activated epithelium suggest that in a short term study, Brm does not attenuate or accelerate tumour development.

4.3.2 Brm deficiency has a dual role in small intestinal epithelium by enhancing some histological effects of activated Wnt signalling with concomitant suppression of Wnt target genes

As suggested in previous reports, due to the role of Brm ATPase subunit in transcriptional activation and repression rather than acting as a direct tumour suppressor of signalling pathways in human cancers, I investigated the effects of Brm deficiency in the context of aberrant Wnt signalling in the small intestinal epithelium. The activation of Wnt pathway was achieved by conditional deletion of both alleles of *Apc* gene in the context of constitutive loss of Brm (Brm null) under the expression of intestinal-specific Cre recombinase AhCreER.

Initial analysis of Apc-deficient epithelium with and without Brm loss revealed characteristic phenotype associated with initiation and early development of intestinal lesions, mimicking features of conditional Apc loss under control of the AhCre promoter observed by Sansom *et al.* (2004). Further analysis of the histological parameters such as crypt length, proliferation, apoptosis and differentiation revealed the exacerbation of cellular responses mediated by stabilized β-catenin in the Brm-deficient epithelium. In contrast, the gene expression analysis showed a significantly reduced Wnt target gene expression in DKO animals in comparison to levels observed in Brm-proficient Apc-deficient animals. Overall, these observations from the small intestinal epithelium suggest that Brm plays a dual role in enhancing the effects of Wnt activation on processes such as proliferation and apoptosis as well as in parallel mediating suppression of expression of Wnt target genes.

Microscopic analysis of small intestinal epithelium of DKO animals identified numerous high-grade dysplastic cells characterized by the presence of nuclear β-catenin staining within the crypt-villus structures. The general architecture of the epithelium was altered with a distinct crypt compartment no longer identifiable whereas in some areas of tissue with a much higher than other regions number of Apc-deficient cells, the architecture along the crypt-villus axis was dysmorphic and significantly altered. Enlarged abnormal crypts, increase in apoptosis levels and a significant expansion of proliferative compartment measured by Ki67 distribution analysis – all features of acute activation of Wnt signalling (Sansom *et al.* 2004) were shown to be even more pronounced in the small intestine of Brm

deficient mice. Notably, the same morphological parameters were altered in the small intestinal epithelium of Brm null animals (section 3.2.4) and consistent with studies reporting a marked increase in Ki67 proliferation index in epithelial compartment of murine prostate cancers (Shen *et al.* 2008) furthermore indicating that functional Brm might be required for the maintenance of the required levels of proliferating cells in the normal as well as Wnt-activated small intestinal epithelium. Expanding number of tumour cells featuring progenitor-like phenotype and upregulation of intestinal stem cell-specific genes *Ascl2*, *Lrg5* and *Olfm4* are presumably additionally causing perturbations in proliferation and further development of intestinal lesions (Merlos-Suarez *et al.* 2011). Surprisingly in the epithelium of Brm deficient animals, elevated levels of proliferation concurred with a marked depletion of the Wnt-independent stem cell marker gene Olfm4. Both gene expression analysis by qRT-PCR and *in situ* hybridization of *Olfm4*-specific riboprobe showed a significant decrease when compared to Apc-deficient epithelium. In the normal intestinal homeostasis, the stem cell niche is located at the base of the crypt and actively supported by neighbouring Paneth cells however in the case of aberrant Wnt signalling in Brm deficient epithelium Paneth cells are localised at higher positions along the crypt-villus axis whereas remarkably, *Olfm4* expression is restricted to the base of the crypt. A significant decline in *Olfm4* expression and its restoration to the normal stem cell niche compartment suggest the attenuation of an expansion of the stem cell-like populations in the small intestinal epithelium of DKO animals.

Although cellular migration in the epithelium of Apc-deficient animals was not quantified in the course of this study, previous reports by Sansom *et al.* (2004) showed that inactivation of Apc under the expression of AhCre recombinase completely abrogated migration of BrdU-labelled cells along the crypt-villus axis. The absence of functional Brm did not have any effect on cell migration in the epithelium of Brm null animals in comparison to controls therefore taken together these results suggest that observed changes in the populations of proliferating cells are not caused by abrogation of migration and failure of removal of dysplastic cells.

As described in the previous chapter, Brm was shown to play an important role in the differentiation of mature epithelial cell types by modulation of Notch pathway effectors. Furthermore Brm deficiency was also found to affect the cell differentiation in response to activated Wnt signalling. The most pronounced changes were the reduction in the brush border enterocytes accompanied by an increase in the population of goblet cells. Wnt and

Notch pathways are the key regulators of the maintenance of stem cells and progenitor cells whereas Notch effector Hes1 and its antagonist Math1 direct the differentiation of those progenitor cells towards either absorptive or secretory cell lineage (Jensen *et al.* 2000). Wnt-activated small intestinal epithelium has been previously shown to display significantly reduced alkaline phosphatase and *Villin* expression indicating the diminished numbers of brush border enterocytes (Sansom *et al.* 2004). A concomitant decline in the secretory cell populations was observed in the Apc-deficient epithelium with an exception of Paneth cells whose very low numbers and confinement to the crypt base were lifted under acute Wnt signalling (Battle *et al.* 2002, Sansom *et al.* 2004). Loss of functional Brm expression in the small intestinal epithelium resulted in a further decline in the population of brush border enterocytes in the DKO animals. However a homogenous decline in all secretory cell lineage populations as described by Sansom *et al.* (2004) in a model of Apc loss was not observed in this study. In contrast, along with decrease in enterocytes a simultaneous increase in goblet cell numbers was detected in the epithelium of DKO animals. The increase in Alcian Blue-positive goblet cells was significant in comparison to Apc-deficient epithelium as well as in comparison to controls expressing functional Brm indicating that loss of Brm has led to an intermediate effect on goblet cell differentiation between the normal numbers of goblet cells in the normal intestinal epithelium and Wnt-activated Apc-deficient epithelium. Scoring of enteroendocrine cell numbers and Paneth cell numbers as expected have identified a significantly underrepresented population of enteroendocrine cells and a marked increase in Paneth cells and their mislocalisation from crypt base along the crypt-villus axis in the Apc-deficient epithelium of both Brm-proficient and Brm-deficient animals. However the differentiation patterns of those two cell types was not altered by the absence of functional Brm in DKO animals. In parallel to quantification of differentiation traits on the histological sections, the analysis of gene expression of Notch effectors detected a significant fluctuation of expression of *Hes1* and *Math1* in the intestinal epithelium of Apc-deficient cohorts. Downregulation of *Hes1* expression in the epithelium of DKO animals further confirmed transcriptional repression of this gene in the absence of functional Brm. Strikingly, a significant up-regulation of *Math1* levels was detected in both Apc-deficient cohorts suggesting that the intermediate numbers of Goblet cells in the small intestinal epithelium of DKO animals may be a result of concomitant down-regulation of Hes1 and up-regulation of Math1 which overdrives Hes1-driven suppression of differentiation towards secretory lineage differentiation. To summarize, consistent with previous reports showing that Brm-containing remodelling complexes are preferentially recruited to Hes1 and Hes5 promoters these results

suggest that Brm is involved in transcriptional activation of particular subsets of genes regulating proliferation and apoptosis as well as concomitant activation and repression of separate genes governing cell differentiation. Therefore the lack of homogenous response to activation of Wnt signalling by Brm accounts for the enhancement of some and attenuation of other histological parameters of small intestinal epithelium. While some differences in the overall experimental design between our study and that of Sansom *et al.* (2004) should be noted such as use of dually-regulated Cre recombinase with a lower recombination efficiency and slightly different criteria of histological scoring and therefore could account for the magnitude of the effects observe, the phenotype in animals that lost both copies of *Apc* gene appears to be quite consistent in both studies.

Taken together, in the context of aberrant Wnt signalling, Brm deficiency enhanced some of the cellular responses mediated by activated Wnt pathway such as proliferation, apoptosis and impaired enterocyte differentiation. Further attenuation of differentiation of absorptive lineage cells was parallel with lifted impairment of goblet cell differentiation and its restoration to levels intermediate between normal and Apc-deficient epithelium. No observed effect of Brm on the enteroendocrine and Paneth cell populations suggested that the expansion of goblet cell population by Brm deficiency is a direct effect of this ATPase subunit of Notch signalling effectors which is independent of acute activation of Wnt pathway.

The aggravation of some of the histological parameters in a response to Wnt activation in the small intestinal epithelium of DKO animals suggests a possible link between the Brm chromatin remodelling factor and the Wnt pathway. However the precise mechanism of how this enhancement of phenotype occurs remained unclear. Previous reports showed that components of Wnt pathway including β-catenin have failed to interact with SWI/SNF complexes in ChIP experiments indicating the absence of direct interaction and suggesting that Wnt pathway may require different types of complexes in order to mediate its downstream effects (Kadam and Emerson 2003). Therefore whereas Brm is not capable of regulation of β-catenin expression, it could possibly be involved in the transcriptional activation of Wnt receptors or promote active translocation of β-catenin into the nucleus. Immunohistochemical analysis of Wnt activated epithelium of Brm proficient and Brm-deficient animals revealed that many cells expressed nuclear β-catenin staining however the comparison between both cohorts of the level of Wnt activation was not possible using this method. To explore this possibility of indirect regulation of Wnt pathway by Brm, I have

quantified the levels of active β-catenin in the small intestinal epithelium of DKO mice. Western blotting analysis detected no differences in the levels of stabilized β-catenin between those two cohorts of Apc-deficient animals further confirming that Brm does not play role in the stabilization and accumulation of β-catenin. These results demonstrate that exacerbation of the effects of Apc loss on proliferation, apoptosis and differentiation potential of progenitor cells in the small intestinal epithelium of DKO animals do not occur as a consequence of elevated levels of main Wnt pathway effector β-catenin.

The other possible mechanism of Wnt-driven phenotype modulation by Brm was the trans-activation of downstream of β-catenin Wnt target genes. The expression levels of genes involved in the transcriptional program activated in response to aberrant Wnt signalling such as *CD44*, *c-Myc*, *cyclin D1* and *E-cadherin*. Surprisingly, *CD44*, *c-Myc* and *cyclin D1* were downregulated in the small intestinal epithelium of DKO animals in comparison to Apc-deficient mice. Similar transcription levels of Wnt target genes were reported by Holik *et al.* (2014) suggesting that deficiency in either ATPase of chromatin remodelling complex results in the attenuation of the Wnt transcriptional program. Whereas CD44 and c-Myc immediate Wnt targets are overexpressed in all colorectal tumours, cyclin D1 expression become up-regulated upon the progression of small neoplastic lesions into adenomas (Sansom *et al.* 2005). These observations suggest that although many parameters of Wnt-activated Brm-deficient epithelium are enhanced suggesting acceleration in tumorigenesis, the absence of functional Brm might result in the repression of transcriptional program activated by β-catenin stabilization and translocation to the nucleus. However the expression levels of E-cadherin remained significantly up-regulated in the small intestinal epithelium of both Apc-deficient cohorts. Previous reports have indicated that the CD44 promoter becomes hypermethylated and silenced in the Brm null model as well as numerous Brm-deficient cancer cell lines (Banine *et al.* 2005, Batsché *et al.* 2006), moreover ChIP assays showed the association of Brm chromatin remodelling factor with this region of CD44 suggesting that Brm is required for transcriptional activation of CD44 with Brm deficiency directly influencing the transcription of *CD44* gene. Brm-induced changes in the methylation status of CD44 promoter region could occur directly by Brm promoting the activities of genes that are capable of alteration of DNA methylation or indirectly by promoting the transcription of those genes through via two possible routes: blocking of abilities of methyltransferases to methylate CD44 promoter or recruitment of demethylases to these promoter sequences. The exact mechanism by which Brm is affecting the transcriptional activation of CD44 has not yet

been confirmed. ChIP-seq experiments by Damiano *et al.* (2013) showed that c-Myc was found to bind the core promoter region of Brm and MEK-ERK signalling pathway is capable of activating c-Myc to reduce the transcription of Brm SWI/SNF subunit. However c-Myc was also indicated as a direct target for Brm-mediated transcriptional repression (Coisy-Quivy *et al.* 2006) suggesting that the mechanism underlying the transcriptional repression of *c-Myc* in the DKO small intestinal epithelium appears to be driven by more complex and two-way interactions between c-Myc and Brm.

Taken together, the data presented in this chapter suggest that the modulation of Wnt-driven tumorigenesis in the small intestinal epithelium of Brm-deficient animals occurs at different levels. First of all, enhanced crypt length, proliferation and apoptosis suggest an enhanced phenotype, which is however not consistent with the survival probability analysis. Furthermore, Brm loss results in the impaired expression of Wnt target genes as well as reduced expression of the stem cell marker Olfm4. The net result of these changes is the development of only small lesions and low-grade adenomas in the small intestinal epithelium of DKO. Ablation of transcriptional program activated by aberrant Wnt signalling can consequently lead to less severe than expected responses in proliferation, apoptosis and differentiation to Wnt activation.

4.3.3 Brm deficiency has mild effects on the Wnt-activated colonic epithelium

The data obtained in the chapter 3 suggested that the effects of Brm loss differ between the small intestinal and colonic epithelium indicating some tissue-specificity of functional Brm. Therefore I aimed to investigate whether those differences in the response to Brm deficiency are also present in the context of aberrant Wnt signalling in the colonic epithelium. As previously described in section 2.1.1 the activation of Wnt pathway was achieved by conditional deletion of loxP-flanked *Apc* allele under the expression of AhCreER recombinase together with constitutive loss of functional Brm.

Morphological analysis of Apc-deficient epithelium with and without Brm deficiency revealed the presence of multiple lesions expressing stabilized β-catenin in the colonic epithelium however those morphological changes in the architecture were far less pronounced and occur less frequently than those observed in the small intestinal epithelium. Notably, these observations would be consistent with the hypothesis that a variation in the

physiological levels of Wnt activity across the length of intestines influences the distribution of lesions and tumours (Leedham *et al.* 2012). Equally some of these changes might reflect differences in Cre mediated recombination levels between those animals.

The phenotypic responses in the Wnt-activated colonic epithelium should closely resemble those reported in the small intestine by Samson 2004 including elongated crypts, increase in proliferation and apoptosis, expansion of proliferative compartment and up-regulation of transcriptional program mediated by β-catenin stabilization. Histological analysis of colonic epithelium of DKO animals detected significantly increased proliferation and apoptosis levels with no alterations of crypt length in comparison to Apc-deficient animals. These results are in contrast to previous data from large intestine (section 3.2) showing the opposite phenotype in context of Brm loss – enlarged crypts coincide with no changes in either proliferation or apoptosis. Independently of the population size of Ki67-positive cells, Brm-deficiency appears to induce the shift and extension of proliferative compartment in the colonic epithelium of both Brm null and DKO animals. The shift in the alterations of cellular responses in the Wnt-activated Brm-deficient epithelium suggest that some modulations of phenotype by Brm loss may be highly dependent on the level of activity of Wnt pathway for regulation of cellular processes along the crypt-villus axis of colonic epithelium.

Subsequently, qRT-PCR gene expression analysis showed a significant down-regulation of Wnt target gene expression in DKO animals in comparison to levels observed in Brm-proficient Apc-deficient animals whereas no changes in the expression levels of genes such as *cyclin D1* and *E-cadherin* were detected. In overall, these observations from small intestinal epithelium suggest that Brm plays a dual role in enhancing the effects of Wnt activation on processes such as proliferation and apoptosis as well as in parallel mediating suppression of expression of Wnt target genes.

As described in the previous chapter, Brm was shown to play an important role in the differentiation of mature epithelial cells of secretory lineage by modulation of Notch pathway effectors. Similarly, the size of the populations of differentiated cell types, in particular goblet cells, is affected by the loss of functional Brm in the Wnt-activated small intestine. Notably, a marked decrease in the populations of goblet and enteroendocrine cells was observed in Apc-deficient epithelium when compared to controls however no alterations in the secretory cell populations were shown between DKO and Apc-deficient mice. The absence of response to Brm deficiency in the context of aberrant Wnt pathway in colonic epithelium might further

indicate that the extent of Apc phenotype modulation is highly dependent upon the local levels of Wnt activation.

To summarize, Brm deficiency has very mild effects on the Wnt-activated colonic epithelium resulting in an enhancement of both proliferation and apoptosis. However the absence of severe effects in the colonic morphology due to those alterations suggests that other mechanisms may counteract the response. The repression of β-catenin-mediated transcriptional program of immediate Wnt targets CD44 and c-Myc which concurs with increased proliferation and apoptosis may in longer term halt the exacerbation of Wnt-driven tumorigenesis. Furthermore, Brm was shown to be capable of compensating for loss of Brg1 ATPase subunit in the colonic but not small intestinal epithelium suggesting that some of the modifications of phenotype driven by Apc loss in context of Brm deficiency might indeed be a response to fluctuations in the expression of its paralogue, Brg1.

4.3.4 Conclusions

Taken together, the observations described in this chapter indicate that small intestinal and colonic epithelium substantially differ in their response to activation of Wnt signalling in the context of Brm deficiency. In both cases, the maintenance of "progenitor-like" phenotype of Apc-mutant cells is accompanied by distinct pattern of cellular changes characteristic for Wnt activation via loss of Apc however the direction and the magnitude of those alterations is very specific to either small intestinal or colonic epithelium. In normal epithelium, homeostasis is maintained by a very discreet interplay between pathways and numerous components of Wnt, Notch, Hedgehog and TGF-β/BMP signalling, similarly in Wnt-activated epithelium, the optimal but not excessive level of β-catenin activation is required for tumorigenesis and its development (Albuquerque *et al.* 2002). The discrepancy between small intestinal and colonic epithelium could be a result of two separate mechanisms. Firstly, the phenotype coinciding Brm deficiency may be context-dependent and result in different array of responses in different type of epithelium. This would be consistent with the assumption that the basal gradient of Wnt activity and therefore the extent of the activation of Wnt pathway via Apc loss differs between proximal small intestine and the colon. Therefore different level of Wnt activation in different type of intestinal epithelium would influence the

severity of changes due to Brm deficiency. Secondly, the perturbations of histological parameters associated with Apc loss may also reflect β-catenin-independent effects, notably the up-regulation of Brm paralogue Brg1in order to compensate for Brm function. Both ATPases of SWI/SNF complex have been previously shown to be partially redundant in their functions however this mechanism appears to be tissue-specific and often cell type-specific.

In all, the effects of Brm deficiency on the small intestinal and colonic epithelium in the contexts of both – normal homeostasis and Wnt-driven tumorigenesis should be additionally considered in the context of Brg1 expression in those tissues in regard to reveal the function of Brm chromatin remodelling subunit in the intestinal tract.

Chapter 5

Investigating the effects of Brg1 loss in the epithelium of small and large intestine in the context of Brm deficiency

5.1 Introduction

The data presented in the previous two chapters revealed that Brm deficiency results in a wide range of cellular responses whose effects on phenotype differ between small intestine and colonic epithelium as well as between normal homeostatic and Wnt-activated tissue. Previous studies on Wnt pathway effects on intestinal tissue indicate that such discrepancies between the phenotypes could occur due to differential levels of basal Wnt signalling activity (Leedham *et al.* 2012). As suggested before, the role of Brm may also be partially compensated by its paralogue Brg1.

Catalytic subunits of SWI/SNF chromatin remodelling complex Brm and Brg1 have been implicated in regulating transcriptional activation and repression of numerous genes regulating a variety of cellular processes. Both ATPases share 75% sequence homology and share a core consisting of functional domains: QLQ, proline-rich, HSA, ATPase, Rb-binding and Bromo domain (Kadam and Emerson 2003). The evidence from cell line studies speculated that ATPase subunits might be redundant for homeostasis of the tissue and share many common cellular functions. However further reports conducted on both cell lines and murine models of disease revealed that Brm and Brg1 catalytic subunits are recruited in response to specific signalling pathways by unique interactions with different protein domains (Kadam and Emerson 2003) indicating that some form of compensation mechanism may exist between those ATPases however it would be partial and result in a particular tissue-specific response.

Although no evidence exists supporting the possibility of interaction between Brm and the Wnt pathway, there is evidence of involvement of the Brm paralogue Brg1 in a direct interaction with the Wnt pathway through its capacity of regulating Wnt target genes such as Cyclin D1 and CD44 (Baker *et al.* 2001, Kadam and Emerson 2002, 2003).

Both considered as putative tumour suppressor genes, Brm and Brg1 have been shown to be frequently lost concomitantly in lung, pancreas, skin, ovary and breast cancers (Numata *et al.* 2013, Liu *et al.* 2011, Reisman *et al.* 2009, Glaros *et al.* 2007, Reisman *et al.* 2005, Yamamichi *et al.* 2005, Fukuoka *et al.* 2004, Reisman *et al.* 2002, reviewed in Weissman and Knudsen 2009). Moreover in contrast to deficiency in either of the subunits individually, concomitant loss of activity of both ATPases has been correlated to poor prognosis in lung and prostate cancer. Previous data obtained by Holik *et al.* (2013, 2014) indicated that Brg1 is required for maintenance of intestinal stem cells and in the absence of functional Brg1 attenuates Wnt-driven tumorigenesis in the small intestinal epithelium suggesting that Brm and Brg1 play important but distinct roles in modulation of cancer phenotype.

In order to explore the effects of concomitant loss of both ATPase subunits on the small intestinal and colonic epithelium I have explored the consequences of loxP targeted deletion of *Brg1* allele (using AhCreER recombinase) in the context of constitutive loss of Brm as described in section 2.1.1. The evaluation of the effects of deficiency in both Brm and Brg1 appears appropriate to distinguish between those histological changes described in the previous two chapters due to Brm deficiency and possible Brg1 compensation. Additionally I aimed to investigate the respective levels of Brm and Brg1 in Brg1- and Brm-deficient lesions in the context of Wnt activation induced by Apc loss in the small intestinal and colonic epithelium. This chapter will aim to characterise the effects of Brm and Brg1 deficiency on the small and large intestinal epithelium.

5.2 Results

5.2.1 Concomitant loss of Brm and Brg1 results in animals that are viable and not prone to tumorigenesis

Mating of animals carrying the Brg1 targeted allele under the expression of AhCreER recombinase ($AhCreER^{+}Brg1^{fl/fl}$) with Brm null ($Brm^{-/-}$) resulted in the absence of neonatal lethality, litters of normal size and fertility of resulting progeny. No differences were observed in viability between DKO, Brm null and wild-type (control) littermates.

Similarly as with the Brm null animals, Brm null Brg1 KO mice were monitored for signs of illness or tumour formation, twice a week for a period of a year but no abnormalities were

observed. Morphological analysis of H&E sections revealed no dysplasia of the epithelium of small or large intestinal tissue.

5.2.2 AhCreER recombinase drives mosaic loss of Brg1 and subsequent repopulation in the small intestinal epithelium of AhCre^{+}Brg1$^{fl/fl}$Brm null mice

As previously reported by Holik (PhD Thesis, 2011), a mosaic pattern of Brg1 loss was observed in Brg1-deficient small intestinal epithelium under the control of AhCreER recombinase. Histological analysis of further time-points post induction showed that the number of crypts retaining Brg1-deficient cells decreased at regular intervals and by day 35 post induction no crypts containing Brg1-deficient cells were detected indicating that the small intestinal epithelium was repopulated with wild-type cells. Due to limited expression of AhCreER recombinase in the intestinal epithelium, being restricted to stem cell and progenitor cells and being activated at the frequency lower than 100%, Brg1-deficient cells were identified predominantly in the crypt compartment or along the crypt-villus axis and were present in small clusters of cells neighbouring with Brg1-proficient cells. Although AhCreER recombinase enforces some limitations to the histological analysis of tissue, the mechanism of activation evades the presumed off-target lethality observed in the animals expressing AhCre recombinase.

Cohorts of AhCreER^{-} (control), AhCreER^{+}Brg$^{fl/fl}$Brm$^{+/+}$ and AhCreER^{+}Brg1$^{fl/fl}$Brm null animals at 70 days of age were induced with five bi-daily daily intraperitoneal injections of 80mg/kg β-naphthoflavone with Tamoxifen at 12 hour intervals. All mice were then aged for a maximum of 50 days and were sacrificed at appropriate time-points (day 3, day 5, day 7, day 10, day 15, day 30, day 50, n≥4) when intestinal tissues were harvested. No animals from induced cohorts became ill within the timeframe of the experiment. Identification of Brg1-deficient cells in the AhCreER^{+}Brg$^{fl/fl}$Brm$^{+/+}$ and AhCreER^{+}Brg1$^{fl/fl}$Brm null small intestinal epithelium was performed using immunohistochemical staining against Brg1. Consistent with the previous study (Holik *et al.* 2013), a pattern of mosaic loss of Brg1 was observed in both AhCreER^{+}Brg$^{fl/fl}$Brm$^{+/+}$ and AhCreER^{+}Brg1$^{fl/fl}$Brm null animals as early as 3 days post induction. Quantification of the number of crypts containing Brg1-deficient cell clusters at all time-points showed a decrease in the frequency of deficient crypts in the small intestinal epithelium of both Brg1KO and DKO animals. By day 15, less than 5% of all small intestinal

crypts contained Brg1-deficient cell clusters in both DKO and Brg1KO animals. The vast majority of crypts consisted of Brg1-proficient cells only, indicating that Brg1-deficient cells are slowly eliminated from the epithelium and replaced by wild-type cells (Figure 5.1). Interestingly, on day 3 post induction the proportion of Brg1-deficient versus Brg1-proficient crypts was significantly lower in the context of Brm null epithelium. In contrast, at day 30 post induction qualitative assessment of Brg1 expression failed to detect any crypts with Brg1-deficient cell clusters in Brg1KO animals whereas such crypts were retained for longer in the epithelium of DKO mice. However by day 50 post induction, microscopic analysis failed to identify any Brg1-deficient cells in either experimental cohort suggesting that eventually all epithelium is Brg1-profiecient.

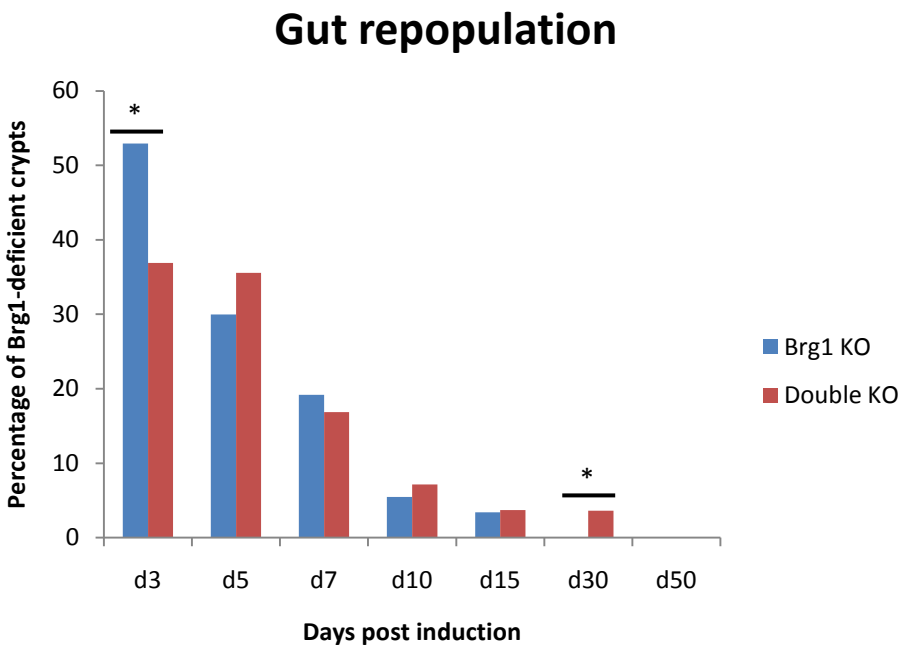

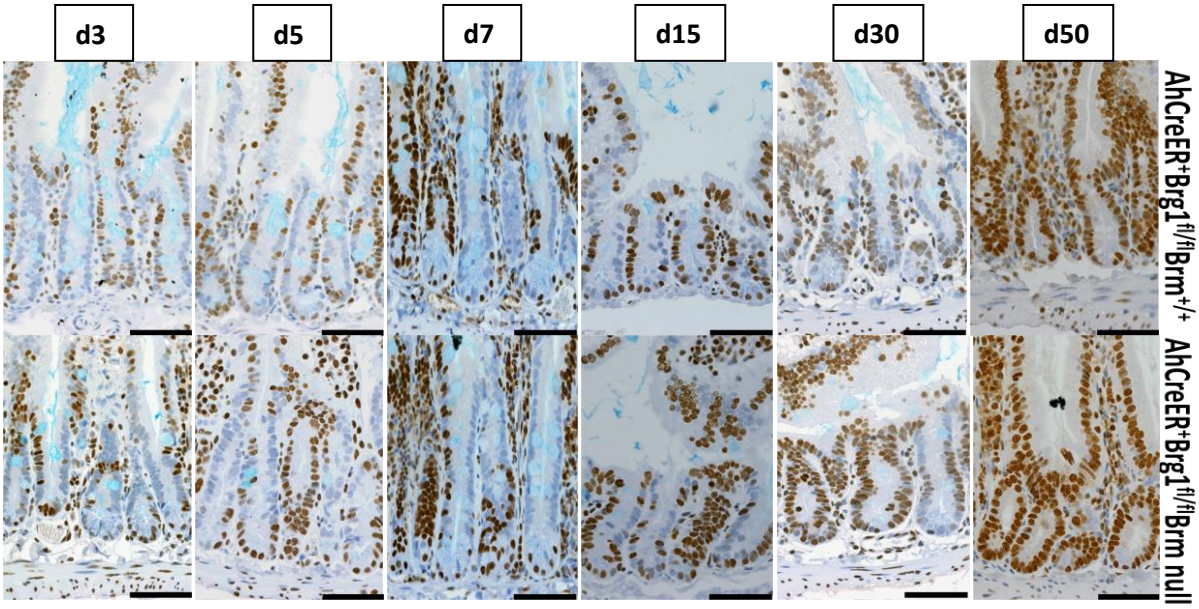

Figure 5.1 Brg1 loss under the expression of AhCreER recombinase is characterized by mosaic pattern of Brg1-deficient and Brg1-proficient crypts. AhCreER^{+}Brg1$^{fl/fl}$ and AhCreER^{+}Brg1$^{fl/fl}$Brm null animals were induced according to an appropriate protocol and tissues were harvested at day 3, 5, 7, 10, 15, 30 and 50 post induction. Immunohistochemical staining against Brg1 was conducted to assess Brg1 expression where crypts containing more than 6 Brg1-deficient cells were counted across small intestinal epithelium. The quantification of Brg1 expression revealed a trend of decrease in the frequency of Brg1-deficient crypts in both cohorts with a significantly lower number of crypts at day 3 post induction in DKO mice. Scale bar represents 100 μm.

5.2.3 Brg1 loss in the context of a Brm null allele has mild effects on small intestinal homeostasis

Due to the short-term retention of Brg1-deficient cells in the small intestinal epithelium repopulation under the expression of AhCreER recombinase, an appropriate time-point along the gut repopulation timeline had to be selected in order to allow further histological analysis of concomitant loss of both ATPases in the small intestinal epithelium. In regards to the numbers of crypts displaying Brg1-deficient cell clusters as well as the uniform pattern of Brg1 loss in AhCreER^{+}Brg1$^{fl/fl}$Brm null mice, day 5 post induction was selected for this purpose. Consistency between the time-points at which animals were sacrificed allowed for the analysis between DKO, Brm null and control cohorts. Serial sections of small intestinal epithelium tissue were stained against Brg1 and antibodies against Cleaved Caspase-3 and Ki67 for subsequent histological analysis conducted only in Brg1-deficient intestinal crypts.

Microscopic analysis of H&E sections of AhCreER^{+}Brg1$^{fl/fl}$Brm null animals revealed no obvious morphological abnormalities or tumorigenesis. The quantitative analysis of functional parameters of the epithelium detected some fine differences between DKO, Brm null and control animals. The results of quantitative analysis of those histological parameters are summarized in Table 5.1.

Crypt and villus lengths were assessed on H&E stained sections as the average number of cells (± standard deviation) from the bottom of the crypt upwards to the crypt-villus junction and from the crypt-villus junction upwards to the top of the villus where the cell shedding occurs. Assessment of crypt size showed that crypt length remained unaltered in the DKO epithelium in comparison to both control and Brm null (22.27±0.265 versus 21.617±0.920 and 22.564±0.156, $p=0.097$ and $p=0.109$ respectively, $n\geq4$, Figure 5.2a). Similarly, the quantification of the villus length detected no change in the villus size (72.997±1.358 versus 73.402±1.478 and 71.668±1.475, $p=0.954$ and $p=0.162$, $n\geq4$, Figure 5.2b).

The scoring of apoptosis levels detected a significant decrease in the number of cleaved Caspase-3- positive cells in DKO epithelium in comparison to control animals (0.025±0.01 versus 0.866±0.06, $p<0.001$, $n\geq4$). The decline in the apoptosis levels was equally abrupt when compared to Brm null mice (0.025±0.01 versus 0.744±0.338, $p<0.001$, $n\geq4$, Figure 5.2c). Strikingly, the quantification of proliferating cells showed a significant depletion of Ki67-positive cells in the epithelium of DKO animals in comparison to both controls and

Brm null (6.116±0.257 versus 13.395±0.762 and 13.513±0.702 respectively, $p<0.0001$ for either comparison, $n\geq4$, Figure 5.2d).

Therefore in the context of Brm loss, Brg1 deficiency in the small intestinal crypts results in a decrease in the numbers of both apoptotic and proliferating cells when compared to either control or Brm null tissue. Quantitative analysis of other morphological factors such as crypt and villus size detected no alterations in DKO animals.

Parameter	Cohort	Mean	SD	p-values	
				Control vs DKO	Brm null vs DKO
Crypt length	Control	21.617	0.920	0.097	0.109
	Brm null	22.564	0.156		
	DKO	22.27	0.265		
Villus length	Control	73.402	1.478	0.954	0.162
	Brm null	71.668	1.475		
	DKO	72.997	1.358		
Caspase positive cells	Control	0.866	0.060	0.001	0.001
	Brm null	0.744	0.338		
	DKO	0.025	0.010		
Ki67 positive cells	Control	13.395	0.762	0.000	0.000
	Brm null	13.513	0.702		
	DKO	6.116	0.257		

Table 5.1 Quantitative analysis of the effects of Brg1 deficiency on the small intestinal histology in the context of constitutive Brm loss. Epithelium from small intestine from AhCreER^{-} Brm$^{+/+}$ (marked as Control) and AhCreER^{+} Brm null (marked as Brm null) was harvested at day 70 of age and AhCreER^{+}Brg1$^{fl/fl}$Brm null (marked as DKO) was harvested from animals at 5 days post induction. Histological parameters including crypt and villus length, apoptosis and proliferation were assessed and the comparison between those three experimental cohorts was conducted using statistical software.

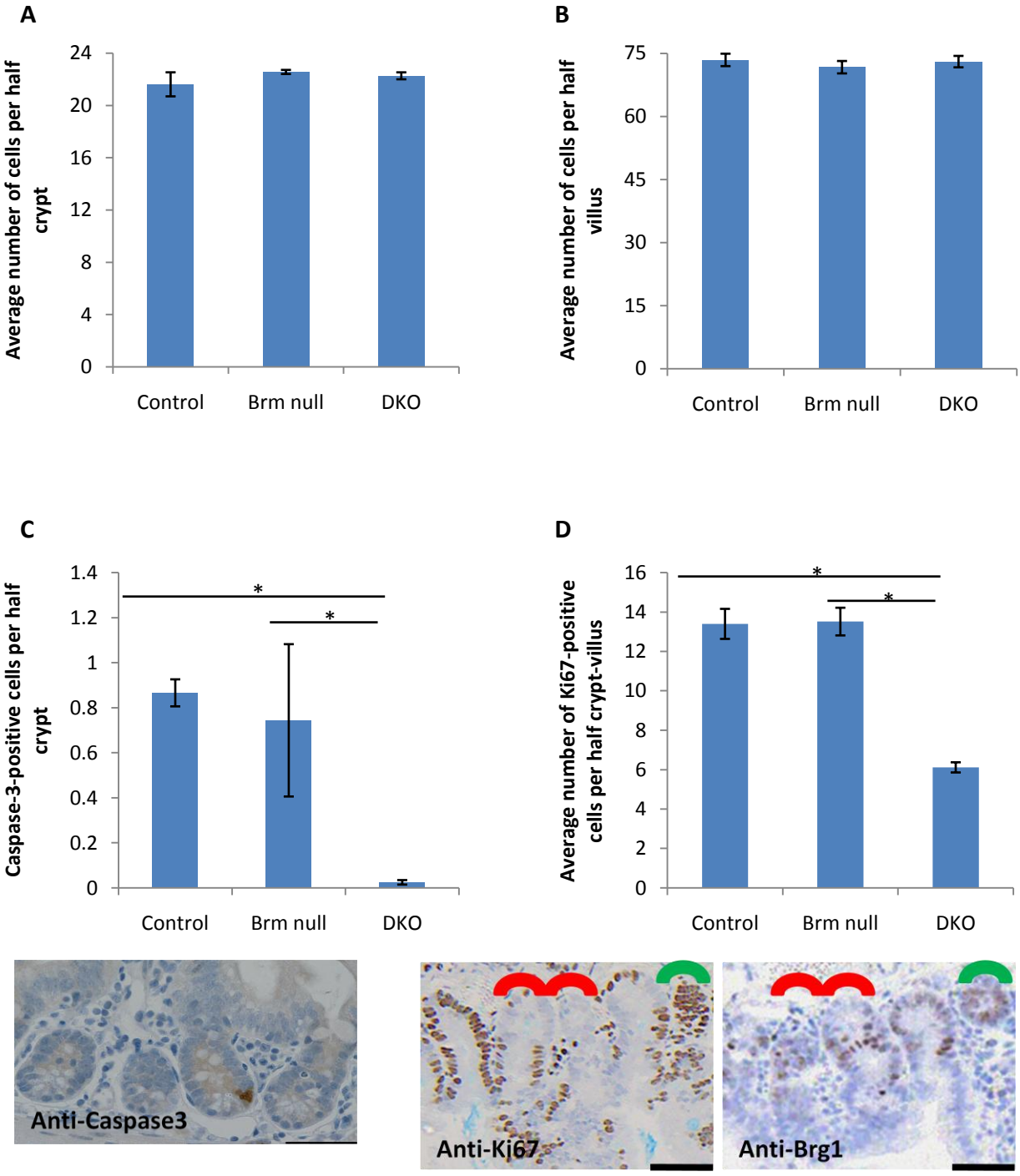

Figure 5.2 Histological analysis of the effects of mosaic Brg1loss in the small intestinal epithelium of Brm null animals. Control, Brm null and DKO experimental animals were harvested at day 5 post induction. A-D bar graphs represent histological parameters such as (A) crypt length (B) villus length that were counted on H&E sections for all animals. The average number of (C) Cleaved Caspase 3 (D) Ki67-positive cells was quantified on the corresponding immunostained sections. Error bars represent standard deviation and asterisk symbol indicates those histological parameters that showed a statistically significant difference (p value<0.05) between cohorts of mice. Exact values, standard deviations, p values and numbers of animals included in the experiments are provided in Table 5.1. Scale bar represents 100 µm.

5.2.4 Mosaic loss of Brg1 changes the pattern of distribution of proliferating cells in the Brm null epithelium of small intestine

Further to the analysis of the size of the proliferating compartment of the small intestinal epithelium, the distribution of Ki67-positive cells was assessed in order to investigate whether the reduction in the numbers of proliferating cells led to changes in the shape of the proliferative compartment. The analysis of cumulative frequency of Ki67-positive cells revealed a significant expansion of the zone occupied by proliferating cells along the length of the intestinal crypt in the epithelium of DKO animals in comparison to control and Brm null (Kolmogorov-Smirnov Z test, p=0.015 and p=0.001 respectively, n≥4, Figure 5.3). This observation suggested that the distribution of Ki67-positive cells is altered and more irregular along the crypt-villus axis in the Brg1- and Brm-deficient small intestinal epithelium however it did not result in the reduction of proliferative compartment.

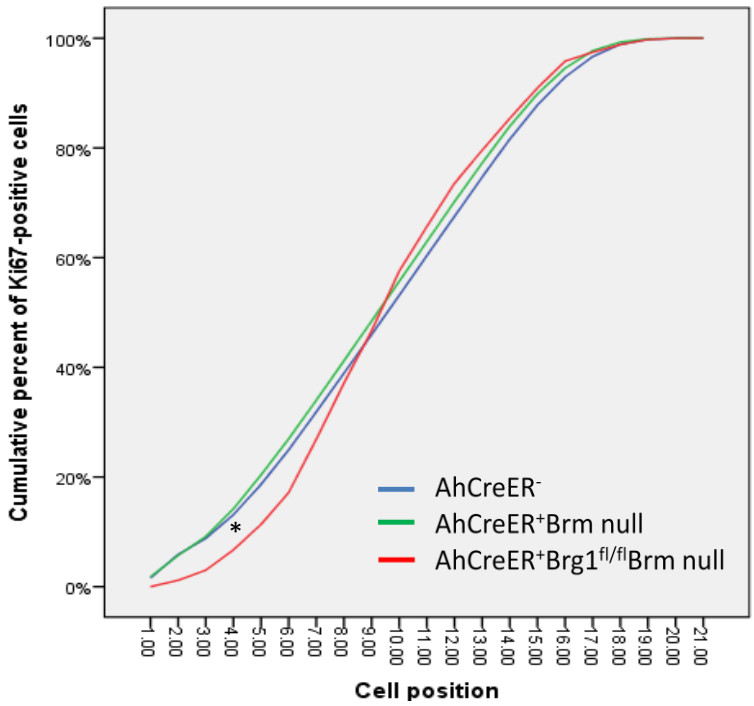

Figure 5.3 A change in shape of proliferative zone in the small intestinal epithelium of AhCreER^{+}Brg1$^{fl/fl}$Brm null animals. Tissues of control, Brm and DKO mice were harvested and immunohistochemical analysis of Ki67 staining was performed. Cumulative frequency analysis of Ki67-positive cells revealed significant change in the shape of proliferative compartment in the DKO epithelium in comparison to both control and Brm null (Kolmogorov-Smirnov Z test p=0.015 and p=0.001 respectively, n≥4) with an expansion at the base of the intestinal crypt.

5.2.5 Brg1-deficiency affects the differentiation of goblet cells in the small intestinal epithelium of AhCreER^{+}Brg1$^{fl/fl}$Brm null animals

As evidenced in the previous sections, Brg1 loss in the context of Brm null allele results in the depletion of the Ki67 proliferative compartment. In order to assess whether these changes in the proliferation affect the differentiation processes in the epithelium, the quantitative analysis of mature epithelial cell types found in the small intestinal epithelium was conducted in AhCreER^{+}Brg1$^{fl/fl}$Brm null mice at day 5 post induction and compared to the data from control and Brm null mice at day 70 of age (section 3.2.6) in order to further characterise the effects of Brm loss on the maintenance of small intestinal homeostasis. Brg1-deficient crypts have been identified by the presence of minimum 5 adjacent Brg1-deficient cells on the basis of Brg1 immunohistochemical staining conducted on the serial section of the epithelial tissue.

The only differentiated cells belonging to an absorptive lineage, enterocytes were assessed using alkaline phosphatase staining. The abundance in enterocytes is marked by brush border thickness and revealed a marked decrease in the intensity and thickness of the staining in the DKO animals compared to control and Brm null animals (Figure 5.4)

Secretory lineage goblet cells were identified using Alcian Blue staining. The performed staining allowed for quantification of the numbers of goblet cells in the small intestine of AhCreER^{+}Brg1$^{fl/fl}$Brm null animals (Figure 5.5). Scoring of the Alcian Blue-positive cells detected a significant decline in the number of goblet cells in the DKO animals per half crypt-villus in comparison to controls (4.830±0.158 versus 6.375±0.185, $p<0.0001$, $n\geq4$). Parallel pattern of decrease in the frequency of goblet cells in DKO epithelium was found when compared to Brm null epithelium (4.830±0.158 versus 7.402±0.304, $p<0.0001$, $n\geq4$ Figure 5.5a). The presence of enteroendocrine cells within small intestinal epithelium was assessed using Grimelius staining. The scoring of the enteroendocrine cells detected no difference in the number of Grimelius-positive cells in Brm null Brg1 KO animals in comparison to controls (2.052±0.172 versus 2.142±0.050 and 2.24±0.078, $p=0.375$ and $p=0.114$ respectively, $n\geq4$, Figure 5.5b).

The quantification of Paneth cells numbers as well as distribution was performed using lysozyme immunohistochemistry carried out on the appropriate sections of small intestinal epithelium (Figure 5.6). The quantification of the Paneth cells showed no difference in the number of cells present in the half-crypt between DKO and controls (1.767±0.103 versus

1.725±0.153, p=0.585, n≥4) or DKO and Brm null animals (1.767±0.103 versus 1.837±0.264, p=506, n≥4, Figure 5.6).

The quantification of differentiated cell types in the small intestinal epithelium of Brg1 and Brm deficient mice revealed that Brg1 loss in context of Brm null allele leads to severe depletion in brush border enterocytes and goblet cells. Together with depletion in the numbers of Ki-67-positive cells in the proliferative compartment, this shift in the differentiation suggests that concomitant loss of both catalytic subunits attenuated differentiation of specific mature cell types belonging to both absorptive and secretory lineage.

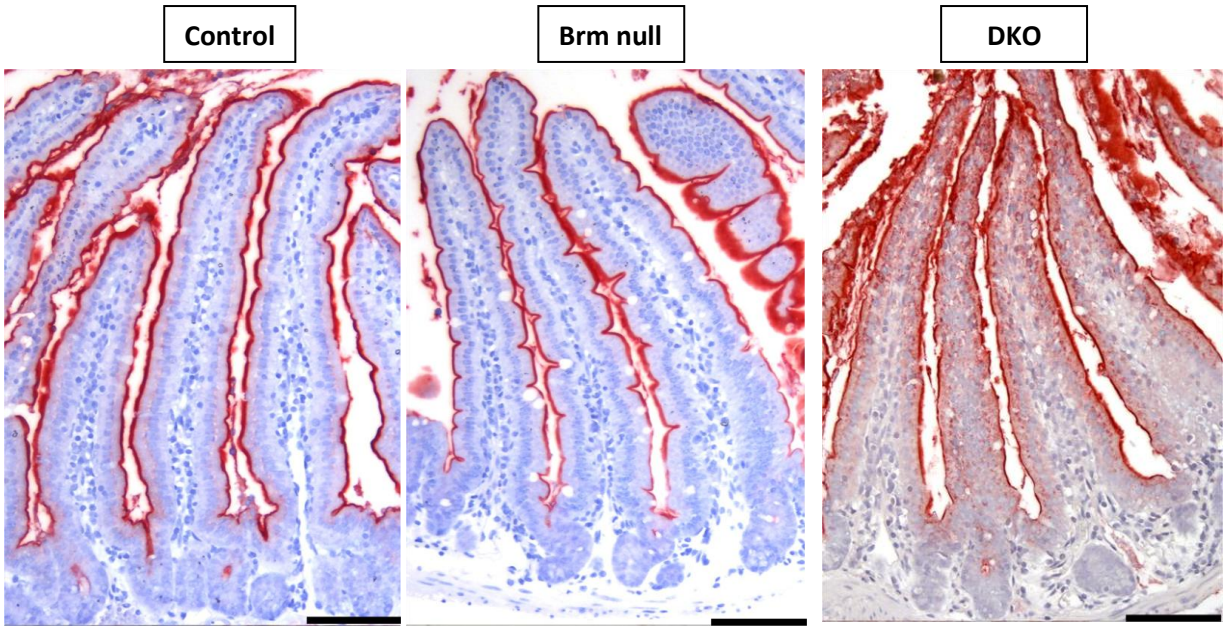

Figure 5.4 Alkaline phosphatase staining detected the normal brush border pattern corresponding to the membrane of differentiated enterocytes. The small intestinal sections of control, Brm null and DKO mice were stained for alkaline phosphatase. Brush border staining revealed a decline in the alkaline phosphatase expression in the epithelium of Brm null Brg1KO animals when compared to sections of control and Brm experimental animals. However in case of DKO animals, alkaline phosphatase staining appears to be present in the epithelial cells as well as on their surface. The scale bar represents 100µm.

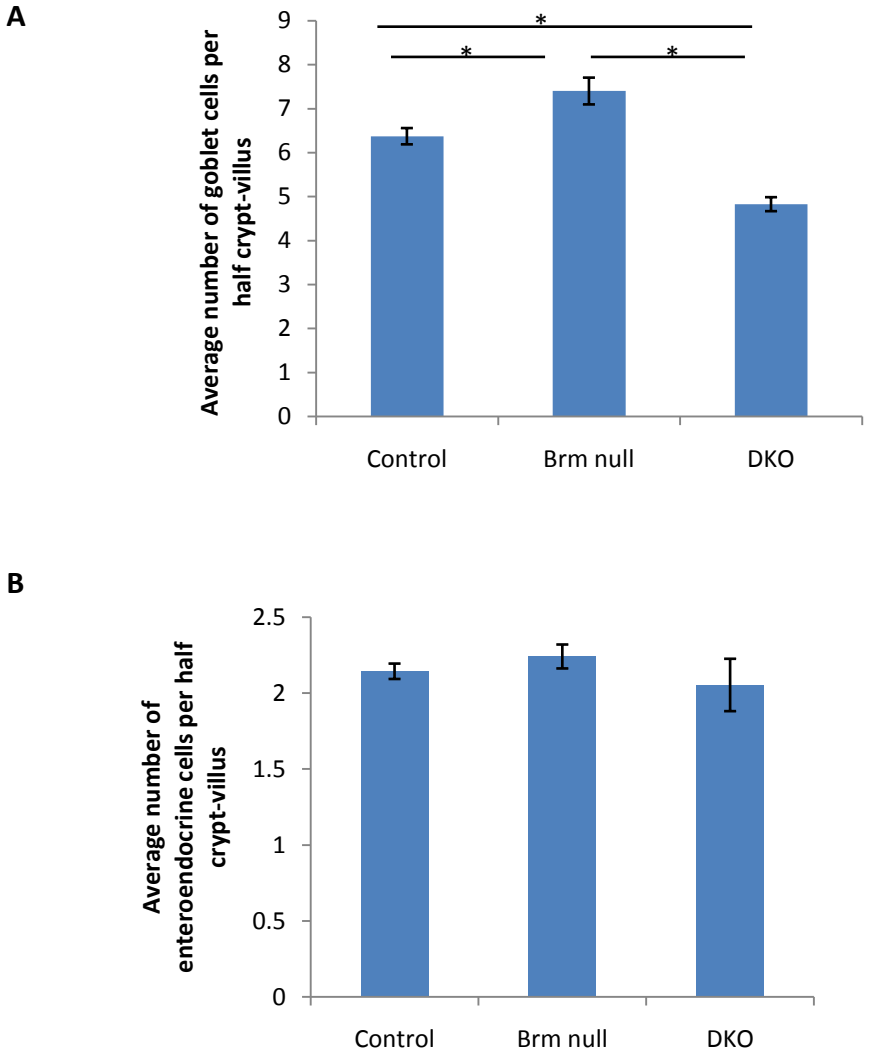

Figure 5.5 Cell-specific stains were performed for identification of cells of secretory lineage. Alcian Blue staining was used in order to detect goblet cells whereas Grimelius staining was carried out to visualize enteroendocrine cells within small intestinal epithelium. The small intestinal sections of control, Brm null and DKO mice were stained and the populations of mature cells were quantified. (A) Analysis of small intestinal tissue for Alcian Blue-stained cells revealed a significant decline in the goblet cells in the epithelium of DKO animals in comparison to control and Brm animals. (B) In contrast, the assessment of enteroendocrine cells revealed no change in the number of stained cells between the epithelium of DKO and control or Brm null animals.

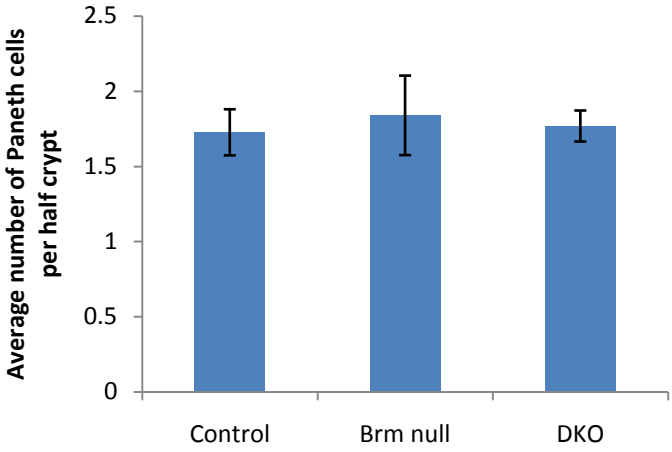

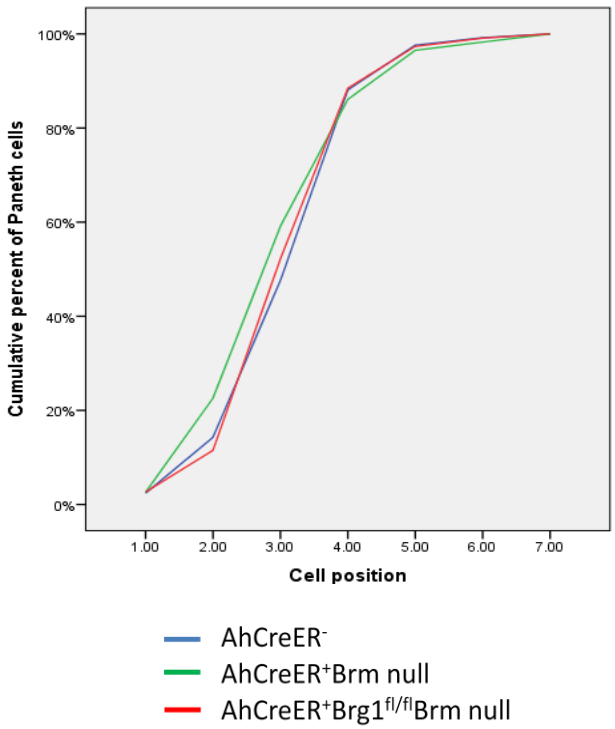

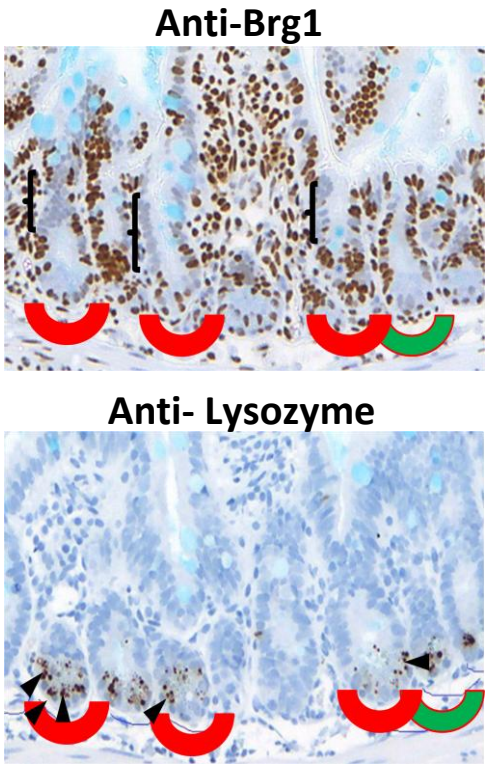

Figure 5.6 Immunohistochemistry against lysozyme was performed to mark Paneth cells within small intestinal epithelium. The small intestinal sections of control, Brm null and DKO mice were stained to reveal the number and localisation of Paneth cells. The red semi-circle marks Brg1-deficient crypts with more than 5 adjacent Brg1 deficient cells whereas green semi-circle marks a Brg1-proficient crypt. The analysis of both number and position of lysozyme-positive cells in the small intestinal epithelium showed no differences in DKO mice when compared to control and Brm animals. The scale bar represents 100µm.

5.2.6 Mosaic loss of Brg1 in Brm-deficient colonic epithelium of AhCreER^{+}Brg1$^{fl/fl}$Brm null animals is characterized by a long-term retention of Brg1–negative clusters of epithelial cells

As previously described for small intestine, furthermore I aimed to analyse the consequences of Brg1-deficiency in the context of Brm null allele on the colonic epithelium. Parallel to the experiment conducted in the small intestinal tissue, mosaic pattern of Brg1 loss was observed in Brm- and Brg1-deficient colonic epithelium under control of AhCreER recombinase.

Cohorts of AhCreER^{-} (control), AhCreER^{+}Brg$^{fl/fl}$Brm$^{+/+}$ and AhCreER^{+}Brg1$^{fl/fl}$Brm null animals at 70 days of age were induced with five bi-daily daily intraperitoneal injections of 80mg/kg β-naphthoflavone with Tamoxifen at 12 hour intervals (n≥28 for all cohorts). Colonic tissues were harvested from induced animals that have been aged until particular experimental time-points (n≥4) with no lethality observed during the timeframe of the experiment.

Identification and subsequent quantification of Brg1-deficient colonic crypts in the AhCreER^{+}Brg$^{fl/fl}$Brm$^{+/+}$ and AhCreER^{+}Brg1$^{fl/fl}$Brm null epithelium was carried out using immunohistochemical staining against Brg1. Similar to small intestinal pattern of mosaic loss of Brg1 across the colonic tissue was observed however in contrast to small intestine characterized by small clusters of Brg1-deficient cells, colonic crypts frequently were completely devoid of Brg1 expression.

Further quantification of the colonic crypts consisting of Brg1-deficient cell at all time-points showed a steady decline in the frequency of such a crypts in the epithelium of DKO in the first 7 days post induction followed by a two-fold decrease observed at day 10 and the maintenance of the proportion of Brg1-deficient to Brg1-proficient crypts till the end of experimental timescale. However in the context of functional Brm, the initial proportion of Brg1-deficient crypts in the colonic epithelium was significantly lower in Brg1 KO than in DKO animals. The elimination of Brg1-deficient colonic crypts occurred at much slower rate in Brg1 KO epithelium with less fluctuation in the frequency of Brg1-deficient crypt and from day 10 post induction between 10-15% of all colonic crypts retained Brg1-deficient clusters of cells (Figure 5.7).

Although the frequency of Brg1-deficient cell clusters in the colonic epithelium of both DKO and Brg1 KO animals display a trend of decrease, in contrast to small intestine those cells are retained within the epithelium for a long-term (Figure 5.7). Interestingly, whereas in small

intestine of DKO animals the proportion of Brg1-deficient crypts on day 3 post induction is significantly lower than in Brg1 KO, in the colonic epithelium this situation is inversed.

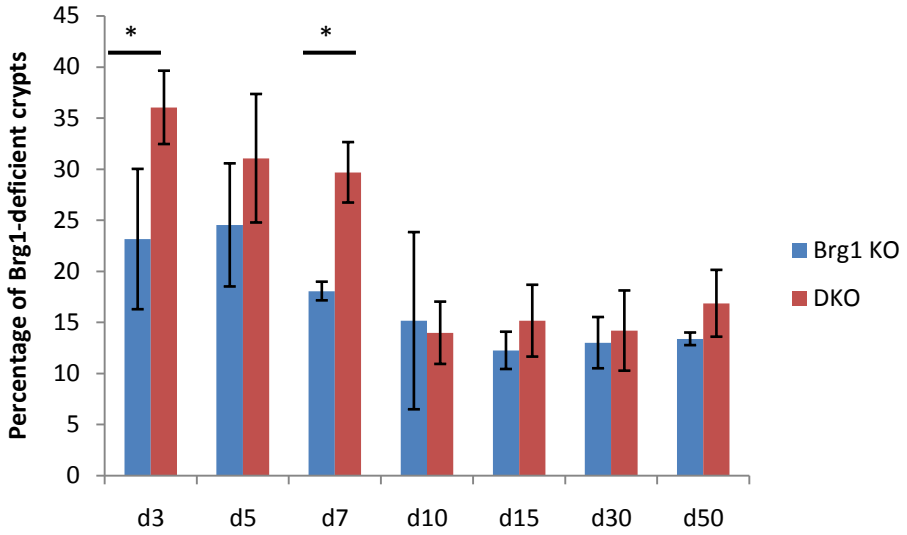

Figure 5.7 Mosaic loss of Brg1 under the expression of AhCreER recombinase is maintained within the colonic epithelium. AhCreER^{+}Brg1$^{fl/fl}$ and AhCreER^{+}Brg1$^{fl/fl}$Brm null animals were induced according to an appropriate protocol and tissues were harvested at day 3, 5, 7, 10, 15, 30 and 50 post induction in a same manner as in small intestine. Immunohistochemical analysis of Brg1 expression conducted on the colonic epithelium in both experimental cohorts of animals was used to score the number of crypts containing more than 6 Brg1-deficient cells relative to the total number of colonic crypts. The quantification of Brg1 expression revealed a trend of decrease in the frequency of Brg1-deficient crypts in both cohorts concomitant with the long-term retention of Brg1-deficient crypts in both epithelia.

5.2.7 Brg1 loss in the context of Brm null allele leads to severe decrease in apoptosis levels and an expansion of proliferative zone in colonic epithelium

As described in the previous chapter (section 3.2.11) homeostasis of colonic epithelium in the context of Brm loss appears to be well-maintained with no perceptible differences from normal Brm-proficient epithelium. I aimed to investigate the effects of combined loss of Brm and Brg1 on the morphology of colonic epithelium. The deficiency in the functional catalytic subunits of SWI/SNF chromatin remodelling complex failed to results in macroscopic abnormalities or tumorigenesis in the cohort of DKO animals. Quantitative analysis of histological parameters revealed significant changes in the level of apoptosis and when compared to control and Brm null mice. The effects of mosaic loss of Brg1 in the context of constitutive Brm deficiency on the large intestinal epithelium were investigated in AhCreER^{+}Brg1$^{fl/fl}$Brm null (DKO), AhCreER^{+}Brm null (Brm null) and AhCreER^{-} (control) animals at day 5 post induction. A quantitative analysis carried out is summarized in Table 5.2.

The length of colonic crypt was assessed on H&E stained sections as the average number of cells (± standard deviation) from the bottom of the crypt upwards till the flat surface of the epithelium. No change in the crypt size of DKO mice was observed when compared to control and Brm null colonic epithelium (24.64±0.311 versus 24.309±0.319 and 24.497±0.431, $p>0.05$ for either comparison, $n\geq4$, Figure 5.8a).

The levels of apoptosis within the colonic epithelium were quantified using Cleaved Caspase-3 immunohistochemical staining. The assessment of stained cells showed a significant decrease in the number of apoptotic cells in the epithelium of AhCreER^{+}Brg1$^{fl/fl}$Brm null in comparison to both control and Brm null mice (0.005±0.01 versus 0.060±0.016 and 0.064±0.022, $p=0.002$ for either comparison, $n\geq4$, Figure 5.8b). However, the analysis of proliferating cells on colonic epithelium by Ki67 immunohistochemistry detected no difference between the average number of proliferating cells per crypt in DKO and control and Brm-deficient cohort (5.48±1.077 versus 6.609±1.039 and 7.921±2.547, $p=0.182$ and $p=0.104$ respectively, $n\geq4$, Figure 5.8c) similarly to the quantification of apoptosis by Cleaved Caspase-3. In contrast to the quantification of proliferating cell population in the colonic epithelium which revealed no alterations, the analysis of the cumulative frequency of Ki67-positive cells detected a significant shift in the shape of proliferating zone in DKO animals. Proliferative compartment marked by Ki67 distribution revealed a great expansion

in AhCreER^{+}Brg1$^{fl/fl}$Brm null epithelium in comparison to both control and Brm null tissue (Kolmogorov-Smirnov Z test p=0.0001 for either comparison, n≥4, Figure 5.8d). This result is parallel to the small intestinal analysis indicating that the distribution of proliferating cells and therefore the shape of proliferative compartment in the DKO mice is affected by Brm loss.

Taken together, Brg1 loss in the context of Brm deficiency within the colonic epithelium affects several histological parameters leading to a severe depletion in the number of apoptotic cells concurring with an expansion in shape of proliferative compartment. Strikingly, no increase in the total number of Ki67-labelled proliferating cells was noted in parallel to the change in the shape of proliferative compartment. No gross morphological abnormalities or tumorigenesis were observed in the colonic tissue of AhCreER^{+}Brg1$^{fl/fl}$Brm null suggesting that in a short-term the homeostasis in the large intestinal epithelium is maintained even in the absence of both ATPase subunits of SWI/SNF chromatin remodelling complex.

Parameter	Cohort	Mean	SD	p-values	
				Control vs DKO	Brm null vs DKO
Crypt length	Control	24.309	0.319	0.428	0.581
	Brm null	24.497	0.431		
	DKO	24.670	0.311		
Caspase positive cells	Control	0.060	0.016	0.001	0.001
	Brm null	0.064	0.021		
	DKO	0.005	0.010		
Ki67 positive cells	Control	6.609	1.039	0.182	0.104
	Brm null	7.921	2.547		
	DKO	5.480	1.077		

Table 5.2 Quantitative analysis of the effects of Brg1 deficiency on the histology of Brm null colonic epithelium. Epithelium from large intestine from AhCreER^{-}Brm$^{+/+}$ (marked as control), AhCreER^{+}Brm null (marked as Brm null) and AhCreER^{+}Brg1$^{fl/fl}$Brm null (marked as DKO) was harvested from animals and histological parameters including crypt length, apoptosis and proliferation were quantified and the comparison between those experimental cohorts was conducted using statistical software.

A

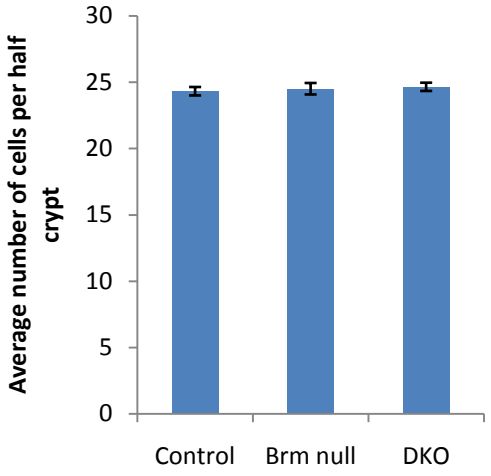
Average number of cells per half crypt
30
25
20
15
10
5
0
Control
Brm null
DKO

B

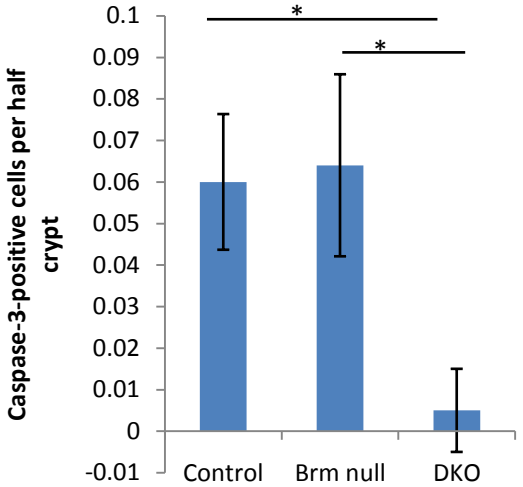
Caspase-3-positive cells per half crypt
0.1
0.09
0.08
0.07
0.06
0.05
0.04
0.03
0.02
0.01
0
-0.01
*
*
Control
Brm null
DKO

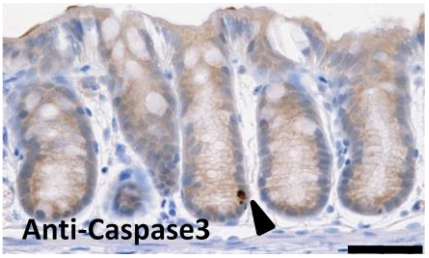
Anti-Caspase3

C

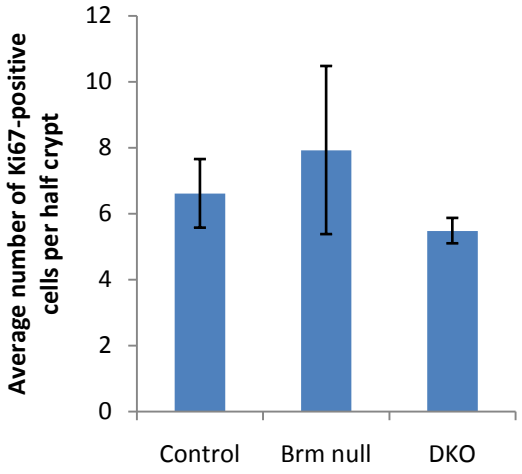
Average number of Ki67-positive cells per half crypt
12
10
8
6
4
2
0
Control
Brm null
DKO

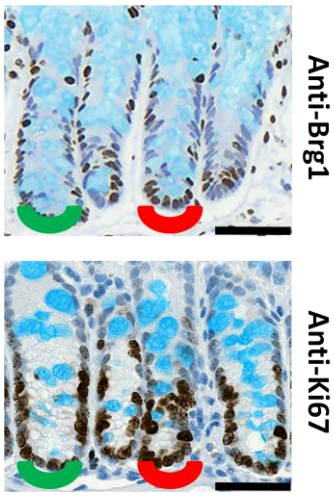
Anti-Brg1
Anti-Ki67

D

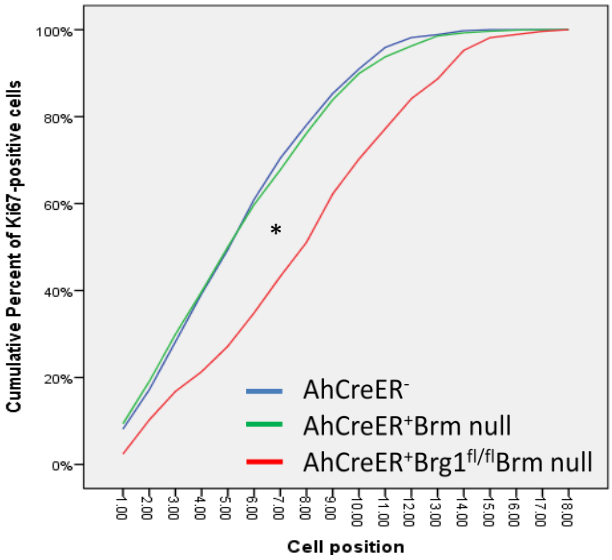

Figure 5.8 Histological analysis of the effects of induced mosaic Brg1 loss in the Brm null colonic epithelium. AhCreER^{+}Brg1$^{fl/fl}$Brm null animals were harvested at day 5 post induction whereas Brm null and control animals were dissected at day 70 of age. A-D histological parameters of (A) crypt length were counted on H&E sections for control and Brm deficient animals. The average number of (B) Cleaved Caspase3 and (C) Ki67-positive cells was scored on the appropriately stained sections. (D) Cumulative frequency analysis detected a significant expansion of the proliferative compartment in DKO animals in comparison to Brm null and control animals. The green half-circle indicates colonic crypts Brg1 proficient crypts whereas red half-circle indicates Brg1-deficient crypts with 5 or more adjacent Brg1-deficient epithelial cells. The black arrow indicates cell positive for Cleaved Caspase 3 staining. Error bars represent standard deviation and asterisk symbol indicates those histological parameters that showed a statistically significant difference (p value <0.05) between cohorts of mice. Exact values, standard deviations, p values and numbers of animals included in the experiments are provided in Table 5.2

5.2.8 Brg1 deficiency in the context of concomitant Brm loss results in a decrease in the differentiation of epithelial cells along the secretory lineage

Although homeostasis in the colonic epithelium in the context of Brm and Brg1 loss appears to be maintained in a short-term, the fluctuations in the numbers of apoptotic and actively proliferating cells might affect the differentiation potential within the epithelium. Therefore I aimed to quantify the size of mature epithelial cell populations in the colonic epithelium of AhCreER^{+}Brg1$^{fl/fl}$Brm null at day 5 post induction and compared it to both Brm null and control cohorts.

Alcian Blue staining was carried out to identify the most abundant cell type of colonic epithelium goblet cells. The scoring of the numbers of those secretory lineage cells revealed a severe depletion in DKO animals in comparison to Brm null and control animals (5.495±0.041 versus 7.630±0.405 and 6.50±0.071, $p<0.0001$ for either comparison, $n\geq4$, Figure 5.9a).

The presence of enteroendocrine cells in the epithelium was confirmed using grimelius staining. The quantification of enteroendocrine cells per half colonic crypt detected a marked decrease in the population of those cells in the epithelium of DKO mice compared to control and Brm-deficient cohorts (0.865±0.055 versus 1.61±0.052 and 1.47±0.066, $p<0.0001$, $n\geq4$, Figure 5.9b).

To summarize, the quantification of the predominant differentiated cell types of the colonic epithelium revealed a marked depletion in both goblet and enteroendocrine cells of secretory lineage suggesting a shift in the differentiation pattern in the Brm- and Brg1-deficient large intestine.

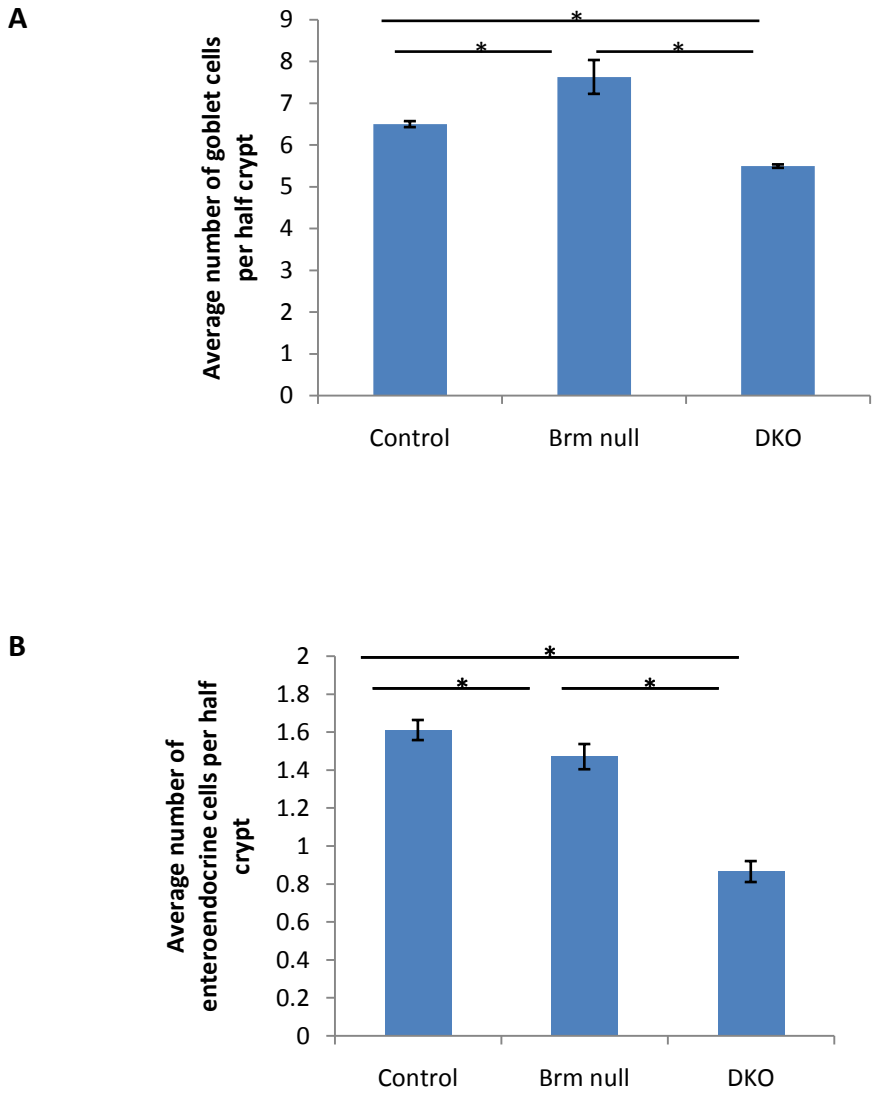

Figure 5.9 Brg1 loss in the context of Brm null epithelium leads to significant reduction in the goblet and enteroendocrine cells of large intestine. The colonic sections of control, Brm null and DKO mice were stained and the populations of mature cells were quantified. (A) Analysis of goblet cells stained with Alcian Blue showed a significant decline in the goblet cells in the epithelium of DKO animals in comparison to control and Brm animals. (B) Similarly, the quantification of the frequency of enteroendocrine cells detected a significant change in the number of grimelius-stained cells between the epithelium of DKO and control or Brm null animals.

5.2.9 Concomitant deficiency in Brm and Brg1 under the expression of AhCreER in the context of Apc loss results in the abrogation of intestinal architecture

As described in the previous sections of this chapter, the effects of mosaic Brg1 loss in the context of both small intestinal and colonic epithelium were investigated in order to assess whether the magnitude of the effects observed in the intestinal epithelia of Brm null allele is due to the modification of phenotype by Brm itself or other parallel mechanisms such as upregulation of Brg1 expression. Concomitant loss of both ATPase subunits of SWI/SNF chromatin remodelling complex is a frequent event in many types of human cancer and furthermore both cell line and murine studies indicated that the compensatory mechanism between Brm and Brg1 is tissue-specific and limited to only some particular transcriptional regulatory functions. Therefore I aimed to explore the effects of induced loss of Brg1 and constitutive loss of Brm in the context of Wnt activation. This was achieved by exploiting Cre loxP-mediated conditional knock-out of Brg1 and Apc alleles in the intestinal epithelium.

In order to investigate the long-term effects of concomitant loss of Brm and Brg1 in the context of Wnt signalling activation and tumorigenesis, the cohorts of AhCreER^{+}Apc$^{fl/fl}$Brg1$^{fl/fl}$Brm$^{+/+}$ (named as ApcBrg1KO) and AhCreER^{+}Apc$^{fl/fl}$Brg1$^{fl/fl}$Brm null (named as TripleKO) animals at 70 days of age were induced with five bi-daily intraperitoneal injections of 80mg/kg β-naphthoflavone with Tamoxifen at 12 hour intervals along with AhCreER^{-} controls (n≥7). All animals were aged for maximum 100 days or until they have developed signs of ill health and had to be sacrificed and appropriate tissues were harvested. As observed previously in chapter 4, none of control animals became ill within the time course of the experiment. In contrast, some of AhCreER^{+}Apc$^{fl/fl}$Brg1$^{fl/fl}$Brm$^{+/+}$ and AhCreER^{+}Apc$^{fl/fl}$Brg1$^{fl/fl}$Brm null animals began displaying signs of ill health as early as 3 days post induction respectively. Whereas none of Triple KO animals survived past day 12 post induction, many AhCreER^{+}Apc$^{fl/fl}$Brg1$^{fl/fl}$Brm$^{+/+}$ mice survived longer with few until 100 days post induction and were sacrificed at the experimental end-point. The analysis of the overall survival probability revealed no significant difference between the AhCreER^{+}Apc$^{fl/fl}$Brg1$^{fl/fl}$Brm null, AhCreER^{+}Apc$^{fl/fl}$Brm null and AhCreER^{+}Apc$^{fl/fl}$ cohorts (median survival for TripleKO=9 days, Figure 5.10, Log-Rank test p=0.127). In contrast a significantly longer survival observed in AhCreER^{+}Apc$^{fl/fl}$Brg1$^{fl/fl}$Brm$^{+/+}$ in comparison to AhCreER^{+}Apc$^{fl/fl}$ (Figure 5.10, Log-Rank test p=0.001) and trends of increase in survival

when compared to AhCreER^{+}Apc$^{fl/fl}$Brg1$^{fl/fl}$Brm null animals (Figure 5.10, Log-Rank test p=0.064) and AhCreER^{+}Apc$^{fl/fl}$Brm null (Figure 5.10, Log-Rank test p=0.072).

The morphological examination of TKO intestinal tissue as day 8-10 post induction revealed no macroscopic tumours in either small intestinal or colonic epithelium. Further histological analysis of small intestine showed a high degree of intestinal dysplasia (Figure 5.11). Wnt-activation-driven changes in the architecture of small intestinal epithelium were severe and distinguishing between crypt and villus region was not possible for the vast majority of the tissue. These observations resulted in the subsequent failure to conduct detailed analysis of histological parameters and cell populations. In parallel, the analysis of the frequency of Brg1-deficient crypts in Wnt-activated epithelium was impossible.

In contrast to small intestine, the morphology of colonic tissue was less dysplastic enabling the quantification of Brg1-deficient crypts in the colonic epithelium of AhCreER^{+}Apc$^{fl/fl}$Brg1$^{fl/fl}$Brm$^{+/+}$ and AhCreER^{+}Apc$^{fl/fl}$Brg1$^{fl/fl}$Brm null mice at days 8-10 post induction. The comparison between two cohorts revealed a significant decline in the number of Brg1-deficient colonic crypts in the epithelium of AhCreER^{+}Apc$^{fl/fl}$Brg1$^{fl/fl}$Brm null animals compared to AhCreER^{+}Apc$^{fl/fl}$Brg1$^{fl/fl}$Brm$^{+/+}$ (24.346±10.204 versus 41.605±4.845, p=0.018, n≥4, Figure 5.12). This result suggested that in the context of Wnt activation mediated by β-catenin, much lower levels of Brg1-deficiency are tolerated in the Brm null in contrast to Brm-proficient epithelium.

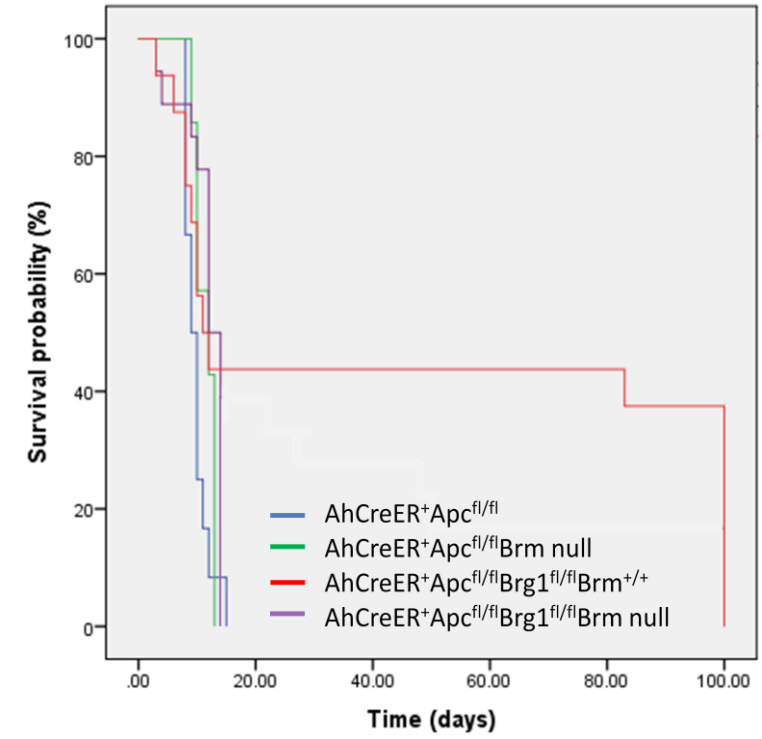

Genotype	ApcKO	ApcBrm KO	ApcBrg1KO	TripleKO
APC KO	**-**	**0.144**	**0.001**	**0.127**
APC BRM	**0.144**	**-**	**0.072**	**0.341**
APC BRG1	**0.001**	**0.072**	**-**	**0.064**
TRIPLE	**0.127**	**0.341**	**0.064**	**-**

Figure 5.10 Deficiency in both Brm and Brg1 does not alter the survival of animals with a homozygous inactivation of Apc. Cohorts of AhCreER^{+}Apc$^{fl/fl}$Brm$^{+/+}$, AhCreER^{+}Apc$^{fl/fl}$Brm null, AhCreER^{+}Apc$^{fl/fl}$Brg1$^{fl/fl}$ Brm$^{+/+}$ and AhCreER^{+}Apc$^{fl/fl}$Brg1$^{fl/fl}$Brm null were induced using an appropriate protocol along with AhCreER^{-} control mice (n≥7). Animals were aged for 100 days post induction or until they have developed signs of ill health. (A) Survival was presented as a Kaplan-Meier plot revealed no significant difference in the survival probability of TripleKO experimental mice in comparison to other Apc-deficient animals (Log-Rank test p values indicated in the table, n≥7 for either cohort).

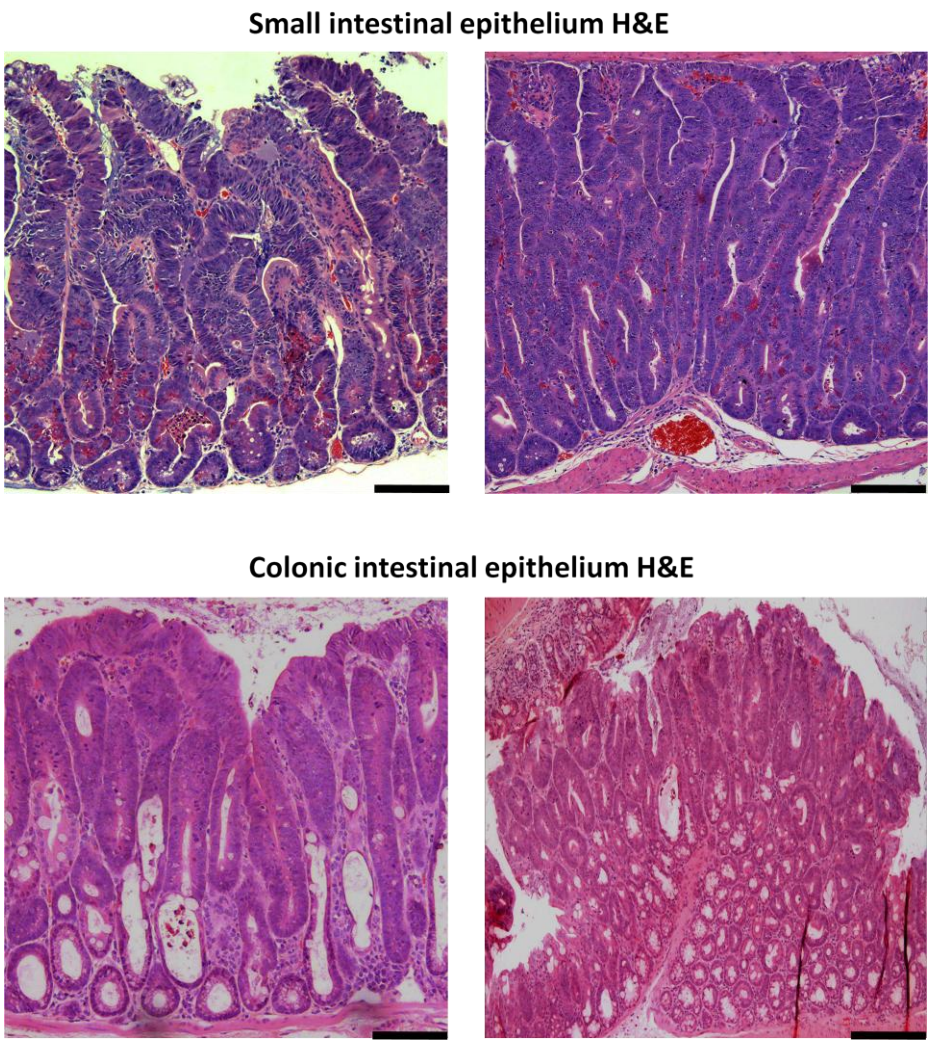

Figure 5.11 Microscopical analysis of H&E sections of small intestinal and colonic epithelium of AhCreER^{+}Apc$^{fl/fl}$Brg1$^{fl/fl}$Brm null animals reveals severe intestinal dysplasia across the tissue. The intestinal epithelium from all animals within TKO cohort underwent a morphological analysis revealing enlarged crypts characteristic for Wnt-activated epithelium furthermore showing no tumours in either type of epithelium. The scale bar represents 100 µm.

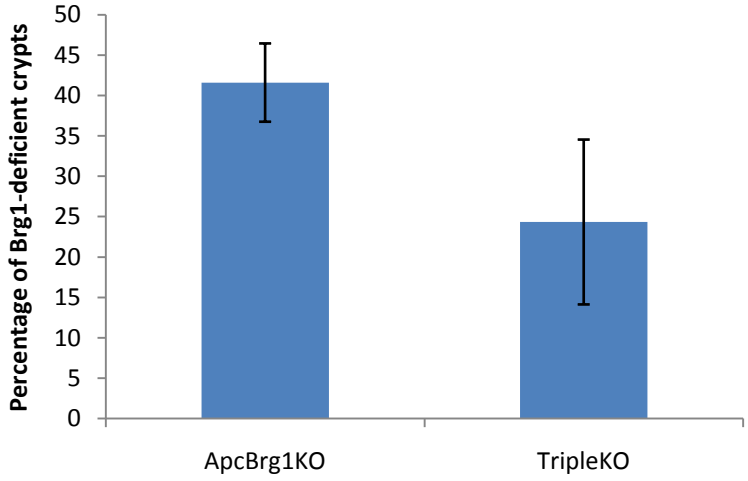

Figure 5.12 Deficiency in Brm and Brg1 ATPases is tolerated at much lower levels in the colonic epithelium of animals carrying a homozygous inactivation of Apc. Cohorts of AhCreER^{+}Apc$^{fl/fl}$Brg1$^{fl/fl}$Brm$^{+/+}$ and AhCreER^{+}Apc$^{fl/fl}$Brg1$^{fl/fl}$Brm null were induced using an appropriate protocol and tissues of intestinal tissue was harvested. The immunohistochemical analysis of Brg1 expression in the colonic epithelium revealed a significant difference in the number of Brg1-deficient crypts between TripleKO and ApcBrg1KO experimental mice (24.346±10.204 versus 41.605±4.845, n≥4, p=0.018).

5.2.10 Brg1 deficiency potentiates the effects of Brm loss on the transcriptional program of Wnt target genes in the context of Wnt activation

Previous reports suggested that Brg1 can act as a trans-activator of transcription of Wnt target genes in colorectal cancer (Baker 2001) indicating that mutations or inactivation of Brg1 would result in the alteration of the expression of Wnt genes. Therefore I aimed to explore whether the absence of both functional ATPase subunits leads to the failure of SWI/SNF complexes to remodel chromatin which subsequently alters the transcriptional program of epithelial cells of small and large intestine in the AhCreER^{+}Apc$^{fl/fl}$Brg1$^{fl/fl}$Brm null epithelium.

The cohorts of control, AhCreER^{+}Apc$^{fl/fl}$Brm null and AhCreER^{+}Apc$^{fl/fl}$Brg1$^{fl/fl}$Brm null animals were induced according to an appropriate protocol at 70 days of age and their intestinal tissues were harvested. mRNA was extracted and qRT-PCR analysis of the expression levels of *β-catenin*, *c-Myc*, *CD44* and *Cyclin D1* was conducted for small intestine and colon. A significant down-regulation of *CD44* and *Cyclin D1* in the small intestine of AhCreER^{+}Apc$^{fl/fl}$Brg1$^{fl/fl}$Brm null mice was detected in comparison to epithelium of both AhCreER^{+}Apc$^{fl/fl}$ and AhCreER^{+}Apc$^{fl/fl}$Brm null (for both comparisons $p<0.05$, $n\geq4$, Figure 5.13a) however no difference in the levels of c-Myc were detected between TripleKO and ApcBrmKO animals. Strikingly, in the colonic epithelium of AhCreER^{+}Apc$^{fl/fl}$Brg1$^{fl/fl}$Brm null a marked up-regulation of all Wnt target genes was detected (for all comparisons $p<0.05$, $n\geq4$, Figure 5.13b) when compared with the gene expression levels in AhCreER^{+}Apc$^{fl/fl}$ and AhCreER^{+}Apc$^{fl/fl}$Brm null colonic epithelium.

These results indicate that small intestinal and colonic epithelium deficient in both Brm and Brg1 response in an inverse manner to Wnt activation. More specifically it revealed that the effects of concomitant loss of both ATPases on the gene expression are not consistent with severe morphological changes observed in the epithelium of AhCreER^{+}Apc$^{fl/fl}$Brg1$^{fl/fl}$Brm null animals therefore indicating that the high level of dysplasia reported in the small intestinal epithelium is not due to transcriptional activation of Wnt target genes mediated by β-catenin.

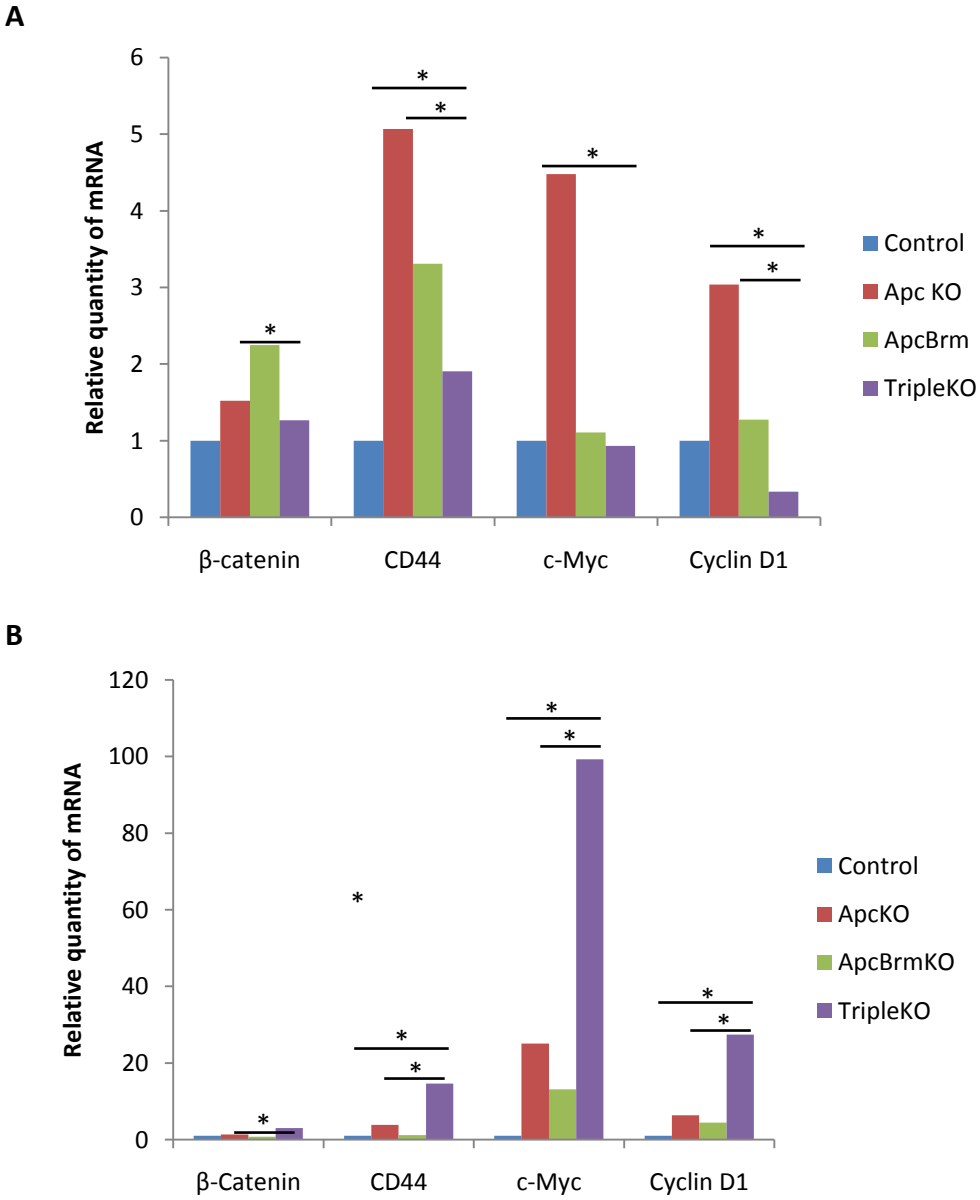

Figure 5.13 Brg1 deficiency suppresses the expression of the Wnt target genes in the small intestine with concurring upregulation of the same genes in the colonic epithelium of AhCreER^{+}Apc$^{fl/fl}$Brg1$^{fl/fl}$Brm null animals. The transcriptional levels of Wnt targets *CD44*, *c-Myc* and *Cyclin D1* genes were quantified by quantitative real-time-PCR (qRT-PCR) as shown in bar graph form. The data from qRT-PCR are normalised with *β-actin* and the asterisks indicate comparisons that were found to be significantly different ($p<0.05$, $n\geq4$). (A) Analysis of levels of *CD44*, *c-Myc* and *Cyclin D1* mRNA revealed a significant decline in expression of *CD44* and *Cyclin D1* genes in the small intestinal epithelium when compared to AhCreER^{+}Apc$^{fl/fl}$ and AhCreER^{+}Apc$^{fl/fl}$Brm null animals. (B) In contrast, colonic epithelium was characterized by a marked upregulation of *CD44*, *c-Myc* and *Cyclin D1* in AhCreER^{+}Apc$^{fl/fl}$Brg1$^{fl/fl}$Brm null mice in comparison to ApcKO and ApcBrmKO cohorts.

5.2.11 The upregulation of Brm in the Brg1-deficient neoplastic lesions of AhCreER^{+}Apc$^{fl/fl}$Brg1$^{fl/fl}$ colonic epithelium

In order to investigate whether Brm is capable of compensating for loss of Brg1 in the context of Apc deficiency, I aimed to explore the expression of Brm in the intestinal neoplasia Wnt-activated small intestinal and colonic epithelium. Intestinal tissue harvested at days 8-10 from AhCreER^{+}Apc$^{fl/fl}$Brg1$^{fl/fl}$Brm$^{+/+}$ and AhCreER^{+}Apc$^{fl/fl}$Brg1$^{fl/fl}$Brm null animals induced at 70 days of age with five bi-daily intraperitoneal injections of 80mg/kg β-naphthoflavone with Tamoxifen at 12 hour intervals was used to perform immunofluorescence for Brm and Brg1. Both small intestinal and colonic epithelium was examined for the presence of the neoplastic lesions characterized by neighbouring Brg1-deficient and Brg1-proficient crypts and the levels of Brm expression within those lesions were qualitatively analysed.

In the small intestine of AhCreER^{+}Apc$^{fl/fl}$Brg1$^{fl/fl}$Brm$^{+/+}$ animals, the analysis of the dysplastic areas of epithelium containing both Brg1-deficient and Brg1-proficient lesions revealed no perceptible changes in Brm expression. This observation suggested that Brm is not playing a compensatory role for Brg1 loss in the small intestinal epithelium (Figure 5.14).

In contrast to this data, the neoplastic areas of colonic epithelium revealed that Brg1-deficient lesions show higher levels of Brm expression in comparison to neighbouring Brg1-proficient lesions indicating that in the context of large intestinal mosaic loss of Brg1, Brm becomes upregulated and may possibly compensate for some of the functions of Brg1 specific for colonic tissue (Figure 5.14). The examination of TripleKO epithelium further confirmed that in the absence of Brm expression in AhCreER^{+}Apc$^{fl/fl}$Brg1$^{fl/fl}$Brm null epithelium this mechanism fails to compensate for Brg1 loss further modulating colonic phenotype of Apc-deficient animals.

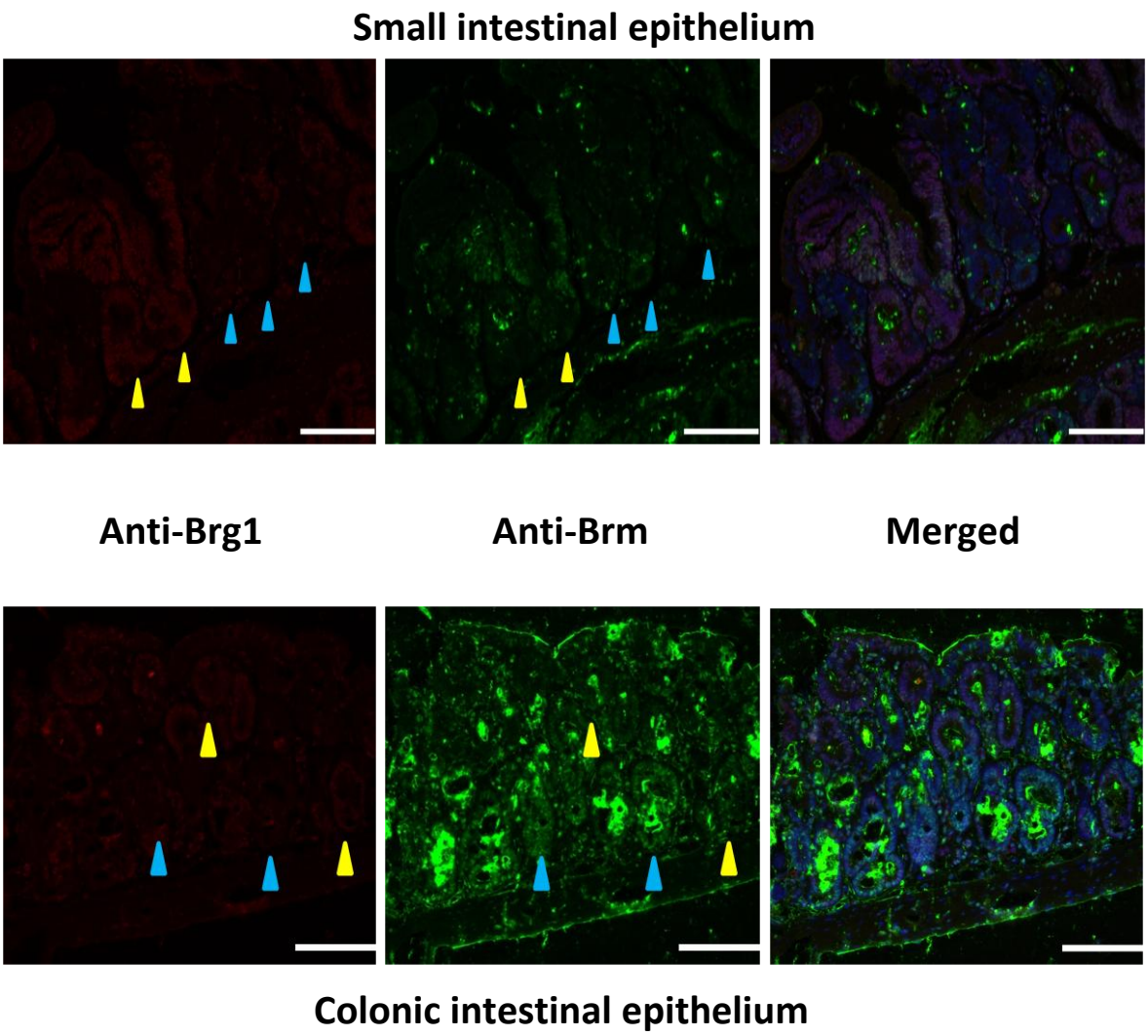

Figure 5.14 The upregulation of the expression of Brm in the colonic epithelium of AhCreER^{+}Apc$^{fl/fl}$Brg1$^{fl/fl}$ animals. Double immunofluorescence for Brm and Brg1 was conducted on the small intestinal and colonic tissue sections of AhCreER^{+}Apc$^{fl/fl}$Brg1$^{fl/fl}$ induced using an appropriate protocol. The immunohistochemical analysis of Brm expression in the neighbouring Brg1-proficient (yellow arrow) and Brg1-deficient (blue arrow) lesions in both types of the epithelium revealed higher expression levels of Brm in the Brg1-deficient lesions of colon. The comparison conducted in the small intestinal epithelium detected no changes in the Brm expression independent upon the Brg1 status. The scale bar represents 100 μm.

5.2.12 The expression levels of Brm and Brg1 in the small intestinal and colonic epithelium are context- and tissue-dependent

Taking into the account numerous reports indicating structural and biochemical similarities, redundancy in the function in murine models of human cancers and fluctuations in the expression in the human tumour tissue between Brm and Brg1, there have been several questions remaining through the course of experiments conducted within this thesis. Upregulated levels of Brm were found frequently in many Brg1-deficienct human cancer cell lines (Reyes *et al.* 1998, Bultman *et al.* 2000, Muchardt and Yaniv 2001, Strobeck *et al.* 2002) suggesting that Brm could compensate for the loss of its paralogue ATPase however in the absence of data from murine models of cancer or human neoplastic tissue, fluctuations in expression between Brm and Brg1 could not be appropriately assessed. Therefore I aimed to quantify the gene expression levels of both Brm and Brg1 in all experimental cohorts used in this thesis to explore the possibility of existence of compensatory mechanism between Brm and Brg1 in the intestinal epithelium as well as to further assess the impact of a deficiency in a single catalytic subunit on the SWI/SNF mediated chromatin remodelling. mRNA was extracted from small intestinal and colonic epithelium of AhCreER^{-}Brm$^{+/+}$ (control), AhCreER^{+}Brm null (Brm null), AhCreER^{+}Brg1$^{fl/fl}$ (Brg1KO), AhCreER^{+}Brg1$^{fl/fl}$Brm null (BrmBrg1KO), AhCreER^{+}Apc$^{fl/fl}$ (ApcKO), AhCreER^{+}Apc$^{fl/fl}$Brm null (ApcBrmKO), AhCreER^{+}Apc$^{fl/fl}$Brg1$^{fl/fl}$ (ApcBrg1KO) and AhCreER^{+}Apc$^{fl/fl}$Brg1$^{fl/fl}$Brm null (TripleKO) and qRT-PCR analysis using TaqMan probes for *Brg1* and *Brm* was conducted.

The analysis of *Brm* and *Brg1* expression in the colonic epithelium in the context of maintained homeostasis revealed 1.5 fold upregulation of Brg1 in the Brm null tissue, 10 fold increase in Brm in the mosaic Brg1KO and remarkably over a 50 fold increase in the gene expression levels of Brg1 in the AhCreER^{+}Brg1$^{fl/fl}$Brm null epithelium (Figure 5.15a). Surprisingly, in the small intestinal tissue no upregulation but diminished levels of Brg1 were detected in the Brm null epithelium. However consistent with observations in the colon, qRT-PCR analysis showed a marked increase in Brm levels in the epithelium of AhCreER^{+}Brg1$^{fl/fl}$ animals as well as 4 fold upregulation in Brg1 in the BrmBrg1KO cohort (Figure 5.15a).

Moreover the parallel gene expression analysis was conducted for both types of intestinal epithelium in the context of Wnt activation via deletion of Apc. Similar pattern of fluctuation in the expression of Brm and Brg1 were detected with a significant downregulation of Brg1 in the ApcBrmKO small intestinal and colonic epithelium. A marked 8 fold increase in Brm mRNA levels was found in the small intestine of AhCreER^{+}Apc$^{fl/fl}$Brg1$^{fl/fl}$ however in the

context of colon it was only equal to 2 fold increase (Figure 5.15b). Importantly in contrast to homeostatic tissues, a sharp decline in the levels of Brg1 was observed in both types of epithelium in the AhCreER^{+}Apc$^{fl/fl}$Brg1$^{fl/fl}$Brm null samples. Taken together these results suggest that the pattern of fluctuation between Brm and Brg1 levels is different in the context of normal or neoplastic epithelium with some perceptible changes in the magnitude of changes between small intestinal and colonic epithelium.

In summary, the analysis of *Brm* and *Brg1* gene expression in the context of both normal intestinal homeostasis and Wnt-driven tumorigenesis showed significant fluctuations of mRNA levels of either ATPase depending upon the status of its respective paralogue. These changes were observed in both small intestinal and colonic epithelium however the fold changes of a greater magnitude were observed in the homeostatic in contrast to Wnt-activated epithelium.

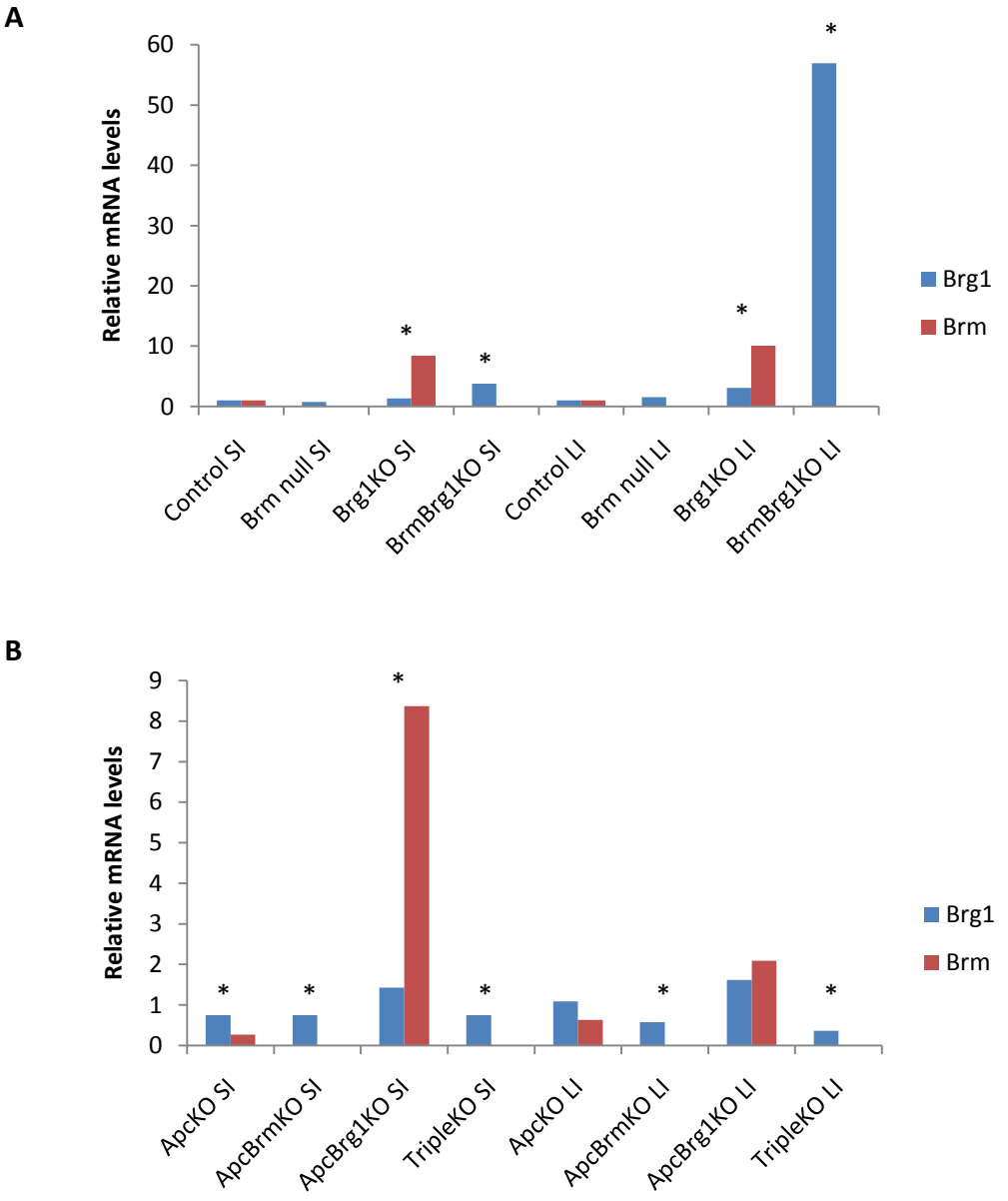

Figure 5.15 The fluctuations in the gene expression of Brm and Brg1 in the small intestinal and colonic epithelium in the context of normal homeostasis and Wnt-driven tumorigenesis. The transcriptional levels of Brm and Brg1 were quantified by quantitative real-time-PCR (qRT-PCR) as shown in bar graph form. The data from qRT-PCR are normalised with *β-actin* and the asterisks indicate comparisons that were found to be significantly different ($p<0.05$, $n\geq4$). Analysis of levels of Brg1 ATPase revealed a significant decline in expression in the small intestinal epithelium of Brm-deficient animals with a mild increase observed in the colon. In contrast, Brm was shown to be upregulated 10 fold in the intestinal epithelium of Brg1KO mice. In the context of Wnt-activation, Brg1 is characterized by significant downregulation in all Brm-deficient tissues whereas Brm transcription levels are maintained at very high levels in the Brg1-deficient epithelium.

5.3 Discussion

5.3.1 Loss of Brg1 under the expression of AhCreER recombinase leads to repopulation by wildtype Brg1-proficient cells in the context of Brm null epithelium of small intestine with concomitant retention of Brg1-deficient crypts in the colon

Previous reports by Holik (PhD Thesis, 2011) showed that Brg1 was characterized by a mosaic pattern of loss under control of AhCreER recombinase in the small intestinal and colonic epithelium. Further histological analysis of experimental time-points post induction showed that the number of crypts retaining Brg1-deficient cells gradually decreased resulting in the absence of crypts containing Brg1-deficient cells by day 35 post induction indicating that in the context of small intestine, the epithelium became repopulated with wildtype cells expressing Brg1. In contrast, the colonic epithelium could be distinguished by the long term retention of Brg1-deficient crypts as long as 490 days post induction.

I aimed to investigate further this pattern of Brg1 loss, repopulation of epithelial cells and the fate of Brg1-deficient crypts in the context of Brm null allele. Similar time-points to those set-out by Holik (2011) were analysed for the frequency of Brg1-deficient intestinal crypts detecting a parallel mechanism of elimination of Brg1-deficient cells and slow repopulation of epithelium by Brg1-proficient cells. By day 15 post induction less than 5% of all crypts in Brg1KO and DKO animals were Brg1-deficient. As quantitative analysis of $AhCreER^{+}Brg1^{fl/fl}$Brm null epithelium showed low levels of apoptosis in Brg1-deficient small intestinal crypts, the decrease in the frequency of Brg1-deficient crypts is unlikely to occur due to programmed cell death of Brg1-deficient cells. Although the rates of repopulation of small intestinal epithelium seem indistinguishable between Brg1KO and DKO animals, the initial frequency of Brg1-deficient crypts indicate that in the context of Brm allele, Brg1 is lost as significantly lower rate in Brm null rather than Brm-proficient animals and those crypts require a longer time to regain their Brg1-proficient status.

These results suggest that in the small intestinal epithelium there is a strong selection against the presence Brg1-deficient cells which further magnifies in the context of constitutive Brm loss. Considering the expression pattern of AhCreER recombinase, the mosaic loss of functional Brg1 specifically in stem cell and early progenitor cell populations could possibly be a driver of crypt repopulation as non-recombined stem and progenitor cells could rescue the small intestinal epithelium from the long-term consequences of Brg1 deficiency.

Concomitant deficiency in both ATPases within those crypts may however result in the extension of time required for turnover of epithelial cells and therefore complete elimination of Brg1-deficient crypts in the AhCreER^{+}Brg1$^{fl/fl}$Brm null epithelium.

In parallel, the analysis of the Brg1 expression in the colonic epithelium of AhCreER^{+}Brg1$^{fl/fl}$Brm null animals was conducted revealing a contrasting effects of a long-term retention of Brg1-deficient colonic crypts in both AhCreER^{+}Brg1$^{fl/fl}$Brm null and AhCreER^{+}Brg1$^{fl/fl}$Brm$^{+/+}$ animals. The frequency of Brg1-deficient colonic crypts remains at a steady rate of approximately 15% throughout all experimental time-points in both Brm-deficient and Brm-proficient epithelium.

In summary, Brm and Brg1 might both be dispensable for proliferation of the large intestinal epithelium and a long-term retention of crypts however in the context of small intestine, a reduction in the frequency of Brg1-deficient cells suggests that expression of functional Brg1 is important for the maintenance of intestinal architecture independently of its Brm status.

5.3.2 The repopulation of small intestinal epithelium is halted by reduced proliferation levels in AhCreER^{+}Brg1$^{fl/fl}$Brm null concomitant with the dysregulation of differentiation along the secretory lineage

In the absence of induced pan-epithelial loss of Brg1 similar to the constitutive loss of Brm in the intestinal epithelium, I aimed to conduct a quantitative characterization of small intestinal and colonic epithelium at day 5 post induction ensuring that over 30% of the crypts within epithelium are Brg1-deficient.

The morphological analysis of small and large intestine revealed no architectural abnormalities with crypts retaining their normal appearance in comparison to neighbouring Brg1-proficient counterparts. The intestinal crypt in both small intestine and colon represents a proliferative compartment of the epithelium which is regulated predominantly by Wnt signalling (reviewed in Pinto and Cleavers 2005). In the small intestine, the concomitant deficiency in Brm and Brg1 resulted in the significant decrease in the number of proliferating cells marked by Ki67 immunohistochemistry. Analysis of the distribution of Ki67-positive cells further revealed that this severely reduced pool of proliferating cells is localized predominantly towards the base of the crypt. In contrast, in the colonic epithelium the proliferation levels in DKO crypts are indifferent from those observed in Brm null and controls. Taken together, it can be extrapolated that the longer retention of Brg1-deficient crypts in the small intestinal epithelium is partially due to the significantly reduced levels of

proliferation in the DKO epithelium allowing for slower rate of repopulation by Brg1-proficient cells. The notion of diminished population of proliferating Ki67-positive cells in the homeostatic intestinal epithelium of AhCreER^{+}Brg1$^{fl/fl}$Brm null mice is not supported by experiments in human cancer cell lines and prostate cancer reporting that the deficiency in both Brm and Brg1 results in the abrogation of the ability of Rb to arrest cellular proliferation (Strobeck *et al.* 2002, Marshall *et al.* 2003, Shen *et al.* 2008). In this case the disparity between our observations and mentioned reports might be due to the context – homeostasis versus tumorigenesis - in which the tissue was found rather than tissue-specific alterations.

Previous reports indicated Notch and Wnt as the key signalling pathways regulating the differentiation of epithelial cells along the absorptive and secretory lineage. Brg1 has previously been proposed as a factor required for the trans-activation of Wnt target genes regulating a wide array of cellular processes such as apoptosis and proliferation (Baker 2001). In contrast, Brm has been shown to be preferentially recruited to the promoters of Hes1 and Hes5 Notch genes (Kadam and Emerson 2003) as well as to interact with ICD22 and CBF-1 Notch proteins (Kadam and Emerson 2003). The decline in the number of goblet cells accompanied by the decrease in brush border enterocytes in the DKO crypts of small intestine is contradictory to the increase in the size of goblet cells population in Brm null. However, a trend of decrease in the number of goblet cells was reported in the context of small intestinal Brg1 loss under the expression of *VillinCre* recombinase (Holik A, PhD thesis 2011). In parallel, colonic crypts of DKO are characterized by the depletion in the numbers of goblet and enteroendocrine cells which is again in contrast to observations by Holik (PhD thesis, 2011). In the light of those contrasting data and the results presented in chapter 3, Brm status is crucial for the differentiation of the epithelial cells along the secretory lineage in intestinal epithelium whereas the dynamics of the changes occurring in the AhCreER^{+}Brg1$^{fl/fl}$Brm null animals indicates that the concomitant deletion of Brm and Brg1 may possibly establish a unique phenotype different of those observed in the cases of loss of either particular ATPase.

5.3.3 Concomitant loss of both Brm and Brg1 does not exacerbate the phenotype of Wnt activation in the colonic epithelium

Whereas the effects of pan-epithelial deletion of Brg1 in the intestinal epithelium were previously reported by Holik *et al.* (2013, 2014) along with the consequences of constitutive loss of Brm described in the chapter 3, I aimed to characterize the effects of concomitant loss in Brm and Brg1 in the intestinal epithelium in the context of Wnt activation in order to further characterize the roles of both ATPase subunits in colorectal cancer.

Concomitant loss of both ATPases of SWI/SNF chromatin remodelling complex was reported to occur at a higher frequency than a deficiency in only one subunit in lung cancers whereas the situation is *vice versa* in gastric cancer (Reisman *et al.* 2003, Fukuoka *et al.* 2004, Yamamichi *et al.* 2007). Furthermore, the same non-small cell lung cancer study showed that deficiency in Brm and Brg1 is associated with a poor prognosis for the patients (Reisman *et al.* 2002) whereas another study in prostate cancer correlated reduction in the expression of Brm in particular as a marker for worse survival (Sun *et al.* 2007).

In order to investigate the effects of concomitant loss of Brm and Brg1 in the context of epithelium of intestine I initially conducted a morphological analysis of the intestinal epithelium of AhCreER^{+}Apc$^{fl/fl}$Brg1$^{fl/fl}$Brm null animals revealed a severe dysplasia in the small intestine whereas colonic tissue was less severely affected. The survival probability analysis revealed no significant differences in the lifespan between AhCreER^{+}Apc$^{fl/fl}$, AhCreER^{+}Brm null and AhCreER^{+}Apc$^{fl/fl}$Brg1$^{fl/fl}$Brm null mice however a trend of decrease in survival was observed comparing AhCreER^{+}Apc$^{fl/fl}$Brg1$^{fl/fl}$Brm null and AhCreER^{+}Apc$^{fl/fl}$Brg1$^{fl/fl}$ indicating that supplemental deficiency in Brm factor leads to reduced lifespan of animals. These data suggest that small intestinal epithelium is dependent upon the normal functioning of either of ATPases in a much higher degree than large intestine. The reduction in lifespan of animals carrying a deletion of Apc and Brg1 indicated that whereas Brm does not affect the Wnt-driven tumorigenesis mediated by Apc loss it might act in a tumour suppressor manner in the context of Wnt-activated intestinal epithelium deficient in its paralogue Brg1.

One of the hallmarks of colorectal tumorigenesis is the activation of β-catenin-mediated transcriptional program that occurs in the context of Wnt activation. Therefore I aimed to investigate whether a reduction in liferspan of AhCreER^{+}Apc$^{fl/fl}$Brg1$^{fl/fl}$Brm null mice in comparison to AhCreER^{+}Apc$^{fl/fl}$Brg1$^{fl/fl}$ animals is due to the modulation of Wnt signalling. The assessment of the expression levels of several Wnt target genes such as *c-Myc*, *CD44* and *Cyclin D1* was conducted using qRT-PCR revealing significant downregulation of *CD44* and *Cyclin D1* in the small intestine of AhCreER^{+}Apc$^{fl/fl}$Brg1$^{fl/fl}$Brm null animal. Interestingly the expression of *c-Myc* was not altered between AhCreER^{+}Apc$^{fl/fl}$Brm null, AhCreER^{+}Apc$^{fl/fl}$Brg1$^{fl/fl}$ and AhCreER^{+}Apc$^{fl/fl}$Brg1$^{fl/fl}$Brm null animals. In parallel, the expression analysis in the colonic epithelium showed similar but less severe reduction in the expression in Wnt target genes. The discrepancy between the Wnt signalling levels in small

and colonic epithelium might explain the differences in the degree of intestinal dysplasia observed in the either type of epithelium.

Taken together, in the context of Wnt activation it appears Brm is playing an auxiliary role to Brg1 in the modulation of lifespan and histological phenotype.

Chapter 6
General discussion

Colorectal cancer remains one of the most frequently diagnosed malignancies in the developed countries accounting for over13% of all new cancer cases annually. Although the survival rates have increased over the last two decades, colorectal cancer is still characterized by a high mortality rate, being the 2nd most common cause of cancer death. Dysregulation of Wnt signalling via Apc loss or stabilizing mutations in β-catenin is at the core of over 80% of all CRC cases. The current treatments of CRC involve surgical removal of the tumour mass combined with neoadjuvant and adjuvant care using chemotherapy or radiotherapy or both in some cases of rectal cancer. The concept of stratified medicine in cancer treatment culminated in the large-scale genetic profiling of colorectal tumours combined with extensive analyses of molecular events occurring during cancer initiation and progression. Importantly, numerous potential markers and therapeutic candidates have been identified throughout this process implicating both genetic and epigenetic changes that may play an important role in the modulation of many cancers including CRC.

The potential role of the SWI/SNF chromatin remodelling complex and more specifically its catalytic ATPases Brm and Brg1 as *bona fide* tumour suppressor genes in contributing towards tumorigenesis in a tissue-specific manner was suggested as a promising avenue for development of novel therapeutic strategies. Importantly, in contrast to many other tumour suppressor genes which are frequently mutated, Brm is rather silenced in the context of human solid tumours. The notion that the expression and therefore the function of Brm could possibly be restored provides some serious implications for clinical targeted therapy of tissues dependent on Brm functioning. Moreover numerous cell line studies have indicated that histone deacetylase acid (HDAC) inhibitors are capable of re-induction of Brm expression in Brm-deficient cell lines and this re-expression is sufficient for restoration of Rb-mediated growth inhibition and expression of Wnt target CD44 (Strobeck *et al.* 2002, Glaros *et al.* 2007, Kahali *et al.* 2013). As targeting of developmental pathways involved in tumorigenesis such as Hedgehog, Wnt and Notch pathways could be achieved at multiple levels within the signalling cascade like ligand expression or interactions between ligand and

receptor, modulation of the expression of downstream Wnt target genes like CD44 and β-catenin would be an interesting alternative to explore.

Furthermore in light of the fact that both Wnt and Notch signalling are implicated in intestinal homeostasis involving stem cell maintenance as well as in colorectal tumorigenesis, the interaction of the Brg1 catalytic subunit with β-catenin (Baker *et al.* 2001), together with exclusive interactions of Brm with CBF-1 and ICD-22 Notch pathway effectors (Kadam and Emerson 2003) all suggest that the ATPase subunits of the SWI/SNF chromatin remodelling complex might act as good potential therapeutic targets in CRC. One of the potential obstacles to this is the notion in regards to the high degree of homology (~75% amino acid sequence identity), between Brm and Brg1,which suggests they may be capable of compensating for each other in case of loss of either ATPase. This is not a common consensus as other sources in dicate tissue-specificity and gene-selectivity of interactions of Brm-containing and Brg1-containing complexes suggesting distinct roles for each catalytic subunit of SWI/SNF in regulating gene expression (Kadam and Emerson 2003, Marshall *et al.* 2003).

In the absence of data regarding a role of Brm in the intestinal tissue, the potential of ATPases of SWI/SNF chromatin remodelling complex to act as tumour suppressor genes, as well as potential clinical targets remained undetermined. Therefore, I aimed to investigate the effects of Brm deficiency in the normal intestinal epithelium in the context of homeostasis and further in the context of Wnt pathway activation via loss of Apc. Whereas the small intestine is recognized as a tissue that accurately recapitulates many aspects of human CRC tumorigenesis, due to some differences in the morphology of the epithelium and the fact that a primary site of human tumours is in the colonic epithelium, both small intestine and colon were investigated.

As described in this thesis, these notions have been explored leading to the following findings:

1) Brm is redundant for the maintenance of intestinal homeostasis in the context of functional Brg1 paralogue
2) In the context of Wnt activation, loss of Brm modulates Wnt-driven intestinal neoplasia by suppression of Wnt target genes and attenuation of the expansion of stem cells which concurs with expansion of the proliferative compartment

3) Differences in the mRNA levels of Brm and Brg1 were found between the intestinal and colonic epithelium and the severity of phenotypes observed appears to be dependent upon the status of both ATPases of SWI/SNF

Taken together, in this chapter I will discuss all of the above notions summarized in the Table 6.1.

	SMALL INTESTINE			COLONIC EPITHELIUM		
	Brm null	**BrmBrg1 KO**	**BrmApc KO**	**Brm null**	**BrmBrg1 KO**	**BrmApc KO**
Histology:						
Crypt length	↑	↔	↑	↔	↔	↔
Villus length	↓	↔	↔	N/A	N/A	N/A
Cell death:	↔	↓	↑	↔	↓	↑
Proliferation:						
Cell numbers	↔	↓	↔	↔	↔	↑
Cell distribution	changes	changes	changes	↔	changes	↔
Cell differentiation:						
Enterocytes	↔	↓	↓	N/A	N/A	N/A
Goblet cells	↑	↓	↑	↑	↓	↔
Enteroendocrine cells	↑	↔	↔	↓	↓	↔
Paneth cells	↔	↔	↔	N/A	N/A	N/A
Wnt pathway:		N/A		N/A	N/A	
At protein level	IHC βcat ↓		βcat ↔	IHC βcat ↔		
At mRNA level	βcat ↔ CD44 ↔		CD44 ↓ c-myc ↓ cyclinD1 ↓			βcat ↔ CD44 ↓ c-myc ↓
Notch pathway:		N/A		N/A	N/A	N/A
At protein level	Math1 ↑ HES5 loss ↓					
At mRNA level	Math1 ↑		HES1 ↓			
Stem cell niche:				N/A	N/A	N/A
Olfm4 in situ	↑		↓			
At mRNA level	No changes		Olfm4 ↓			
Brg1 expression:	↔	↑	↑	↔	↑	↑
Other notes:		Repopulation by Brg1 wildtype cells			Retention of Brg1 deficient cell	

<u>In the context of homeostasis:</u>

- Brm is redundant for the maintenance of SC zone
- Brm imposes restriction to the proliferative compartment expansion
- Brm together with Brg1 maintains the expression of CD44 Wnt target gene
- Brg1 might partially compensate for Brm function, in particular in colonic epithelium

<u>In the context of Wnt signalling activation:</u>

- Brm is redundant for the Wnt activation via Apc loss
- Brm regulates the expression of Wnt target genes via β-catenin-independent mechanism
- Brm regulates the expression of Olfm4 Wnt-independent SC marker
- Brg1 has antagonistic effects on the Wnt target gene expression in Wnt-activated small intestine and colon in the context of Brm loss

Table 6.1 The summary of histological analyses of all phenotypes involving Brm null allele in both small intestinal and colonic epithelium. Red arrow indicates statistically significant increase/upregulation, green arrow – statistically significant reduction/downregulation and purple arrow – the parameters that no difference/change. N/A refers to the parameters which have not been investigated or are small intestinal/colonic-specific. The impact of Brm on the homeostasis of small intestinal and colonic epithelium and tumour suppressing function of Brm and its requirement in the Wnt-activated epithelium is dependent upon the status of Brg1 paralogue in the respective tumours. The disparity in the results between small intestinal and colonic epithelium are associated with differential Wnt gradient and limiting capacities of Brg1 to compensate for Brm function.

6.1 The effects of Brm loss on the intestinal epithelium are dependent on the physiological levels of Wnt activity

The role of SWI/SNF chromatin remodelling complexes in facilitating the accessibility of DNA sequence is a fundamental requirement for transcription to occur and coincident with this notion, complexes associated with either of catalytic subunits Brm or Brg1 have been implicated in regulation of a plethora of cellular processes and signalling pathways involved in cell self-renewal, proliferation, differentiation and cell death (reviewed in Narlikar *et al.* 2002). While numerous in vivo studies on human cancer cell lines suggested that ATPases of the SWI/SNF complex share some common functions (Chiba 1994, Strober *et al.* 1996, Bourachot *et al.* 2003), the differential distribution in the preimplantation stages of mouse development between Brm and Brg1 (LeGouy 1998) together with experiments conducted in a model of osteoblast differentiation revealed that Brm and Brg1 might indeed function in an antagonistic manner and be associated with either repression or activation of particular promoters in the tissue-specific context (Flowers 2009). Furthermore the same reports suggest that Brm is frequently functionally redundant and therefore plays an auxiliary role in the regulation of gene expression, a notion consistent with the Brg1 null phenotype which is embryonic lethal (Bultman *et al.* 2000), and the Brm null phenotype which is characterized by animals that are viable and overtly no different to their wildtype littermates (Reyes *et al.* 1998). Although the role of Brm have been described in several reports investigating the effects of Brg1 loss, limited data exists on the role of Brm on the homeostasis or tumorigenesis of differentiated tissue types. The results presented in this thesis represent an extensive analysis of the effects of Brm deficiency in the context of homeostasis and Wnt-driven tumorigenesis in the murine small intestinal and colonic epithelium.

A comparison of the consequences of Brm and Brg1 loss in the small intestinal epithelium (Brg1 data presented by Holik A in the PhD thesis 2011) revealed a degree of specialization of Brm-containing complexes in performing particular function in tissue-dependent context. Analysis of the proliferation levels using Ki67 and BrdU markers showed no differences in the size of the population of proliferating cells measured by the number of positive cells across the crypt-villus axis, however the distribution of those cells revealed an expansion of the proliferating compartment in the epithelium of Brm null mice. This is in contrast to the data by Reyes (1998) indicating a 4 fold increase in the number of BrdU-positive cells in the livers of Brm null animals. However, this observed disparity in the results might be due to the morphological differences between those tissues where similar effects – pro-proliferative

capacities in Brm deficient context - are differentially expressed in the spatial setting of a particular tissue type – increase the number of proliferating cells in the liver in comparison to an expansion of the proliferating compartment in the small intestine. In the context of concomitant loss of both Brm and Brg1 driven by the expression of the AhCreER recombinase transgene, a marked decline in the number of proliferating cells was detected coinciding with changes in the distribution of Ki67-positive cells indicating that whereas Brm does not appear to display pro-proliferative effects in a form of alterations to cell numbers such as those observed in case of pan-epithelial loss of Brg1 (Holik PhD thesis 2011), the expansion of proliferative compartment is a Brm-dependent process. Perturbations in the proliferation of Brm-deficient cells has been previously reported in numerous cell lines characterized by Rb-insensitivity as a result of Brm loss, however the analysis of the cell cycle regulators p21 and p17 did not provide any further insight into the possible mechanism by which Brm mediates its anti-proliferative functions (Kadam and Emerson 2003).

One tissue-specific effect observed in the small intestinal epithelium of Brm null animals was CD44 expression. Interestingly, no changes at the transcriptional level of CD44 were detected in the Brm null experimental animals while the pattern of CD44 loss was reported *in vivo* in Brm-deficient human cancer cell lines (Reisman *et al.* 2002, 2003) as well as in multiple tissues including gut epithelium of Brm null mice (Reisman *et al.* 2002). Whereas there is a possibility of transient repression of CD44 expression in all investigated systems however taking into the account the timeframe of experiments and the extensive differences in the data obtained, this seems unlikely. One other possibility is that there is a difference in the requirement for CD44 function between those cells, which subsequently would imply reliance of small intestinal epithelium on CD44 for the maintenance of homeostasis as the presence of CD44 on the cell surface is recognised as a marker for intestinal progenitors (Fevr 2007). Lastly, considering that Brg1 expression is retained in the epithelium of Brm null animals, the levels of Brg1 ATPase may be sufficient for the activation of the CD44 promoter ensuring that the appropriate levels of CD44 expression are maintained within this tissue. It could therefore be extrapolated that no specific compensatory mechanism would be needed but rather a shift between Brm-containing and Brg1-containing complexes at the level of CD44 promoter.

These observations suggest that Brm might play a similar or parallel role to Brg1 in intestinal homeostasis, however the extent of the effects would be more limited and less severe than those one observed in the Brg1-deficient tissue.

In regards to the anti-proliferative capacities of Brm, in the context of Wnt-driven tumorigenesis Brm loss was found to lead to an expansion of Ki67-positive cell distribution, therefore again the spatial distribution of proliferating cells can be influenced by Brm status.

In the context of active Wnt signalling, qRT-PCR analysis detected an extensively downregulated CD44 expression in both small intestine and colon which was further confirmed by immunohistochemical analysis of Apc-deficient epithelium in the context of Brm proficiency and Brm loss. The expression of CD44 expression is a well-known hallmark of colorectal tumorigenesis (Shibata 1997, Huh 2009) implicating that Brm may be directly interacting with Wnt pathway downstream of β-catenin through the regulation of target genes expression. The lack of any effect of Brm null allele on the expression of CD44 in the normal small intestinal homeostasis might be unexpected when compared to the diminished expression of CD44in the context of aberrant Wnt signalling. However taking into the account the gradient of active Wnt signalling and stem cells ranging from very high in the proximal small intestine and relatively low in the colon in CRC (Leedham *et al.* 2012) in regards to what appears to be low levels of Wnt which are required for normal intestinal homeostasis, the response to Brm deficiency as evidenced by the changes in CD44 expression would indicate an extensive reliance of Brm effects on underlying Wnt activity within the intestinal epithelium. A "just right hypothesis" suggesting that the impairment of Apc-containing β-catenin destruction complex must result in the β-catenin accumulation and Wnt activation sufficiently high to generate tumours (Albuquerque *et al.* 2002) is consistent with the above data and provides further evidence for the differential responses to Brm deficiency in the context of Wnt-driven tumorigenesis between the small intestinal and colonic epithelium.

The absence of a lethal phenotype for Brm null animals as well as increased Brm expression during cellular differentiation (LeGouy 1998, Reyes *et al.* 1998) both indicate that Brm is redundant for the maintenance of stem cells. Following Wnt activation there is a Wnt-driven expansion of the stem cell population (Jubb 2006) however, in the context of Brm deficiency, Wnt-activated epithelium of small intestine revealed a significant decrease in the intestinal stem cell marker Olfm4. Both *in situ* hybridization using an*Olfm4* riboprobe and analysis of gene expression detected diminished levels of Olfm4 in the small intestinal epithelium of AhCreER^{+}Apc$^{fl/fl}$Brm null mice. No alterations were observed in the gene expression of other intestinal stem cell markers(*Lgr5* and *Ascl2*) which are direct Wnt target genes, suggesting a lack of interaction between the Wnt pathway elements and Brm function as suggested by

Kadam and Emerson (2003). The speculation that Brm is capable of regulating the stem cell compartment of intestinal epithelium and that this interaction is limited to the Wnt-independent stem cell marker Olfm4 would implicate that signalling pathways regulating self-renewal and maintenance of stem cells and progenitors other than Wnt must be mediating these effects. The control of self-renewal and the fate of intestinal progenitors have been attributed to interaction between Wnt and Notch pathway (Fre 2005, 2009, van Es 2005, reviewed in Noah 2013), suggesting that signalling through the Notch cascade could provide Brm with an alternative option for by-passing Wnt pathway. The mediation of Brm consequences through Notch without further activation of Wnt signalling via the β-catenin pathway effector would be consistent with other reports indicating that in the context of aberrant Wnt signalling, Notch is present downstream of β-catenin (Rodilla *et al.* 2009, Peignon *et al.* 2011).

6.2 *Bona fide* role of Brm as a tumour suppressor gene in Wnt-driven colorectal tumorigenesis is dependent upon the Brg1 status indicating a synthetic lethality relationship between ATPases of SWI/SNF chromatin remodelling complex

Alteration in the catalytic subunits of the SWI/SNF chromatin remodelling complex have been implicated in human diseases as factors contributing towards tumorigenesis in a tissue-specific manner (reviewed in Wilson and Roberts 2011). Loss of Brm expression in the context of UV-induced skin cancer mouse model (Halliday *et al.* 2012) was associated with higher growth rate of skin tumours consistent with the role of Brm in the cell cycle control (Reyes *et al.* 1998). Analysis of human skin lesions was indicative of a tumour suppressive role for both Brm and Brg1 in the progression of skin cancer towards more invasive tumours (Bock *et al.* 2011, Moloney *et al.* 2009) suggesting that whereas Brm appears to not be necessary for tumour initiation, loss of expression occurs as a late event in the skin tumorigenesis. The role of Brm in Rb-mediated cell cycle arrest and its pro-proliferative capacities provide skin tumours with a growth advantage consistent with a tumour suppressor loss phenotype. Consistent with the above, a downregulation in Brm expression has been observed in non-small cell lung cancer where it was frequently lost along with Brg1 expression indicating poor prognosis (Reisman *et al.* 2002, 2003). Similarly, the loss of Brm expression in prostate tumours has been reported to correlate to a higher proliferative index and overall poor survival probability in comparison to Brm-proficient counterparts (Sun *et al.* 2007,Shen *et al.* 2008). The prognostic potential of Brm for classification of gastric cancer

was explored by Yamimichi *et al.* (2007), who showed a positive correlation between deficiency in Brm expression and poorly differentiated tumour phenotype. In parallel, the same study indicated that Brm expression is present in all colorectal cancer cell lines whereas staining of colonic mucosa against Brm revealed no decrease in Brm expression suggesting that Brm is a marker for gastric but not colorectal tumorigenesis.

In the chapter 4 of this PhD thesis I explored the possibility that Brm plays a tumour suppressor role in the epithelium of the small intestine and colon. Due to previous notions suggesting that the loss of both alleles of Brm was required in a murine model of UV-induced photocarcinogenesis (Halliday *et al.* 2012), I assessed the effects of Brm null status on the Wnt-driven tumorigenesis of intestinal epithelium.

Whereas loss of Brm expression in human lung and prostate tumours was associated with a poor prognosis and decrease in survival, parallel studies using murine models reported increased growth potential of Brm-deficient lung and skin tumours with no indications in regards to survival probability of experimental animals (Glaros *et al.* 2007, Halliday *et al.* 2012). The analysis of Brm loss in the context of aberrant Wnt signalling mediated through Apc loss failed to reveal an alteration of survival probability dependent upon Brm expression status.While conditional loss of Apc under the expression of AhCreER recombinase results in the perturbation of normal intestinal homeostasis and initiation of tumorigenesis, the activation of Wnt signalling leads to very short lifespan of experimental animals making the analysis of frequency or size of tumours very limited. In addition, Brm status does not appear to alter the survival probability of Apc-deficient animals as seen by a median survival, however Brm null mice are characterized by an earlier onset of symptoms suggesting that tumour initiation and early neoplastic change occurs at the faster rate in Brm-deficient epithelium. Consistent with that, the ethyl carbamate model of lung carcinogenesis indicated loss of Brm as factor potentiating the initiation and development of lung tumours (Glaros *et al.* 2007).These results suggest that Brm plays a tumour suppressing role in the epithelium of lung and intestine, however the acceleration tumorigenesis occurs through the changes in the proliferation rates and gene expression rather that do not translate into dramatic differences in survival probability.

The significance of Brm in the context of Wnt-driven colorectal tumorigenesis in a short-term study was further explored by comparing Brm-deficient, Brg1-deficient as well as Brm and Brg1-deficient intestinal epithelium to elaborate the impact of loss of a particular ATPase to

determine whether the reported effects on colorectal tumorigenesis are caused directly by the loss of catalytic subunit or by alteration in the remaining SWI/SNF chromatin remodelling complexes through a shift in their subunit reliance. Analysis of the survival probability between AhCreER^{+}Apc$^{fl/fl}$Brg1$^{fl/fl}$Brm null and AhCreER^{+}Apc$^{fl/fl}$Brm null showed no significant differences in the survival suggesting that in the context of Brm null allele Brg1 proficiency or deficiency does not alter tumorigenesis. Moreover, in response to Wnt activation, the expression levels of Wnt target genes in the small intestine were suppressed in a similar manner between those two cohorts of animals suggesting similar mechanism of tumorigenesis. Whilst conditional loss of Brg1 in the intestinal epithelium is incompatible with β-catenin accumulation and Wnt activation leading to improved survival of Apc-deficient mice and (Holik 2014), either loss of its paralogue Brm or concomitant loss of both Brm and Brg1 does not display a similar effect on the survival probability. The upregulation of Brm at the transcription level in the Brg1-deficienct Wnt-activated small intestinal epithelium together with survival data suggest that Brm might be capable of partial compensation for Brg1 function extending the survival of Apc-deficient animals. In the context of concomitant loss of both Brm and Brg1 the same compensation mechanism would be absent leading to the survival probability being indistinguishable from that of AhCreER^{+}Apc$^{fl/fl}$ mice. Analysis of mRNA levels of Brg1 in the small intestinal epithelium of Apc-deficient animals carrying the Brm null allele indicate that low levels of Brg1 expression cannot compensate for the loss of Brm subunit. Moreover, consistent with the notion that only Brg1-proficient lesions of the epithelium become Wnt-activated, cells with high levels of Brg1 expression would express the stabilized form of β-catenin and subsequently higher Wnt activity potentially accelerating tumorigenesis in theAhCreER^{+}Apc$^{fl/fl}$Brm null cohort and eventually resulting in the poor prognosis of those animals and similar survival to both AhCreER^{+}Apc$^{fl/fl}$ and AhCreER^{+}Apc$^{fl/fl}$Brg1$^{fl/fl}$Brm null mice. A similar notion exploiting the existence of a compensatory mechanism between Brm and Brg1 *in vivo* was explored by Oike *et al.* (2013), suggesting that silencing of Brm would provide a therapeutic window for Brg1-deficient cancers however this synthetic lethality relationship between two catalytic subunits of SWI/SNF complex relies on the strong tumour suppressor role of Brg1 in the context of lung epithelium. Moreover, whereas Brm was previously found to functionally compensate for Brg1 in Brg1-deficient human cancer cell lines leading to the restoration of Rb signalling and cell cycle arrest as well as re-expression of CD44 (Bultman *et al.* 2000, Reisman *et al.* 2002, 2003, Glaros *et al.* 2007). However the

extent of the compensation or the mechanism by which it occurs has not been explored within this PhD thesis.

6.3 Future directions

The data presented in chapter 4 and 5 together demonstrate that the loss of Brm is capable of modulation of Wnt-driven tumorigenesis in the intestinal epithelium and furthermore that additional deficiency of Brm in the context of Brg1 loss in Wnt-activated tissue exacerbates the effects of Brg1 loss. Taken together these results implicate that the presence of Brm provides a survival advantage in Brg1-deficient intestinal epithelium and subsequently might be a marker for a better prognosis in the colorectal tumorigenesis. In order to explore the anti-cancer potential of Brm, a long-term study investigating the effects of Brm loss on the intestinal tumorigenesis in animals carrying a heterozygous loss of Apc driven by the expression of AhCre or AhCreER recombinase transgene would be necessary.

Several findings in this study suggest the potential for Brm as a novel therapeutic in colorectal tumorigenesis. There are a number of possible routes forward to explore this further. Firstly, chromatin immunoprecipitation analysis of the small intestinal and colonic epithelium would be required in order to establish whether Brm is associated with promoters of the Wnt and Notch target genes reported as modulated in this thesis. Genome-wide expression analysis in the context of Brm loss, Brg1 loss and concomitant Brm and Brg1 loss in the Wnt-activated epithelium would provide a greater insight into the role of SWI/SNF chromatin remodelling in CRC.

In regards to the animal model used in the experiments, the construction of a conditional Brm knock-down allele that could be expressed under the pan-intestinal VillinCre or other intestinal-specific recombinase would eliminate Brm effects on other tissues and more specifically on the intestinal microenvironment. Stem-cell-specific loss of Brm using Lgr5CreER could be used to exclude the possibility of Brm modulating stem cell population however due to extremely low levels of recombination a high risk of false negatives exists in using this system. In contrast, Apc^{Min} mouse model could replace conditional deletion of both Apc alleles driven by AhCreER recombinase. The use of this model of CRC would allow for the development of multiple intestinal tumours in the murine epithelium around 6 months of age facilitating the observations of the effects of SWI/SNF complex loss in long-term by traditional knock-down using Cre-loxP system or using Clustered Regularly Interspaced Short Palindromic Repeats (CRISPR) to silence Brm in the pre-existing tumours.

5.3.4 Concomitant loss of both Brm and Brg1 does not exacerbate the phenotype of Wnt-driven tumorigenesis in the colonic epithelium

Previous *in vivo* studies detected an increase in the expression of Brm in the Brg1-deficient human cancer cell lines which concurred in some cases with the compensation of Brg1 function by Brm in mediating the Rb-mediated signalling and restoration of CD44 expression (Muchardt and Yaniv 2001, Strobeck *et al.* 2003). These observations indicate that whereas the functional compensation could lessen the impact of deficiency in one catalytic subunit, other experiments suggested that Brm and Brg1 display partially redundant functions and therefore a disparity may exist in their interactions with target genes regulating tumorigenesis (Strobeck *et al.* 2000, Reisman *et al.* 2002).

Therefore I aimed to establish the transcriptional levels of Brm and Brg1 in the small intestinal and colonic epithelium across all experimental cohorts used in the preparation of this thesis. mRNA from small intestinal and colonic tissue of AhCreER^{-}Brm$^{+/+}$ (control), AhCreER^{+}Brm null (Brm null), AhCreER^{+}Brg1$^{fl/fl}$ (Brg1KO), AhCreER^{+}Brg1$^{fl/fl}$Brm null (DKO), AhCreER^{+}Apc$^{fl/fl}$ (ApcKO), AhCreER^{+}Apc$^{fl/fl}$Brm null (ApcBrmKO), AhCreER^{+}Apc$^{fl/fl}$Brg1$^{fl/fl}$ (ApcBrg1KO) and AhCreER^{+}Apc$^{fl/fl}$Brg1$^{fl/fl}$Brm null (TripleKO) was extracted and qRT-PCR analysis of mRNA levels of *Brm* in Brm-proficient animals and *Brg1* in both Brg1-proficient and Brg1-deficient cohorts. The analysis of the intestinal epithelium in the context of the homeostasis revealed that *Brg1* is 1.5 fold upregulated in the Brm null colonic tissue while in the small intestine a decline rather than an increase in the Brg1 is reported. In contrast, in the Brg1KO epithelium of both small and large intestine we noted a 10 fold increase in the *Brm* expression. Nonetheless, combined loss in Brm and Brg1 detected over 50 fold change in *Brg1* in the colon in comparison to 4 fold increase in the small intestine. Taken together these results suggest that in the context of small intestinal epithelium the fluctuations in the gene expression of Brm and Brg1 are substantially high suggesting that intestinal epithelium is not SWI/SNF-independent and requires the function of chromatin remodelling complexes containing either Brm or Brg1 at a very discreet levels.

In the context of Apc deletion and thus Wnt-driven tumorigenesis in the intestinal epithelium, the fluctuations in Brm and Brg1 expression were detected by qRT-PCR analysis. A significant downregulation of Brg1 in the small intestine and colon of Wnt-activated Brm-deficient epithelium similar to the effect observed in the Brm null homeostatic tissue indicates that in the context of small intestinal epithelium Brg1 is not capable of replacing Brm in SWI/SNF chromatin remodelling complexes lacking Brm catalytic subunit.

Importantly in contrast to homeostatic tissues, levels of Brg1 were downregulated significantly in the intestinal epithelium in the AhCreER^{+}Apc$^{fl/fl}$Brg1$^{fl/fl}$Brm null suggesting that in the context of Wnt activation, compensation mechanism may be damaged and therefore the shift to the large numbers of Brg1-containing complexes is not viable.

Interestingly, in both types of Brg1-deficient epithelium we have detected 10 fold increases in Brm expression however previous reports investigating pan-epithelial loss of Brg1 under the expression of VillinCre indicated that deficiency in Brg1 results in the abrogation of stem cell maintenance and rapid disruption of crypt-villus architecture therefore suggesting that Brm is not capable of compensating for Brg1 function in the maintenance of homeostasis. The discrepancies in those observations would be consistent with notion that post-transcriptional mechanism such as translation of existing mRNA or protein stability could be responsible for the expression levels and therefore possibly compensation between Brm and Brg1. Moreover 4 fold upregulation in small intestine and 56 fold in colon in the epithelium of AhCreER^{+}Brg1$^{fl/fl}$Brm null in contrast to a decrease in the Brg1 expression levels in AhCreER^{+}Apc$^{fl/fl}$Brg1$^{fl/fl}$Brm null animals might potentially be responsible for very mild phenotype of concomitant loss of Brm and Brg1 in normal epithelium in comparison to the high level of dysplasia and destruction of crypt-villus architecture in the AhCreER^{+}Apc$^{fl/fl}$Brg1$^{fl/fl}$Brm null epithelium.

Furthermore, in order to investigate whether Brm is upregulated at the protein level in the epithelium and therefore capable of compensating for Brg1 loss in the context of Wnt activation, double immunofluorescence against Brg1 and Brm was conducted on the small intestinal and colonic epithelium of AhCreER^{+}Apc$^{fl/fl}$Brg1$^{fl/fl}$ animals. Importantly, the comparison between neighbouring Brg1-proficient and Brg1-deficient lesions revealed that Brm expression is upregulated in the colonic but not small intestinal epithelium in contrast to fold changes detected by qRT-PCR. Several considerations should be taken into account while analyzing the changes observed. Notably, Leedham *et al.* (2012) assessed the physiological levels of Wnt activity and the size of stem cell population across the length of intestines in the murine model of stabilizing β-catenin mutation showing that a differential Wnt activity and therefore differential response to aberrant Wnt signalling. The same study also reported that neoplastic transformation of the epithelium is more severe in the proximal small intestine in contrast to very mild effects on the colonic epithelium (Leedham 2012). Whereas the authors did not establish the levels of Wnt signalling in the normal intestinal epithelium, it is plausible that parallel gradient should be observed in the homeostatic tissue.

Taken together these results could provide some insight into the existence of a great discrepancy between small intestinal and colonic epithelium and the fluctuations in *Brm* and *Brg1* gene expression between those two types of epithelium. This notion however does not explain the changes in the gene expression quantified by qRT-PCR and the observations conducted using double immunofluorescence in the context of Wnt activation by Apc loss. Although mRNA levels of Brm in the small intestine of AhCreER^{+}Apc$^{fl/fl}$Brg1$^{fl/fl}$ mice are 4 fold higher than in the respective colonic epithelium, the disparity of these results with reported protein levels of Brm in the same tissue could further indicate that despite of the high levels of mRNA further changes occur at the translational or protein level that could lead to degradation of existing mRNA template and lower Brm expression. Moreover, we previously showed that deficiency in both Brm and Brg1 is well-tolerated in a large intestine of AhCreER^{+}Brg1$^{fl/fl}$Brm null mice in contrast to small intestinal epithelium. The magnitude of changes in Brm and Brg1 expression could be tissue-specific where particular mRNA level is “enough” for functional compensation in colon yet “not sufficient” in the context of small intestine. This notion would be consistent with more prominent transcriptional upregulation of Brm in the small intestine rather than in the colon which however concurs with increased expression of Brm and milder phenotype in the large intestinal tissue. The differential expression between Brm and Brg1 as described in the mouse embryo showing ubiquitous expression of Brg1 throughout the development and higher levels of Brm specifically during the differentiation (LeGouy 1998) could account for some of the extent of fold changes between Brm-deficient and Brg1-deficient experimental cohorts. Another possible explanation for the differences ATPase gene expression levels between homeostatic and Wnt-activated epithelium could be the impairment of the compensation mechanism in cancer cells. The damage in the compensation between Brm and Brg1 is consistent with the increased severity of the phenotype in cells carrying Apc deletion than the consequences of deficiency in either catalytic subunit in the normal intestinal epithelium.

Therefore data presented in this chapter suggested that there is a requirement for functional Brm or Brg1 ATPase for the maintenance of homeostasis of the epithelium as well as for Wnt-driven tumorigenesis. The disparity in the compensation level between Brm and Brg1 are dependent upon the context of small intestinal or colonic epithelium. While the maintenance of homeostasis in Brg1-deficient colonic epithelium requires higher levels of Brm upregulation, this prerequisite is less rigorous in the context of Wnt activation as transformation and neoplastic response to aberrant Wnt signalling is diminished to a great

degree due to gradient in physiological Wnt activity. It can be extrapolated that in the small intestinal epithelium the dependency upon respective levels of Brm and Brg1 is inversed due to higher gradient of underlying Wnt signalling. Taken together, the results from this and previous chapters reveal that Brm and Brg1 ATPases of SWI/SNF chromatin remodelling complex show an exceptional tissue-specificity for their functions. Tissue-specificity, Wnt gradient and functional redundancy between Brm and Brg1 would therefore account for a wide array of the phenotypes and transcriptional responses reported in the intestines of various cohorts of experimental animals. SWI/SNF chromatin remodelling complexes containing either Brm or Brg1 are subjected to the delicate equilibrium with some limited potential of replacement and compensation and with the alterations in the proportions of Brm-associated and Brg1-associated complexes generating alternative phenotypes characterized by various severities.

7 Reference List

Abecassis I, Maes J, Carrier JL, Hillion J, Goodhardt M, Medjber K, Wany L, Lanotte M, Karniguian A. (2008, March) Re-expression of DNA methylation-silenced CD44 gene in a resistant NB4 cell line: rescue of CD44-dependent cell death by cAMP. *Leukemia. 22*(3):511-20. Epub 2007 Dec 20. PMID: 18094716

Albuquerque C, Breukel C, van der Luijt R, Fidalgo P, Lage P, Slors FJ, Leitão CN, Fodde R, Smits R. (2002, June). The 'just-right' signaling model: APC somatic mutations are selected based on a specific level of activation of the beta-catenin signaling cascade. *Hum Mol Genet.*;11(13):1549-60.

Andrae J, Gallini R, Betsholtz C. (2008, May) Role of platelet-derived growth factors in physiology and medicine.*Genes Dev. 22*(10):1276-312. Review.PMID: 18483217

Andreu, P., S. Colnot, C. Godard, S. Gad, P. Chafey, M. Niwa-Kawakita, P. Laurent-Puig, A. Kahn, S. Robine, C. Perret, and B. Romagnolo (2005, March). Cryptrestricted proliferation and commitment to the paneth cell lineage following apc loss in the mouse intestine. *Development 132* (6), 1443 -1451.

Asp P, Wihlborg M, Karlén M, Farrants AK. (2002, July) Expression of BRG1, a human SWI/SNF component, affects the organisation of actin filaments through the RhoA signalling pathway. *J Cell Sci. 115*(Pt 13):2735-46. PMID: 12077364

Banine F, Bartlett C, Gunawardena R, Muchardt C, Yaniv M, Knudsen ES, Weissman BE, Sherman LS. (2005, May) SWI/SNF chromatin-remodeling factors induce changes in DNA methylation to promote transcriptional activation. *Cancer Res. 65*(9):3542-7. PMID: 15867346

Barker, N. and Clevers, H. (2006, December).Mining the Wnt pathway for cancer therapeutics.*Nat Rev Drug Discov,* 5**,** 997-1014.

Barker, N., Ridgway, R. A., van Es, J. H., van de Wetering, M., Begthel, H., van der Born, M., Danenberg, E.,Clarke A. R., Sansom, O. J. and Clevers, H. (2009, January). Crypt stem cells as the cells-of-origin of intestinal cancer.*Nature,* 457**,** 608-11.

Barker, N., van Es, J. H., Kuipers, J., Kujala, P., van den Born, M., Cozijnsen, M., Haegeberth, A., Korving, J., Begthel, H., Peters, P. J. and Clevers, H. (2007, October). Identification of stem cells in small intestine and colon by marker gene Lgr5. *Nature,* 449**,** 1003-7.

Bos, J. L., E. R. Fearon, S. R. Hamilton, M. V.-d.Vries, J. H. van Boom, A. J. van derEb, and B. Vogelstein (1987, May).Prevalence of ras gene mutations in human colorectal cancers.*Nature* 327 (6120), 293-297.

Batlle, E., J. T. Henderson, H. Beghtel, M. M. van den Born, E. Sancho, G. Huls, J. Meeldijk, J. Robertson, M. van de Wetering, T. Pawson, and H. Clevers (2002, October). beta-Catenin and TCF mediate cell positioning in the intestinal epithelium by controlling the expression of EphB/EphrinB. *Cell 111* (2), 251-263.

Batsché E, Yaniv M, Muchardt C. (2006, January) The human SWI/SNF subunit Brm is a regulator of alternative splicing. *Nat Struct Mol Biol. 13*(1):22-9. Epub 2005 Dec 11. PMID: 16341228

Biegel JA, Zhou JY, Rorke LB, Stenstrom C, Wainwright LM, Fogelgren B. (1999, January) Germ line andacquired mutations of INI1 in atypical teratoid and rhabdoid tumors. *Cancer Res 59*:74-9. PMID:9892189

Biggs JR, Yang J, Gullberg U, Muchardt C, Yaniv M, Kraft AS. (2001, March) The human brm protein is cleaved during apoptosis: the role of cathepsin G.*Proc Natl Acad Sci U S A. 98*(7):3814-9. Epub 2001 Mar 20. PMID: 11259672

Bourgo RJ, Siddiqui H, Fox S, Solomon D, Sansam CG, Yaniv M, Muchardt C, Metzger D, Chambon P, Roberts CW, Knudsen ES. (2009, July) SWI/SNF deficiency results in aberrant chromatin organization, mitotic failure, and diminished proliferative capacity. *Mol Biol Cell. 20*(14):3192-9. Epub 2009 May 20. PMID: 19458193

Büller NV, Rosekrans SL, Westerlund J, van den Brink GR.(2012, June) Hedgehog signaling and maintenance of homeostasis in the intestinal epithelium. *Physiology (Bethesda). 27*(3):148-55. PMID: 2268979

Bultman S, Gebuhr T, Yee D, La Mantia C, Nicholson J, Gilliam A, Randazzo F, Metzger D, Chambon P, Crabtree G, Magnuson T. (2000, December) A Brg1 null mutation in the mouse reveals functional differences among mammalian SWI/SNF complexes. *Mol Cell. 6*(6):1287-95. PMID: 11163203

Bultman, S. J., J. I. Herschkowitz, V. Godfrey, T. C. Gebuhr, M. Yaniv, C. M. Perou, T. Magnuson (2007, July).Characterization of mammary tumors from brg1 heterozygous mice.*Oncogene 27* (4), 460-468.

Cairnie, A. B., L. F. Lamerton, and G. G. Steel (1965, September). Cell proliferationstudies in the intestinal epithelium of the rat : II. theoretical aspects. *ExperimentalCell Research* 39 (2-3), 539-553.

Carpten, J. D., Faber, A. L., Horn, C., Donoho, G. P., Briggs, S. L., Robbins, C. M., Hostetter, G., Boguslawki, S., Moses, T. Y., Savage, S., Uhlik, M., Lin, A., Du, J., Qian, Y. W., Zeckner, D. J., Tucker-Kellogg, G., Touchman, J., Patel, K., Mousses, S., Bittner, M., Schevitz, R., Lai, M. H., Blanchard, K. L. and Thomas, J. E. (2007, July). A transforming mutation in the pleckstrin homology domain of AKT1 in cancer.*Nature,* 448**,** 439-44.

Cheng, H. and Leblond, C. P. 1974.Origin, differentiation and renewal of the four main epithelial cell types in the mouse small intestine. V. Unitarian Theory of the origin of the four epithelial cell types. *Am J Anat,* 141**,** 537-61.

Cheng, H., J. Merzel, and C. P. Leblond (1969, December). Renewal of paneth cells in the small intestine of the mouse. *The American Journal of Anatomy 126* (4), 507-525. PMID: 5369113.

Chi TH, Wan M, Lee PP, Akashi K, Metzger D, Chambon P, Wilson CB, Crabtree GR. (2003, August) Sequentialroles of Brg, the ATPase subunit of BAF chromatin remodeling complexes, in thymocyte development. *Immunity. 19*(2):169-82. PMID: 12932351

Chiba H, Muramatsu M, Nomoto A, Kato H. (1994, May) Two human homologues of Saccharomyces cerevisiae SWI2/SNF2 and Drosophila brahma are transcriptional coactivators cooperating with the estrogen receptor and the retinoic acid receptor. *Nucleic Acids Res. 22*(10):1815-20. PMID: 8208605

Clevers H. (2006, November) Wnt/beta-catenin signaling in development and disease.*Cell. 127*(3):469-80. PMID: 17081971

Cohet N, Stewart KM, Mudhasani R, Asirvatham AJ, Mallappa C, Imbalzano KM, Weaver VM, Imbalzano AN, Nickerson JA. (2010, June) SWI/SNF chromatin remodeling enzyme ATPases promote cell proliferation in normal mammary epithelial cells. *J Cell Physiol. 223*(3):667-78. PMID: 20333683

Coisy M, Roure V, Ribot M, Philips A, Muchardt C, Blanchard JM, Dantonel JC. (2004, July) Cyclin A repression in quiescent cells is associated with chromatin remodeling of its promoter and requires Brahma/SNF2alpha. *Mol Cell. 15*(1):43-56. PMID: 15225547

Conboy IM, Conboy MJ, Wagers AJ, Girma ER, Weissman IL, Rando TA. (2005, February) Rejuvenation of aged progenitor cells by exposure to a young systemic environment. *Nature. 433*(7027):760-4. PMID: 15716955

Coopersmith, C. M., C. Chandrasekaran, M. S. McNevin, and J. I. Gordon (1997, July).Bi-transgenic mice reveal that K-rasVal12 augments a p53-independent apoptosis when small intestinal villus enterocytes reenter the cell cycle. *The Journal of CellBiology* 138 (1), 167-179.

de la Chapelle A. (2004, October). Genetic predisposition to colorectal cancer.*Nat Rev Cancer*.;4(10):769-80.

Crabtree M, Sieber OM, Lipton L, Hodgson SV, Lamlum H, Thomas HJ, Neale K, Phillips RK, Heinimann K, Tomlinson IP.(2003, July). Refining the relation between 'first hits' and 'second hits' at the APC locus: the 'loose fit' model and evidence for differences in somatic mutation spectra among patients. *Oncogene*;22(27):4257-65.

de la Serna, I. L., Y. Ohkawa, and A. N. Imbalzano (2006, June). Chromatin remodelling in mammalian differentiation: lessons from ATP-dependent remodellers. *Nat Rev Genet 7* (6), 461-473.

Dalerba, P., S. J. Dylla, I. Park, R. Liu, X. Wang, R. W. Cho, T. Hoey, A. Gurney, E. H. Huang, D. M. Simeone, A. A. Shelton, G. Parmiani, C. Castelli, and M. F. Clarke (2007, June). Phenotypic characterization of human colorectal cancer stem cells.*Proceedings of the National Academy of Sciences* 104 (24), 10158 -10163.

Dalhamn T, Rhodin J. (1956, April). Mucous flow and ciliary activity in the trachea of rats exposed to pulmonary irritant gas. *Br J Ind Med. 13*(2):110-3.

Damiano L, Stewart KM, Cohet N, Mouw JK, Lakins JN, Debnath J, Reisman D, Nickerson JA, Imbalzano AN, Weaver VM. (2013, June). Oncogenic targeting of BRM drives malignancy through C/EBPβ-dependent induction of α5 integrin. *Oncogene.* [Epub ahead of print]

DelBove J, Rosson G, Strobeck M, Chen J, Archer TK, Wang W, Knudsen ES, Weissman BE. (2011, December).Identification of a core member of the SWI/SNF complex, BAF155/SMARCC1, as a human tumor suppressor gene.*Epigenetics. 6*(12):1444-53. PMID: 22139574

Dhawan P, Wieder R, Christakos S. (2009, March) CCAAT enhancer-binding protein alpha is a molecular target of 1,25-dihydroxyvitamin D3 in MCF-7 breast cancer cells. *J Biol Chem. 284*(5):3086-95. Epub 2008 Dec 3. Erratum in: *J Biol Chem.284*(12):8208. Weider, Robert [corrected to Wieder, Robert]. PMID: 19054766

Di Cristofano A, Pesce B, Cordon-Cardo C, Pandolfi PP.(1998, August). Pten is essential for embryonic development and tumour suppression. *Nat Genet*.;19(4):348-55.

Dunaief JL, Strober BE, Guha S, Khavari PA, Alin K, Luban J, Begemann M, Crabtree GR, Goff SP. (1994, October) The retinoblastoma protein and BRG1 form a complex and cooperate to induce cell cycle arrest. *Cell.79*(1):119-30. PMID: 7923370

Dunican DS, McWilliam P, Tighe O, Parle-McDermott A, Croke DT.(2002, May). Gene expression differences between the microsatellite instability (MIN) and chromosomal instability (CIN) phenotypes in colorectal cancer revealed by high-density cDNA array hybridization.*Oncogene.*;21(20):3253-7.

Dymecki, S. M. (1996, June). Flp recombinase promotes site-speci_c DNA recombination in embryonic stem cells and transgenic mice. *Proceedings of the National Academy of Sciences* 93 (12), 6191-6196.

el Marjou, F., K. Janssen, B. H. Chang, M. Li, V. Hindie, L. Chan, D. Louvard, P. Chambon, D. Metzger, and S. Robine (2004, July). Tissue-specific and inducible cre-mediated recombination in the gut epithelium.*Genesis* (New York, N.Y.: 2000) *39* (3), 186-93. PMID: 15282745.

Eng, C. and H. Ji (1998, May). Molecular classification of the inherited hamartomapolyposis syndromes: Clearing the muddied waters. *The American Journal of Human Genetics* 62 (5), 1020-1022.

Eppert, K., S. W. Scherer, H. Ozcelik, R. Pirone, P. Hoodless, H. Kim, L. Tsui, B. Bapat, S. Gallinger, I. L. Andrulis, G. H. Thomsen, J. L.Wrana, and L. Attisano (1996, August). MADR2 maps to 18q21 and encodes a TGF[beta]-Regulated MAD-Relatedprotein that is functionally mutated in colorectal carcinoma. *Cell* 86 (4), 543-552.

Fazeli, A., Dickinson, S. L., Hermiston, M. L., Tighe, R. V., Steen, R. G., Small, C. G., Stoeckli, E. T., Keino-Masu, K., Masu, M., Rayburn, H., Simons, J., Bronson, R. T., Gordon, J. I., Tessier-Lavigne, M. and Weinberg, R. A. (1997, April). Phenotype of mice lacking functional Deleted in colorectal cancer (Dcc) gene.*Nature,* 386**,** 796-804.

Fearon, E. R., K. R. Cho, J. M. Nigro, S. E. Kern, J. W. Simons, J. M. Ruppert,S. R. Hamilton, A. C. Preisinger, G. Thomas, and K. W. Kinzler (1990, January).Identification of a chromosome 18q gene that is altered in colorectal cancers.*Science*(New York, N.Y.) 247 (4938), 49-56. PMID: 2294591.

Fearon, E. R. and B. Vogelstein (1990, June).A genetic model for colorectal tumorigenesis.*Cell* 61 (5), 759-767.

Fedirko V., I. Tramacere V. Bagnardi M. Rota L. Scotti F. Islami E. Negri K. Straif I. Romieu C. La Vecchia P. Bofietta and M. Jenab (2011, February). Alcoholdrinking and colorectal cancer risk: an overall and dose-response meta-analysis ofpublished studies. *Annals of Oncology: Official Journal of the European Society forMedical Oncology / ESMO*. PMID: 21307158.

Fevr, T., S. Robine, D. Louvard, and J. Huelsken (2007, November). Wnt/beta-Catenin is essential for intestinal homeostasis and maintenance of intestinal stem cells. *Mol. Cell. Biol. 27* (21), 7551-7559.

Flowers, S., Nagl, N. G., Jr, Beck, G. R., Jr & Moran, E. (2009, April) Antagonistic roles for BRM and BRG1 SWI/SNF complexes in differentiation. *J. Biol. Chem.* 284, 10067–10075. Epub 2009 Jan 14. PMID: 19144648

Fodde, R., W. Edelmann, K. Yang, C. van Leeuwen, C. Carlson, B. Renault, C. Breukel,E. Alt, M. Lipkin, and P. M. Khan (1994, September). A targeted chain-terminationmutation in the mouse apc gene results in multiple intestinal tumors. *Proceedingsof the National Academy of Sciences of the United States of America* 91 (19), 8969-8973. PMID: 8090754.

Fodde, R., R. Smits, and H. Clevers (2001, October).APC, signal transduction andgenetic instability in colorectal cancer.*Nat Rev Cancer* 1 (1), 55-67.

Foulds L. (1958, July). The natural history of cancer.*J Chronic Dis*.;8(1):2-37.

Fre, S., M. Huyghe, P. Mourikis, S. Robine, D. Louvard, and S. Artavanis-Tsakonas (2005, June). Notch signals control the fate of immature progenitor cells in the intestine. *Nature 435* (7044), 964-968.

Gebuhr TC, Kovalev GI, Bultman S, Godfrey V, Su L, Magnuson T. (2003, December) The role of Brg1, a catalytic subunit of mammalian chromatin-remodeling complexes, in T cell development. *J Exp Med. 198*(12): 1937-49. PMID: 14676303

Gerbe, F., Brulin, B., Makrini, L., Legraverend, C. and Jay, P. (2009, December). DCAMKL-1 expression identifies Tuft cells rather than stem cells in the adult mouse intestinal epithelium. *Gastroenterology,* 137**,** 2179-80; author reply 2180-1.

Gerbe F., van Es J. H., Makrini L., Brulin B., Mellitzer G., Robine S., Romagnolo B., Shroyer, N. F., Bourgaux J. F., Pignodel C., Clevers, H.and& Jay P. (2011, March). Distinct ATOH1 and Neurog3 requirements define tuft cells as a new secretory cell type in the intestinal epithelium. *J Cell Biol*, 192**,** 767-80.

Gerbe F, Legraverend C, Jay P. (2012, September). The intestinal epithelium tuft cells: specification and function. *Cell Mol Life Sci. 69*(17):2907-17.

Giles, R. H., J. H. van Es, and H. Clevers (2003, June).Caught up in a wnt storm:Wnt signaling in cancer.*Biochimica et Biophysica Acta* (BBA) - *Reviews on Cancer* 1653 (1), 1-24.

Gossen, M. and H. Bujard (1992, June).Tight control of gene expression in mammalian cells by tetracycline-responsive promoters.*Proceedings of the National Academy of Sciences of the United States of America* 89 (12), 5547-5551. PMID: 1319065.

Gossen, M., S. Freundlieb, G. Bender, G. Mller, W. Hillen, and H. Bujard (1995, June). Transcriptional activation by tetracyclines in mammalian cells.*Science* (New York, N.Y.) 268 (5218), 1766-1769. PMID: 7792603.

Glaros S, Cirrincione GM, Muchardt C, Kleer CG, Michael CW, Reisman D. (2007, October). The reversible epigenetic silencing of BRM: implications for clinical targeted therapy. *Oncogene. 26*(49):7058-66. Epub 2007 Jun 4.

Glaros S, Cirrincione GM, Palanca A, Metzger D, Reisman D. (2008, May) Targeted knockout of BRG1 potentiates lung cancer development.*Cancer Res. 68*(10):3689-96. PMID: 18483251

Genetic evaluation of candidate genes for the Mom1 modifier of intestinal neoplasia in mice. Gould KA, Luongo C, Moser AR, McNeley MK, Borenstein N, Shedlovsky A, Dove WF, Hong K, Dietrich WF, Lander ES. (1996, December) *Genetics*.;144(4):1777-85.

Grady, W. M., L. L. Myerofi, S. E. Swinler, A. Rajput, S. Thiagalingam, J. D. Lutterbaugh, A. Neumann, M. G. Brattain, J. Chang, S. Kim, K. W. Kinzler, B. Vogelstein, J. K. V. Willson, and S. Markowitz (1999, January). Mutational inactivation of transforming growth factor receptor type II in microsatellite stable colon cancers.*Cancer Research* 59 (2), 320-324.

Greenow, K. R., A. R. Clarke, and R. H. Jones (2009, January). Chk1 deficiency in the mouse small intestine results in p53-independent crypt death and subsequent intestinal compensation. *Oncogene 28* (11), 1443-1453.

Gregorieff, A. and H. Clevers (2005, April). Wnt signaling in the intestinal epithelium:from endoderm to cancer. *Genes & Development 19* (8), 877-90. PMID: 15833914.

Gregorieff, A., D. Pinto, H. Begthel, O. Destre, M. Kielman, and H. Clevers (2005, August).Expression pattern of wnt signaling components in the adult intestine.*Gastroenterology 129* (2), 626-638.

Griffin CT, Brennan J, Magnuson T. (2008, February) The chromatin-remodeling enzyme BRG1 plays an essential role in primitive erythropoiesis and vascular development. *Development. 135*(3):493-500. Epub 2007 Dec 19. PMID: 18094026

Griffin, C. T., C. D. Curtis, R. B. Davis, V. Muthukumar, and T. Magnuson (2011, February). The chromatin-remodeling enzyme BRG1 modulates vascular wnt signalling at two levels. *Proceedings of the National Academy of Sciences 108* (6), 2282-2287.

Groden, J., A. Thliveris, W. Samowitz, M. Carlson, L. Gelbert, H. Albertsen, G. Joslyn,J. Stevens, L. Spirio, M. Robertson, L. Sargeant, K. Krapcho, E. Wol_, R. Burt,J. P. Hughes, J. Warrington, J. McPherson, J. Wasmuth, D. Le Paslier, H. Abderrahim,D. Cohen, M. Leppert, and R. White (1991, August). Identification andcharacterization of the familial adenomatous polyposis coli gene.*Cell* 66 (3), 589-600.

Guerra, C., N. Mijimolle, A. Dhawahir, P. Dubus, M. Barradas, M. Serrano, V. Campuzano,and M. Barbacid (2003, August). Tumor induction by an endogenous k-rasoncogene is highly dependent on cellular context. *Cancer Cell* 4 (2), 111-120.

Guidi CJ, Sands AT, Zambrowicz BP, Turner TK, Demers DA, Webster W, Smith TW, Imbalzano AN, Jones SN. (2001, May) Disruption of Ini1 leads to peri-implantation lethality and tumorigenesis in mice. *Mol Cell Biol 21*:3598-603. PMID: 11313485

Halliday GM, Zhou Y, Sou PW, Huang XX, Rana S, Bugeja MJ, Painter N, Scolyer RA, Muchardt C, Di Girolamo N, Lyons JG. (2012, August). The absence of Brm exacerbates photocarcinogenesis. *Exp Dermatol. 21*(8):599-604.

Hampel H, Frankel WL, Martin E, Arnold M, Khanduja K, Kuebler P, Nakagawa H, Sotamaa K, Prior TW, Westman J, Panescu J, Fix D, Lockman J, Comeras I, de la Chapelle A. (2005, May). Screening for the Lynch syndrome (hereditary nonpolyposis colorectal cancer).*N Engl J Med*.;352(18):1851-60.

Harada, N., Y. Tamai, T. Ishikawa, B. Sauer, K. Takaku, M. Oshima, and M. M. Taketo(1999, November).Intestinal polyposis in mice with a dominant stable mutation ofthe beta-catenin gene.*The EMBO Journal* 18 (21), 5931-42. PMID: 10545105.

Haramis, A. G., H. Begthel, M. van den Born, J. van Es, S. Jonkheer, G. J. A. Offerhaus, and H. Clevers (2004, March).De novo crypt formation and juvenile polyposis on BMP inhibition in mouse intestine.*Science 303* (5664), 1684 -1686.

Harikrishnan KN, Chow MZ, Baker EK, Pal S, Bassal S, Brasacchio D, Wang L, Craig JM, Jones PL, Sif S, El-Osta A. (2005, May) Brahma links the SWI/SNF chromatin-remodeling complex with MeCP2-dependent transcriptional silencing. *Nat Genet. 37*(3):254-64. Epub 2005 Feb 6. PMID: 15696166

He S, Pirity MK, Wang WL, Wolf L, Chauhan BK, Cveklova K, Tamm ER, Ashery-Padan R, Metzger D, Nakai A, Chambon P, Zavadil J, Cvekl A. (2010, November) Chromatin remodeling enzyme Brg1 is required for mouse lens fiber cell terminal differentiation and its denucleation. *Epigenetics Chromatin. 3*(1):21. PMID: 21118511

He XC, Zhang J, Tong WG, Tawfik O, Ross J, Scoville DH, Tian Q, Zeng X, He X, Wiedemann LM, Mishina Y, Li L. (2004, October) BMP signaling inhibits intestinal stem cell self-renewal through suppression of Wnt-beta-catenin signaling.*Nat Genet. 36*(10):1117-21. Epub 2004 Sep 19. PMID: 15378062

Hinnebusch BF, Siddique A, Henderson JW, Malo MS, Zhang W, Athaide CP, Abedrapo MA, Chen X, Yang VW, Hodin RA. (2004, January).Enterocyte differentiation marker intestinal alkaline phosphatase is a target gene of the gut-enriched Kruppel-like factor. *Am J Physiol Gastrointest Liver Physiol.*;286(1):G23-30.

Holik AZ, Krzystyniak J, Young M, Richardson K, Jardé T, Chambon P, Shorning BY, Clarke AR. (2013, November). Brg1 is required for stem cell maintenance in the murine intestinal epithelium in a tissue-specific manner. *Stem Cells.*;31(11):2457-66.

Holik AZ, Young M, Krzystyniak J, Williams GT, Metzger D, Shorning BY, Clarke AR. (2014, July). Brg1 loss attenuates aberrant wnt-signalling and prevents wnt-dependent tumourigenesis in the murine small intestine. *PLoS Genet*. 10;10(7):e1004453

Howe, J. R., J. L. Bair, M. G. Sayed, M. E. Anderson, F. A. Mitros, G. M. Petersen,V. E. Velculescu, G. Traverso, and B. Vogelstein (2001, June). Germline mutationsof the gene encoding bone morphogenetic protein receptor 1A in juvenile polyposis.*Nat Genet* 28 (2), 184-187.

Howe, J. R., S. Roth, J. C. Ringold, R. W. Summers, H. J. Jrvinen, P. Sistonen, I. P. M. Tomlinson, R. S. Houlston, S. Bevan, F. A. Mitros, E. M. Stone, Aaltonen L.A (1998, May). Mutations in the SMAD4/DPC4 gene in juvenile polyposis.
Science 280 (5366), 1086-1088.

Höcker M, Wiedenmann B. (1998, November). Molecular mechanisms of enteroendocrine differentiation.*Ann N Y Acad Sci. 17*;859:160-74.

Iacopetta B., Russo, A., Bazan V., Dardanoni G., Gabbia N., Soussi T., Kerr D., Elsaleh H., Soong R., Kandioler, D., Janschek, E., Kappel S., Lung M., Leung C. S., Ko J. M., Yuen S., Ho J., Leung S. Y., Crapez E., Duffouyr J., Ychou M., Leahy D. T., O'Donoghue D. P., Agnese, V., Cascio S., di Fede G., Chieco-Bianchi, L., Bertorelle R., Bellucco C., Giaretti W., Castagnola P., Ricevuto, E., Ficorella C., Bosari S., Arizzi, C. D., Miyaki M., Onda M., Kampman E., Diergaarde B., Royds, J., Lothe, R. A., Diep C. B., Meling G. I., Ostrowski J., Trzeciak L., Guzinska-Ustymowicz K., Zalewski B., Cappela G. M., Moreno V., Peinado M. A., Lonnroth C., Lundholm, K., Sun, X. F., Jasnsson, A., Bouzouhene H., Hsieh L. L., Tang R., Smith D. R., Allen-Mersh T. G., Khan Z. A., Shorthouse A. J., Silverman M. L., Kato S., Ishioka C. and Group TP53.-CRC Collaborative Group. 313 (2006, May). Functional categories of TP53 mutation in colorectal cancer: results of an International Collaborative Study. *Ann Oncol,* 17(5)**,** 842-7.

Ireland, H., C. Houghton, L. Howard, and D. J. Winton (2005, August).Cellular inheritance of a cre-activated reporter gene to determine paneth cell longevity in the murine small intestine.*Developmental Dynamics: An Official Publication of the American Association of Anatomists 233* (4), 1332-1336. PMID: 15937933.

Janssen, K., F. E. Marjou, D. Pinto, X. Sastre, D. Rouillard, C. Fouquet, T. Soussi, D. Louvard, and S. Robine (2002, August). Targeted expression of oncogenic k-rasin intestinal epithelium causes spontaneous tumorigenesis in mice. *Gastroenterology* 123 (2), 492-504.

Jarvi O, Keyrilainen O. (1956). On the cellular structures of the epithelial invasions in the glandular stomach of mice caused by intramural application of 20-methylcholantren.*Acta Pathol Microbiol Scand Suppl*. 39(Suppl 111):72-3.

Jensen J, Pedersen EE, Galante P, Hald J, Heller RS, Ishibashi M, Kageyama R, Guillemot F, Serup P, Madsen OD. (2000, January).Control of endodermal endocrine development by Hes-1.*Nat Genet. 24*(1):36-44.

Kadam, S. & Emerson, B. M. (2003, February) Transcriptional specificity of human SWI/SNF BRG1 and BRM chromatin remodeling complexes. *Mol. Cell* 11, 377–389. PMID: 12620226

Karlsson L, Lindahl P, Heath JK, Betsholtz (2000, August) Abnormal gastrointestinal development in PDGF-A and PDGFR-(alpha) deficient mice implicates a novel mesenchymal structure with putative instructive properties in villus morphogenesis.*C. Development. 127*(16):3457-66. PMID: 10903171

Katoh, Y. and M. Katoh (2006, December). Hedgehog signaling pathway and gastrointestinal stem cell signaling network (review). *International Journal of Molecular Medicine 18* (6), 1019-1023. PMID: 17089004.

Katoh M, Katoh M. (2007, January) Notch signaling in gastrointestinal tract (review).*Int J Oncol. 30*(1):247-51. Review.PMID: 17143535

Kemp, R., H. Ireland, E. Clayton, C. Houghton, L. Howard, and D. J. Winton (2004). Elimination of background recombination: somatic induction of cre by combined transcriptional regulation and hormone binding affinity. *Nucleic Acids Research 32* (11), e92. PMC443557.

Keshav S. (2006, September). Paneth cells: leukocyte-like mediators of innate immunity in the intestine. *J Leukoc Biol.* 80(3):500-8.

Kim Y, Fedoriw AM, Magnuson T. (2012, March) An essential role for a mammalian SWI/SNF chromatin-remodeling complex during male meiosis. *Development. 139*(6):1133-40. Epub 2012 Feb 8. PMID: 22318225

Kim, B., G. Buchner, I. Miletich, P. T. Sharpe, and R. A. Shivdasani (2005, April).Thestomach mesenchymal transcription factor barx1 speci_es gastric epithelial identitythrough inhibition of transient wnt signaling.*Developmental Cell* 8 (4), 611-622.PMID: 15809042.

Kim, J., H. Crooks, A. Foxworth, and T. Waldman (2002, December). Proof-ofprinciple:oncogenic beta-catenin is a valid molecular target for the developmentof pharmacological inhibitors. *Molecular Cancer Therapeutics* 1 (14), 1355-1359.PMID: 12516970.

Kim, S. H., K. A. Roth, A. R. Moser, and J. I. Gordon (1993, November).Transgenic mouse models that explore the multistep hypothesis of intestinal neoplasia.*The Journal of Cell Biology* 123 (4), 877-893. PMID: 8227147.

Kinzler K. W. and Vogelstein, B. (1996). Lessons from hereditary colorectal cancer.*Cell,* 87**,** 159-70.

Kinzler, K. W. and B. Vogelstein (1998, May).Landscaping the cancer terrain.*Science* 280 (5366), 1036-1037.

Klochendler Yeivin A, Fiette L, Barra J, Muchardt C, Babinet C, Yaniv M. (2000, December) The murineSNF5/INI1 chromatin remodeling factor is essential for embryonic development and tumor suppression. *EMBO Rep 1*:500-6. PMID: 11263494

Korinek, V., N. Barker, P. Moerer, E. van Donselaar, G. Huls, P. J. Peters, and H. Clevers (1998, August). Depletion of epithelial stem-cell compartments in the small intestine of mice lacking tcf-4. *Nature Genetics 19* (4), 379-83. PMID: 9697701.

Kraehenbuhl JP, Neutra MR. (2000) Epithelial M cells: differentiation and function. *Annu Rev Cell Dev Biol. 16*:301-32. Review.

Kucharzik T, Lügering N, Rautenberg K, Lügering A, Schmidt MA, Stoll R, Domschke W. (2000). Role of M cells in intestinal barrier function. *Ann N Y Acad Sci. 915*:171-83. Review.

Kuehn, M. R., A. Bradley, E. J. Robertson, and M. J. Evans (1987, March).A potentialanimal model for Lesch-Nyhan syndrome through introduction of HPRT mutationsinto mice.*Nature* 326 (6110), 295-298.

Kuhnert, F., C. R. Davis, H. Wang, P. Chu, M. Lee, J. Yuan, R. Nusse, and C. J. Kuo (2004, January). Essential requirement for wnt signaling in proliferation of adult small intestine and colon revealed by adenoviral expression of dickkopf-1.*Proceedings of the National Academy of Sciences of the United States of America 101* (1), 266 -271.

Lachlan KL, Lucassen AM, Bunyan D, Temple IK.(2007, September). Cowden syndrome and Bannayan Riley Ruvalcaba syndrome represent one condition with variable expression and age-related penetrance: results of a clinical study of PTEN mutation carriers. *J Med Genet.*;44(9):579-85.

Lamlum H, Ilyas M, Rowan A, Clark S, Johnson V, Bell J, Frayling I, Efstathiou J, Pack K, Payne S, Roylance R, Gorman P, Sheer D, Neale K, Phillips R, Talbot I, Bodmer W, Tomlinson I. (1999, September) The type of somatic mutation at APC in familial adenomatous polyposis is determined by the site of the germline mutation: a new facet to Knudson's 'two-hit' hypothesis.*Nat Med.* 5(9):1071-5.

LeGouy E, Thompson EM, Muchardt C, Renard JP. (1998, May).Differential preimplantation regulation of two mouse homologues of the yeast SWI2 protein.*Dev Dyn. 212*(1):38-48.

Li L. and Clevers H. (2010, January).Coexistence of quiescent and active adult stem cells in mammals.*Science,* 327**,** 542-5.

Lim, W., HearleN., ShahB., Murday V., HodgsonS. V., LucassenA., EcclesD.,Talbot I., Neale K., LimA. G., O'DonohueJ.,. DonaldsonA, MacdonaldR. C., YoungI. D., RobinsonM. H., LeeP. W. R., StoodleyB. J., TomlinsonI., AldersonD.,HolbrookA. G., VyasS., SwarbrickE. T., LewisA. A. M., PhillipsR. K. S., Houlston R.S. (2003, July). Further observations on LKB1/STK11 status andcancer risk in Peutz-Jeghers syndrome. *British Journal of Cancer* 89 (2), 308-313.PMID: 12865922.

Liang, J., M. Wan, Y. Zhang, P. Gu, H. Xin, S. Y. Jung, J. Qin, J. Wong, A. J. Cooney,D. Liu, and Z. Songyang (2008, June). Nanog and oct4 associate with unique transcriptionalrepression complexes in embryonic stem cells. *Nat Cell Biol* 10 (6), 731-739.

Liang, P. S., T. Chen, and E. Giovannucci (2009, May). Cigarette smoking and colorectalcancer incidence and mortality: systematic review and meta-analysis. *International Journal of Cancer. Journal International Du Cancer* 124 (10), 2406-2415.PMID: 19142968.

Lobo N. A., Shimono Y., Qian D., Clarke M. F. (2007).The biology of cancer stem cells.*Annu Rev Cell Dev Biol,* 23**,** 675-99.

Lynch, H. T. and A. de la Chapelle (2003, March). Hereditary colorectal cancer.*The New England Journal of Medicine* 348 (10), 919-932. PMID: 12621137.

Lim, W., Hearle N., Shah B., Murday V., Hodgson S.V., Lucassen A., Eccles D., Talbot D., Neale K., Lim A.G., O'Donohue J., Donaldson A., Macdonald R.C., Young D.C., Robinson M.H., Lee P.W.R., Stoodley B.J., Tomlinson I, Alderson D., Holbrook A.G., S. Vyas, E. T. Swarbrick A., Lewis A.M., Phillips R.K.S., Houlston R.S. (2003, July). Further observations on LKB1/STK11 status and cancer risk in Peutz-Jeghers syndrome. *British Journal of Cancer* 89 (2), 308-313. PMID: 12865922.

Madison, B. B., K. Braunstein, E. Kuizon, K. Portman, X. T. Qiao, and D. L. Gumucio (2005, January). Epithelial hedgehog signals pattern the intestinal crypt-villus axis. *Development 132* (2), 279-289.

Markowitz, S., Wang J., Myerofi L., Parsons R., Sun L., Lutterbaugh J, Fan R., Zborowska E., Kinzler K., Vogelstein B. (1995, June). Inactivation of the type II TGF-beta receptor in colon cancer cells with microsatellite instability. *Science* 268 (5215), 1336 -1338.

Marsh, V., Winton D. J., Williams G. T., Dubois N., Trumpp A., Sansom, O. J, Clarke A.R. (2008, December). Epithelial pten is dispensable for intestinal homeostasisbut suppresses adenoma development and progression after apc mutation.*Nat Genet* 40 (12), 1436-1444.

Davies EJ, Marsh Durban V, Meniel V, Williams GT, Clarke AR.(2014, May).PTEN loss and KRAS activation leads to the formation of serrated adenomas and metastatic carcinoma in the mouse intestine.*J Pathol.*;233(1):27-38.

Marshman, E., C. Booth, and C. S. Potten (2002).The intestinal epithelial stem cell.*BioEssays 24* (1), 91-98.

Matsubara D, Kishaba Y, Ishikawa S, Sakatani T, Oguni S, Tamura T, Hoshino H, Sugiyama Y, Endo S, Murakami Y, Aburatani H, Fukayama M, Niki T. (2013, February). Lung cancer

with loss of BRG1/BRM, shows epithelial mesenchymal transition phenotype and distinct histologic and genetic features. *Cancer Sci. 104*(2):266-73. Epub 2013 Jan 4.

May R., Riehl T. E., Hunt C., Surreban S. M., Anant S. and Houchen C. W. (2008).Identification of a novel putative gastrointestinal stem cell and adenoma stem cell marker, doublecortin and CaM kinase-like-1, following radiation injury and in adenomatous polyposis coli/multiple intestinal neoplasia mice.*Stem Cells,* 26**,** 630-7.

Merlos-Surez, A., F. M. Barriga, P. Jung, M. Iglesias, M. V. Cspedes, D. Rossell, M. Sevillano, X. Hernando-Momblona, V. da Silva-Diz, P. Muoz, H. Clevers, E. Sancho, R. Mangues, and E. Batlle (2011). The intestinal stem cell signature identifies colorectal cancer stem cells and predicts disease relapse. *Cell Stem Cell In Press,Corrected Proof.*

Moghaddam, A. A., M. Woodward, and R. Huxley (2007, December). Obesity and riskof colorectal cancer: a meta-analysis of 31 studies with 70,000 events. *Cancer Epidemiology, Biomarkers & Prevention: A Publication of the American Associationfor Cancer Research, Cosponsored by the American Society of Preventive Oncology* 16 (12), 2533-2547. PMID: 18086756.

Montgomery R. K., Carlone D. L., Richmond C. A., Farrilla L., Kranendonk M. E., Henderson D. E., Baffour-Awuah N. Y., Ambruzs D. M., Fogli L. K., Aolgra S. and Breault, D. T. (2011). Mouse telomerase reverse transcriptase (mTert) expression marks slowly cycling intestinal stem cells. *Proc Natl Acad Sci U S A,* 108**,** 179-84.

Muchardt C, Yaniv M. (1993, November) A human homologue of Saccharomyces cerevisiae SNF2/SWI2 and Drosophila brm genes potentiates transcriptional activation by the glucocorticoid receptor. *EMBO J. 12*(11):4279-90. PMID: 8223438

Muchardt C, Yaniv M. (1999, April) The mammalian SWI/SNF complex and the control of cell growth. *Semin Cell Dev Biol. 10*(2):189-95. PMID: 10441072

Muncan, V., O. J. Sansom, L. Tertoolen, T. J. Phesse, H. Begthel, E. Sancho, A. M. Cole, A. Gregorie, I. M. de Alboran, H. Clevers, and A. R. Clarke (2006, November). Rapid loss of intestinal crypts upon conditional deletion of the Wnt/Tcf-4 target gene c-Myc. *Mol. Cell. Biol. 26* (22), 8418-8426.

Munoz J., Stange D. E., Schepers A. G., van de Wetering M., Koo B. K., Itzkovitz S., Volckmann R., Kung K. S., Koster J., Radalescu S., Myant K., Versteeg R., Sansom O. J., van Es J. H., Barker N., van Oudenaarden A., Mohammed S., Heck A. J. and Cleavers H. (2012). The Lgr5 intestinal stem cell signature: robust expression of proposed quiescent '+4' cell markers. *EMBO J,* 31**,** 3079-91

Nagase, H. and Y. Nakamura (1993).Mutations of the APC (adenomatous polyposiscoli) gene.*Human Mutation* 2 (6), 425-34. PMID: 8111410.

Nagrani SR, Levens ED, Baxendale V, Boucheron C, Chan WY, Rennert OM. (2011, January) Methylation patterns of Brahma during spermatogenesis and oogenesis: potential implications. *Fertil Steril. 95*(1):382-4. Epub 2010 Aug 17. PMID: 20719309

Nigro JM, Baker SJ, Preisinger AC, Jessup JM, Hostetter R, Cleary K, Bigner SH, Davidson N, Baylin S, Devilee P, et al.(1989, December). Mutations in the p53 gene occur in diverse human tumour types. *Nature.*;342(6250):705-8.

Norat, T., Bingham S., Ferrari P., Slimani N., Jenab M., Mazuir M., Overvad K., Olsen A., Tjnneland A., Clavel F., Boutron-Ruault M., Kesse E., Boeing H., Bergmann M. M., Nieters A., Linseisen J., Trichopoulou A., Trichopoulos D., Tountas Y., Berrino F., Palli D., Panico S., Tumino R., Vineis P., Bueno-de-Mesquita H. B., P. H. M. Peeters, D. Engeset, E. Lund, G. Skeie, E. Ardanaz, C. Gonzlez, C. Navarro, J. R. Quirs, M. Sanchez, G. Berglund, I. Mattisson, G. Hallmans, R. Palmqvist, N. E. Day, K. Khaw, T. J. Key, M. San Joaquin, B. Hmon, R. Saracci, R. Kaaks, and E. Riboli (2005, June). Meat, fish, and colorectal cancer risk: the European prospective investigation into cancer and nutrition. *Journal of the National Cancer Institute* 97 (12), 906-916. PMID: 15956652.

Nusse R, Varmus H. (2012, June). Three decades of Wnts: a personal perspective on how a scientific field developed. *EMBO J.* 13;31(12):2670-84.

O'Brien C. A., Pollett A., Gallinger S., Dick J. E. (2007, January).A human colon cancer cell capable of initiating tumour growth in immunodeficient mice.*Nature,* 445**,** 106-10.

Olive, K. P., M. A. Jacobetz, C. J. Davidson, A. Gopinathan, D. McIntyre, D. Honess, B. Madhu, M. A. Goldgraben, M. E. Caldwell, D. Allard, K. K. Frese, G. DeNicola, C. Feig, C. Combs, S. P. Winter, H. Ireland-Zecchini, S. Reichelt, W. J. Howat, A. Chang, M. Dhara, L. Wang, F. Rckert, R. Grtzmann, C. Pilarsky, K. Izeradjene, S. R. Hingorani, P. Huang, S. E. Davies, W. Plunkett, M. Egorin, R. H. Hruban, N. Whitebread, K. McGovern, J. Adams, C. Iacobuzio-Donahue, J. Grifiths, and D. A. Tuveson (2009, June). Inhibition of hedgehog signaling enhances delivery of chemotherapy in a mouse model of pancreatic cancer. *Science* 324 (5933), 1457-1461.

Oshima, H., A. Matsunaga, T. Fujimura, T. Tsukamoto, M. M. Taketo, and M. Oshima(2006, October).Carcinogenesis in mouse stomach by simultaneous activation of thewnt signaling and prostaglandin e2 pathway.*Gastroenterology* 131 (4), 1086-1095.

Oshima, M., H. Oshima, K. Kitagawa, M. Kobayashi, C. Itakura, and M. Taketo (1995,May).Loss of apc heterozygosity and abnormal tissue building in nascent intestinalpolyps in mice carrying a truncated apc gene.*Proceedings of the National Academyof Sciences of the United States of America* 92 (10), 4482-4486. PMID: 7753829.

Ouellette AJ. (2005, September). Paneth cell alpha-defensins: peptide mediators of innate immunity in the small intestine. *Springer Semin Immunopathol. 27*(2):133-46.

Park, C. H., D. E. Bergsagel, and E. A. McCulloch (1971, February). Mouse myelomatumor stem cells: a primary cell culture assay. *Journal of the NationalCancerInstitute* 46 (2), 411-422. PMID: 5115909.

Park, H. S., R. A. Goodlad, and N. A. Wright (1995, November).Crypt fission in the small intestine and colon.a mechanism for the emergence of G6PD locus-mutated crypts after treatment with mutagens. *The American Journal of Pathology* 147 (5), 1416-1427. PMID: 7485404.

Park, J., A. S. Venteicher, J. Y. Hong, J. Choi, S. Jun, M. Shkreli, W. Chang, Z. Meng,P. Cheung, H. Ji, M. McLaughlin, T. D. Veenstra, R. Nusse, P. D. McCrea, andS. E. Artandi (2009, July). Telomerase modulates wnt signalling by association withtarget gene chromatin. *Nature* 460 (7251), 66-72.

Park, S., J. Gwak, M. Cho, T. Song, J. Won, D. Kim, J. Shin, and S. Oh (2006, September). Hexachlorophene inhibits wnt/beta-catenin pathway by promoting siah-mediated beta-catenin degradation. *Molecular Pharmacology* 70 (3), 960-966. PMID: 16735606.

Park, S. Y., J. K. Ryu, J. H. Park, H. Yoon, J. Y. Kim, Y. B. Yoon, J. Park, S. H. Lee, S. Kang, J. W. Park, and J. H. Oh (2011, March). Prevalence of gastric and duodenal polyps and risk factors for duodenal neoplasm in korean patients with familial adenomatous polyposis. *Gut and Liver* 5 (1), 46-51. PMID: 21461071.

Park, Y., D. J. Hunter, D. Spiegelman, L. Bergkvist, F. Berrino, P. A. van den Brandt, J. E. Buring, G. A. Colditz, J. L. Freudenheim, C. S. Fuchs, E. Giovannucci, R. A. Goldbohm, S. Graham, L. Harnack, A. M. Hartman, D. R. Jacobs, I. Kato, V. Krogh, M. F. Leitzmann, M. L. McCullough, A. B. Miller, P. Pietinen, T. E. Rohan, A. Schatzkin, W. C. Willett, A. Wolk, A. Zeleniuch-Jacquotte, S. M. Zhang, and S. A. Smith-Warner (2005, December). Dietary fiber intake and risk of colorectalcancer: a pooled analysis of prospective cohort studies. JAMA*: The Journal ofthe American Medical Association* 294 (22), 2849-2857. PMID: 16352792.

Pino MS, Chung DC. (2010, June) The chromosomal instability pathway in colon cancer.*Gastroenterology. 138*(6):2059-72. PMID: 20420946

Pinto, D., A. Gregorieff, H. Begthel, and H. Clevers (2003, July). Canonical wnt signals are essential for homeostasis of the intestinal epithelium. *Genes & Development 17* (14), 1709-13. PMID: 12865297.

Potten C. S., Booth C., Tudor G. L., Booth D., Brady G., Hurley P., Ashton G., Clarke R., Sakakibara S. and Okano H. (2003). Identification of a putative intestinal stem cell and early lineage marker; musashi-1.*Differentiation,* 71**,** 28-41.

Potten, C. S., G. Owen, and D. Booth (2002, June). Intestinal stem cells protect their genome by selective segregation of template DNA strands. *J Cell Sci* 115 (11), 2381-2388.

Potten C. S., Hume W. J., Reid P. and Cairns J. (1978).The segregation of DNA in epithelial stem cells.*Cell,* 15**,** 899-906.

Potten, C. S., L. Kovacs, and E. Hamilton (1974, May). Continuous labelling studies onmouse skin and intestine. *Cell and Tissue Kinetics* 7 (3), 271-283. PMID: 4837676.

Porter, E. M., C. L. Bevins, D. Ghosh, and T. Ganz (2002, January).The multifaceted paneth cell.*Cellular and Molecular Life Sciences: CMLS 59* (1), 156-170. PMID:11846026.

Powell A. E., Wang Y., Li Y., Poulin E. J., Means A. L., Washington M. K., Higginnotham J. N., Juchheim A., Prasad N., Levy S. E., Guo Y., Shyr Y., Aronow B. J., Haigis K. M., Franklin J. L. & Coffey R. J. (2012). The pan-ErbB negative regulator Lrig1 is an intestinal stem cell marker that functions as a tumor suppressor. *Cell,* 149**,** 146-58.

Rajagopalan, H., A. Bardelli, C. Lengauer, K. W. Kinzler, B. Vogelstein, and V. E. Velculescu(2002). Tumorigenesis: RAF/RAS oncogenes and mismatch-repair status.*Nature* 418 (6901), 934.

Ramalho-Santos, M., D. A. Melton, and A. P. McMahon (2000, June). Hedgehog signals regulate multiple aspects of gastrointestinal development. *Development (Cambridge,England) 127* (12), 2763-2772. PMID: 10821773.

Reisman DN, Strobeck MW, Betz BL, Sciariotta J, Funkhouser W Jr, Murchardt C, Yaniv M, Sherman LS, Knudsen ES, Weissman BE. (2002, February). Concomitant down-regulation of BRM and BRG1 in human tumor cell lines: differential effects on RB-mediated growth arrest vs CD44 expression. *Oncogene. 21*(8):1196-207.

Reisman, D. N., J. Sciarrotta, W.Wang, W. K. Funkhouser, and B. E.Weissman (2003, February). Loss of BRG1/BRM in human lung cancer cell lines and primary lung cancers: Correlation with poor prognosis. *Cancer Res 63* (3), 560-566.

Reisman D, Glaros S, Thompson EA. (2009, April). The SWI/SNF complex and cancer.*Oncogene. 28*(14):1653-68. Epub 2009 Feb 23. Review.

Reya T, Clevers H. (2005, April) Wntsignalling in stem cells and cancer.*Nature. 434*(7035):843-50. PMID: 15829953

Reyes JC, Barra J, Muchardt C, Camus A, Babinet C, Yaniv M. (1998, December) Altered control of cellular proliferation in the absence of mammalian brahma (SNF2alpha). *EMBO J. 17*(23):6979-91. PMID: 9843504

Ricci-Vitiani L, Fabrizi E, Palio E, De Maria R. (2009, November) Colon cancer stem cells. *J Mol Med (Berl). 87*(11):1097-104. Epub 2009 Sep 2. Review.PMID: 19727638

Rijsewijk F, Schuermann M, Wagenaar E, Parren P, Weigel D, Nusse R. (1987, August). The Drosophila homolog of the mouse mammary oncogene int-1 is identical to the segment polarity gene wingless. *Cell.*1987 Aug 14;50(4):649-57.

Roberts CW, Galusha SA, McMenamin ME, Fletcher CD, Orkin SH. (2000, December) Haploinsufficiencyof Snf5 (integrase interactor 1) predisposes to malignant rhabdoid tumors in mice. *Proc Natl Acad Sci USA 97*:13796-800. PMID: 11095756

Roberts CW, Orkin SH.(2004, February).The SWI/SNF complex--chromatin and cancer. *Nat Rev Cancer*.;4(2):133-42.

Salmena L., Carracedo A. and Pandolfi P. P. (2008,May). Tenets of PTEN tumor suppression.*Cell,* 133**,** 403-14.

Samowitz, W. S., M. D. Powers, L. N. Spirio, F. Nollet, F. van Roy, and M. L. Slattery (1999, April).β-Catenin mutations are more frequent in small colorectal adenomas than in larger adenomas and invasive carcinomas. *Cancer Research* 59 (7), 1442-1444.

Sancho, E., E. Batlle, and H. Clevers (2004).Signaling pathways in intestinal development and cancer.*Annual Review of Cell and Developmental Biology 20*, 695-723. PMID: 15473857.

Sander GR, Powell BC.(2004, April).Expression of notch receptors and ligands in the adult gut.*J Histochem Cytochem. 52*(4):509-16.

Sangiorgi E. and Capecchi, M. R. (2008). Bmi1 is expressed in vivo in intestinal stem cells. *Nat Genet,* 40**,** 915-20.

Sansom, O. J., J. Berger, S. M. Bishop, B. Hendrich, A. Bird, and A. R. Clarke (2003, June). Deficiency of mbd2 suppresses intestinal tumorigenesis. *Nat Genet* 34 (2), 145-147
.
Sansom, O. J., F. C. Mansergh, M. J. Evans, J. A. Wilkins, and A. R. Clarke (2007,October). Deficiency of SPARC suppresses intestinal tumorigenesis in APCMin/+ mice. *Gut* 56 (10), 1410-1414. PMID: 17299058.

Sansom, O. J., V. Meniel, J. A. Wilkins, A. M. Cole, K. A. Oien, V. Marsh, T. J. Jamieson, C. Guerra, G. H. Ashton, M. Barbacid, and A. R. Clarke (2006, September).Loss of apc allows phenotypic manifestation of the transforming properties of an endogenous k-ras oncogene in vivo. *Proceedings of the National Academy ofSciences of the United States of America* 103 (38), 1412214127. PMC1599922.

Sansom, O. J., V. S. Meniel, V. Muncan, T. J. Phesse, J. A. Wilkins, K. R. Reed, J. K. Vass, D. Athineos, H. Clevers, and A. R. Clarke (2007b, April). Myc deletion rescues apc deficiency in the small intestine. *Nature* 446 (7136), 676-679

Sansom, O. J., K. R. Reed, A. J. Hayes, H. Ireland, H. Brinkmann, I. P. Newton, E. Batlle, P. Simon-Assmann, H. Clevers, I. S. Nathke, A. R. Clarke, and D. J. Winton (2004, June). Loss of apc in vivo immediately perturbs wnt signaling, differentiation,and migration. *Genes & Development* 18 (12), 1385-90. PMID: 15198980.

Sato, A. (2007, December). Tuft cells. *Anatomical Science International / Japanese Association of Anatomists 82* (4), 187-199. PMID: 18062147.

Sato, T., Vries, R. G., Snippert H. J., van de Wetering, M., Barker N., Stange D. E., van Es J. H., Abo A., Kujala P., Peters P. J. and Cleavers H. (2009, March). Single Lgr5 stem cells build crypt-villus structures in vitro without a mesenchymal niche. *Nature,* 459**,** 262-5.

Sato, T., J. H. van Es, H. J. Snippert, D. E. Stange, R. G. Vries, M. van den Born, N. Barker, N. F. Shroyer, M. van de Wetering, and H. Clevers (2010, November). Paneth cells constitute the niche for lgr5 stem cells in intestinal crypts. *Nature 20*;469(7330):415-8.

Schepers, A. G., R. Vries, M. van den Born, M. van de Wetering, and H. Clevers (2011, March). Lgr5 intestinal stem cells have high telomerase activity and randomly segregate their chromosomes. *EMBO J* 30 (6), 1104-1109.

Schneider, M. R., M. Dahlhoff D. Horst, B. Hirschi, K. Trlzsch, J. Mller-Hcker, R. Vogelmann, M. Allguer, M. Gerhard, S. Steininger, E. Wolf, and F. T. Kolligs (2010). A key

role for e-cadherin in intestinal homeostasis and paneth cell maturation.*PloS One 5* (12), e14325. PMID: 21179475.

Seeley, R. R., T. D. Stephens, and P. Tate (2002, July).*Anatomy and Physiology* 6/e (7th Revised edition ed.). McGraw Hill Higher Education.

Sévenet N, Sheridan E, Amram D, Schneider P, Handgretinger R, Delattre O(1999, November)Constitutional mutations of the hSNF5/INI1 gene predispose to a variety of cancers. *Am J Hum Genet.65*(5):1342-8.PMID: 10521299

Shanahan F, Seghezzi W, Parry D, Mahony D, Lees E. (1999, February) Cyclin E associates with BAF155 and BRG1, components of the mammalian SWI-SNF complex, and alters the ability of BRG1 to induce growth arrest. *Mol Cell Biol.19*(2):1460-9. PMID: 9891079

Shi Y, Massagué (2003, June) Mechanisms of TGF-beta signaling from cell membrane to the nucleus.*J. Cell. 113*(6):685-700. Review.PMID: 12809600

Shibata, H., K. Toyama, H. Shioya, M. Ito, M. Hirota, S. Hasegawa, H. Matsumoto, H. Takano, T. Akiyama, K. Toyoshima, R. Kanamaru, Y. Kanegae, I. Saito, Y. Nakamura, K. Shiba, and T. Noda (1997, October). Rapid colorectal adenoma formation initiated by conditional targeting of the apc gene. *Science 278* (5335),120-123.

Shen H, Powers N, Saini N, Comstock CE, Sharma A, Weaver K, Revelo MP, Gerald W, Williams E, Jessen WJ, Aronow BJ, Rosson G, Weissman B, Muchardt C, Yaniv M, Knudsen KE. (2008, December). The SWI/SNF ATPase Brm is a gatekeeper of proliferative control in prostate cancer. *Cancer Res. 68*(24):10154-62.

Shibata, H., K. Toyama, H. Shioya, M. Ito, M. Hirota, S. Hasegawa, H. Matsumoto, H. Takano, T. Akiyama, K. Toyoshima, R. Kanamaru, Y. Kanegae, I. Saito, Y. Nakamura, K. Shiba, and T. Noda (1997, October). Rapid colorectal adenoma formation initiated by conditional targeting of the apc gene. Science 278 (5335), 120-123.

Shmelkov S. V., ButlerJ. M., HooperA. T., HormigoA., KushnerJ., MildeT., Clair R. S., Baljevic M., White I., Jin D.K., Chadburn A., MurphyA. J., ValenzuelaD. M., Gale N. W., ThurstonG., YancopoulosG. D., DangelicaM., KemenyN., LydenD., Rafi S. (2008, June). CD133 expression is not restricted to stem cells, and both CD133+ and CD133 metastatic colon cancer cells initiate tumors. *The Journal of Clinical Investigation* 118 (6). PMC2391278.

Silverman KA, Koratkar R, Siracusa LD, Buchberg AM.(2002, January).Identification of the modifier of Min 2 (Mom2) locus, a new mutation that influences Apc-induced intestinal neoplasia.*Genome Res*. ;12(1):88-97.

Siminovitch L. and Axelrad A. A. (1963). Cell-cell interactions in vitro: their relation to differentiation and Carcinogenesis. *Proc Can Cancer Conf*, 5**,** 149-65.

Smith, M. W. (1985, October). Expression of digestive and absorptive function in differentiating enterocytes.*Annual Review of Physiology 47* (1), 247-260.

Snippert, H. J., L. G. van der Flier, T. Sato, J. H. van Es, M. van den Born, C. Kroon-Veenboer, N. Barker, A. M. Klein, J. van Rheenen, B. D. Simons, and H. Clevers (2010, October). Intestinal crypt homeostasis results from neutral competition betweensymmetrically dividing lgr5 stem cells. Cell 143 (1), 134-144.

Snippert, H. J., J. H. van Es, M. van den Born, H. Begthel, D. E. Stange, N. Barker, andH. Clevers (2009, June). Prominin-1/CD133 marks stem cells and early progenitorsin mouse small intestine. Gastroenterology 136 (7), 2187-2194.e1.

Strobeck, M. W., M. F. DeCristofaro, F. Banine, B. E. Weissman, L. S. Sherman, and E. S. Knudsen (2001, March). The BRG-1 subunit of the SWI/SNF complex regulates CD44 expression. *J. Biol. Chem. 276* (12), 9273-9278.

StroberBE, Dunaief JL, Guha, Goff SP. (1996, April) Functional interactions between the hBRM/hBRG1 transcriptional activators and the pRB family of proteins. *Mol Cell Biol. 16*(4):1576-83. PMID: 8657132

Su, L. K., K. W. Kinzler, B. Vogelstein, A. C. Preisinger, A. R. Moser, C. Luongo, K. A.Gould, and W. F. Dove (1992, May). Multiple intestinal neoplasia caused by a mutationin the murine homolog of the APC gene. *Science* (New York, N.Y.) 256 (5057), 668-70. PMID: 1350108.

Sumi-Ichinose, C., H. Ichinose, D. Metzger, and P. Chambon (1997, October). SNF2beta-BRG1 is essential for the viability of f9 murine embryonal carcinoma cells. *Molecular and Cellular Biology 17* (10), 5976-5986. PMC232446.

Sun A, Tawfik O, Gayed B, Thrasher JB, Hoestje S, Li C, Li B. (2007, February) Aberrant expression of SWI/SNF catalytic subunits BRG1/BRM is associated with tumor development and increased invasiveness in prostate cancers.*Prostate. 67*(2):203-13. PMID: 17075831

Suzuki, H., D. N. Watkins, K. Jair, K. E. Schuebel, S. D. Markowitz, W. Dong Chen, T. P. Pretlow, B. Yang, Y. Akiyama, M. van Engeland, M. Toyota, T. Tokino, Y. Hinoda, K. Imai, J. G. Herman, and S. B. Baylin (2004, April). Epigenetic inactivation of SFRP genes allows constitutive WNT signaling in colorectal cancer.*Nat Genet* 36 (4), 417-422.

Takaku, K., H. Miyoshi, A. Matsunaga, M. Oshima, N. Sasaki, and M. M. Taketo (1999, December).Gastric and duodenal polyps in smad4 (Dpc4) knockout mice.*Cancer Research* 59 (24), 6113-6117.

Takaku, K., M. Oshima, H. Miyoshi, M. Matsui, M. F. Seldin, and M. M. Taketo (1998,March). Intestinal tumorigenesis in compound mutant mice of both Dpc4(Smad4)and apc genes. *Cell* 92 (5), 645-656.

Takeda N., Jain R., Leboeuf M. R., Wang Q., Lu M. M. and Epestein J. A. (2011, December). Interconversion between intestinal stem cell populations in distinct niches.*Science,* 334**,** 1420-4.

Thibodeau, S. N., G. Bren, and D. Schaid (1993, May).Microsatellite instability in cancer of the proximal colon.*Science* (New York, N.Y.) 260 (5109), 816-819. PMID:8484122.

Tomlinson, I. P. and R. S. Houlston (1997, December).Peutz-Jeghers syndrome.*Journal of Medical Genetics* 34 (12), 1007-1011. PMID: 9429144.

Troughton, W. D. and J. S. Trier (1969, April).Paneth and goblet cell renewal in mouse duodenal crypts.*The Journal of Cell Biology 41* (1), 251-268.

Ueo T, Imayoshi I, Kobayashi T, Ohtsuka T, Seno H, Nakase H, Chiba T, Kageyama R. (2012, March). The role of Hes genes in intestinal development, homeostasis and tumor formation.*Development. 139*(6):1071-82. Epub 2012 Feb 8.

van der Flier, L. G., M. E. van Gijn, P. Hatzis, P. Kujala, A. Haegebarth, D. E. Stange, H. Begthel, M. van den Born, V. Guryev, I. Oving, J. H. van Es, N. Barker, P. J.Peters, M. van de Wetering, and H. Clevers (2009, March). Transcription factorachaete Scute-Like 2 controls intestinal stem cell fate. *Cell* 136 (5), 903-912.

van Es, J. H., P. Jay, A. Gregorie_, M. E. van Gijn, S. Jonkheer, P. Hatzis, A. Thiele, M. van den Born, H. Begthel, T. Brabletz, M. M. Taketo, and H. Clevers (2005, April). Wnt signalling induces maturation of paneth cells in intestinal crypts. *Nat Cell Biol 7* (4), 381-386.

van Es, J. H., M. E. van Gijn, O. Riccio, M. van den Born, M. Vooijs, H. Begthel, M. Cozijnsen, S. Robine, D. J. Winton, F. Radtke, and H. Clevers (2005, June). Notch/[gamma]-secretase inhibition turns proliferative cells in intestinal crypts and adenomas into goblet cells. *Nature 435* (7044), 959-963.

Versteege I, Sevenet N, Lange J, Rousseau Merck MF, Ambros P, Handgretinger R, Aurias A, Delattre O. (1998, July). Truncating mutations of hSNF5/INI1 in aggressive paediatric cancer.*Nature 394*:203-6. PMID: 9671307

Vries R. G., Huch M., Clevers H. (2010, October). Stem cells and cancer of the stomach and intestine. *Mol Oncol,* 4**,** 373-84.

Walther A., Johnstone E., Swanton C., Midgley R., Tomlinson I., Kerr D. (2009, July). Genetic prognostic and predictive markers in colorectal cancer.*Nature Reviews Cancer* 9, 489-499

Wang W, Xue Y, Zhou S, Kuo A, Cairns BR, Crabtree GR. (1996, September) Diversity and specialization of mammalian SWI/SNF complexes. *Genes Dev. 10*(17):2117-30. PMID: 8804307

Willert, K., J. D. Brown, E. Danenberg, A. W. Duncan, I. L. Weissman, T. Reya, J. R. Yates, and R. Nusse (2003, May). Wnt proteins are lipid-modifed and can act as stem cell growth factors. *Nature 423* (6938), 448-52. PMID: 12717451.

Wicha, M. S., S. Liu, and G. Dontu (2006, February). Cancer stem cells: An old Idea-A paradigm shift. Cancer Res 66 (4), 1883-1890.

Wilson BG, Roberts CW. (2011, June) SWI/SNFnucleosomeremodellers and cancer. *Nat Rev Cancer. 11*(7):481-92. PMID: 21654818

Winesett MP, Ramsey GW, Barnard JA. (1996, May). Type II TGF(beta) receptor expression in intestinal cell lines and in the intestinal tract. *Carcinogenesis. 17*(5):989-95.

Wolin, K. Y., Y. Yan, and G. A. Colditz (2011, March). Physical activity and risk ofcolon adenoma: a meta-analysis. *British Journal of Cancer* 104 (5), 8820-885. PMID: 21304525.

Yamamichi-Nishina M, Ito T, Mizutani T, Yamamichi N, Watanabe H, Iba H. (2003, February). SW13 cells can transition between two distinct subtypes by switching expression of BRG1 and Brm genes at the post-transcriptional level. *J Biol Chem. 278*(9):7422-30. Epub 2002 Dec 17.

Yamamichi N, Yamamichi-Nishina M, Mizutani T, Watanabe H, Minoguchi S, Kobayashi N, Kimura S, Ito T, Yahagi N, Ichinose M, Omata M, Iba H. (2005, August). The Brm gene suppressed at the post-transcriptional level in various human cell lines is inducible by transient HDAC inhibitor treatment, which exhibits antioncogenic potential. *Oncogene. 24*(35):5471-81.

Yamamichi N, Inada K, Ichinose M, Yamamichi-Nishina M, Mizutani T, Watanabe H, Shiogama K, Fujishiro M, Okazaki T, Yahagi N, Haraguchi T, Fujita S, Tsutsumi Y, Omata M, Iba H. (2007, November). Frequent loss of Brm expression in gastric cancer correlates with histologic features and differentiation state. *Cancer Res. 67*(22):10727-35.

Yang, Q., N. A. Bermingham, M. J. Finegold, and H. Y. Zoghbi (2001, December).Requirement of math1 for secretory cell lineage commitment in the mouse intestine.*Science 294* (5549), 2155 -2158.

Zhu, L., Gibson P., Currle D. S., Tong Y., Richardson R. J., Bayazitov I. T., Poppleton H., Zakharenko S., Ellison D. W. and Gilberston R. J. (2009, January) Prominin 1 marks intestinal stem cells that are susceptible to neoplastic transformation. *Nature*, 457**,** 603-7.

de Zwaan SE, Haass NK. (2010, May) Genetics of basal cell carcinoma.*Australas J Dermatol. 51*(2):81-92; quiz 93-4. Review. PMID: 2054